The regulation and function of the Rac1 GEF Trio and the Rac1/Cdc42 GAP CdGAP during neuronal development

Jonathan DeGeer

Department of Anatomy & Cell Biology

McGill University, Montréal, Québec, Canada

Submitted April, 2015

A thesis submitted to McGill University in partial fulfillment

of the requirements of the degree of

Doctor of Philosophy

Acknowledgements

I would like to begin by thanking Dr. Nathalie Lamarche-Vane for opening up her door to me in 2008. Her kind support and generous investment in my training have shaped me as a thinker, stoked my interests in science beyond the Petri dish, and have taken me to places in the world I would have never imagined. The times when I thought she would send me packing for home (ie, after the incident with the Beckman Coulter centrifuge), she instead exemplified patience in a manner I have yet to comprehend. I would like to also thank Dr. Chantal Autexier, who has supported me as a mentor from the beginning. Dr. Autexier encouraged me to transfer to the PhD program, and supervised me during my first teaching assistantship. To the other members of my advisory committee, Drs. Elaine Davis and Louise Larose, thank you for your scientific input and encouragement.

For funding support, I would like to thank the Fonds de Recherche en Santé Québec, Canadian Institutes for Health Research (CIHR), McGill Faculty of Medicine/Department of Anatomy & Cell Biology for: the Master's Training Award, Lab Operational Grants, GREAT Travel Awards and Merit Awards, respectively. To my colleagues in the Department both past and present, thank you for your collaboration, reagents (whether you realized it or not), troubleshooting/advice, and putting up with my practical jokes. Thanks to Josée-France, Martin and Judith for helping me to start in the lab, and to Vilay, Yi, Ali, Hidetaka, Fereshteh, Philippe, and Tristan for the scientific and not-so-scientific discussions/support. I was blessed to have been able to train excellent undergraduate students, Morgane and Lou—thank you for catching on quickly to my

“this is how you shouldn’t be doing it” lessons (the fact you are both starting PhD programs is certainly independent of my supervisory skills). I offer an especially important thanks to my friends Carlos and Lance for dropping all things and supporting me when I was at my lowest low—you are both exceptional friends. Also to my dear friend Megan, thanks for the constant encouragement and for your part in forcing me to finally write this thesis.

I wouldn’t be here if it wasn’t with the support of my loving family. Thanks to my parents Peter and Kayla for letting me run off at seventeen and explore the world. You gave me the wings and means to pursue my dreams whether or not we realized it at the time. Thanks to my brothers Tim and Bryan, for not sharing your friends or my hobbies and forcing me to make it on my own. I’m grateful that you’ve kept my picture on your fridges and still remind your beautiful children that I exist—I love them immensely more than I can show from afar. To my sister in spirit, Mary Ann, thanks for helping me keep it together all of these years. To my dear grandma, Maureen – thanks for encouraging me and supporting me in anything I’ve done. You and grandpa both taught me that anything is possible if I work hard enough at it. Thank you for all the precious chats, notes and letters that have helped to shrink the distance between myself and home--I treasure each one. I love you all.

Finally, I would like to thank God for curiosity and for the invention of the microscope—I’ve been blessed to view nature through its lens and I am awestruck.

Abstract

The wiring of the central nervous system during development supports normal physiological function and survival, and as such occurs in a tightly regulated manner. The Rho family of small GTPases are key regulators of cytoskeletal dynamics that have been implicated in neuronal development. Rho proteins are molecular switches, cycling between an inactive GDP-bound and active GTP-bound state. Oversight of Rho GTPase nucleotide cycling is performed by regulatory proteins: guanine nucleotide exchange factors (GEFs) promote GTP-bound state, while GTP hydrolysis is catalyzed by GTPase-activating proteins (GAPs). While Rho GTPase activities contribute to axon outgrowth and guidance, little is known about the spatiotemporal regulation of their cognate GEFs and GAPs. The Rac1 GEF, Trio and Rac1/Cdc42 GAP, CdGAP are highly enriched in the developing mammalian brain. Although Trio is required for the attractive axon guidance cue netrin-1 to induce axon pathfinding, the mechanisms governing Trio function are unknown. In contrast to this, the function of CdGAP in the mammalian brain is completely unknown. In this work we first explore the regulation of Trio by tyrosine phosphorylation in embryonic rat cortical neurons. Using an *in vitro* approach, we show that the Src-kinase Fyn phosphorylates Trio at tyrosine-2622, an event that is required for netrin-1-induced Rac1 activation. Next, we show that the molecular chaperone Hsc70 associates with Trio and the netrin-1 receptor DCC and that Hsc70 chaperone activity is required for Rac1 activation by Trio. Finally, we introduce a CdGAP-null mouse model and reveal a key role for CdGAP in vascular system development and the cytoarchitecture of cortical neurons. Overall, these studies highlight the importance of Rac1 and Cdc42 regulators during development.

Résumé

Le développement du système nerveux central est essentiel au bon fonctionnement physiologique. Les petites protéines G de la famille Rho sont des régulateurs clés du cytosquelette d'actine et des microtubules, lequel est impliqué dans plusieurs aspects du développement neuronal. Les protéines de la famille Rho sont des commutateurs moléculaires qui passent d'un état actif ou inactif par association avec le GTP ou GDP, respectivement. Cet échange nucléotidique est contrôlé par des protéines régulatrices comme les facteurs d'échange de nucléotide (GEFs) qui promouvoient le remplacement du GDP par le GTP ou les « GTPase-activating proteins » (GAPs) qui catalysent l'hydrolyse du GTP en GDP. Bien que l'activation de certaines GTPases Rho contribue à la croissance et au guidage axonale, nous en savons toujours très peu sur la régulation spatiotemporelle de leurs GEFs et GAPs. Trio et CdGAP sont des régulateurs spécifiques de Rac1 et Cdc42, Trio étant une protéine Rac1GEF et CdGAP, une protéine inhibitrice pour Rac1 et Cdc42. Ces protéines sont hautement enrichies dans le cerveau des mammifères en développement. Dans cette thèse, nous avons investigué premièrement la régulation de Trio par la phosphorylation sur ses tyrosines dans le cortex embryonnaire chez le rat. Une approche *in vitro* a révélé que la protéine Src-kinase Fyn phosphoryle Trio sur sa tyrosine-2622, et cette modification est nécessaire pour l'activation de Rac1 en aval de nétrine-1. Ensuite, nous avons démontré que le chaperone moléculaire Hsc70 associe avec Trio et le récepteur DCC et que l'activité de la chaperone Hsc70 est nécessaire pour l'activation de Rac1 par Trio. Enfin, nous avons analysé des embryons de souris dépourvus de l'expression de CdGAP et nous avons révélé un rôle clé pour CdGAP dans le développement du

système vasculaire et la cytoarchitecture des neurones corticaux. En résumé, ces études démontrent l'importance des régulateurs de Rac1 et Cdc42 au cours du développement.

Table of Contents

List of Tables

List of Figures

Chapter 1

Chapter 2

Chapter 3

Chapter 4

Abbreviations

ALS	amyotrophic lateral sclerosis
AOS	Adams-Oliver syndrome
ARHGAP	Rho GTPase-activating protein
Arp2/3	Actin-related protein 2 and 3 complexes
ATP	adenosine triphosphate
AKT	Ak thymoma
BDNF	brain-derived neurotrophic factor
BR	basic region
Cdc42	cell division cycle protein 42
CdGAP	Cdc42 GTPase-activating protein
cDNA	complementary DNA
CRIB	Cdc42 and Rac1 interactive binding
CNS	central nervous system
DAPI	4', 6-diamidino-2-phenylindole
DCC	deleted in colorectal carcinoma
Dbl	proto-oncogene in Diffuse B-cell Lymphoma cells

DH	Dbl homology
DHR	Dock homology region
DIV	days *in vitro*
DMEM	Dulbecco's modified Eagle's medium
Dock	dedicator of cytokinesis
DNA	deoxyribonucleic acid
DTT	dithiothreitol
E#	embryonic day
ECL	enhanced chemiluminescence
EDTA	ethylenediaminetetraacetic acid
EGF	epidermal growth factor
ER	endoplasmic reticulum
ERM	Ezrin, radixin, moesin
EMT	epithelial to mesenchymal transition
ERK	extracellular signal-regulated kinase
FAK	focal adhesion kinase
FBS	fetal bovine serum

Fyn	Fyn proto-oncogene
GAP	GTPase-activating protein
GDI	guanine nucleotide dissociation inhibitor
GDP	guanosine diphosphate
GEF	guanine nucleotide exchange factor
GEFD	GEF domain
GST	glutathione S-transferase
GTP	guanosine triphosphate
HEPES	4-(2-hydroxyethyl)-1-piperazineethanesulfonic acid
HRP	horseradish peroxidase
Ig	immunoglobulin
IPTG	isopropyl β-D-1-thiogalactopyranoside
JNK	c-Jun N-terminal kinase
kDa	kilodalton
LIMK	Lin11, Isl-1 and Mec-3 kinase
MAG	myelin-associated glycoprotein
MAPK	mitogen-activated protein kinase

mDia	mammalian diaphanous formins
MLC	myosin light chain
mRNA	messenger ribonucleic acid
mTOR	mammalian target of rapamycin
Nck	non-catalytic region of tyrosine kinase adaptor protein
NF-κB	nuclear factor-kappa B
NGF	nerve growth factor
NgR	Nogo family receptors
OMgp	oligodendrocyte-myelin glycoprotein
P75NTR	p75 neurotrophin receptor
PAGE	polyacrylamide gel electrophoresis
PAK	p21 activated kinase
PAR	partitioning-defective protein
PBR	polybasic region
PBS	phosphate-buffered saline
PCR	polymerase chain reaction
PDGF	platelet-derived growth factor

PEI	polyethylenimine
PH	Pleckstrin homology
PI3K	phosphatidylinositol 3-kinase
PKA	cAMP-dependent protein kinase A
PKC	protein kinase C
PKG	cGMP-dependent protein kinase G
P-loop	phosphate binding loop
PRD	Proline-rich domain
Rab	Ras in brain
Rac	Ras-related C3 botulinum toxin substrate
Ras	rat sarcoma
Rho	Ras homologous
Rnd	resistance-nodulation-cell division
ROBO	homolog of drosophila roundabout
ROCK	Rho-associated coiled-coil-containing protein kinase
RSK	p90 ribosomal S6 kinase
Sec14	exocyst complex subunit 14

SH2	Src homology 2
SH3	Src homology 3
siRNA	small interfering RNA
SNARE	SNAP receptor
SNAP	synaptosomal-associated protein
Slit	homolog of drosophila slit
Smurf	SMAD ubiquitin regulatory factor
SUMO	small ubiquitin-like modifier
TC10	10^{th} protein cloned from a human teratocarcinoma cell line
TCL	TC10-like
TGFβ	transforming growth factor beta
Tiam1	T-cell lymphoma invasion and metastasis 1
Trio	triple functional domain protein
U2OS	human osteosarcoma cells
VAMP	vesicle-associated membrane protein
VASP	vasodilator-stimulated phosphoprotein
VEGF	vascular endothelial growth factor

WASP	Wiskott-Aldrich syndrome protein
WAVE	WASP family VErprolin homologous protein
Wrch	Wnt-responsive Cdc42 homolog

Contribution of Authors to Manuscripts

Chapter 2:

My contribution to the manuscript entitled “Tyrosine phosphorylation of the RhoGEF Trio regulates netrin-1/DCC-mediated cortical axon outgrowth” included designing and performing all experiments, except for figures 2.3 and 2.6C which were performed in collaboration with J.B. & S.S.. N.L.V. and I each wrote this manuscript.

Chapter 3:

My contribution to the manuscript entitled “Hsc70 chaperone activity underlies Trio GEF function in axon growth and guidance induced by netrin-1” involved designing and performing all experiments, with help from M.M. in figure 3.3, assistance from A.K. and A.E.F. in figure 3.7. U.S. provided the GFP-Hsc70 and mutant constructs and contributed to the design of some experiments. T.E.K. provided the netrin-1 fragment used in figure 3.7. A.D. provided the GFP-Trio mutants and reagents. N.L.V. and I analyzed the data and wrote this manuscript.

Chapter 4:

My contributions to the manuscript entitled “CdGAP-null mouse generation reveals a role for CdGAP in angiogenesis and central nervous system development” involved designing and performing all experiments with help from V.L., H.I., and P.D. in figure 4.2A-B and 4.3D, respectively. L.B.L. assisted with micrograph acquisition and data analysis in figures 4.4-4.7. N.L.V., L.B.L. and I wrote this manuscript.

Submitted Manuscripts

Chapter 3:

Hsc70 chaperone activity underlies Trio GEF function in axon outgrowth and guidance induced by netrin-1 (2015). Jonathan DeGeer, Andrew Kaplan, Morgane Morabito, Ursula Stochaj, Timothy E. Kennedy, Anne Debant, Alyson Fournier and Nathalie Lamarche-Vane. **In revision, Journal of Cell Biology.**

Chapter 1: Introduction and Literature Review

1.0 General Introduction

It was 1665 when the English physicist Robert Hooke coined the biological term "cell". This term arose from his description of the discrete, porous units that constituted the cork shaving that he viewed under a simple magnifying lens [1]. Not long thereafter, in the 1670s, the development of magnifying lenses by Netherlander Antonie Van Leeuwenhoek led to the first detailed descriptions of tiny, living "animalcules" (likely protozoa) which were noted to be capable of propagating movement [2]. It was these founding observations that stoked preoccupation with microorganisms and inspired the development of modern microscopes. Further developments in the 20th century, including the ability to culture and observe living mammalian cells *in vitro* has birthed the field of cell biology, and we have since then begun to unravel the inner workings of this small unit of life.

We now know that mammalian cells are densely packed, lipid bilayer-bound entities comprising various organelles and biomolecules, suspended in a cytoplasmic matrix with the support of a cytoskeleton. The cell's ability to propagate movement and to respond to its extracellular environment is a feature that is conserved among both prokaryotes and eukaryotes and in the latter, involves the dynamic modulation of the actin cytoskeleton. The cell migration is a complex and tightly regulated process necessary for survival and development of multicellular organisms. During embryogenesis for example, the collective migration of cells and morphogenesis of tissues underlies the developmental program. On the other hand, deregulation of cell motility can lead to disastrous consequences. For example, enhanced motility and invasion of transformed cells contributes to metastasis and cancer progression, while

the inhibition of neurons to project axons following nerve injury can lead to neuronal death, motor and/or cognitive deficits. Whether physiological or pathological, the intracellular events that underlie cell migration are highly conserved. The Rho family of small GTPases are master regulators of cell motility and cell migration, acting as molecular switches to regulate the actin cytoskeleton. To date many regulators of Rho GTPases have been identified, however the mechanisms of their spatiotemporal modulation in either developmental or pathological contexts have been incompletely characterized. In this work, I investigate the regulation of Rho GTPase modulators in the developing mammalian brain: the Rac1 GEF, Trio and Rac1/Cdc42 GAP, CdGAP.

1.1 Overview of the Rho family of GTPases

The Rho family of GTPases are members of the Ras superfamily, which is composed of small G protein enzymes that bind guanosine triphosphate (GTP) and catalyze its hydrolysis to guanosine diphosphate (GDP). As was first determined with Ras proteins, Rho GTPases have been identified as key components of molecular signaling pathways induced by extracellular stimuli. The first Rho family member identified was RhoA in 1985, which was cloned from a cDNA library from the sea mollusc *Aplysia* and termed a ***R***as ***ho***mologue [3]. Since then, 20 genes encoding members of the Rho family have been discovered in mammals, and their gene products have been found to function from the earliest stages of development, and throughout the lifespan of multicellular organisms [4]. By the nature of their enzymatic activity, Rho GTPases act as molecular switches, regulating downstream pathways via effector proteins that preferentially associate with GTP-bound members [5]. Rho proteins have

been sub-classified into various families based on sequence homology: Rac (Rac1-3, RhoG), Rho (RhoA-C), Cdc42 (Cdc42, TC10, TCL), Wrch (Wrch-1, Chp/Wrch2), Rnd (Rnd1-2, Rnd3/RhoE), RhoD (RhoD, Rif/RhoF), RhoBTB (RhoBTB1-2) and RhoH [6]. Oversight of Rho GTPase nucleotide cycling is performed by regulatory proteins: guanine nucleotide exchange factors (GEFs) enhance the GTP-bound state, while GTP hydrolysis is catalyzed by GTPase-activating proteins (GAPs) [7,8]. Additionally, guanine nucleotide dissociation inhibitors (GDIs) bind to some Rho GTPases and restrict them in an inactive state within the cytoplasm, preventing them from associating with their downstream effectors [9]. The following section is a summary of the structure and regulation of the Rho family of GTPases, providing insights into their function in mammalian cells and tissues.

1.1.1 Rho GTPase structure and regulation

Similar to other GTP-binding proteins, Rho GTPases contain a G-domain fold consisting of a six-stranded β-sheet, flanked by six α-helices on either side (Fig. 1.1A) [10]. Rho GTPases contain a 13 amino acid insert between the fifth β strand and fourth α-helix termed the “Rho insert” thereby differentiating these proteins from their Ras family cousins [11]. Nucleotide binding and exchange activity of Rho GTPases is facilitated by the dynamic “switch I” and “switch II” regions. Water-mediated contact of an Mg^{2+} ion in the phosphate-binding loop (P-loop) pocket between switch I and II is critical for tight nucleotide binding [12] (Fig. 1.1B). GTP-binding to Rho proteins is stabilized by hydrogen bonds between amide groups in switch I (threonine-35) and II (glycine-60) regions and the oxygen atoms of the γ-phosphate group of GTP, in a manner that has been likened

A

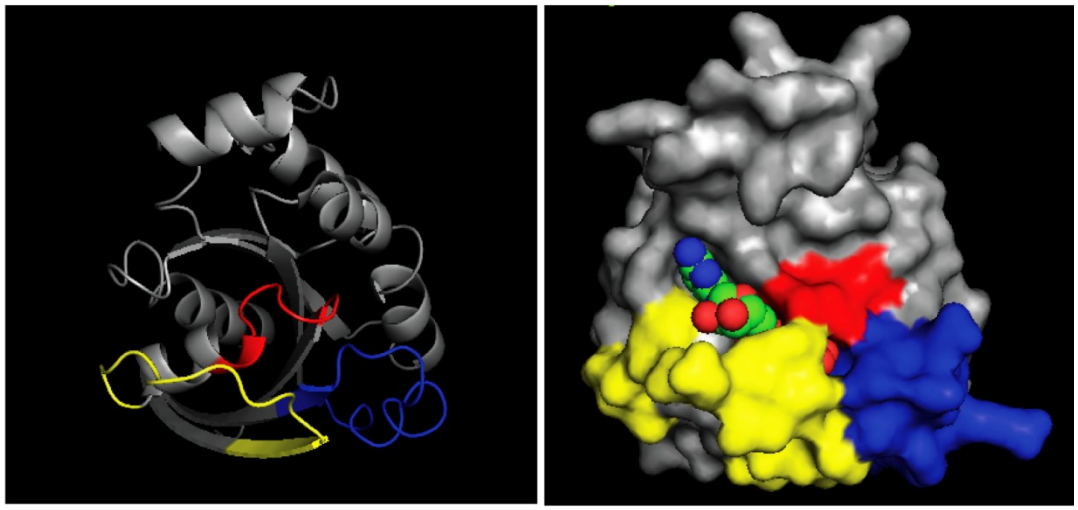

B

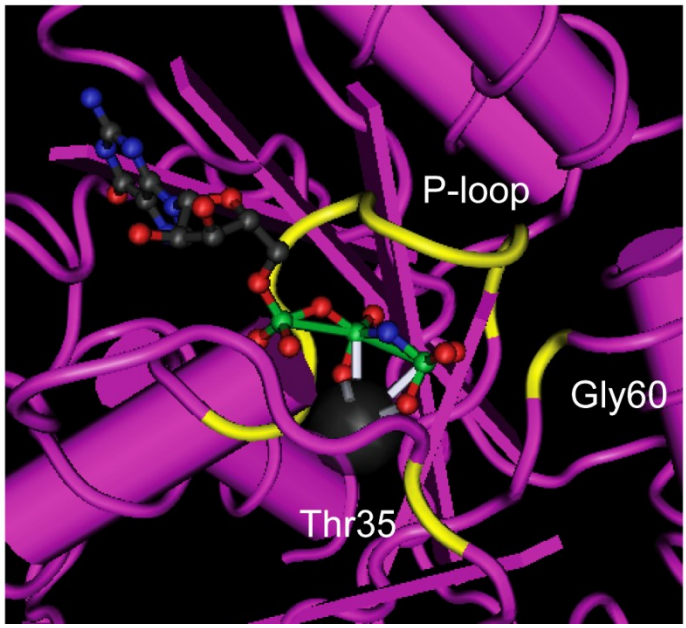

Figure 1.1 – Crystal structure of Rac1 and nucleotide binding

(A) Left: Secondary structure of Rac1 reveals the characteristic G-domain fold with a six-stranded β-sheet (oriented outwards) surrounded by six α-helices, shared by Rho family proteins. The P-loop domain (red), switch I (yellow) and switch II (blue) are indicated. Right: Surface mask demonstrating the electron density of Rac1 structure binding a GTP analogue. This view demonstrates the nucleotide (green) binding pocket provided by the P-loop, switch I and switch II regions (generated from [13] using PyMOL software). (B) Highlighted regions of the P-loop in close association with Mg^{2+} (black), Thr-35 of switch I and Gly-60 of switch II coordinating the tight association with the γ-phosphate of GTP ("loaded spring"). Hydrolysis of GTP results in release of these tight contacts and conformational change in Rac1 underlying its specificity for effector proteins in the GTP-bound conformation (generated from [13] using Cn3D software [NCBI]).

to a “loaded spring” [10,12] (Fig. 1.1B). Upon GTP hydrolysis, loss of these stabilizing interactions results in a change in switch I/II conformation of GDP-bound Rho GTPases, and a resulting loss of association with downstream effector proteins due to unfavorable sterics [14].

Whether targeted to the cytosol or to the membranes, the proper localization of Rho GTPases is imperative for their biological functioning within the cell. Various indispensible post-translational mechanisms have evolved that regulate Rho GTPase localization, the first of which to be discussed is lipid modification. Before being released into the cell, a lipid moiety is conjugated to the C-terminus of most newly synthesized Rho family proteins, which serves to increase hydrophobicity and acts as a membrane anchor. Prenylation of Rho GTPases occurs at the C-terminal CAAX motif (C-cysteine, A-aliphatic residue, X-any amino acid) which is present on all Rho proteins except Wrch-1/2, and RhoBTB1/2 [15]. Targeted Rho GTPases undergo either farnesylation or geranylgeranylation via irreversible covalent addition of the 15 carbon farnesyl- or 20 carbon geranylgeranyl-lipid groups to the C-terminal cysteine residues. Selection of either farnesyl- or geranylgeranyl-transferases to target the CAAX motif of Rho GTPases is mediated by the “X” residue following the targeted cysteine. Generally, geranylgeranyltransferases are preferentially guided by non-polar, hydrophobic residues such as a leucine, phenylalanine, isoleucine, or valine (ie: -CLV**L** of RhoA) [15,16]. Farnesyltransferases are directed by polar, uncharged residues such as a glycine, cysteine, serine, threonine or alanine which flank the cysteine targeted for prenylation (ie: -CLI**T** of TC10), with the exception of non-polar methionine, which directs both farnesyl- and geranylgeranyltransferases [15,16]. At this stage, the functional modification

of target proteins remains incomplete. Following prenyl moiety addition, lipid-modified Rho GTPases are translocated to the surface of the endoplasmic reticulum, where the Ras-converting enzyme 1 endoprotease trims the C-terminal –AAX residues [17,18], freeing the C-terminal cysteine to undergo methylation by isoprenylcysteine-*O*-carboxyl methyltransferase [19]. In addition to prenylation, some Rho GTPases are modified by the reversible addition of a 16 carbon palmitoyl group to free cysteines at or near the C-terminus. Notably, Wrch1/2 which lack a C-terminal CAAX motif, as well as Rac1, RhoB, and TC10 are modified by palmitoylation, either alone or accompanying isoprenylation [20]. For example, palmitoylation of Rac1 at cysteine-178 follows prenylation, promoting its GTP-loading and targets Rac1 for stabilization at actin cytoskeleton-linked membranes [21].

In addition to lipid modification, some Rho GTPases are regulated by other post-translational modifications including phosphoryation. Phosphorylation is the mechanism by which a γ-phosphate group of adenosine triphosphate (ATP) is transferred to an amino acid via the activity of a protein kinase [22]. Although a reversible, covalent phosphorylation event does little to alter the structure of the target Rho GTPases, they generally alter the favourability of association with downstream effectors and as such alter the biological activity of Rho GTPases. For example, RhoA becomes phosphorylated at serine-188 by both cAMP-dependent protein kinase A (PKA) and cGMP-dependent protein kinase G (PKG) [23,24]. Phosphorylation of RhoA at serine-188 results in an enhanced association with the Rho guanine-dissociation inhibitor (RhoGDI) while in its GTP-bound conformation, resulting in its sequestration in the cytoplasm and inactivation [25]. Similarly, while phosphorylation of Cdc42 by Src-family kinases at

tyrosine-64 does not directly alter its nucleotide binding or association with effectors, it leads to an enhanced interaction with the negative regulator RhoGDI, leading to its cytoplasmic sequestration or differential subcellular targeting [26]. The biological function of Rho GTPase phosphorylation is less clear than with lipid modification. For example, phosphorylation of Rac1 by Akt at serine-71 results in impaired GTP binding, but this has no effect on its GTPase activity either *in vitro* or in cells [27].

Many Rho GTPases are also modified by covalent addition of polypeptides including polyubiquitination or SUMOylation. Ubiquitination is the reversible process by which covalent addition of 8 kilodalton (kDa) ubiquitin polypeptides are added to lysine residues of particular eukaryotic proteins, resulting in the targeting of proteins to specific subcellular structures, or proteasome-mediated degradation (reviewed in [28]). Protein ubiquitination is highly conserved and requires the sequential contribution of activating, conjugating and ligating enzymes (termed E1-3, respectively). Selective ubiquitination of active Rac1 at lysine-147 occurs at the plasma membrane and precedes downregulation of active Rac1 by the proteasome pathway [29,30]. In epithelial cells, ubiquitination of Rac1 occurs during cell scattering at the earliest stage of epithelial to mesenchymal transition (EMT) and correlates with the loss of cell adhesions [31]. Subsequent study revealed that ubiquitination of active Rac1 is mediated by the ubiquitin E3-ligase HACE1, which negatively regulates Rac1 function in cultured fibroblasts [32]. In addition to Rac1, GTP-bound RhoA is also a target of ubiquitination, which is carried out by the E3 ligase smad ubiquitin regulatory factor-1 (Smurf-1) [33]. Ubiquitination of RhoA induced by Smurf-1 in epithelial cells resulted in reduced stress-fibre formation and an increase in dynamic protrusions, both indicative of reduced RhoA

activation [33]. Subsequent study revealed a second E3 ligase Cullin-3 which also targets RhoA for ubiquitination. Unlike Smurf-1, Cullin-3 preferentially targets GDP-bound RhoA for polyubiquitination and proteasomal degradation, and does not ubiquitinate other Rho GTPases including: RhoB, RhoC, Cdc42 or Rac1 [34]. Cullin-3 also associates with and ubiquitinates the atypical Rho GTPase RhoBTB2, resulting in its downregulation in various cell lines [35].

SUMOylation is the reversible post-translational addition of the 11 kDa small ubiquitin-like modifier (SUMO) to target lysine residues, and is well conserved throughout all eukaryotes [36]. Similar to the ubiquin-conjugation cascade, SUMOylation also requires three sequential enzymatic steps involving different classes of enzymes. SUMOylation of target proteins contributes to protein stability, localization and activity [37]. Although a core consensus motif has been identified: -ψKxD/E- (where ψ is any large hydrophobic residue, x is any residue) [36], many sequences targeted for SUMOylation lack a consensus motif altogether. Recently, Rac1 was revealed as a substrate for the SUMO E3 ligase PIAS3, which preferentially SUMOylates Rac1 at a non-consensus sequence preceding its C-terminal CAAX motif rich in polybasic residues (PBR) [38]. Intriguingly SUMOylation is not required for Rac1-GTP binding, but helped to stabilize active Rac1 and promote lamellipodia induction [38].

In summary, many mechanisms of post-translational modification of Rho GTPases have been described. These modifications directly regulate the subcellular localization of Rho proteins, altering their affinity for both membranes and effectors, independently of GEFs and GAPs.

1.1.2 Rho GTPases and the actin cytoskeleton

Of the Rho GTPases identified, the best characterized are RhoA, Rac1, and Cdc42. Early studies in murine fibroblasts in 2D culture highlighted the fundamental role of these GTPases in mediating cytoskeletal rearrangements: stress fiber and focal adhesion formation by RhoA, lamellipodia and membrane ruffles by Rac1, and filopodia and actin microspikes by Cdc42 [39-41]. The following section is a summary of these major subfamilies of Rho GTPases and their roles in regulating the actin cytoskeleton.

1.1.2.1 RhoA subfamily

RhoA is the founding member of the Rho GTPase family, and was cloned alongside two additional subfamily members with high sequence homology, termed RhoB and RhoC [3]. All three RhoA subfamily members are ubiquitously expressed, and carry out their functions by association with effector proteins, many of which are shared [42]. Rho proteins were largely assumed to play redundant roles due to their overlapping expression and similar abilities to induce stress fibre formation [43]. Despite sharing 85% amino acid identity, subtle differences between Rho subfamily proteins have emerged, thus alluding to divergent cellular functions. The majority of variance in sequence homology among Rho subfamily members is enriched within 15 amino acids of the C-terminus, including the region targeted for isoprenylation. Indeed each RhoA subfamily member is targeted for lipid modification which promotes protein stability, and is required for Rho-induced processes including cell proliferation and cytoskeletal reorganization [44,45]. While both RhoA and RhoC undergo only geranylgeranylation, RhoB can become modified by palmitoylation and either farnesyl- or geranylgeranylation [46]. This correlates with studies showing that RhoA and RhoC are

similarly localized to either the plasma membrane or the cytoplasm associated with RhoGDI, whereas RhoB is mainly targeted to late endosomes and lysosomes [47,48]. A testament to the subtle importance of prenylation on protein localization is exemplified by RhoB; farnesylated RhoB is specifically targeted to the plasma membrane versus geranylgeranylated RhoB which localizes to late endosomes [49].

The biological importance of Rho subfamily proteins has been pursued extensively. Notably upregulation of RhoA has been correlated with various cancers and neurodegeneration [50,51], and as such extensive efforts have been made to determine the downstream signaling pathways induced by Rho activation. The founding observations implicating Rho GTPase activity in the regulation of cytoskeletal dynamics were performed by introducing active GTPases into quiescent fibroblasts. Microinjection of active RhoA resulted in the formation of stress fibres and focal adhesions [39,52,53]. Subsequent studies have further implicated Rho function in maintenance of cell shape, polarity and migration due to regulation of actin polymerization, actomyosin contractility, microtubule dynamics and cell adhesion [54,55]. Downstream of RhoA activation, the Rho-kinase (ROCK) family of protein kinases are stimulated. ROCK1 and ROCK2 are serine/threonine kinases that contribute to cytoskeletal rearrangements by promoting the phosphorylation and activation of myosin light chain (MLC), and inactivation of MLC phosphatase [56,57]. This in turn stimulates myosin II to associate with and move along actin filaments, generating contractile forces within the cell [58]. ROCK also contributes to F-actin dynamics by phosphorylating Lin-11, Isl-1, and Mec-3 (LIM) domain-containing kinases (LIMK), which phosphorylates and inactivates the actin depolymerisation factor cofilin [59,60]. In addition to ROCKs, mammalian Diaphanous formin proteins (mDia) are

effectors of RhoA that bind to and nucleate the elongation of pre-existing actin filaments, while they also contribute to microtubule stabilization at the leading edge during cell migration downstream of RhoA [61]. The first formin to be identified as an effector of RhoA, mDia1 was later confirmed to be a target of RhoB and RhoC [62,63]. Activation of Rho and its resulting association with mDia stimulates the actin-nucleating and microtubule stabilizing functions of mDia1 [64]. This pathway is of particular importance during cytokinesis when RhoA localizes to the cleavage furrow of dividing cells, supporting furrow formation, ingression and stabilization via regulation of microtubule stability [65]. While Rho proteins are able to activate mDia2 and mDia3, these formins also can become activated by Rac1 and Cdc42 [66].

Modulation of the actin cytoskeleton by Rho is particularly important during cell migration. RhoA activation is enriched at the trailing edge of a migrating cell where its activation leads to local actomyosin-induced contractility, degradation of focal adhesions, and resulting retraction of the trailing edge [67,68]. Indeed temporal activation of RhoA occurs at the leading edge of the motile cell to drive cortical actin polymerization and retrograde actin flow (reviewed in [69]). At the leading edge RhoA is negatively regulated by the ubiquitin E3 ligase Smurf1, resulting in local proteasome-mediated degradation of RhoA [33,70]. Upregulation of both RhoA and RhoC have been associated with tumorigenesis and carcinoma invasion, notably by regulation of the actin cytoskeleton and shape of tumour cells [50,71,72]**.** Activation of Rho is associated with the loss of focal adhesions occurring during EMT preceding tumour metastasis, and depends on ROCK activity [50,73]. Furthermore, studies of RhoC-null mice reveal a particular requirement for RhoC in tumour metastasis [71,74]. Generally, RhoB expression

is reduced during tumour progression. This is further supported by studies of RhoB-null mice where the loss of RhoB resulted in enhanced susceptibility to tumour formation, cell adhesion and growth factor signaling in transformed cells [75].

Rho proteins have also been shown to contribute to cell proliferation and survival independently of regulation of the actin cytoskeleton. RhoA has been implicated in the regulation of gene expression by the c-fos serum response factor downstream of mitogenic signaling pathways [76]. Additionally, downstream of RhoA, nuclear NF-kB becomes activated independently of Ras, thereby altering target gene transcription [77]. The differentially localized and less stable Rho protein, RhoB, has also been shown to regulate cell cycle transition and survival [78]. Loss of RhoB expression induces apoptosis of primary endothelial cells during angiogenesis, via dephosphorylation and impaired nuclear trafficking of kinase Akt [79]. Furthermore, treatment of cells with growth factors results in a vesicular localization of RhoB [78], which regulates the trafficking of signaling molecules in non cancerous cells including the epidermal growth factor (EGF) receptor [80] and platelet-derived growth factor receptor [81]. In cancer cells, the loss of RhoB results in an increase in surface localization of the EGFR, leading to enhanced Akt phosphorylation and cell proliferation [82].

1.1.2.2 Rac subfamily

The Rac subfamily of Rho proteins consists of Rac1 and its splice variant Rac1b, Rac2, Rac3 and RhoG. Originally identified as a ***Ra***s-related ***C***3 botulinum toxin substrate, Rac1 is the founding member of the Rac subfamily and is expressed ubiquitously [83]. The alternatively spliced variant of Rac1, Rac1b, is upregulated in various tumours and is constitutively active [84,85]. Rac2 which was cloned at the same

time as Rac1, shares 92% amino acid sequence homology with Rac1 but its expression is restricted to hematopoietic lineages [83]. Rac3, which shares more than 90% of its protein sequence with Rac1 is enriched in the developing mammalian CNS where its expression overlaps substantially with Rac1 [86]. RhoG is the most divergent Rac subfamily member sharing 72% amino acid sequence identity with Rac1, and is ubiquitously expressed [87]. Of the Rac subfamily, Rac1 is the best characterized Rho GTPase, being shown to function in divergent aspects of cell biology such as reorganization of the actin cytoskeleton [40], reactive oxygen species generation [88], oncogenic transformation [89], cell cycle progression [90] and neuronal axon guidance [91].

The identification of Rac1 as a regulator of the actin cytoskeleton resulted from injection of active Rac1 into quiescent fibroblasts, which induced lamellipodia formation and membrane ruffles [40]. One of the first effector proteins of Rac1 identified is the serine/threonine kinase family, p21 activated kinases (PAKs). Upon binding to active Rac1 via its Cdc42 and Rac1 interactive binding domain (CRIB), PAK activity increases more than 50 fold [92], leading to modulation of the actin cytoskeleton by LIMKs, which phosphorylate and inhibit the actin filament depolymerizing factor cofilin [93,94]. Downstream of active Rac1, PAKs also phosphorylate and inactivate myosin light chain kinase (MLCK), which leads to reduced phosphorylation and activity of the MLCK target myosin II regulatory light chain, a molecular motor involved in actin cytoskeletal dynamics [95,96]. In addition to targeting LIMK and MLCK, PAKs also link Rac1 to various signaling pathways including the mitogen-activated protein kinase (MAPK), the c-Jun-NH2-terminal kinase (JNK) and p38 MAPK pathways [90,97-99]. Important downstream effectors of active Rac1, thereby linking these GTPases to actin polymerization, are the

Wiskott-Aldrich-syndrome family scaffold proteins: Wiskott-Aldrich-syndrome Protein (WASP), and WASP family VErprolin homologous (WAVE) proteins [100]. WASP and WAVE proteins associate with the actin cytoskeleton via the Arp 2/3 actin nucleation complex. Direct association of GTP-Rac1 with N-WASP via its CRIB-domain results in activation of N-WASP *in vitro*, and promotes association with the Arp2/3 complex which nucleates new actin filaments [101,102]. Downstream of Rac1 the activation of WAVE occurs indirectly via the release of an inhibitory WAVE complex [103], thus promoting its association with monomeric actin and Arp2/3, producing lamellipodia [104,105]. Owing to its ability to regulate the actin cytoskeleton, Rac1 is also a key regulator of cell migration. The polarized localization and activation of Rac1 at the leading edge during chemotaxis requires WAVE-mediated dendritic actin polymerization and lamellipodia formation [103].

Rac1b, is characterized by a 19 amino acid insertion following the Switch II domain, resulting in a decreased ability to hydrolyze GTP rendering it predominantly active [85]. As with Rac1, Rac1b promotes the transcription of cyclin D1 and contributes to oncogenic transformation by inactivation of the NF-κB inhibitor IκB, leading to stimulation of NF-κB targets [106]. In contrast to Rac1 however, Rac1b only poorly activates PAKs or JNK [85], but promotes survival and cell cycle progression despite serum deprivation [106]. As a result of these mechanistic findings it is not surprising that Rac1b expression is upregulated in breast, colon and lung cancers [84,107,108].

Despite being highly homologous to Rac1, the C-terminus of Rac2 diverges from Rac1 most notably in the PBR upstream of its CAAX motif. As a result, Rac2 does not undergo palmitoylation like Rac1 [21], and in such a manner is differentially regulated in cells expressing both Rac1 and Rac2. For example, Rac2 has a lower affinity for PAK

in a manner that is dependent on its C-terminal sequence [109]. While Rac2 expression is enhanced in some tumours [110], its restricted expression to hematopoetic lineages which also express the highly homologous Rac1 implies a particular requirement for another Rac protein. Rac2-null mice are fertile, and although they exhibit impaired hematopoiesis, they have normal longevity [111]. Although Rac2-deficient neutrophils displayed impaired chemotaxis and superoxide formation in response to various stimuli [111], Rac2 is not required for migration of macrophages [112].

In contrast to Rac1-null mice, which die during early embryogenesis [113], Rac3-deficient mice survive embryogenesis and exhibit an enhanced motor coordination and hyperactivity [86]. Divergences in Rac3 sequence homology relative to Rac1 occurs at the C-terminus and PBR, suggesting that Rac3 may have altered affinity for effector proteins [114]. This is evidenced by Rac3 specific binding with Calmodulin- and integrin-binding protein in a manner that requires and intact C-terminal tail, promoting integrin-mediated adhesion and cell spreading [115]. Despite its differences, Rac3 has been shown to activate many similar downstream pathways to Rac1 including JNK and PAK [114], and active Rac3 can transform fibroblasts and induce foci formation in a similar manner to Rac1 [116,117].

RhoG was originally identified as a gene induced by serum-treatment in fibroblasts [87]. Since then, it has been shown to function during neurite outgrowth [118,119], cell proliferation [120], cell survival [121], as well as macropinocytosis[122]. Despite sharing only 72% sequence identity with Rac1, active RhoG similarly stimulates JNK activity and can also associate with phosphatidylinositol 3-kinase (PI3K) to activate Akt, thereby promoting cell survival [121]. Intriguingly, expression of constitutively activated RhoG

elicits membrane ruffles and lamellipodia, and filopodia as active Rac1 and Cdc42, respectively, in a manner that precludes direct binding with PAK or WASP [123]. A partial explanation for this was revealed when active RhoG was found to associate with the DOCK180-binding protein ELMO, leading to Rac1 activation [124]. In addition to its effects on the actin cytoskeleton RhoG has also been shown to regulate the interferon-gamma promoter and nuclear factor of activated T cells (NFAT) gene transcription in T-cells [125]. The finding that RhoG promotes neural progenitor proliferation in the developing murine cerebral cortex suggests that RhoG also regulates G1 to S phase transition via transcriptional targets in some cell types, as has been demonstrated with other Rho proteins [120].

1.1.2.3 Cdc42 subfamily

The Cdc42 subfamily of Rho GTPases consists of Cdc42 and its splice variant Cdc42b, TC10/RhoQ and TCL/RhoJ. Human ***C***ell-***d***ivision-***c***ycle protein ***42*** (Cdc42a/ Cdc42Hs, herein Cdc42) was originally cloned in 1990 from a placental cDNA library, and was found to have the highest conserved sequence identity to *Saccharomyces cerevisiae* CDC42 [126]. At the same time, another CDC42-related protein termed G25K (25 kDa GTP-binding protein) was identified from a human fetal brain cDNA library, differing from Cdc42 in the C-terminal 10 amino acids [127,128]. While Cdc42 is expressed ubiquitously and is required for early embryonic development [55,129], Cdc42b is enriched in the brain [128]. TC10 shares roughly 67% amino acid sequence homology to Cdc42, and was found to be expressed ubiquitously [130]. TC10-like (TCL) shares 78% amino acid similarity with Cdc42, and is expressed in various tissues including the heart, lung, liver and kidney [131,132] with a particular function in endothelial cells [133].

Since its identification, Cdc42 subfamily members have been implicated in cancer development [134], cell cycle progression [135], and regulation of the actin cytoskeleton [41]. While the subcellular localization of Cdc42 is regulated by geranylgeranylation at its C-terminus [15], Cdc42b is regulated by both isoprenylation and palmitoylation [136]. The subtlety of palmitoylation of Cdc42b is particularly important, since depalmitoylation results in the dispersal of Cdc42b from the dendritic spine which supports synapse function [137]. Both TC10 and TCL are modified by farnesylation at their C-termini, resulting in their proper perinuclear and endosomal localizations [15]. Additionally, TC10 and not TCL undergoes palmitoylation, but the contribution of this modification to increased membrane localization has remained elusive [15].

The first noted observation that Cdc42 acts as a regulator of the actin cytoskeleton was made when constitutively active Cdc42 was microinjected into fibroblasts. In these cells active Cdc42 induced the formation of filopodia and multi-molecular focal complexes at the plasma membrane, rich in vinculin, paxillin and focal adhesion kinase (FAK) [41]. Intriguingly this study also reported that Cdc42 activation occurs upstream of both Rac1 and Rho activation, suggesting that particular crosstalk between disparate Rho GTPase signaling pathways occurs and underlies such cytoskeletal changes within cultured cells [41]. Exogenous expression of TC10 has also been shown to induce filopodia and microspike formation similar to Cdc42 [138]. While TCL expression in fibroblasts supports filopodia formation [131] and regulates early endocytosis [139], a recent study has also implicated its function in the disassembly of focal adhesions [133].

One of the first effector proteins of active Cdc42 identified is the PAK family of protein kinases. As with Rac1, binding of active Cdc42 to PAKs stimulate its kinase activity [92] and regulates actin filament turnover via the LIMK/cofilin pathway [93,94]. As described with Rac1, PAK activation also links Cdc42 regulation with diverse signaling pathways within the cell including the MAPK and JNK pathways [90,97-99]. Cdc42 induces filopodia formation via binding to and activating the WASP family of proteins [100]. Direct association of GTP-Cdc42 with WASP via its CRIB domain results in activation of WASP *in vitro*, and promotes association with the Arp2/3 complex which nucleates new actin filaments [102]. While both TC10 and TCL also associate with WASP and N-WASP, the binding affinity to these effectors is much less than that of Cdc42 [140]. Cdc42 also associates with and activates the formin family members mDia2 and mDia3, which promote the polymerization of unbranched actin thus supporting filopodia formation [141,142]. The insulin receptor substrate p53 (IRSp53) has also been identified as a Cdc42 effector which contributes to filopodia by supporting actin filament bundling and promoting membrane curvature [143].

Since its identification in yeast, Cdc42 has been implicated in the generation of cell polarity [144], a process required for proper cell migration, development, and differentiation. Cdc42 carries out this role in conjunction with the Par polarity complex, consisting of polarity protein partitioning-defective-3 (PAR3), PAR6 and atypical protein kinase C (aPKC), which is required to generate polarity induction in various cell types [145]. In epithelial cells which have a defined apical-basal polarity, Cdc42 is required for the apical targeting of the PAR complex, thereby supporting the asymmetrical distribution of proteins which underlies cell polarity [146-148]. During chemotaxis, active

Cdc42 recruits the PAR complex to the leading edge of the cell, stabilizing extending microtubules and reorienting the microtubule-organizing centre to polarize the cell [149]. Simultaneously active Cdc42 induces Rac1 activation at the leading edge of the cell, via the Rac1 GEF Tiam1 (T-cell lymphoma invasion and metastasis 1) leading to synchronized regulation of the actin cytoskeleton by both Cdc42 and Rac1-dependent mechanisms [149,150] .

In addition to its function in regulating the actin cytoskeleton and cell polarity, Cdc42 is an important regulator of cell cycle regulation. As Rac1, activation of Cdc42 results in cell cycle progression through G1 and activation of the JNK pathway [151]. Furthermore, active Cdc42 and TC10 induce the transcription of the cyclin D1 promotor independent of ERK activation, in part by activation of nuclear NF-kB [77,152]. An additional mechanism by which Cdc42 regulates cell cycle progression is by the regulation of chromosome segregation during mitosis. Cdc42-dependent activation of mDia3 is required for the proper attachment of spindle microtubules to the kinetochores of sister chromatids during mitosis [153]. This function of Cdc42 is further supported by the observation of defective alignment of chromosomes during cell division and abundance of multinucleated cells depleted of all Cdc42 subfamily members [154]. Dysregulation of cell cycle progression is a key driver of oncogenic transformation. While active Cdc42 and TC10 are sufficient to transform cells, they are also required for Ras-induced oncogenic transformation [155,156]. *In vivo* TCL-deficient mice have reduced tumour vascularisation and growth, further underscoring the importance of Cdc42 subfamily members in tumorigenesis [133].

1.2 Regulators of Rho GTPases

In addition to structural post-translational modifications, Rho GTPases are differentially spatiotemporally regulated by various classes of enzymes. The localized modulation of Rho GTPases in particular by GEFs, GAPs and GDIs, varies from cell type to cell type and thus presents a complex network of regulatory mechanisms. Next the major classes of enzymes regulating Rho GTPases will be discussed, with a general emphasis placed on GEF and GAP structure and enzymatic function.

1.2.1 Rho guanine nucleotide exchange factors

Most of the RhoGEFs identified to date have been subdivided into two families: the Dbl-homology domain-containing family and the Dedicator of cytokinesis (Dock) family. GEFs of the former group generally contain a characteristic Dbl-homology (DH) domain directly followed by a Plekstrin homology (PH) domain, which together interact with GDP-bound substrates [8]. The Dock family of GEFs have two characteristic Dock homology regions (DHR) termed DHR1 and DHR2, which are involved in phospho-lipid association and GEF activity, respectively [157]. Additionally, various atypical RhoGEFs which lack either DH or DHR domains entirely have been identified. Despite lacking general amino acid identity across families, RhoGEFs have evolved convergent functions within mammals.

1.2.1.1 Dbl family of exchange factors

To date, more than 70 human Dbl domain-containing Rho GEFs have been identified (Table 1.1)[158]. Among family members, there is a considerable amount of variation in the sequence identities of the namesake Dbl-homolog and PH-domain,

Table 1.1 – Dbl family of guanine nucelotide exchange factor proteins in humans.

Classic DH-PH containing Rho GEFs					
Symbol	**Name**	**Synonyms**	**Chrom.**	**Rho Target(s)**	**Ref**
FARP1	FERM, RhoGEF (ARHGEF) and pleckstrin domain protein 1 (chondrocyte-derived)	CDEP, PLEKHC2	13q32.2	RhoA, Rac1	[159,160]
FARP2	FERM, RhoGEF and pleckstrin domain protein 2	KIAA0793, FIR, PLEKHC3, FRG	2q37.3	Cdc42, Rac1	[161,162]
ABR	Active BCR-related	MDB	17p13	RhoA, Rac1, Rac2, Cdc42	[163]
ALS2	Amyotrophic lateral sclerosis 2 (juvenile)	Alsin	2q33-q35	Rac1	[164]
p115-RHOGEF	P115-rho guanine nucleotide exchange factor (GEF)	SUB1.5, LBCL2, ARHGEF1, Lsc	19q13.13	RhoA, RhoB, RhoC	[165]
GEF-H1	Guanine nucleotide exchange factor (GEF) H1	LFP40, ARHGEF2, Lfc	1q21-q22	RhoA, Rac1	[166]
ARHGEF3	Rho guanine nucleotide exchange factor (GEF) 3	STA3, XPLN, GEF3	3p14.3	RhoA, RhoB	[167]
ASEF	APC-stimulated guanine nucleotide exchange factor 1	STM6, KIAA1112, ARHGEF4	2q22	Rac1, Cdc42	[168,169]
ASEF2	Spermatogenesis associated 13	ARHGEF29, Asef2	13q12.13	Rac1, Cdc42	[170]
EPHEXIN-3	Eph-interacting exchange protein 3	TIM, TIM1, ARHGEF5	7q35	RhoA, RhoB, RhoC, RhoG, Rac1, Cdc42	[171,172]
α-PIX	PAK-interacting exchange factor alpha	Cool-2, Cool2, ARHGEF6	Xq26	Rac1, Cdc42, RhoA	[173]
β-PIX	Rho guanine nucleotide exchange factor (GEF) 7	PIXB, COOL1, P85COOL1, P50BP, ARHGEF7	13q33.3	Rac1, Cdc42	[173]
NET1	Neuroepithelial cell transforming 1	ARHGEF8, NET1A	10p15	RhoA, RhoB	[174,175]
ARHGEF9	Cdc42 guanine nucleotide exchange factor (GEF) 9	KIAA0424, hPEM-2	Xq11.1	Cdc42	[176]
ARHGEF10	Rho guanine nucleotide exchange factor (GEF) 10	KIAA0294, Gef10	8p23	RhoA, RhoB, RhoC	[177]
GrinchGEF	Rho guanine nucleotide exchange factor (GEF) 10-like	ArhGEF10L, KIAA1626	1p36.13	RhoA, RhoB, RhoC	[178]
PDZ-RHOGEF	PDZ-Rho guanine nucleotide exchange factor (GEF)	GTRAP48, ARHGEF11	1q21	RhoA, RhoB, RhoC	[179,180]
LARG	Leukemia-associated RhoGEF (LARG)	KIAA0382, ARHGEF12	11q23.3	RhoA, RhoB, RhoC	[180,181]

AKAP13	A kinase (PRKA) anchor protein 13	Ht31, BRX, AKAP-Lbc, c-lbc, PROTO-LB, HA-3, ARHGEF13	15q24-q25	RhoA, RhoB, RhoC	[182]
DBS	MCF2 cell line derived transforming sequence-like	KIAA0362, DBS, OST, ARHGEF14	13q34	RhoA, Cdc42	[183]
EPHEXIN-5	Eph-interacting exchange protein 5	Vsm-RhoGEF, ARHGEF15	17p13.1	RhoA	[184]
EPHEXIN-4	Eph-interacting exchange protein 4	NBR, neuroblastoma, ARHGEF16	1p36.3	RhoG	[185]
TEM4	Tumor endothelial marker 4	TEM4, p164-RhoGEF, ARHGEF17	11q13.3	RhoA, RhoB, RhoC	[186,187]
P114-RhoGEF	P114-Rho guanine nucleotide exchange factor (GEF)	ARHGEF18	19p13.3	RhoA, Rac1	[188,189]
EPHEXIN-2	Eph-interacting exchange protein 2	FLJ33962, WGEF, ARHGEF19	1p36.13	RhoA, Rac1, Cdc42	[190]
DBL	Diffuse B-cell lymphoma	MCF2, ARHGEF21	Xq26.3-q27.1	RhoA, RhoB, RhoC, Rac1, RhoG, Cdc42, TC10	[191,192]
MCF2L2	MCF.2 cell line derived transforming sequence-like 2	KIAA0861, ARHGEF22	3q27	Unknown	
TRIO-N	Trio Rho guanine nucleotide exchange factor	ARHGEF23, Trio-A, Trio-B, Trio-C, Trio-D	5p14-p15.1	Rac1, RhoG	[193]
TRIO-C	Trio Rho guanine nucleotide exchange factor	ARHGEF23, Trio-A, Trio-D, Trio-E	5p14-p15.1	RhoA	[193]
KALRN-N	Kalirin, RhoGEF kinase	duo, Hs.8004, DUO, Kalirin, ARHGEF24	3q21.2	Rac1, Rac2, RhoC, RhoG	[194,195] (unpublished)
KALRN-C	Kalirin, RhoGEF kinase	DUET, TRAD, Kalirin(iso3), ARHGEF24	3q21.2	RhoG, RhoC	(unpublished) [196]
P63RhoGEF	P63-Rho guanine nucleotide exchange factor (GEF)	GEFT, ARHGEF25	12q13.3	Rac1, Cdc42, RhoA	[197,198]
SGEF	SH3-containing guanine nucleotide exchange factor (GEF)	DKFZP434D146, ARHGEF26	3q25.2	RhoG, Cdc42	[122]
EPHEXIN-1	Eph-interacting exchange protein 1	ARHGEF27, NGEF	2q37	Rac1, RhoA, Cdc42	[199]
P190-RhoGEF	P190-Rho guanine nucleotide exchange factor (GEF)	RIP2, ARHGEF28	5q13.2	RhoA, RhoB, RhoC	[180]

OBSCN	Obscurin, cytoskeletal calmodulin and titin-interacting RhoGEF	KIAA1556, UNC89, KIAA1639, ARHGEF30	1q42	RhoA	[200]
ECT2	epithelial cell transforming sequence 2	ARHGEF31	3q26.1-q26.2	RhoA, Rac1, Cdc42	[201]
ECT2L	epithelial cell transforming sequence 2 like	ARHGEF32, FBXO49, LFDH	6q24.1	Unknown	
ARHGEF39	Rho guanine nucleotide exchange factor (GEF) 39	AAH33666, FLJ14642	9p13.3	Unknown	
ARHGEF40	Rho guanine nucleotide exchange factor (GEF) 40	Solo, FLJ10357, Trio8, Scambio	14q11.2	RhoA, RhoC, Rac1	[202,203]
PLEKHG1	pleckstrin homology domain containing, family G member 1	KIAA1209, ARHGEF41	6q25.1	Unknown	
PLEKHG2	pleckstrin homology domain containing, family G member 2	CLG, FLJ00018, ARHGEF42	19q13.2	Rac1, Cdc42	[204]
PLEKHG3	pleckstrin homology domain containing, family G member 3	ARHGEF43	14q23.3	Unknown	
PLEKHG4	pleckstrin homology domain containing, family G member 4	DKFZP434I216, ARHGEF44	16q22.1	RhoA, Rac1, Cdc42	[205]
PLEKHG4b	pleckstrin homology domain containing, family G member 4b	KIA1909	5p15.33	Unknown	
PLEKHG5	pleckstrin homology domain containing, family G member 5	KIAA0720, TECH, Syx	1p36	RhoA	[206]
PLEKHG6	pleckstrin homology domain containing, family G member 6	BAA91741, MyoGEF	12p13.31	RhoA, RhoC, Rac1, RhoG	[207-209]
PLEKHG7	pleckstrin homology domain containing, family G member 7	FLJ46688	12q22	Unknown	
BCR	breakpoint cluster region	D22S662, CML, PHL, ALL	22q11	RhoA, Rac1, Rac2, Cdc42	[163]
FGD1	FYVE, RhoGEF and PH domain containing 1	ZFYVE3	Xp11.21	Cdc42	[210]
FGD2	FYVE, RhoGEF and PH domain containing 2	ZFYVE4	6p21.2	Cdc42	[211]
FGD3	FYVE, RhoGEF and PH domain containing 3	FLJ00004, ZFYVE5	9q22	Cdc42	[212]
FGD4	FYVE, RhoGEF and PH domain containing 4	FRABP, frabin, ZFYVE6, CMT4H	12p11.1	Cdc42	[213]
FGD5	FYVE, RhoGEF and PH domain containing 5	ZFYVE23, FLJ39957, FLJ00274	3p25.1	Cdc42	[214]
FGD6	FYVE, RhoGEF and PH domain containing 6	ZFYVE24, FLJ11183	12q23.1	Cdc42	[215]
ITSN1	intersectin 1 (SH3 domain protein)	SH3P17	21q22.1-q22.2	Cdc42	[216]

ITSN2	intersectin 2	SWAP, SH3P18	2p23.3	Cdc42	[217]
P-REX1	phosphatidylinositol-3,4,5-trisphosphate-dependent Rac exchange factor 1	KIAA1415, PREX1	20q13.13	Rac1, Rac2, Cdc42, RhoA	[218]
P-REX2	phosphatidylinositol-3,4,5-trisphosphate-dependent Rac exchange factor 2	DEP.2, FLJ12987, PREX2, PPP1R129	8q13.1	Rac1, Cdc42	[219]
RASGRF1	Ras protein-specific guanine nucleotide-releasing factor 1	CDC25L, CDC25, GRF55, H-GRF55, GNRP, PP13187	15q24	Rac1	[220]
RASGRF2	Ras protein-specific guanine nucleotide-releasing factor 2	GRF2, Ras-GRF2	5q13	Rac1	[221]
SOS1	son of sevenless homolog 1 (Drosophila)	HGF, GF1	2p21	Rac1	[222]
SOS2	son of sevenless homolog 2 (Drosophila)		14q21	Rac1	[222]
TIAM1	T-cell lymphoma invasion and metastasis 1		21q22.1	RhoA, Rac1, Cdc42	[223]
TIAM2	T-cell lymphoma invasion and metastasis 2	STEF	6q25	Rac1	[224]
VAV1	vav 1 guanine nucleotide exchange factor		19p13.2	Rac1, Rac2, RhoG, Cdc42, RhoA	[225,226]
VAV2	vav 2 guanine nucleotide exchange factor		9q34.1	RhoA, RhoB, Rac1, RhoG, Rac3, Cdc42	[122,227]
VAV3	vav 3 guanine nucleotide exchange factor		1p13.3	RhoA, Rac1, RhoG, Cdc42	[228,229]
Non-classical DH-domain containing GEFs					
Symbol	**Name**	**Synonyms**	**Chrom.**	**Rho Target(s)**	**Ref**
ARHGEF33	Rho guanine nucleotide exchange factor (GEF) 33		2p22.1	Unknown	
TUBA	Dynamin binding protein	KIAA1010, Tuba, ARHGEF36, DNMBP	10q24.31	Cdc42	[230]
TUBA2	Rho guanine nucleotide exchange factor (GEF) 38	FLJ20184, Tuba-like, ARHGEF38	4q24	Unknown	
TUBA3	Rho guanine nucleotide exchange factor (GEF) 37	FLJ41603, ARHGEF37	5q32	Unknown	

nonetheless resulting in the modulation of common GTPases [158]. In general, Dbl-family GEFs carry out their enzymatic activity in an allosteric fashion. Sequence comparisons and structural analysis have revealed three conserved alpha helical sequences (CR1-3) within the DH domain of Rho GEFs responsible for GTPase association [231,232]. Indeed amino acid substitutions in the DH domain of some Rho GEFs interfering with these alpha helices result in loss of exchange activity [233]. This is in part explained by the finding that CR1 and 3 directly contact the switch I and II regions of GTPases (Fig. 1.2 A, B), while CR2 acts to stabilize the engaged helices [158,232]. The DH domain helical bundle association with the cognate GTPase results in reshaping of the switch I and II regions, resulting in a concomitant loss of Mg^{2+} binding in the P-loop and nucleotide binding [10]. Nucleotide-free Rho protein intermediates in complex with Dbl-GEFs readily bind GTP·Mg^{2+}, since the GTP concentration in cells is much greater than that of GDP and this results in dissolution of the GEF/GTPase complex **[158]**.

Although the PH domain (located C-terminal to the DH domain of most Dbl GEFs) has been shown to enhance nucleotide exchange activity of Dbl-family GEFs [234], the variable distance and orientation between DH and PH domains among Rho GEFs complicates a general contribution of the PH domain to enzymatic activity. A direct binding of the PH domain of some Rho GEFs to cognate GTPases has been documented, such as with LARG-RhoA [235], Trio-Rac1 [236] and Dbs-Cdc42 [237], but it does not appear to be a universal mechanism [158]. Since Rho GTPases are targeted to lipid bilayers via C-terminal prenylation, it has been proposed that the PH domain contributes to the membrane-recruitment of Rho GEFs [158]. Indeed, PH domains of various proteins have been documented to bind with phospholipids [238], and in this way promote

A

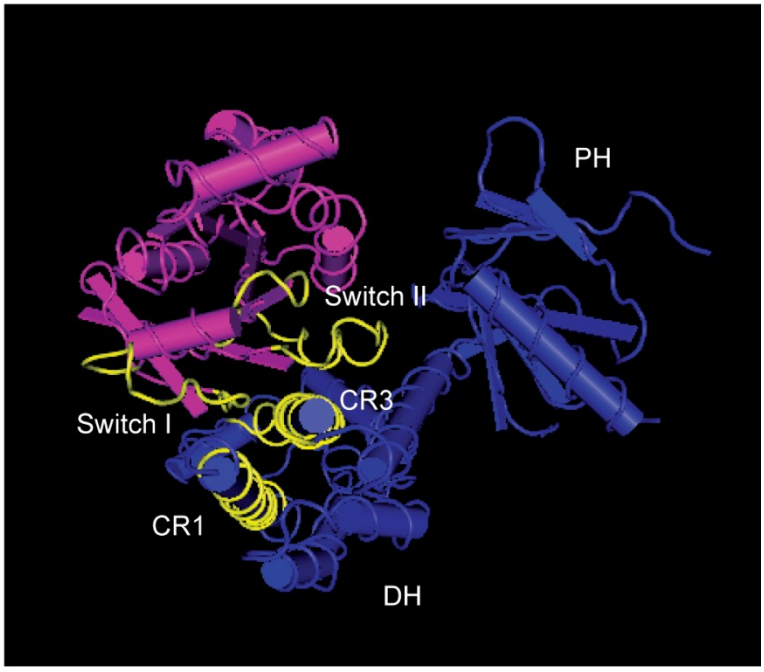

B

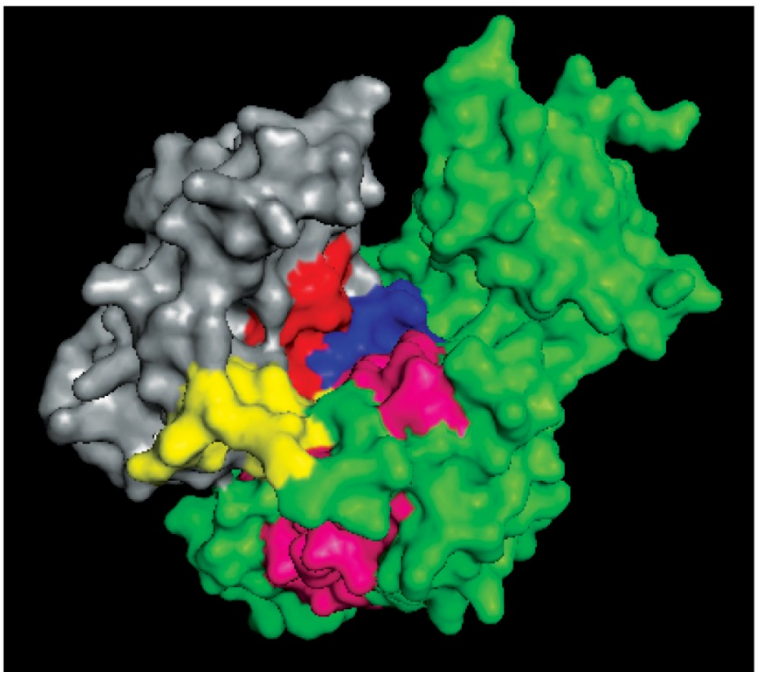

Figure 1.2 – Crystal structure of Rac1 in complex with Trio DH-PH domains

Tertiary structure of Rac1 crystalized with the DH-PH domain of the GEF Trio reveals the Rho GTPase and Dbl GEF interface (nucleotide-free). (A) Switch I and II regions of Rac1 closely juxtapose the alpha helical sequences CR1 and CR3 of the DH domain, respectively. (B) Surface mask demonstrating the electron density of the Rac1 (grey) and Trio (green) interface. These direct interactions of the CR domains (magenta) with Rac1 switch I (yellow) and switch II (blue) regions favour the release of Mg^{2+} from P-loop binding (red) and loss of GDP association (Generated from [236] using PyMOL software).

membrane localization of proteins. Although the PH domains of some Rho GEFs bind phospholipids, the relatively low efficiency with which they bind suggests a more subtle contribution of the PH domain to Rho GEF membrane localization [239]. The PH domain of Rho GEFs may effectively promote exchange activity by re-orienting the DH domain toward membrane-localized Rho GTPases via engagement with phosphoinositides of lipid bilayers [10]. However the observation that some Rho GEFs lack a PH domain all together would imply that the PH domain is more of an accessory to Rho GEF function and is not solely responsible for Rho GEF activity. These GEFs include: Arhgef10L, Arhgef33, and TUBA1-3 (Table 1.1).

1.2.1.2 Trio subfamily of Dbl GEFs

Trio along with its paralog, Kalirin, constitute this subfamily of Dbl Rho GEFs, which contain two tandem DH-PH GEF domains (GEFDs). Trio was originally identified by yeast two-hybrid screen, using the LAR transmembrane tyrosine phosphatase as bait [193]. Trio, as its name implies, contains three enzymatic domains: two Dbl GEFDs and a serine/threonine kinase domain, for which a substrate has yet to be identified. Kalirin was identified shortly after Trio, as a protein associated with the secretory pathway peptide processing enzyme, peptidylglycine alpha-amidating monooxygenase [240]. Kalirin shares 60% of its protein sequence identity with Trio, including its highly conserved tri-enzymatic domain structure [241]. Invertebrates express one protein encoded by a single Trio-like gene: UNC-73 in the nematode *Caenorhabditis elegans* (30% homologous), and D-Trio in *Drosophila melanogaster* (40% homologous). Thus it is likely that the duplication of a common gene resulting in two Trio-like proteins is of great biological significance in the function of higher organisms. Of this subfamily Trio is

the most widely distributed being expressed ubiquitously [242] and it is also required for late embryonic development in mice [243,244]. Conversely, Kalirin is mainly enriched in the central nervous system, and while Kalirin-null mice have neurological deficits, they are viable and fertile [245]. Due to the objectives of this thesis, the remainder of this section will focus on the biological role of Trio in regulating Rho GTPases.

At nearly 350 kDa, Trio is a massive, multi-domain containing protein (Figure 1.3). In addition to the two DH-PH domains, Trio contains an N-terminal Sec14 domain, various Spectrin-like repeats, SH3 domains following each GEFD, an immunoglobulin (Ig)-like domain, and a serine/threonine kinase domain at the C-terminus. Although Trio has two GEFDs, the first GEFD (GEFD1) appears to function as the dominant exchange factor upon over-expression in cells [246]. Trio has been shown to function as an exchange factor for both RhoG and Rac1 via GEFD1, while the GEFD2 binds to and activates RhoA *in vitro* [193,246,247]. As Kalirin, Trio is also abundant in the mammalian brain where five Trio isoforms are generated by alternative-splicing, four containing the GEFD1 (Trio-A-D) and a second consisting of the C-terminal portion of Trio containing the GEFD2 and kinase domain (Trio-E; Table 1.3) [242]. An additional isoform Tgat has been isolated from adult-T cell leukemia patients, consisting of only the RhoA DH domain with additional 15 C-terminal amino acids, and possesses transforming abilities [248]. Trio-null mice die between embryonic day 15.5 (E15.5) and birth and display a general impairment of commissural projections in the spinal cord and brain [243,244]. Specifically in the brain Trio-null embryos lack anterior commissures, and commissural projections crossing the corpus callosum and internal capsule are misguided, due to defects in axon pathfinding governed by the guidance cue netrin-1 [244]. In addition to

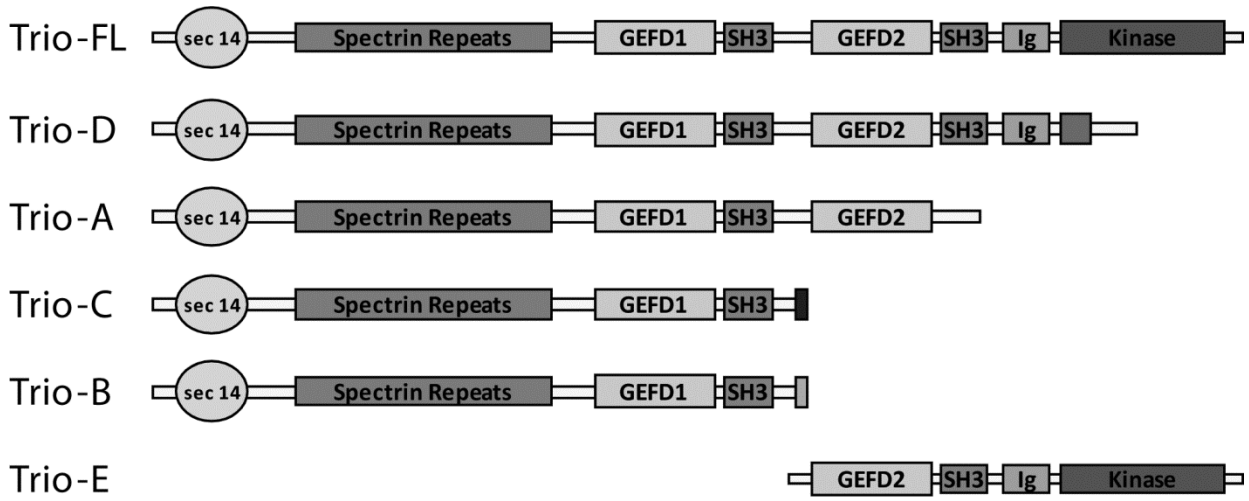
Trio-FL
sec 14
Spectrin Repeats
GEFD1
SH3
GEFD2
SH3
Ig
Kinase
Trio-D
sec 14
Spectrin Repeats
GEFD1
SH3
GEFD2
SH3
Ig
Trio-A
sec 14
Spectrin Repeats
GEFD1
SH3
GEFD2
Trio-C
sec 14
Spectrin Repeats
GEFD1
SH3
Trio-B
sec 14
Spectrin Repeats
GEFD1
SH3
Trio-E
GEFD2
SH3
Ig
Kinase

Figure 1.3 – Trio domain structure and neural isoforms

Full length Trio (Trio-FL) contains a Rac1 and RhoG-specific DH-PH GEFD (GEFD1), followed by the RhoA GEFD (GEFD2). Additional domains include a Sec14 domain and Spectrin-like repeats N-terminal to GEFD1, SH3 domains following each GEFD, and an immunoglobulin (Ig)-like domain and kinase domain at the C-terminus. The domain structure of the neural Trio isoforms: Trio-A-E. This figure was based on previously published reports [241,242].

neural defects, Trio-null embryos also exhibit underdeveloped skeletal muscles due to impaired myoblast fusion, further contributing to the embryonic lethal phenotype [243].

It has been reported that Rho GEFs can be differentially spatiotemporally regulated by various mechanisms including: protein-protein interactions and phosphorylation [7], and Trio is no exception to this. Trio regulates the actin cytoskeleton via close association with various cytoskeleton-associated proteins. For example, the PH domain of Trio GEFD1 binds to the actin cross-linking protein Filamin A, and in this manner directly targets Trio to the cytoskeleton [249]. Furthermore, the Trio-associated repeat on actin (Tara) protein was identified by its direct interaction with Trio GEFD1 [250], which localizes to adherens junctions with E-cadherin but negatively regulates Trio-dependent Rac1 activation [251]. Trio function has also been implicated during cell adhesion induced by cadherins. For example, the importance of Trio-dependent Rac1 activation occurring downstream of M-cadherin during myoblast fusion *in vitro* [252] *,* is underscored by the defects in myogenesis in Trio-null embryos [243]. More recently, Trio has been identified as the Rac1 GEF that regulates F-actin remodeling during cytokinesis of HeLa cells, a function which is impaired by the Rac1/Cdc42 GAP, MgcRacGAP [253]. In addition to regulating actin networks, Trio regulates microtubule dynamics in extending neurites via its association with the microtubule plus-end-tracking protein Navigator 1 (NAV1). Binding of Trio to NAV1 at the ends of dynamic microtubules increases the association of Trio with Rac1 and RhoG, and stimulates its Rac1 exchange activity [254].

It has been proposed that the Spectrin repeats N-terminal to the GEFD1 act to impair Trio Rac1 GEF function by an intramolecular inhibition. In *C. elegans* Disrupted-

in-schizophrenia 1 (DISC1) binds to the N-terminal Spectrin repeats of Trio, releasing the GEFD1 and promoting Rac1 activation [255]. Similarly, the integral membrane protein Kidins220/ARMS associates with the N-terminus of Trio, thereby promoting its Rac GEF activity [256]. Since Trio Spectrin repeats are functionally required for Trio-induced neurite outgrowth in PC12 cells [118], it is more likely that the N-terminus of Trio serves as a binding site for regulatory proteins required for its proper targeting and activation, than an inhibitory module. In further support of this, Pak1 association with Trio occurs via the Spectrin repeats, which is necessary for association of Trio with the receptor deleted in colorectal cancer (DCC) during netrin-1-induced neurite outgrowth [244]. Since Trio is a large protein, it is likely that it is regulated by association with additional proteins that have yet to be identified, which will be explored in Chapter 3.

Trio was originally reported as serine phospho-protein [193], but whether serine phosphorylation regulates Trio function remains to be shown. As I will detail in Chapter 2, phosphorylation of Trio at tyrosine-2622 by the Src-family kinase Fyn is required for Rac1-dependent axon outgrowth induced by the axon guidance cue netrin-1 in embryonic cortical neurons [257]. Phosphorylation by Fyn promotes the association of Trio with the receptor DCC, and Trio expression potentiates the surface enrichment of DCC in cortical neuron growth cones [257]. In *Drosophila*, although Trio directly associates with Abl tyrosine kinase during nervous system development, whether Trio is a direct substrate of Abl kinase activity has yet to be determined [258,259].

In addition to its physiological function in regulating neurite outgrowth, aberrant Trio regulation has been reported in many different types of cancers. In general, high Trio expression is often correlated with a poor degree of patient survival [260]. For

example, Trio is highly upregulated in invasive glioblastomas, where it promotes tumour invasion via dysregulation of Rac1 [261].

1.2.1.3 Dock family of exchange factors

Despite being functionally similar to Dbl GEFs, Dock family Rho GEFs lack sequence homology to Dbl proteins and are structurally distinct enzymes. To date, 11 Dock family Rho GEFs have been identified (Table 1.2) [262]. Dock family GEFs have been further sub-divided into four groups based on sequence homology/domain structure: Group A (Dock1, 2 and 5), Group B (Dock 3 and 4), Group C (Dock 6, 7, and 8) and Group D (Dock9, 10, and 11) [263]. Unlike Dbl family GEFs, Dock proteins have been reported to act only as exchange factors for either Rac1 or Cdc42 (Table 1.2). Each Dock family member contains both DHR1 and DHR2 domains. The DHR1 domain, which lies N-terminal to the DHR2, is roughly 200 amino acids in length and lacks intrinsic GEF activity. The DHR1 contributes to the enzymatic activity of Dock GEFs by mediating binding to lipids, and promoting membrane localization. Particularly, the DHR1 domain of Dock1 binds to phosphotidylinositol (3,4,5)-triphosphate (PIP(3,4,5)P3) downstream of phosphatidylinositol 3-kinase (PI3K) which is required for cell migration independently of Rac1 activation [157]. Structural analysis of the DHR1 domain of Dock1 has revealed positively charged lysine residues within the DHR1 that are required for specific PI(3,4,5)P3 binding [264]. In contrast, the conserved sub-domain within the DHR1 domain of dual specificity Dock-C GEFs was found to bear fewer positively charged residues, and bound with both PI(4,5)P2 and PI(3,4,5)P3 [265]. These findings emphasize the importance of the spatiotemporal regulation of Rho GEFs and the contribution of membrane composition and substrate specificity. Additionally, the

Table 1.2 – Dock family and atypical Rho guanine nucleotide exchange factors

Dock family of GEFs					
Symbol	**Name**	**Synonyms**	**Chrom.**	**Rho Target(s)**	**Ref**
DOCK1	Dedicator of cytokinesis 1	Dock180	10q26	Rac1	[266]
DOCK2	Dedicator of cytokinesis 2	KIAA0209	5q35.1	Rac1, Rac2	[267,268]
DOCK3	Dedicator of cytokinesis 3	KIAA0299, MOCA, PBP	3p21.2	Rac1	[269]
DOCK4	Dedicator of cytokinesis 4	KIAA0716	7q31.1	Rac1	[270]
DOCK5	Dedicator of cytokinesis 5		8p21.2	Rac1	[271]
DOCK6	Dedicator of cytokinesis 6	AOS2, KIAA1395, ZIR1	19p13.2	Rac1, Cdc42	[272]
DOCK7	Dedicator of cytokinesis 7	ZIR2, KIAA1771	1p31.3	Rac1, Rac3, Cdc42	[273,274]
DOCK8	Dedicator of cytokinesis 8	MRD2, HEL-205, Zir8	9p24.3	Cdc42	[275]
DOCK9	Dedicator of cytokinesis 9	Zizimin1, ZIZ1, KIAA1058	13q32.3	Cdc42	[276]
DOCK10	Dedicator of cytokinesis 10	Zizimin3, ZIZ3, KIAA0694, DRIP2	2q36.2	Cdc42	[277]
DOCK11	Dedicator of cytokinesis 11	Zizimin2, ZIZ2	Xq24s	Cdc42	[278]
Unclassified atypical Rho GEFs					
Symbol	**Name**	**Synonyms**	**Chrom.**	**Rho Target(s)**	**Ref**
SWAP-70	switch-associated protein 70	KIAA0640	11p15	Rac1	[279]
DEF6	differentially expressed in FDCP 6 homolog	IBP, SLAT, SWAP70L	6p21.33	RhoA, Rac1, Cdc42	[280,281]
SMGGDS	SMG P21 stimulatory GDP/GTP exchange protein	RAP1GDS1	4q23	RhoA, RhoC	[282]
PLD2	Phospholipase D2	PLD1C	17p13	Rac2, RhoA	[283,284]

DHR1 domain is required for the direct binding of WAVE proteins by Dock1-4, further emphasizing the importance of DHR1 in modulating the actin cytoskeleton via Rac1 regulation [285].

The DHR2 domain is the minimal unit required to confer the GEF activity of Dock proteins. Despite being selective for Rac1 and/or Cdc42, there is a high level of divergence among the roughly 450 amino acid DHR2 sequences of Dock proteins [286]. The structures of Dock2 DHR2-Rac1 and Dock9 DHR2-Cdc42 have revealed both the mechanism of exchange activity and also the selectivity of Dock proteins for their respective substrates. Upon binding the DHR2, the switch I of either Rac1 or Cdc42 undergo conformational changes, thereby easing the association of phenylalanine-28 with the bound nucleotide [287]. Furthermore, the projection of an aliphatic side chain of valine residue of either DHR2 domain into the Mg^{2+}-binding site displaces Mg^{2+} from the bound nucleotide resulting in loss of nucleotide binding [287]. Ultimately, the substrate specificity for the respective DHR2 is mediated by the P-loop of Cdc42 and Rac1 and the differential changes in switch I conformation of either GTPase [287]. Notably, the DHR2 domain of Dock1 binds Rac1, but it requires the cooperative binding of ELMO in cells to induce its full GEF activity [288].

In addition to functioning as an exchange factor, the DHR2 of Dock proteins can mediate protein dimerization. Both Dock2 and Dock9 have been reported to form homodimers , and in the case of Dock2 homodimerazation is necessary for Rac1 activation [289,290]. Structurally the interface of homodimerization of the DHR2 of Dock2 and Dock9 were found to be similar, and it was suggested that other Dock proteins may form homodimers [287]. Furthermore, the finding that Dock1 and Dock5 can form

heterodimers [291] implies that dimerization may be an intrinsic characteristic of Dock family GEFs, pending further investigation.

1.2.1.4 Atypical Rho GEFs

Thus far, a few exchange factors for Rho proteins lacking the classical DH-PH or DHR domains have been identified (Table 1.2). While SWAP-70 and DEF6 both lack a DH domain, they each contain a "coiled coil" domain with 17% homology to the DH domain of Dbl GEFs which coordinates nucleotide exchange of target Rho proteins in conjunction with a PH domain [279,280]. The atypical GEF SmgGDS relies on a conserved electronegative patch and binding pocket located on its surface to bind and activate its substrates RhoA and RhoC [282]. Lastly, the atypical GEF PLD2 carries out its exchange activity via a Phox (PX) domain sequence upstream of its PH domain [283]. Although the PX domain is sufficient to bind both Rac and Rho substrates, residues of the adjacent CRIB motifs support nucleotide exchange by PLD2 [292].

1.2.2 Rho GTPase activating proteins

As indicated by their name, Rho GTPase themselves are enzymes that bind to GTP and catalyze its hydrolysis independently of modifying enzymes. Despite this fact, Rho proteins are highly inefficient at hydrolyzing GTP and GAP proteins accelerate this step by several orders of magnitude [293]. There are more than 70 RhoGAP proteins encoded within the human genome, which are characterized by a trademark RhoGAP domain (Table 1.3) [8]. Generally, RhoGAPs bind to their cognate GTP-bound Rho proteins and stabilize the switch I and switch II conformation. Hydrolysis of GTP occurs

Table 1.3 – Rho GTPase activating proteins expressed in human

RhoGAP Proteins					
Symbol	**Name**	**Synonyms**	**Chrom.**	**Rho Target(s)**	**Ref**
ARHGAP1	Rho GTPase activating protein 1	RhoGAP, p50RhoGAP, CDC42GAP, Cdc42GAP	11p11.2	Cdc42	294,295
CHN1	chimerin 1	RhoGAP2, ARHGAP2, n-chimerin	2q31-q32.1	Rac1, Cdc42	296
CHN2	chimerin 2	ARHGAP3, RhoGAP3	7p15.3	Rac1, Cdc42	297
ARHGAP4	Rho GTPase activating protein 4	KIAA0131, C1, p115, RhoGAP4, SrGAP4	Xq28	RhoA	298
ARHGAP5	Rho GTPase activating protein 5	RhoGAP5, p190-B, p190BRhoGAP	14q12	Rac1, Cdc42, RhoA	299,300
ARHGAP6	Rho GTPase activating protein 6	rhoGAPX-1	Xp22.3	RhoA	301,302
ARHGAP8	Rho GTPase activating protein 8	FLJ20185, BPGAP1	22q13.3	Cdc42	303
ARHGAP9	Rho GTPase activating protein 9	MGC1295, 10C	12q13.3	Rac1, Cdc42	304
ARHGAP10	Rho GTPase activating protein 10	FLJ20896, FLJ41791, GRAF2; PSGAP	4q31.23	Cdc42, RhoA	305
ARHGAP11A	Rho GTPase activating protein 11A	KIAA0013	15q13.3	RhoA	306
ARHGAP11B	Rho GTPase activating protein 11B	B'-T	15q13.2	Unknown (not RhoA)	307
ARHGAP12	Rho GTPase activating protein 12	FLJ20737, FLJ10971, FLJ21785	10p11.22	Rac1	308
SRGAP1	SLIT-ROBO Rho GTPase activating protein 1	KIAA1304, ARHGAP13	12q13.13	Cdc42	309
SRGAP3	SLIT-ROBO Rho GTPase activating protein 3	KIAA0411, MEGAP, WRP, ARHGAP14	3p25.3	Rac1, Cdc42	310
ARHGAP15	Rho GTPase activating	BM046	2q22.2-	Rac1	311

	protein 15		q22.3		
ARHGAP17	Rho GTPase activating protein 17	RICH1, FLJ10308, NADRIN, FLJ13219	16p12.2-p12.1	Rac1, Cdc42, RhoA	[312,313]
ARHGAP18	Rho GTPase activating protein 18	MacGAP, bA307O14.2	6q23.1	RhoA	[314]
ARHGAP19	Rho GTPase activating protein 19	FLJ00194, MGC14258	10q24.2	RhoA	[315]
ARHGAP20	Rho GTPase activating protein 20	KIAA1391; RARHOGAP	11q23.2	unknown	
ARHGAP21	Rho GTPase activating protein 21	KIAA1424, ARHGAP10	10p12.31	RhoA, RhoC	[316]
ARHGAP22	Rho GTPase activating protein 22	RhoGAP2	10q11.23	Rac1	[317]
ARHGAP23	Rho GTPase activating protein 23	KIAA1501	17q12	Unknown	
ARHGAP24	Rho GTPase activating protein 24	DKFZP564B1162, FLJ33877, FilGAP	4q22.1	Rac1, Cdc42	[318]
ARHGAP25	Rho GTPase activating protein 25	KIAA0053	2p13.3	Rac1	[319]
ARHGAP26	Rho GTPase activating protein 26	GRAF, KIAA0621, OPHN1L, OPHN1L1	5q31	RhoA, Cdc42	[320]
ARHGAP27	Rho GTPase activating protein 27	CAMGAP1, FLJ43547, SH3P20	17q21.31	Rac1, Cdc42	[321]
ARHGAP28	Rho GTPase activating protein 28	KIAA1314, FLJ10312	18p11.23	RhoA	[322]
ARHGAP29	Rho GTPase activating protein 29	PARG1	1p22.1	RhoA, Rac1, Cdc42	[323]
ARHGAP30	Rho GTPase activating protein 30	FLJ00267	1q23.3	RhoA, Rac1	[324]
ARHGAP31	Rho GTPase activating protein 31	CDGAP	3q13.33	Rac1, Cdc42	[325]
ARHGAP32	Rho GTPase activating protein 32	GRIT, KIAA0712, RICS, GC-GAP	11q24.3	Cdc42, RhoA, Rac1	[326]
ARHGAP33	Rho GTPase activating protein 33	FLJ39019, TCGAP, SNX26, NOMA-GAP	19q13.13	Cdc42, TC10, Rac1	[327]

SRGAP2	SLIT-ROBO Rho GTPase activating protein 2	KIAA0456, ARHGAP34, FNBP2	1q32.1	Rac1	[328]
ARHGAP35	Rho GTPase activating protein 35	GRF-1, p190ARhoGAP, P190A, p190RhoGAP	19q13.32	Rac1, Cdc42, RhoA	[329]
ARHGAP36	Rho GTPase activating protein 36	FLJ30058	Xq26.1	Unknown (lacks R-finger)	[330]
ARHGAP39	Rho GTPase activating protein 39	KIAA1688, Vilse, CrGAP	8q24.3	Rac1, Cdc42	[331]
ARHGAP40	Rho GTPase activating protein 40	dJ1100H13.4; ; C20orf95	20q11.23	Unknown	
OPHN1	oligophrenin 1	OPN1, ARHGAP41	Xq12	RhoA, Rac1, Cdc42	[332]
ARHGAP42	Rho GTPase activating protein 42	FLJ32810, GRAF3	11q22.1	RhoA	[333]
SH3BP1	SH3-domain binding protein 1	ARHGAP43; 3BP-1	22q13.1	Rac1	[334]
ARHGAP44	Rho GTPase activating protein 44	KIAA0672, RICH-2, RICH2	17p12	Rac1, Cdc42	[313]
HMHA1	histocompatibility (minor) HA-1	KIAA0223, HA-1, ARHGAP45	19p13.3	Rac1, RhoA	[335]
GMIP	GEM interacting protein	ARHGAP46	19p13.11	RhoA	[336]
TAGAP	T-cell activation RhoGTPase activating protein	FLJ32631, IDDM21, ARHGAP47	6q25.3	Unknown	
FAM13A	family with sequence similarity 13, member A	KIAA0914, ARHGAP48	4q22.1	Unknown	
FAM13B	family with sequence similarity 13, member B	N61, KHCHP, ARHGAP49	5q31	Unknown	
STARD8	StAR-related lipid transfer (START) domain containing 8	ARHGAP38, DLC3, STARTGAP3	Xq13.1	RhoA, Cdc42	[337]
DLC1	DLC1 Rho GTPase activating protein	HP, ARHGAP7, STARD12, DLC-1, p122-RhoGAP	8p22	RhoA, RhoB, RhoC, Cdc42	[338]

STARD13	StAR-related lipid transfer (START) domain containing 13	GT650, DLC2, ARHGAP37	13q13.1	RhoA, Cdc42	[339]
DEPDC1	DEP domain containing 1	DEP.8; SDP35	1p31.2	Unknown	
RACGAP1	MgcRacGAP	CYK4; HsCYK-4; KIAA1478	12q13.12	Rac1, Cdc42	[340]
ARAP1	ArfGAP with RhoGAP domain, Ankyrin repeat and PH domain 1	CENTD1; KIAA0782	11q13.4	RhoA, Cdc42	[341]
ARAP2	ArfGAP with RhoGAP domain, Ankyrin repeat and PH domain 2	CENTD2; KIAA0580	4p14	RhoA (no hydrolysis; lacks R finger)	[342]
ARAP3	ArfGAP with RhoGAP domain, Ankyrin repeat and PH domain 3	CENTD3, DRAG1	5q31.3	RhoA	[343]
BCR	Breakpoint Cluster Region	BCR1;	22q11.23	RhoA, Rac1 and Cdc42	[163,344]
MYO9B	Myosin IXb	MYR5; CELIAC4	19p13.1	RhoA	[345]
RALBP1	RalA binding protein 1	RIP1; RLIP1	18p11.22	Rac1, Cdc42	[346]
IQGAP1	RasGAP-like with IQ motifs 1	P195; SAR1; KIAA0051	15q26.1	Cdc42, Rac1 (no hydrolysis)	[347,348]
IQGAP2	RasGAP-like with IQ motifs 2		5q13.3	Rac1, Cdc42 (no hydrolysis)	[349]
IQGAP3	RasGAP-like with IQ motifs 3		1q21.3	Rac1, Cdc42 (no hydrolysis)	[350]
PIK3R1	Phosphoinositide-3-Kinase, regulatory subunit 1 (alpha)	GRB1; p85-alpha	5q13.1	Unknown	
PIK3R2	Phosphoinositide-3-Kinase, regulatory subunit 2 (beta)	P85; p85-beta	19p13.11	Unknown	
INPP5B	Inositol polyphosphate-5-phosphatase, 75-KD	5PTase; 75-KD	1p34	Unknown	
OCRL	Oculocerebrorenal syndrome of Lowe	OCRL1	Xq25	Rac1	[351]

as a result of an in-line nucleophilic attack of the γ-phosphate of GTP by a water molecule, which is oriented by glutamine-61 in the switch II region by the GAP protein [352]. Subsequently, an arginine residue of the RhoGAP (termed “arginine finger”) becomes inserted into the phosphate-binding site to stabilize the transition state of the GTPase by neutralizing the negative charge of the γ-phosphate [352]. There are a few exceptional RhoGAP domain-containing proteins, including ARHGAP36 and ARAP2, which lack an arginine finger required for stabilizing the GTPase/GAP interface to induce GTP-hydrolysis (Table 1.3). As a result these proteins likely function in a GAP-independent manner.

Since nearly all RhoGAP proteins contain additional signaling motifs and domains, it is widely accepted that they also serve as signaling modules or hubs that integrate various inputs via intermolecular associations [353]. These additional domains may also act to properly position RhoGAPs within the cell, thereby regulating the particular biological outputs of each protein complex.

1.2.2.1 ARHGAP31/ Cdc42 GTPase-activating protein

ARHGAP31 or Cdc42 GTPase-activating protein (CdGAP) is a RhoGAP protein with activity directed towards Rac1 and Cdc42 [354]. CdGAP was originally identified in a yeast two-hybrid screen, using the Q61L/Y40C mutant Cdc42 as bait [354]. CdGAP is composed of a PBR and a GAP domain at the N-terminal region, a basic-rich (BR) stretch in the central region, a proline rich domain (PRD) and a C-terminal region [355]. In the mouse, CdGAP is expressed ubiquitously with an enrichment in the lungs, brain and liver tissues [355]. CdGAP over-expression in diverse cell lines has been shown to reduce cell spreading and lamellipodia formation, due to the disruption of cortical actin and loss

of focal adhesions [356,357]. In U2OS osteoblasts CdGAP is reported to be localized at focal adhesions, and overexpression of CdGAP results in impaired cell polarity and random migration [358]. Localization of CdGAP to focal adhesions occurs via actopaxin, through its interaction with the GAP and BR regions of CdGAP [358].

Earlier studies have noted that CdGAP expression is readily upregulated downstream of growth factor treatment [359], suggesting that CdGAP may function during cell proliferation or migration. While enhanced expression of a Cdc42 and Rac1 GAP should result in impaired cell migration and invasion, studies have revealed the inverse is true. In fact, CdGAP is required for TGFβ and Neu/ErbB2-mediated breast cancer cell migration and invasion, and does so in a GAP-independent manner [360]. Downregulation of CdGAP induces the expression of E-cadherin in Neu/ErbB2-expressing breast cancer cells, but the precise mechanism of this GAP-independent function for CdGAP has not yet been reported.

CdGAP is highly phosphorylated on serine and threonine residues[355]. While phosphorylation of the PRD of CdGAP at threonine-776 by ERK1/2 and GSK-3 results in reduced GAP activity [355,361], whether it regulates CdGAP subcellular localization has not been investigated. CdGAP has been reported to associate with the neural-enriched Cdc42 GEF and endocytic scaffolding protein, Intersectin [356]. Association occurs via an atypical xKx(K/R) motif (x-any amino acid, K- lysine, R- arginine) within the BR domain of CdGAP and the SH3D domain of Intersectin, thereby inhibiting CdGAP Rac1 GAP activity [356,362]. CdGAP localization is part regulated by binding to lipids in the plasma membrane. CdGAP was found to be preferentially associated with phosphatidylinositol

3,4,5-trisphosphate via a stretch of N-terminal polybasic residues, resulting in its membrane recruitment downstream of PDGF [363].

Human CdGAP, ARHGAP31, has recently been identified as an inherited factor associated with a rare developmental disorder, Adams-Oliver Syndrome (AOS) characterized by the combination of *aplasia cutis congenita* and terminal transverse limb defects [364,365]. AOS-causing CdGAP mutants have C-terminal truncations, exhibit enhanced *in vitro* GAP activity which result in enhanced cell rounding [366]. Some patients with AOS also present with vascular anomalies including cutis marmorata, cardiac and vascular defects [367]. Since ARHGAP31 was also reported to be among the 17 RhoGAPs most highly expressed in human umbilical vein endothelial cells (HUVECs) [368], it may be possible that ARHGAP31/CdGAP contributes to vascular homeostasis or angiogenesis. This possibility will be discussed in chapter 4.

1.2.3 Rho guanine dissociation inhibitors

The final class of proteins that are well documented as regulators of Rho GTPases are the RhoGDIs. Generally, RhoGDIs act by sequestering the hydrophobic tail of lipid-modified Rho GTPases, thereby retaining them in the cytosol out of the reach of effector proteins [48]. Whereas RhoGEFs and GAPs are composed of numerous members, only three genes encode Rho GDIs in humans (RhoGDI1-3) [369]. RhoGDI1 is ubiquitously expressed and has broad association with many geranylgeranylated Rho GTPases including: RhoA, RhoC, Rac1, Rac2 and Cdc42 [370,371]. Of note, RhoGDI1 does not associate with Rho GTPases that undergo farnesylation, palmitoylation or lack prenylation [369]. RhoGDI2 is enriched in haematopoetic cells, and has been shown to regulate various Rho GTPases *in vitro* [48,372]. RhoGDI3 is the most divergent RhoGDI,

mainly targeted to the Golgi [373] and associated most notably with RhoG and RhoB [374]. Traditionally, RhoGDI proteins are classified as negative regulators of Rho GTPase signaling, however, this view is over simplified. Rho GDI activity is credited with chaperoning newly synthesized Rho GTPases from the ER to the plasma membrane, guarding Rho GTPases from proteasome-mediated degradation, and creating a pool of inactive proteins primed for activation by extracellular stimuli (reviewed in [48]).

1.3 Neuronal development and Rho GTPases

The mammalian nervous system is composed of billions of neurons and supports normal physiological function and survival. The wiring of the central nervous system during mammalian development occurs in a tightly regulated and precise manner. Following their specification, neurons migrate *in vivo*, undergo a polarization program and project axons toward their often distant targets. Although the mechanisms of neuronal development are only beginning to be revealed, many Rho family proteins have been found to regulate some aspects of neuronal development, including: axon specification, axon outgrowth and guidance, synaptogenesis and synaptic plasticity [375]. The following section will focus on the general mechanisms of axon polarization and outgrowth, and the contribution of Rho GTPases to these processes.

1.3.1 Neuronal polarization

Following differentiation, neurons become highly polarized with domains that either receive inputs (dendrites) or transmit electrochemical impulses (axon). Before neurons can form mature connections, they must first transform identical primary processes into functionally distinct, polarized units. Neuronal polarization is dependent

on an internal program that is regulated by factors including: kinases, lipids, small GTPases, and Par polarity proteins [376-378]. Since cultured neurons are able to polarize without the addition of extracellular cues, it was originally assumed that an intrinsic program is sufficient to induce axon formation [379]. In recent years however, extracellular molecules such as Wnts [380], netrin-1 [381], Semaphorin 3A (Sema3A) [382,383], laminin and neuron-glia cell adhesion molecule (NgCAM) [384] have been shown to influence which neurite becomes an axon, thus suggesting a more complex mechanism of axon specification *in vivo*.

During the intrinsic program of neuronal polarization, the Par polarity complex has been shown to play a crucial role [145,385]. Par3 and Par6 localize to the tips of axons with Cdc42 in primary hippocampal neurons in a PI3K-dependent process [150,378]. Notably, the expression of constitutively active Cdc42 or the Rac1 GEF Tiam1 induces multiple immature axon-like neurites [150], suggesting that the physiological cycling of Cdc42 and Rac1 at the neurite tips is required for both neuronal polarization and maturation [150,386]. The activation of PI 3-kinase (PI3K) activity and production of its lipid product $PI(3,4,5)P_3$ is a key feature during the initiation of axon specification. A signaling cascade by which PI3K acts on Akt/GSK3β has been shown to influence cell polarity in various cell types, including neurons [387,388]. In brief, PI3K stimulates the Akt-mediated inactivation of GSK3β at the plasma membrane, stimulating the formation of multiple axons by Collapsin response mediator protein (CRMP)-2 [387,388]. CRMP-2 accumulates at the distal portion of a growing axon [389] and promotes microtubule assembly and actin filament stability in a non-phosphorylated state [388]. Furthermore, the ability of GSK3β to phosphorylate and inhibit the microtubule-associated proteins

(MAPs) MAP1B and APC suggests a function of GSK3β in regulating neuronal polarity by modulating cytoskeletal dynamics [390].

Another kinase that has been shown to regulate neuronal polarity *in vivo* is the serine/threonine specific liver kinase B1 (LKB1) [391]. The *C. elegans* homolog of LKB1, Par4 is a member of the Par polarity family and regulates embryonic polarity [392]. Expression of LKB1 is required for axon initiation *in vivo*, while the ectopic stimulation of LKB1 by its co-activator Stradα induces the formation of multiple axons in cortical neurons [391]. LKB1 activation by PKA, leads to its accumulation in the neurite which is to be the prospective axon [393]. Downstream of LKB1, Synapses of the amphid defective (SAD) kinases are activated and phosphorylate Tau and potentially other MAPs, resulting in modulation of microtubule dynamics within the neurite [391]. Axon specification induced by brain derived neurotrophic factor (BDNF) also requires the PKA-dependent phosphorylation of LKB1[393], and thus is a crucial step during early axon specification.

In addition to BDNF, it has been shown that other extracellular cues may lead to axon specification during neuronal development. UNC-6/netrin, a well defined axon guidance cue, is involved in the initial break in neuronal symmetry which precedes axonal extension [381]. Netrin causes MIG10/lamellipodin to become restricted to the leading edge of the neurite in a mechanism dependent on PI3K/PI3K phosphatase (PTEN) lipid signaling [394]. In addition to netrin, both Wnts and Sema3A signaling have been implicated in neuronal polarization in *C. elegans* and mice, suggesting that additional extracellular cues that induce neuronal polarization *in vivo* exist (reviewed in [395]).

1.3.2 Axon outgrowth and guidance

During development, the extension and pathfinding of neurons of the CNS is governed in part by environmental guidance cues, namely: netrins, semaphorins, slits and ephrins [396-398]. Guidance cues act as either short range (membrane-bound) or long range (diffusible) signals, the both of which are transduced intracellularly by means of conserved receptors expressed at the distal axon growth cone [399]. The growth cone emanating from the axon tip is a highly dynamic area, where drastic rearrangements of actin filaments, microtubules and adhesions complex turnover occur during neurite elongation [400,401]. The growth cone can be subdivided into two functional regions: the peripheral domain which is rich in actin structures, namely filopodia and lamellipodia, and the microtubule and organelle-rich central domain [402]. In addition to actin cytoskeleton remodelling, axonal transport of cargo by molecular motors, and local protein translation within the growth cone occur during neurite extension, branching and guidance [403,404]. In the presence of attractive guidance cues, the asymmetrical enrichment of actin and the formation of filopodia and lamellipodia in the direction of attraction occur in a manner which is dependent on Rho GTPase activity [401]. Simultaneously, microtubule polymerization into the growth cone periphery, delivery of plasma membrane at the leading edge, and collapse of the lagging growth cone around the axon propels the growth cone forward [401,405].

Rho GTPases are important signaling elements during neurite outgrowth and axon guidance, with Cdc42 and Rac1 [406] acting to induce neurite extension, while net RhoA activation stimulates neurite retraction or failure to extend neurites [375,407]. The latter finding is of particular importance, since RhoA activation is elevated during nerve

injury and in various neurodegenerative diseases [51]. Although they are studied less extensively, other Rho GTPases have been found to support neurite outgrowth and axon guidance, including: Rnd3 [408], RhoG [119], TC10 and TCL [131].

Many regulators of Rho GTPases have been implicated in neurite outgrowth mechanisms. In particular, many Rac1 and/or Cdc42 GEFs are expressed in the brain and contribute to neurite outgrowth pathways including: Tiam1 [409], Tiam2 [410], Trio [242], βPIX [411], GEFT [412], Vav2/3 [413], RasGRF1[414], Alsin [415], Intersectin1 [416], Dock1 [124], Dock3 [285], Dock4 [417], Dock6 [272], and Dock7 [273]. Although IQGAP3 is a Rac1/Cdc42-binding GAP protein, its lack of arginine finger renders it GAP-dead and it acts instead as an effector protein, promoting neurite outgrowth of PC12 cells [350]. Also, though α2-chimaerin is a Rac/Cdc42 GAP that has been implicated in Eph4A-dependent growth cone collapse [418], its expression in neuroblastoma cells promotes neurite outgrowth [419] and promotes neuronal migration *in vivo* [420]. These results suggest that α2-chimaerin has both GAP dependent and independent functions in neurons. In addition to inducing neurite outgrowth via Rac1 activation, Trio has also been shown to induce NGF-mediated neuritogenesis in PC12 cells via RhoG activation [118]. Similarly, Kalirin-expressing primary sympathetic neurons extended axons in a RhoG-dependent manner [195]. Since activation of RhoA or its effectors counters neurite outgrowth[421], it is not surprising that several RhoA GAPs have been shown to promote neurite extension, including: Nadrin [422], p190RhoGAP [423], GRIT [424] and p200RhoGAP [425] .

Downstream of Rac1 and Cdc42, induced neurite outgrowth is mediated in part by the Pak-induced signaling pathways. The membrane targeting of Pak1 is sufficient to stimulate neurite outgrowth in PC12 cells, indicating that Pak1 acts downstream of Rac

and Cdc42 in polarized neurites [426]. Neural-expressed Pak5, which also contains a CRIB binding motif, induces the formation of filopodia and neurites in neuroblastoma cells, via activation of the JNK pathway and antagonizing Rho signaling [427]. Downstream of Cdc42 the WASP family member, N-WASP is required for induced neurite outgrowth [428]. Additionally, the brain-enriched myotonic dystrophy kinase-related Cdc42-binding kinases (MRCKs) were identified as effectors of Cdc42 and also play a key role in neurite outgrowth. Although the kinase domain of MRCKs resembles ROCK and phosphorylates non-muscle MLC to promote myosin contractility in non-neuronal cells, MRCK is required for neurite outgrowth induced by NGF via the activity of Cdc42 [429].

Despite their function in regulating the actin cytoskeleton being well defined, a recent study has shed light on an alternative role for Rho GTPases during neurite outgrowth. Fujita and colleagues revealed that the Cdc42-related TC10 promotes neurite outgrowth via regulating exocytic fusion at growth cone tips [430]. TC10 was localized to Rab11-labelled vesicles, and its activation induced the translocation of the exocyst component Exo70 to the plasma membrane at the extending growth cone tip [430]. Although the association of TC10 with Exo70 impaired local WASP activity, Exo70 may regulate actin dynamics by its own association with Arp2/3 [431]. Considering other Rho proteins are brain-localized and have alternate functions in cultured cells, it is probable that future study will link these components to neuronal function in some manner.

1.3.2.1 Netrin-1 induced axon growth and guidance

Netrins constitute a family of axon guidance cues that are required for proper neural specification [432]. The first netrins, named from the Sanskrit "Netr" for 'guide', (netrin-1 and netrin-2) were identified from the embryonic chick brain and found to be homologous with UNC-6 in *C. elegans* [433,434]. Netrins are laminin-related extracellular matrix-binding proteins [434], of which three are secreted: netrin-1, -3, -4, and two are membrane-anchored: netrin -G1 and -G2 [435]. The secreted netrin proteins can act as bi-functional chemotropic cues[436], promoting either the attraction or repulsion of various cell types [436]. To date, netrin-1 signals through at least four distinct families of transmembrane receptors: Down's syndrome cell adhesion molecule (DSCAM), the UNC-5 family (UNC5A-D), amyloid precursor protein (APP) and the DCC family (DCC and neogenin) [437-442]. In vertebrates, netrin-1 was first demonstrated to promote the outgrowth of commissural axons of embryonic spinal cord explants [443], a function that is mediated by DCC [438]. In mammals, netrin-1 is secreted by the ventral floor plate of the developing spinal cord [443], and facilitates midline attraction of DCC and neogenin-expressing commissural projection neurons [444-446]. Netrin-1 is also required for forebrain commissure formation in mammals [444,447]. The remainder of this section will focus on netrin-1-mediated signaling pathways in axon outgrowth and guidance.

In neurons, netrin-1 can promote either growth cone attraction or repulsion [436]. This bifunctional response is generally thought to be dependent on the composition of receptor complexes induced by netrin-1: DCC homodimers mediate attraction [448], while UNC-5/DCC heterodimers or UNC-5 homodimers induce repulsion [449]. DCC is a transmembrane receptor, with an extracellular domain comprised of four Ig-like domains

and six fibronectin type III repeats (FN) [450]. Recent structural studies have revealed that netrin-1 binding to DCC is accommodated by FN-5 and -6 [451]. The intracellular portion of DCC contains three well conserved regions, termed P1-3, which are important for initiating molecular signaling events downstream of netrin-1 [452]. DCC acts as a dependence receptor, and was identified originally as a putative tumor suppressor based on its deletion in colorectal cancer cells [453,454]. UNC-5 receptors are also transmembrane proteins, containing an extracellular domain with two Ig motifs and two thrombospondin type-I domains [439]. Binding of netrin-1 to UNC-5 is mediated by the Ig-like repeats [455], but the molecular mechanisms occurring downstream of UNC-5 are much less characterized relative to DCC. In humans, mutations of the *DCC* gene have been associated with congenital mirror movements [456], and small nucleotide polymorphisms within the genes encoding *DCC* and *netrin-1* have been associated with schizophrenia [457], Parkinson's disease and amyotrophic lateral sclerosis [458,459]. As a result, considerable efforts have been made to understand the signaling mechanisms downstream of DCC.

DCC is a tyrosine kinase-associated receptor, and upon netrin-1 stimulation, DCC becomes highly phosphorylated on serine, threonine and tyrosine residues [460]. In particular, specific phosphorylation of rat DCC at tyrosine-1418 by Src family kinases is required for netrin-1-mediated axon outgrowth and guidance in vertebrates [460-462]. Furthermore, downstream of netrin-1 treatment, phosphorylation and activation of focal adhesion kinase (FAK) [461] and ERK 1/2 [463] occur, and although inhibitors of these kinases block axon extension in response to netrin-1, the precise targets of these kinases have not been fully explored. ERK2 associates with the C-terminus of DCC,

and is reported to phosphorylate DCC at consensus ERK phosphorylation sites *in vitro*, but whether this occurs in cells or has a biological function remains to be demonstrated [464]. Since netrin-1-induced activation of ERK1/2 occurs despite Src-kinase inhibition, which functionally impairs neurite outgrowth, it is probable that the receptor proximal activation of ERK is secondary to its function during neurite outgrowth [257].

As described earlier, Rho family GTPases are key components of neurite outgrowth. Downstream of netrin-1/DCC, Rac1 becomes activated in neurons and drives axonal extension, while RhoA activity is inhibited [244,465-467]. Although activation of RhoA in neurons is most commonly correlated with growth cone collapse and RhoA inactivation increases the attractive turning response of axons to netrin-1 [467], transient RhoA activation indeed occurs downstream of netrin-1/DCC [468] . Specifically RhoA/Rho kinase and Src kinases induce ezrin-radixin-moesin (ERM) protein phosphorylation downstream of netrin-1-treatment, which is necessary for induced cortical axon outgrowth [467,469]. Ezrin becomes activated and associates with the C-terminal tail of DCC via phosphorylated tyrosine-1418, thus linking DCC to the actin cytoskeleton during axon outgrowth [469]. It is probable that novel SH2-domain containing proteins will be identified that preferentially associate with tyrosine-phosphorylated DCC in neurons.

Downstream of netrin-1-treatment a DCC signaling complex of proteins forms to mediate intracellular signaling. The SH2-SH3 domain containing adaptor protein Nck1 associates with the C-terminus of DCC, and is required for Rac1 activation and DCC-induced neurite outgrowth in N1E-115 neuroblastoma cells [470]. Subsequently, Pak1 and the Rac1 GEF Trio were identified as members of the DCC signaling complex required for Rac1 activation by netrin-1 [244]. Studies of Trio-null mice revealed that Trio is required

for the netrin-1-dependent Rac1 activation and projection of commissural neurons in the spinal cord and forebrain [244]. But, since the commissural neurons in the spinal cord of Trio-null mice still projected axons somewhat toward the ventral floor plate, it is certainly likely that other Rac GEFs are involved in this process. Indeed, the Rac1 GEF Dock1 was reported to be involved in netrin-1-induced Rac1 activation [471]. Although downregulation of Dock1 in the developing chick spinal cord impaired commissural projections, the lack of DCC expression in the chick model and unreported CNS defects in Dock1-null mice (to date) complicate the importance of Dock1 *in vivo*.

The long range efficacy of netrin-1-induced axon outgrowth depends on the regulation of DCC levels at the plasma membrane of the extending growth cone. In commissural neurons, netrin-1 treatment mobilizes DCC from intracellular pools to the plasma membrane by exocytosis in a process that is enhanced by cAMP-dependent protein kinase (PKA) activation [472]. Recently, PKA was shown to bind DCC via ERM proteins, which are required for netrin-1-induced PKA activation and downstream activation of Mena/VASP (vasodilator-stimulated phosphoprotein) proteins [473]. This finding highlights a feedback loop by which netrin-1 stimulates receptor proximal modulations of the actin cytoskeleton, and enhances delivery of surface DCC for long-range signaling. In support of this, Trio expression in cortical neurons drives the growth cone enrichment of surface DCC further implicating Rac1 activation in DCC surface dynamics [257].

In addition to DCC dynamics, the general delivery of plasma membrane to the leading edge of extending growth cones is imperative for netrin-1-dependent axon guidance. The phenomenon of membrane delivery downstream of netrin-1 requires

local exocytosis of vesicles [405,474]. Local exocytosis and membrane fusion are mediated by the SNARE complex comprising a v-SNARE such as VAMP-2 (vesicle-associated membrane protein 2) and plasma membrane t-SNAREs, SNAP25 (synaptosomal-associated protein 25) and syntaxin-1 [475]. DCC forms a complex with syntaxin-1 downstream of netrin-1, and in this way induces the local exocytosis of VAMP-2-expressing vesicles during axon outgrowth [405]. Furthermore, the E3 ubiquitin ligase TRIM9 associates directly with both SNAP-25 and DCC, and promotes netrin-1-dependent axon branching in cortical neurons [474]. Taken together, netrin-1-induced axon outgrowth and guidance in neurons requires tight regulation of the actin cytoskeleton, receptor and membrane dynamics, and regulation of Rho GTPase activity has proven to be instrumental in these processes.

1.4 Rho GTPases in nerve injury

Whether in response to an intrinsic program or a traumatic injury, the loss of functional connections within the nervous system can lead to severe detrimental consequences. Loss of active neural connections and induction of axon degeneration are characteristic of many incapacitating neurodegenerative diseases. Though the mechanisms of neurodegeneration are not fully understood, recent findings indicate that Rho GTPases are key components of neuronal cell degeneration pathways, including during: Amyotrophic lateral sclerosis, Alzheimer's disease, Huntington's disease, Parkinson's disease, Glaucoma and Charcot-Marie-Tooth disease (reviewed in [51]; See Neurodegeneration Review in Appendix). Next, the mechanisms of nerve injury and dysregulation of Rho protein signaling pathways will be briefly discussed.

In the injured CNS, regeneration of neural tracts is impeded by formation of astroglial scars and the expression of inhibitory myelin-associated molecules: Nogo, myelin-associated glycoprotein (MAG), and oligodendrocyte-myelin glycoprotein (OMgp). Nogo, MAG and OMpg bind to and signal through the neuronal Nogo family receptors (NgR) or the paired Ig receptor B [476,477]. Additionally, NgR-mediated signaling by myelin-associated molecules occurs via the partnering with either p75 neurotrophin receptor (p75NTR) or the orphan receptor TROY [476-478]. p75NTR has been previously implicated in local neurodegeneration, where under physiological conditions p75NTR-expressing sympathetic neurons undergo a neurotrophin-dependent myelin-mediated degeneration program [479]. In this context, p75NTR binds to and sequesters RhoGDI downstream of BDNF during axon pruning, leading to elevation of active RhoA [480,481]. In addition, the Rac1 and RhoA GEF Kalirin 9 competes with RhoGDI for binding to p75NTR in cerebellar granule neurons downstream of MAG, suggesting an interplay between these GTPase regulators underlies the RhoA-mediated inhibitory functions of myelin-associated molecules downstream of p75NTR [482]. Further evidence showing that Nogo-A-mediated activation of RhoA antagonizes Rac1 activity during neurite growth inhibition indicates cross-talk between GTPase signaling pathways occurs during inhibition of nerve growth due to injury [483].

In accordance with the finding that RhoA is activated during local axon pruning and degeneration, inhibition of the RhoA effector ROCK has been shown to promote neuronal growth on inhibitory substrates in culture and promote nerve regeneration and locomotor recovery *in vivo* [484,485]. In addition to its role in nerve growth, RhoA regulation is also important in peripheral nerve axon integrity. In a recent study, Schulz and

colleagues identified that RhoA/ROCK act downstream of the cytoskeletal protein merlin isoform 2 (merlin-iso2), which was required for the maintenance of peripheral axon integrity [486]. Axonal merlin-iso2, which is closely associated with neurofilaments, acts as a scaffold, tethering both p190RhoGAP and RhoGDI, leading to local RhoA regulation [486]. Intriguingly, a patient-derived mutation of merlin at C784T resulted in impaired sequestering of RhoGDI resulting in reduced RhoA activity and programmed axonal atrophy, clinically manifesting as severe neuropathy [486].

In response to axonal transection, molecular mechanisms within the proximal axon are stimulated by the extracellular environment, the sum of which lead to demyelination, axonal die-back and distal axonal clearance typical of Wallerian type degeneration. During peripheral nerve injury a subtype of activated macrophages synthesize *de novo* NgR1 and NgR2, which promotes the clearance of macrophages and signals termination of inflammation via myelin-dependent RhoA activation and repulsion [487]. Furthermore during demyelination, myelin undergoes fragmentation as Schwann cells dedifferentiate. The injury-induced demyelination leads to Rac1-dependent modulation of actin dynamics within the Schwann cell [488]. Together these few examples demonstrate the implication of Rho GTPase signaling in response to nerve injury.

1.5 Rationale & Objectives

While the modulation of Rac1, Cdc42 and RhoA activities support neuronal development, the regulatory mechanisms of their cognate GEFs and GAPs are much less understood. The Rac1 GEF activity of Trio is required for the attractive axon guidance cue netrin-1 to induced axon pathfinding; and while the Cdc42/Rac1 GAP, CdGAP, is enriched in the mammalian brain, whether it contributes to neuronal development is completely unknown. The objectives of my thesis are to investigate the molecular mechanisms of Trio regulation and to characterize CdGAP function in the developing brain. More specifically:

1) To investigate the regulation of Trio by phosphorylation during netrin-1/DCC-mediated axon outgrowth. The first project will investigate the role of Trio tyrosine phosphorylation during netrin-1/DCC-mediated signalling. Serine phosphorylation of Trio downstream of netrin-1/DCC in the embryonic rat brain will also be investigated.

2) To identify novel Trio interacting proteins that may regulate Trio and/or DCC during netrin-1/DCC-mediated axon outgrowth.

3) To characterize CdGAP expression in the developing brain and determine whether CdGAP is required for normal neuronal development.

Chapter 2: Tyrosine phosphorylation of the RhoGEF Trio regulates netrin-1/DCC-mediated cortical axon outgrowth

Jonathan DeGeer, Jérôme Boudeau, Susanne Schmidt, Fiona Bedford, Nathalie Lamarche-Vane, and Anne Debant. (2013). **Molecular and Cellular Biology**. 33(4) 739-751.

Preface to Chapter 2

It has been documented that Rho GEFs can be regulated by several molecular mechanisms including phosphorylation. Indeed, Trio has been shown to be highly phosphorylated on serine residues, and was originally identified via direct association with a tyrosine phosphatase. Despite the association, no evidence has indicated that Trio may be directly regulated by tyrosine phosphorylation within the cell. We hypothesized that the direct association of Trio with a tyrosine phosphatase may mask Trio tyrosine phosphorylation. In order to determine whether Trio is regulated by tyrosine phosphorylation during netrin-1/DCC-induced cortical axon outgrowth, we applied inhibitors of tyrosine phosphatases and assessed by classical biochemical techniques the phosphorylation status of Trio. In this way we demonstrate that endogenous neuronal Trio isoforms become tyrosine phosphorylated. Using various cell culture lines, we show that Trio is a substrate of the Src-kinase Fyn and map the site at which Fyn phosphorylates Trio *in vitro*. Furthermore we go on to characterize the function of Trio tyrosine phosphorylation during neurite outgrowth downstream of netrin-1 at the sub-cellular level.

Abstract

The chemotropic guidance cue netrin-1 mediates attraction of migrating axons during central nervous system development through the receptor Deleted in Colorectal Cancer (DCC). Downstream of netrin-1, activated Rho GTPases Rac1 and Cdc42 induce cytoskeletal rearrangements within the growth cone. The Rho guanine nucleotide exchange factor (GEF) Trio is essential for Rac1 activation downstream of netrin-1/DCC, but the molecular mechanisms governing Trio activity remain elusive. Here, we demonstrate that Trio is phosphorylated by Src-family kinases in the embryonic rat cortex in response to netrin-1. *In vitro*, Trio was predominantly phosphorylated at Tyr^{2622} by the Src-kinase Fyn. Though the phospho-null mutant $Trio^{Y2622F}$ retained GEF activity towards Rac1, its expression impaired netrin-1-induced Rac1 activation and DCC-mediated neurite outgrowth in N1E-115 neuroblastoma cells. $Trio^{Y2622F}$ impaired netrin-1-induced axonal extension in cultured cortical neurons, and was unable to colocalize with DCC in growth cones, in contrast to wild type Trio. Furthermore, depletion of Trio in cortical neurons reduced the level of cell surface DCC in growth cones, which could be restored by expression of wild type Trio but not $Trio^{Y2622F}$. Together, these findings demonstrate that $Trio^{Y2622}$ phosphorylation is essential for the regulation of the DCC/Trio signalling complex in cortical neurons during netrin-1-mediated axon outgrowth.

Introduction

During central nervous system development, neurons extend axons across great distances toward their associated targets. The process of axon extension and path-finding is mediated by the growth cone, a structure which emanates from the distal axon, composed of F-actin and microtubule networks [396,399]. The growth cone is able to sense and integrate a diverse range of extracellular guidance cues (secreted or membrane-bound), which in turn trigger signalling pathways downstream of conserved receptors [397,398]. The netrin family of guidance cues are vital in neural development of both vertebrates and invertebrates [432]. Netrin-1 has been shown to interact with at least four distinct families of transmembrane receptors: the Deleted in Colorectal Cancer (DCC) family, including DCC and its paralog neogenin, as well as DSCAM, the UNC-5 family, and more recently the amyloid precursor protein [437-442]. Netrin-1 acts as a bi-functional guidance cue, promoting either attraction or repulsion of extending growth cones of various classes of neurons by signalling through its receptors and co-receptors [435]. In the developing spinal cord and cerebral cortex of vertebrates, netrin-1 exerts its attractive functions through the receptor DCC [438,443,447]. The significance of this pathway during neural development is underscored by the absence of spinal and cerebral commissures when expression of netrin-1 or DCC is disrupted [444,445]. Considerable efforts have been made to elucidate the molecular pathways downstream of the netrin-1/DCC interaction. Upon netrin-1 stimulation, DCC becomes highly phosphorylated on serine, threonine and tyrosine residues [460]. Phosphorylation of DCC at Tyr^{1418} by the

Src-kinase Fyn occurs downstream of netrin-1 stimulation and is required for axon outgrowth and guidance [460-462,465].

Rho GTPases are molecular switches that regulate multiple intracellular processes, including actin remodelling, by cycling between an inactive GDP-bound and active GTP-bound state [5,158]. During axon outgrowth and guidance, the recruitment and localized regulation of the Rho GTPases Rac1, Cdc42, and RhoA, is fundamental for translating extracellular cues into cytoskeletal rearrangements within the growth cone [375,397,401,489,490]. Downstream of netrin-1/DCC, both Rac1 and Cdc42 become activated and drive axonal extension, while RhoA activation occurs most prominently during growth cone collapse [465-467]. More recently, we have shown that RhoA/Rho kinase and Src kinases induce ezrin-radixin-moesin (ERM) protein phosphorylation, which is required to mediate netrin-1/DCC-induced cortical axon outgrowth [469]. Rho GTPases are activated by guanine nucleotide exchange factors (GEFs), a family of proteins that stimulate GDP/GTP exchange [7]. Recent studies have identified two mammalian GEFs mediating Rac1 activation downstream of netrin-1/DCC: DOCK180 and Trio [244,471]. Trio is the founding member of a family of GEFs, which contain two Dbl-homology/pleckstrin-homology (DH-PH) GEF domains (GEFDs). Trio has activity towards both RhoG and Rac1 by its first GEFD (GEFD1), while the second GEFD (GEFD2) activates RhoA *in vitro* [193,246,247,491]. Although its expression is ubiquitous, Trio is enriched in the brain where it is present in 5 isoforms generated by alternative-splicing [242]. The genetic ablation of Trio in the mouse is lethal between embryonic day 15.5 (E15.5) and birth [243], with embryos presenting disorganization of neuronal projections in the developing spinal cord and brain [244]. Although we have shown that Trio interacts in a signalling complex

with DCC, the SH2/SH3 adaptor protein Nck-1 and p21-activated kinase (Pak1) *in vitro* [244], the mechanisms governing Trio localization and activity within the growth cone remain unknown. GEFs can be regulated by several molecular mechanisms, including phosphorylation, inter- and intra-molecular interactions and lipid binding [7]. Here we demonstrate that Trio is a substrate of Src-kinases downstream of netrin-1/DCC in the embryonic rat cortex. Concomitantly, netrin-1 stimulation enhanced Trio interaction with DCC in the developing cortex. We show that Trio is phosphorylated by the Src-kinase Fyn at Tyr^{2622}, and phosphorylation of this site is potentiated by co-expression of DCC in cultured cells. Although point mutation at Tyr^{2622} did not affect the *in vitro* GEF activity of Trio, it impaired netrin-1-induced Rac1 activation. Expression of phospho-null $Trio^{Y2622F}$ mutant resulted in impaired DCC-mediated neurite outgrowth in N1E-115 neuroblastoma cells, and inhibited axonal responsiveness to netrin-1 in cultured cortical neurons. Furthermore, $Trio^{Y2622F}$ blocked netrin-1-mediated Trio/DCC interaction in the growth cone of cortical neurons and depletion of Trio in cortical neurons reduced the level of cell surface DCC in growth cones, which could be restored by expression of wild type Trio but not $Trio^{Y2622F}$. In addition, Trio participates in the dynamics of DCC surface localization in response to netrin-1. Together, these data suggest a novel regulatory mechanism wherein Trio, in addition to regulating Rac1, also modulates the function of DCC *via* its Tyr^{2622} phosphorylation site during netrin-1-induced axon extension.

Materials and methods

DNA constructs and antibodies. pGEX-5X constructs encoding Trio protein fragments #1 to #8 were cloned using standard cloning procedures (cloning details can be obtained upon request). Fragment #1 corresponds to Trio amino acids 1-232, fragment #2: 1-702, fragment #2a: 1-485, fragment #2b: 464-699, fragment #3: 700-1157, fragment #4: 1157-1203, fragment #5: 1204-1701, fragment #6: 1848-2298, fragment #7: 2299-2627, and fragment #8 : 2627-3038. Green fluorescent protein (GFP)-Trio single and double point mutants were derived from the wild type form of GFP-Trio [118] using the QuickChange Site-Directed Mutagenesis Kit (Stratagene), according to the manufacturer's instructions. pRK5-Fyn and pRK5-DCC constructs have been described previously [118,460,492]. All constructs were verified by sequencing. The polyclonal anti-TrioMTP antibody was raised against a fragment encompassing residues 1581-1849 of the Trio-C isoform expressed as a GST fusion protein in *E. coli* [242]. The antibody was affinity-purified on Affi-Gel sepharose (BioRad) coupled to the same protein antigen. The resulting antibody preparation was then passed through an Affi-Gel sepharose column coupled to the GST protein in order to retain the anti-GST antibodies contained in the preparation. The TrioMTP antibody immunoprecipitates and recognizes by western blotting all Trio isoforms. Additional antibodies: anti-DCC_{INT} (clone G97-449, BD Biosciences), anti-DCC_{EXT} (clone AF5, Calbiochem), anti-phosphotyrosine (clone 4G10) and anti-tubulin (Upstate), anti-GFP (Invitrogen), anti-Pak (C-12) and anti-Fyn (Santa Cruz), anti-pFAK (pY861) and anti-FAK (Invitrogen), anti-Rac1 (BD Transduction Laboratories), anti-pERK1/2 (pThr202/pThr204) and anti-ERK1/2 (Cell Signaling), anti-rabbit-Alexa-488 and anti-mouse-Cy3 (Molecular Probes).

Cell culture and transfection. HEK293, COS-7, and N1E-115 cells were cultured at 37°C in Dulbecco's modified Eagle's medium (DMEM, Wisent Bioproducts) supplemented with 10% fetal bovine serum, 2mM L-Glutamine, penicillin and streptomycin (Invitrogen) under humidified conditions with 5% CO_2. N1E-115 cells were plated on laminin-coated 100-mm dishes (25 µg/ml, BD Biosciences). For the neurite outgrowth assays, N1E-115 cells were plated in 35-mm dishes (1.25 x 10^6 cells/plate) containing glass coverslips coated with laminin. Cells were transfected with the indicated constructs using linear polyethylenimine (PEI, PolySciences) at a 1:6 ratio (cDNA: PEI) as described previously [469].

Primary cortical neuron culture and electroporation. Cortical neurons from E17 rat embryos were dissociated mechanically, and electroporated with cDNA constructs encoding wild-type or mutant forms of GFP-Trio using the Amaxa Rat Neuron Nucleofector Kit (Lonza). Post-electroporation, neurons were plated on poly-L-lysine (0.1 mg/ml, Sigma-Aldrich)-treated coverslips in 24-well plates at a density of 200,000 cells/well. Neurons were cultured in attachment medium (Minimal Essential Medium (Invitrogen) supplemented with 1 mM sodium pyruvate (Invitrogen), 0.6% D-glucose (Sigma-Aldrich) and 10% horse serum). After 2 hours, the medium was replaced with maintenance medium (Neurobasal-A medium (Invitrogen), supplemented with 2% B27 (Invitrogen) and 1% L-Glutamine). At DIV1, the neurons were treated for the indicated times with purified recombinant chick myc-netrin-1 (500 ng/ml), which was produced and purified as described previously [444]. Down-regulation of endogenous Trio was achieved by electroporating dissociated E17 rat cortical neurons with 300 nM synthetic

Trio siRNAs designed to target the 5'-UTR of the rat Trio mRNA (siRNA #1: 5'-GUAAAUAUCAACCGCAUAAUU-3', siRNA #2: 5'-GAACAUGAUUGACGAGCAUUU-3', Dharmacon/Thermo Scientific) together with 2 µg of pmaxGFP vector (Lonza) used as a reporter. Only GFP-expressing neurons were assessed. The siRNA-resistant GFP-Trio point mutant plasmids were co-electroporated where indicated, and expression of the exogenous proteins was verified by western blotting (Fig. 2.5F).

Cortical tissue culture. Cortical tissues were dissected from E17 rat embryos. After light mechanical dissociation, tissues were transferred to a 4-well plate containing pre-warmed maintenance medium and allowed equilibrate to 37°C. For pervanadate treatment, pervanadate (10 mM sodium orthovanadate, 10 mM hydrogen peroxide in PBS) was added to tissue cultures to a final concentration of 0.1 mM for 15 minutes prior to netrin-1 stimulation, and total duration of pervanadate treatment was identical for each condition. Immediately following netrin-1 stimulation, samples were transferred on ice, collected and processed as described.

GST-protein purification. Recombinant proteins corresponding to Trio fragments #1 to #8 were expressed in *E. coli* BL21 (DE3) cells, except for fragment #2 which was expressed in *E. coli* Rosetta, and were purified as described previously [256]. Briefly, 1 liter of log phase bacteria was induced with 1 mM IPTG (isopropylthio-galactopyranoside) and shaken overnight at 22°C. The bacteria were lysed in 20 ml of lysis buffer (20 mM Tris-HCl, pH 7.5, 0.1% Triton X-100, 1 mg/ml lysosyme, 1 mg/ml DNAse I), sonicated, and the lysates were centrifuged at 20,000 × *g* for 20 minutes at

4°C. The clarified lysate was mixed for 1 hour at 4°C with glutathione-Sepharose 4B beads (GE Healthcare) equilibrated with 20 mM Tris-HCl pH 7.5, 0.1% Triton X-100. The beads were washed four times with the same buffer, once with 50 mM Tris-HCl pH 8.0, and the proteins were eluted in 20 mM Tris-HCl pH 8.0 containing 10 mM reduced Glutathione. Proteins were stored at -80°C in the presence of 30% glycerol.

***In vitro* kinase assays.** The GST-tagged fragments of Trio (1 µg) purified from *E. coli* were incubated in a 20 µl reaction mixture containing 50 mM Tris-HCl pH 7.5, 1 µM DTT, 5 mM manganese chloride, 5 mM magnesium chloride, and 100 µM [γ-^{32}P] ATP (Perkin Elmer; 5 mCi/µmole; 10 µCi/reaction) in the presence of 50 ng recombinant active Fyn (Millipore). After incubation for 30 min at 30°C, the reactions were terminated by the addition of 10 µl of SDS sample buffer. Proteins were resolved by SDS-PAGE, and coomassie blue-stained gels were dried and subjected to autoradiography.

Immunoprecipitation and Western blotting. Cell lines expressing GFP-Trio constructs and cortical tissues were lysed in lysis buffer containing 20 mM HEPES, pH 7.5, 100 mM NaCl, 10% glycerol, 1% Triton X-100, 20 mM sodium fluoride, 1 mM sodium orthovanadate, 1 mM phenylmethylsulfonyl fluoride (PMSF), and 1 µM complete protease inhibitor cocktail (Roche Diagnostics). Protein lysates were subjected to centrifugation at 10,000 × *g* for 2 minutes at 4°C to remove insoluble materials. For assays using exogenous GFP-Trio, 1 mg of protein lysate was incubated for 3 hours at 4°C with 20 µl of protein A-Sepharose beads and 2.5 µg of GFP antibody. In the case of primary cortical lysates, 2.5 mg of protein lysate was incubated for 1 hour at 4°C with 6

μg/mL of anti-TrioMTP antibody followed by 2-hour incubation with 40 μl protein-A-Sepharose beads (GE Healthcare). Beads were washed three times with ice-cold lysis buffer and heated to 95°C in SDS sample buffer. Protein samples were resolved by SDS-PAGE, transferred to nitrocellulose membrane for western blotting with the appropriate antibodies, and visualized by enhanced chemiluminescence (ECL; PerkinElmer).

Rac1 activation assay. Transfected HEK293 cells were serum-starved overnight, then lysed in buffer containing 25 mM HEPES, pH 7.5, 1% NP-40, 10 mM $MgCl_2$, 100 mM NaCl, 5% glycerol, 1 mM PMSF, 1 μM protease inhibitor cocktail. Protein lysates were subjected to centrifugation at 10,000 × *g* for 2 minutes at 4°C to remove insoluble materials. Endogenous GTP-Rac1 was pulled down by incubating the protein lysates for 30 minutes at 4°C with the Cdc42/Rac interactive binding domain (CRIB) of mouse PAK3 (amino acids 73-146) fused to GST and coupled to glutathione-sepharose beads [465,468]. The beads were washed twice with 25 mM HEPES, pH 7.5, 1% NP-40, 30 mM MgCl2, 40 mM NaCl, and 1 mM DTT and resuspended in SDS sample buffer. For the assays following netrin-1 stimulation, transfected COS-7 cells (which do not secrete endogenous netrin-1) were serum-starved overnight before stimulation with netrin-1 (500 ng/ml), and the assays were performed using a Rac1 activation kit (Cytoskeleton) according to the manufacturer's instructions. In both cases, protein samples were resolved by SDS-PAGE and transferred onto nitrocellulose membranes for western blotting using the anti-Rac1 antibody. The levels of GTP-bound proteins were assessed

by densitometry using Quantity One software (Bio-Rad) and normalized to the total amount of GTPases detected in the total cell lysates.

Immunofluorescence, microscopy and Pearson's correlation coefficient

Transfected N1E-115 cells were fixed and permeabilized as described previously [465]. Co-immunostaining was carried out with the indicated primary antibodies and the respective Cy3 or Alexa-488-conjugated secondary antibodies. Cells were examined with an Axiovert 135 Carl Zeiss microscope using a 63 x PLAN-Neofluar objective lens. Images were recorded with a digital camera (DVC Co) and analyzed with Northern Eclipse software (Empix Imaging Inc.). Cortical neurons (DIV1 or 2) were fixed with 3.7% formaldehyde (Sigma-Aldrich) in 20% sucrose/PBS for 30 minutes at 37°C and permeabilized as described previously [469] unless otherwise indicated. Cortical neurons were visualized using an Olympus IX81 motorized inverted microscope using the 40X U PLAN Fluorite and 60X U PLAN S-APO oil objective lenses. Images were recorded with a CoolSnap 4K camera (Photometrics) and analyzed with the Metamorph software (Molecular Devices). For surface DCC detection, cortical neurons remained unpermeabilized, were blocked in 1% BSA/PBS and incubated with anti-DCC_{EXT} in 1% BSA/PBS at 4°C overnight. Cy3-conjugated secondary antibodies were used to label surface DCC. Average pixel intensity of DCC fluorescence on growth cones and axonal surfaces was measured from acquired images by Metamorph software, using exclusive thresholding to eliminate background fluorescence. Co-immunostaining of cortical neurons was carried out as indicated and GFP-positive neurons were imaged on a Zeiss LSM510 laser-scanning confocal microscope with a PLAN-Apochromat 63x/1.4 oil

objective lens and analyzed with Zen2009 software (Carl Zeiss Microscopy). Quantification of colocalization using Pearson's correlation coefficient (*r*) was performed using MetaMorph software, analyzing more than 10 growth cones per condition in at least 4 independent experiments. A student's unpaired t-test was used for statistical analysis, and the data were presented as a mean *r* ± SEM.

Neurite outgrowth analysis. More than 100 transfected N1E-115 cells were analyzed for each condition. A neurite was defined as a process that measured at least one length of the cell body, and the proportion of transfected cells expressing a neurite was determined manually. To analyze axon outgrowth of primary cortical neurons, 30 electroporated (GFP-positive) cells were analyzed for each condition. Axonal lengths were measured manually from acquired images using MetaMorph software. A student's unpaired t-test was used for statistical analysis, and the data were presented as the mean cortical neuron axon length ± SEM.

Results

Netrin-1 induces Src-kinase-dependent phosphorylation of Trio in the developing cortex

To investigate whether endogenous Trio is tyrosine phosphorylated in response to netrin-1, embryonic E17 rat cortices were dissected and cultured in the presence of the tyrosine phosphatase inhibitor pervanadate prior to netrin-1 stimulation. After 5 and 10 minute stimulations with netrin-1, the cortices were lysed and Trio was

immunoprecipitated. Netrin-1 stimulation of cortical tissues induced a marked increase in tyrosine phosphorylation of full length Trio and isoforms Trio-D and Trio-A at 5 minutes and 10 minutes, as shown by western blotting with an anti-phosphotyrosine antibody (Fig. 2.1A, B). Netrin-1 stimulation also induced FAK phosphorylation (Fig. 2.1A), which has been previously reported in commissural and cortical neurons, thereby serving as a positive control for a stimulated state in our model system [461]. In addition to tyrosine phosphorylation of Trio, netrin-1 stimulation for 5 minutes resulted in an increased association of Trio with DCC in the embryonic cortex (Fig. 2.1C). Since the Src-kinase Fyn has been reported to be part of the signalling complex downstream of netrin-1/DCC [460], we sought to determine whether Src-family kinases mediate tyrosine phosphorylation of Trio in response to netrin-1. To this means, we pre-incubated rat embryonic cortical tissue with the Src-kinase inhibitor PP2 before stimulating with netrin-1 (Fig. 2.1D). The inhibition of Src-kinases by PP2 resulted in a complete block in tyrosine phosphorylation of the three Trio isoforms induced by netrin-1 (Fig. 2.1D, E). In addition, Src-kinase inhibition led to a reduction in FAK phosphorylation induced by netrin-1 (Fig. 2.1D), but not ERK1/2 phosphorylation (Fig. 2.1F). Therefore, netrin-1 induces tyrosine phosphorylation of Trio in a Src kinase-dependent manner, and a concomitant association with DCC in the developing cortex.

Phosphorylation of Trio downstream of the Src-family kinase Fyn is enhanced by DCC in N1E-115 neuroblastoma cells

We have previously demonstrated that phosphorylation of DCC at Tyr^{1418} by the tyrosine kinase Fyn is required for Rac1 activation, and that Trio is required for this

activation downstream of netrin-1 [244,460]. This led us to investigate whether Fyn could phosphorylate and thereby regulate Trio activity. To this means, we cultured N1E-115 neuroblastoma cells, which express netrin-1 but not DCC [465], and exogenously expressed Trio together with wild type or constitutively active Fyn, with or without DCC. Trio tyrosine phosphorylation was observed in the presence of wild type or active Fyn (Fig. 2.2A, B). Furthermore, co-expression of DCC with Trio and Fyn resulted in an additional increase in tyrosine phosphorylation levels of Trio induced by both wild type and constitutively active Fyn (Fig. 2.2A, B). To investigate this increase in Trio phosphorylation induced by both Fyn and DCC, we co-expressed DCC mutants truncated in their intracellular domain, together with Fyn and Trio in N1E-115 cells. The removal of the C-terminal extremity of DCC, comprising the conserved P2 (residues 1327-1363) and P3 (residues 1421-1445) domains [452], significantly reduced the ability of DCC to enhance Fyn-induced phosphorylation of Trio (Fig. 2.2 C, D). In correlation to this, when DCC mutant proteins lacking P2 and P3 domains were expressed in N1E-115 cells, their ability to induce neurite formation compared to the wild type protein was significantly impaired (Fig. 2.2E). This result is consistent with previous reports showing that the P3 intracellular domain of DCC is required for attractive signalling of the growth cone in response to netrin-1 [448]. Altogether, these data suggest that Trio is tyrosine phosphorylated downstream of Fyn and that an intact intracellular domain of DCC potentiates Fyn-induced tyrosine phosphorylation of Trio.

Trio^{Y2622} is a major *in vitro* phosphorylation site of the tyrosine kinase Fyn

To determine whether Trio is directly phosphorylated by Fyn, N-terminal GST-tagged protein fragments spanning the full length of Trio were employed in an *in vitro* kinase assay with recombinant Fyn (Fig. 2.3A). In this way we identified two protein fragments of Trio to be highly phosphorylated by Fyn, one at the N-terminus (fragment #2) and one at the C-terminus (fragment #7) (Fig. 2.3B). Each of the five tyrosine residues in fragment #7 were replaced by a phenylalanine residue and subsequent *in vitro* kinase assays revealed that mutation of Tyr^{2622} significantly reduced the overall phosphorylation of this fragment by Fyn, while mutation of adjacent Tyr^{2600} only slightly reduced phosphorylation (Fig. 2.3C, right panel). When the amino acid substitution Tyr^{2622F} was introduced into the full-length GFP-tagged Trio protein, tyrosine phosphorylation of Trio with Fyn co-expression was significantly reduced compared to the wild-type Trio protein in HEK293 cells, whereas the Tyr^{2600F} substitution had no effect on Trio tyrosine phosphorylation (Fig. 2.3D). For fragment #2, two sub-fragments (fragments #2a and #2b) spanning the length of fragment #2 were generated, and each tyrosine residue contained within these fragments was replaced by a phenylalanine residue. Subsequent *in vitro* kinase assays revealed Tyr^{432} or Tyr^{439} to be Fyn phosphorylation sites (Fig. 2.3C, left panel). However, when tyrosine-to-phenylalanine substitutions were introduced at these sites into full-length GFP-Trio, phosphorylation of Trio downstream of Fyn was not noticeably reduced in HEK293 cells (Fig. 2.3E). In addition, combined mutations of either Tyr^{432} or Tyr^{439} with Tyr^{2622} did not further reduce tyrosine phosphorylation of Trio compared to the single Tyr^{2622F} substitution, indicating that the phosphorylation events observed on Tyr^{432} or Tyr^{439}*in vitro* within fragment #2a do not occur in the context of full-length Trio expressed in cells. Therefore, these data

show that Fyn phosphorylates Trio directly *in vitro* and that Tyr^{2622} is the major Fyn phosphorylation site.

Tyr^{2622} is not required for Trio intrinsic GEF activity towards Rac1 but participates in netrin-1-induced Rac1 activation and neurite outgrowth

We have previously shown that the expression of DCC in N1E-115 cells induces neurite outgrowth in a netrin-1 and Trio-dependent manner through activation of Rac1 [244,465]. To determine the role of Trio phosphorylation by Fyn on its ability to induce neurite outgrowth in these cells, wild-type Trio, phospho-mimicking $Trio^{Y2622E}$, or phospho-null $Trio^{Y2622F}$ were expressed (Fig. 2.4A, B). Both Trio and $Trio^{Y2622E}$ stimulated neurite outgrowth of N1E-115 cells either alone, or with DCC co-expression; in contrast the ability of $Trio^{Y2622F}$ to induce neurite outgrowth was reduced significantly compared to wild type Trio ($p<5E-9$; Fig. 2.4A, B). Furthermore, $Trio^{Y2622F}$ impaired the ability of DCC to induce neurite outgrowth in N1E-115 cells, acting as a dominant negative protein ($p=0.003$; Fig. 2.4A, B). These results suggest that phosphorylation of Trio at Tyr^{2622} participates in DCC-mediated neurite outgrowth.

In order to determine if the reduction in neurite outgrowth by $Trio^{Y2622F}$ was due to an impaired GEF activity towards Rac1, we performed Rac1-pull down assays to assess the levels of activated, endogenous GTP-Rac1 trapped by specific binding to the Cdc42/Rac interactive binding (CRIB) domain of Pak fused to GST [244,468]. As expected, Trio expression in HEK293 cells increased Rac1-GTP levels (Fig. 2.4C, D), and we observed no significant difference in the ability of the $Trio^{Y2622E}$ and $Trio^{Y2622F}$ mutant proteins to increase Rac1-GTP levels (Fig. 2.4C, D). We next investigated whether

phosphorylation of Trio at Tyr^{2622} plays a role in netrin-1-induced Rac1 activation. For that purpose, we co-expressed wild type, phospho-mimicking or phospho-null Trio with DCC in COS-7 cells, which do not secrete netrin-1. In this context expression of the phospho-null $Trio^{Y2622F}$ completely inhibited netrin-1-mediated Rac1 activation after 5 minutes in comparison to the expression of wild-type Trio, while it did not affect netrin-1-induced ERK1/2 phosphorylation (Fig. 2.4E, F). Curiously, expression of phospho-mimicking $Trio^{Y2622E}$ did not significantly restore netrin-1-induced Rac1 activation (Fig. 2.4E, F) however it was not as inhibitory as the phospho-null $Trio^{Y2622F}$ (Fig. 2.4F). This result suggests that replacing Tyr^{2622} with a negatively charged residue only is not sufficient to restore netrin-1-induced Rac1 activation. Together, these data demonstrate that Tyr^{Y2622} does not play a role in the intrinsic GEF activity of Trio towards Rac1, but is required for netrin-1 and DCC to mediate Rac1 activation and neurite outgrowth.

Phosphorylation of Trio at Tyr^{2622} is required for netrin-1-mediated cortical axon outgrowth

Next, we explored the role of Trio tyrosine phosphorylation in netrin-1-mediated axon outgrowth of dissociated rat embryonic cortical neurons depleted of Trio expression. Endogenous Trio expression was downregulated in E17 rat cortical neurons by electroporation of synthetic siRNA targeting the 5'UTR of Trio mRNA, leading to down-regulation of Trio, Trio-A, and Trio-D isoforms (Fig. 2.5A, B). Consistent with our previous study on Trio -/- embryos [244], downregulation of Trio expression led to inhibition of netrin-1-induced axon outgrowth in cortical neurons (Fig. 2.5C), as illustrated by the percentage of axons greater than 100 μm (Fig. 2.5D) or by the

distribution of axon lengths (Fig. 2.5E). Interestingly, re-expression of wild-type Trio or the phospho-mimicking Trio^{Y2622E} was able to restore netrin-1-induced axon outgrowth (Fig. 2.5C, D, E). Expression of the phospho-null Trio^{Y2622F} was however ineffective in rescuing netrin-1-mediated axon extension (Fig. 2.5C-E). Therefore, these data show that Trio^{Y2622} phosphorylation is required for netrin-1 to mediate cortical axon extension. The finding that Trio^{Y2622E} was capable of recovering netrin-1-mediated axon outgrowth suggests that replacing the tyrosine by a negatively charged residue was sufficient to mimick the role of Tyr^{2622} in Trio function in this cellular context.

Phosphorylation of Trio at Tyr^{2622} is required for netrin-1-enhanced Trio/DCC interaction in the growth cone

Since netrin-1 stimulation of cortical tissues enhances the interaction of Trio with DCC (Fig. 2.1C), we next investigated the role of Tyr^{2622} in this process. Wild-type Trio, phospho-mimicking Trio^{Y2622E}, or phospho-null Trio^{Y2622F} were expressed in isolated embryonic cortical neurons, and after a five-minute netrin-1 stimulation, the cell cultures were fixed and immunostained with antibodies against GFP and the intracellular domain of DCC (Fig. 2.6A). Netrin-1 promoted a significantly enhanced co-localization of DCC with Trio (r=0.474, p=0.031) but not with the phospho-null Trio^{Y2622F} mutant (r=0.295, p=0.996) in the growth cones, as determined by quantification of the Pearson's correlation coefficient (r) (Fig. 2.6A, B). The phospho-mimicking amino acid substitution Y2622E slightly increased co-localization of Trio with DCC at the growth cone in response to netrin-1 (r=0.434, p=0.18), although this was not statistically significant (Fig. 2.6A, B).

We next examined the contribution of Trio^{Y2622} phosphorylation in the interaction with DCC biochemically. Wild-type and mutant GFP-Trio constructs were co-expressed with DCC in COS-7 cells prior to netrin-1 stimulation (Fig. 2.6C). After 5 minutes of netrin-1 stimulation, an increase in the amount of DCC co-immunoprecipitating with GFP-Trio was observed (Fig. 2.6C). Although Trio^{Y2622F} and Trio^{Y2622E} were still able to interact with DCC, no enhancement of DCC interaction was observed with either protein in response to netrin-1 stimulation (Fig. 2.6C). Altogether, these results are consistent with the observation that netrin-1 stimulation of cortical tissues enhances the interaction between wild type Trio and DCC (Fig.2.1C), and show that the phosphorylation of Trio at Tyr^{2622} is required for this netrin-1-induced association in neurons (Fig. 2.6A, B).

Trio is required to maintain DCC surface expression in the growth cone of cortical neurons

To determine if Trio influences DCC function by altering its localization, we assessed the surface expression of DCC in neurons depleted of endogenous Trio by immunostaining with antibodies against the extracellular domain of DCC under non-permeabilizing conditions. When endogenous Trio expression was silenced, the intensity of cell surface DCC as detected by epifluorescence was reduced in the growth cones compared to cells expressing control siRNA (Fig. 2.7A, B). Intriguingly, re-expression of either siRNA-resistant wild-type Trio or Trio^{Y2622E} enhanced the average intensity of DCC at the growth cone surface, whereas Trio^{Y2622F} did not (Fig. 2.7A, B).

We next investigated whether Trio participates in the dynamics of DCC surface localization in response to netrin-1. For that purpose, we performed a netrin-1 time

course experiment with cortical neuron cultures and assessed surface DCC enrichment in the growth cones relative to axons of the same cells. When cortical neurons expressing control siRNA were stimulated with netrin-1 for 5-minutes, we observed a significant reduction in cell surface DCC intensity at the growth cones (Fig. 2.7C). Between 5 and 15-minutes of netrin-1 treatment, cell surface DCC was restored and was maintained until at least 30 minutes post-stimulation. The observed increase in DCC surface intensity correlates well with the netrin-1-induced Trio tyrosine phosphorylation observed at 5 and 10-minutes in cortical tissues (Fig. 2.1A, B). Conversely, Trio-depleted neurons exhibited a reduced level of cell surface DCC intensity, and netrin-1-mediated DCC surface dynamics of these cells were abrogated throughout the time course (Fig. 2.7C). Taken together, these results suggest that Trio is required for a proper expression of DCC at the plasma membrane of growth cones, and that phosphorylation at Tyr^{2622} on Trio plays an imperative role in this process.

Discussion

Previous studies have implicated the Rho GEF Trio as an important player during netrin-1-mediated axon outgrowth and guidance [244,258,493,494]. In this study, we provide evidence for a novel mechanism of regulation of Trio by tyrosine phosphorylation in response to the axon guidance cue netrin-1. We present biochemical and cellular evidence aligning the tyrosine phosphorylation of Trio by Src family kinases downstream of netrin-1/DCC in the mammalian embryonic cortex. We show that Trio is phosphorylated by the Src-kinase Fyn at Tyr^{2622}. Although this residue is not involved in the regulation of the intrinsic Trio GEF activity towards Rac1, it is important for netrin-1-

mediated Rac1 activation and DCC-induced neurite outgrowth in N1E-115 neuroblastoma cells, and for netrin-1-induced axon extension in cultured cortical neurons. Furthermore, phosphorylation of Trio^{Y2622} is required for Trio/DCC interaction in response to netrin-1 and contributes to the proper localization of Trio and DCC at the growth cones of cultured cortical neurons stimulated with netrin-1. We also present evidence that Trio participates in maintaining DCC at the cell surface of neuronal growth cones, and that phosphorylation of Trio^{Y2622} is required for this process. In addition, Trio is also necessary for the dynamics of DCC surface localization in response to netrin-1. Therefore, we propose that Trio^{Y2622} is essential for the proper assembly and stability of DCC/Trio signalling complexes at the cell surface of growth cones in order to mediate netrin-1-induced cortical axon outgrowth (Fig. 2.8).

Neural isoforms of Trio, which are generated by alternative splicing, have previously been reported by Portales-Casamar et al [242]. Trio-D, Trio-A, and Trio-C are highly expressed in both the embryonic and adult mammalian brains, with Trio-C being enriched in the cerebellum [242]. Here, we show that Trio-D and Trio-A are highly expressed in the embryonic rat cortex compared to full-length Trio. Furthermore, we demonstrate that full-length Trio, Trio-D, and Trio-A are tyrosine phosphorylated upon netrin-1 stimulation in a Src-kinase-dependent manner in the rat embryonic cortex. We show that Trio is predominantly phosphorylated by Fyn at Tyr^{2622}, which is present in full-length Trio and Trio-D. Since the most abundant isoform (Trio-A), which lacks Tyr^{2622} is also highly tyrosine-phosphorylated in response to netrin-1, we reason that additional Src-kinase phosphorylation sites of Trio are likely induced by netrin-1, but are rendered inaccessible in the context of the full-length protein.

We demonstrate that the increased tyrosine phosphorylation of Trio by Fyn requires an intact C-terminus of DCC. The phospho-null DCC^{Y1418F} mutant was still able to increase Trio phosphorylation by Fyn, suggesting that phosphorylation of DCC at Tyr^{1418} is not sufficient to potentiate Trio tyrosine phosphorylation by Fyn (data not shown). However, removal of the conserved P2 and P3 regions of DCC significantly reduced its ability to increase Fyn-mediated tyrosine phosphorylation of Trio. These results are in agreement with previous studies showing the importance of the carboxy tail of DCC during netrin-1-mediated axon growth and guidance [452]. Since our previous results have shown that the interaction between DCC and Trio is indirect, possibly occurring through Pak1 and/or Nck1, an intact C-terminal domain of DCC is likely required for binding of these intermediate docking-partners with Trio, thereby facilitating enhanced Src-kinase-dependent phosphorylation of Trio [244].

Phosphorylation is a commonly used mechanism of regulation for both GEFs and GAPs in response to extracellular stimuli in various cellular systems [7]. In the case of ephrin-Eph signalling, phosphorylation of GEFs and GAPs has been reported to play a predominant role in the regulation of axon guidance [495]. For instance tyrosine phosphorylation of Ephexin1, a GEF for RhoA, Cdc42 and Rac1, induces a shift in its exchange activity towards RhoA, thus promoting ephrinA-mediated growth cone collapse [496]. Vav2 and Tiam1 are also two GEFs that are regulated by phosphorylation during ephrin-Eph-mediated axon guidance [497,498]. Furthermore, the activity of the Rac-GAP α2-chimaerin is stimulated by Src-family kinase-dependent phosphorylation downstream of Ephrin-A1/EphA4, resulting in growth cone collapse [499]. In the case of Trio, its phosphorylation at Tyr^{2622} did not alter its intrinsic GEF activity towards Rac1.

However, in the context of netrin-1 signalling, the phospho-null Trio^{Y2622F} mutant blocked netrin-1-induced Rac1 activation. Consequently, Trio^{Y2622F} expression also inhibited the ability of DCC to induce neurite outgrowth and was not able to rescue netrin-1-mediated axon outgrowth in cortical neurons depleted of Trio. In the present study, we provide the molecular function of Trio tyrosine phosphorylation by showing that Trio^{Y2622} is necessary for netrin-1 to enhance the interaction of Trio with DCC in co-immunoprecipitates and to increase colocalization of the Trio/DCC complex in the growth cones of rat embryonic cortical neurons. Moreover, when cortical neurons are depleted of Trio, we observed a significant decrease in cell surface DCC in growth cones, and the phospho-null Trio^{Y2622F} mutant was not able to rescue this effect. This raises the interesting possibility that Trio may also act upstream of the guidance receptor DCC to regulate its levels at the cell surface of the growth cones and that Tyr^{2622} is required for this function (Fig. 2.8). This proposed mechanism agrees well with previous studies in *C. elegans* that implicate the GEF activity of UNC-73 (Trio) and MIG-2 small GTPase (RhoG) as upstream regulators of the guidance receptors UNC-40 (DCC) and SAX-3 (robo) by affecting their membrane localization [493,494,500].

Our data indicate that the phospho-mimicking Trio^{Y2622E} partially restores Trio functions, showing that replacing a tyrosine by a negatively charged residue is not always sufficient to restore the function of a phosphotyrosine site. Since one notable consequence of protein tyrosine phosphorylation is the regulation of protein-protein interactions via binding to SH2 or PTB domains [501], we cannot exclude that phosphorylation of Trio^{Y2622} induced by netrin-1 may create a binding site for potential PTB- or SH2-containing proteins that would mediate Trio regulation of netrin-1/DCC-

induced signalling pathways. Alternatively, Tyr^{2622} may be a priming site that serves to promote a conformational change of Trio leading to specific protein-protein interactions and regulation of a Trio/DCC complex at the growth cone plasma membrane. In future studies it will be of great interest to identify proteins interacting with Trio in a tyrosine phosphorylation-dependent manner that contribute to the regulation of cell surface DCC and consequently, downstream signalling pathways. Our findings therefore provide the first demonstration of a mechanism of direct regulation of Trio in response to an extracellular stimulus, which echoes the importance of precise, localized regulation of Rho GEFs throughout biological systems.

Acknowledgements

We thank Sylvie Fromont for her support with molecular biology techniques. We are grateful to Dr. Joseph Tcherkezian for providing cDNA constructs encoding DCC C-terminal deletion mutants. Also we thank Dr. Min Fu from the McGill University Health Centre Imaging Facility for her assistance with the confocal microscopy. This research was supported by Canadian Institute of Health Research Grant MOP-14701 and the Canada Foundation for Innovation-Leaders Opportunity Fund to N.L-V. and by Agence Nationale de la Recherche (ANR) Grant 07-Neuro-006-01 to A.D.. J.D. was supported by a Fonds de la Recherche en Santé du Québec (FRSQ) bourse de formation de Maîtrise and N.L.-V. is an FRSQ Chercheur-National. J.B. was supported by a postdoctoral fellowship from Fondation de la Recherche Médicale (FRM).

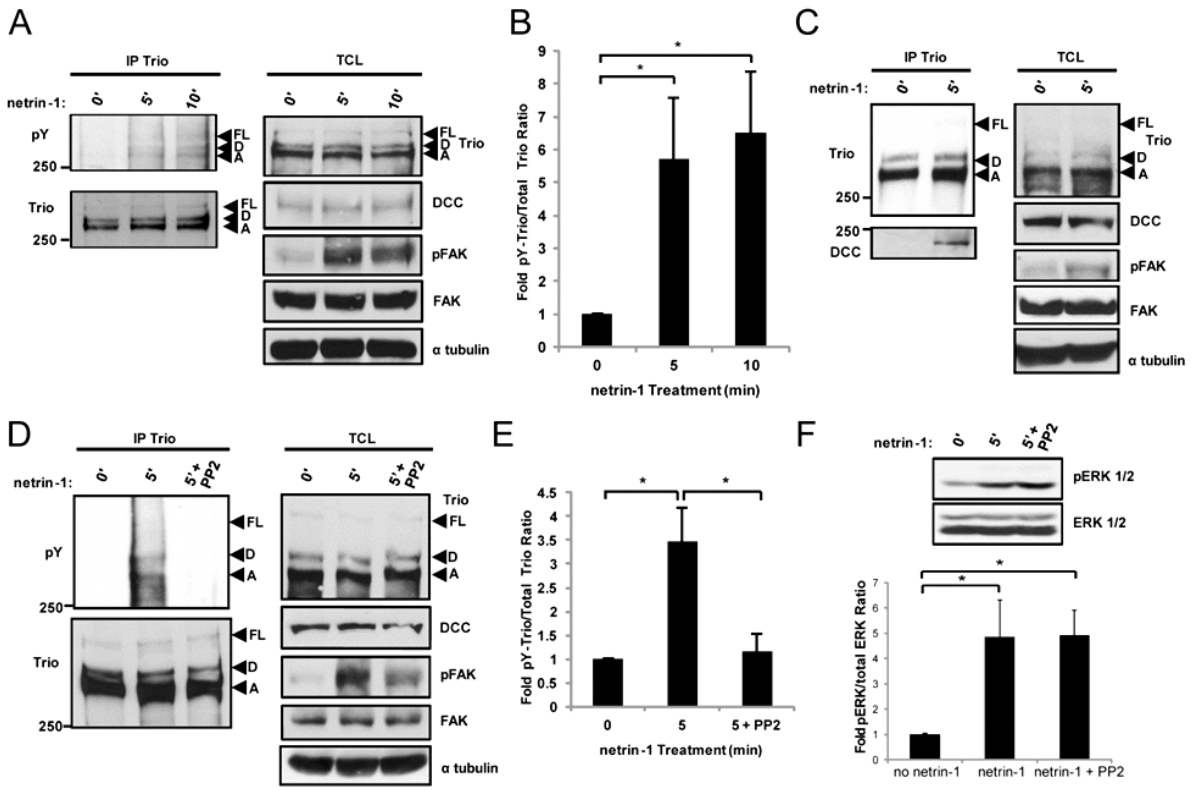
A
IP Trio
TCL
netrin-1:
0'
5'
10'
pY
250
Trio
FL
D
A
DCC
pFAK
FAK
α tubulin
B
Fold pY-Trio/Total Trio Ratio
netrin-1 Treatment (min)
C
IP Trio
TCL
D
5'+ PP2
E
5 + PP2
F
pERK 1/2
ERK 1/2
Fold pERK/total ERK Ratio
no netrin-1
netrin-1
netrin-1 + PP2

Figure 2.1 – Netrin-1 induces Src-kinase-dependent phosphorylation of Trio in the developing cortex.

(A) Isolated E17 rat cortices were stimulated with netrin-1 for the indicated times. Trio isoforms were immunoprecipitated (IP), and phosphotyrosine (pY)-Trio and total Trio were detected by western blotting using anti-phosphotyrosine (4G10) and anti-Trio antibodies, respectively. Netrin-1 stimulation of DCC-induced signalling pathways was verified by FAK phosphorylation in total cell lysates (TCL). (B) Densitometric analysis of Trio-D and Trio-A from A. Error bars indicate the standard error of the mean (SEM) (n=5; *p<0.05). (C) Isolated E17 rat cortices were stimulated with netrin-1 and Trio isoforms were immunoprecipitated (IP) as in A, co-immunoprecipitated DCC was detected by western blotting using an anti-DCC antibody, and total cell lysates were immunoblotted as in A. (D) Isolated E17 rat cortices were stimulated with netrin-1 in the presence or absence of the Src-family kinase inhibitor PP2 (10μM). Trio was immunoprecipitated (IP) as in A, pY-Trio was detected by western blotting, and total cell lysates were immunoblotted as in A. (E) Densitometric analysis of Trio-D and Trio-A from D. Error bars indicate the SEM (n=4; *p<0.05).Trio isoforms: FL= Full length, D = Trio-D, A= Trio-A. (F) As in D, isolated E17 rat cortices were stimulated with netrin-1 in the absence or presence of the Src-kinase inhibitor PP2 before lysis. ERK1/2 phosphorylation was detected by western blotting. Densitometric analysis of pERK1/2/Total ERK1/2 levels. Error bars indicate the standard error of the mean (SEM) (n=4; *p<0.05).

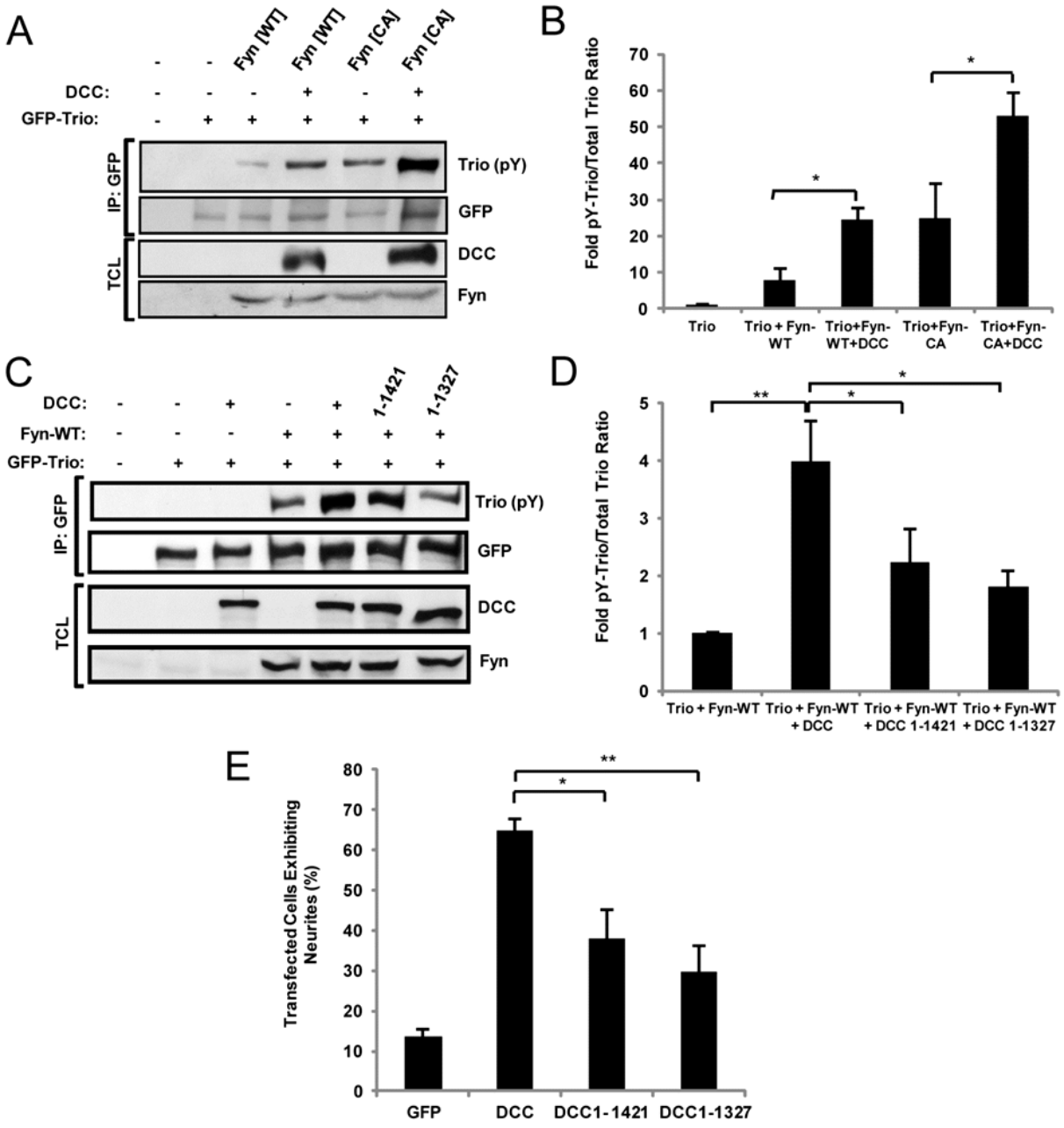
A
Fyn [WT]
Fyn [WT]
Fyn [CA]
Fyn [CA]
DCC:
GFP-Trio:
IP: GFP
TCL
Trio (pY)
GFP
DCC
Fyn
B
Fold pY-Trio/Total Trio Ratio
Trio
Trio + Fyn-WT
Trio+Fyn-WT+DCC
Trio+Fyn-CA
Trio+Fyn-CA+DCC
C
1-1421
1-1327
DCC:
Fyn-WT:
GFP-Trio:
IP: GFP
TCL
Trio (pY)
GFP
DCC
Fyn
D
Fold pY-Trio/Total Trio Ratio
Trio + Fyn-WT
Trio + Fyn-WT + DCC
Trio + Fyn-WT + DCC 1-1421
Trio + Fyn-WT + DCC 1-1327
E
Transfected Cells Exhibiting Neurites (%)
GFP
DCC
DCC1-1421
DCC1-1327

Figure 2.2 – DCC enhances Trio tyrosine phosphorylation by Fyn in N1E-115 neuroblastoma cells.

(A) GFP-Trio was immunoprecipitated (IP) from N1E-115 neuroblastoma cells transfected with pEGFP-Trio, pRK5-Fyn (WT: wild-type, CA: constitutively active), and pRK5-DCC. Phosphotyrosine (pY)-Trio and total Trio were detected by western blotting using anti-phosphotyrosine (4G10) and anti-GFP antibodies, respectively. TCL = total cell lysates (B) Densitometric analysis of A. Error bars indicate the SEM (n=4, *p<0.05). (C) GFP-Trio was immunoprecipitated (IP) from N1E-115 neuroblastoma cells transfected with pEGFP-Trio, pRK5-Fyn, and wild type or truncated forms of pRK5-DCC, as indicated (WT= wild-type). Western blots were conducted as in (A). TCL = total cell lysates. (D) Densitometric analysis of C. Error bars indicate the SEM (n=4, *p<0.05, **p<0.005). (E) N1E-115 neuroblastoma cells were transfected with wild type or truncated forms of pRK5-DCC, as indicated. Neurite outgrowth was assessed by fluorescence microscopy (n=4, *p<0.05, **p<0.005).

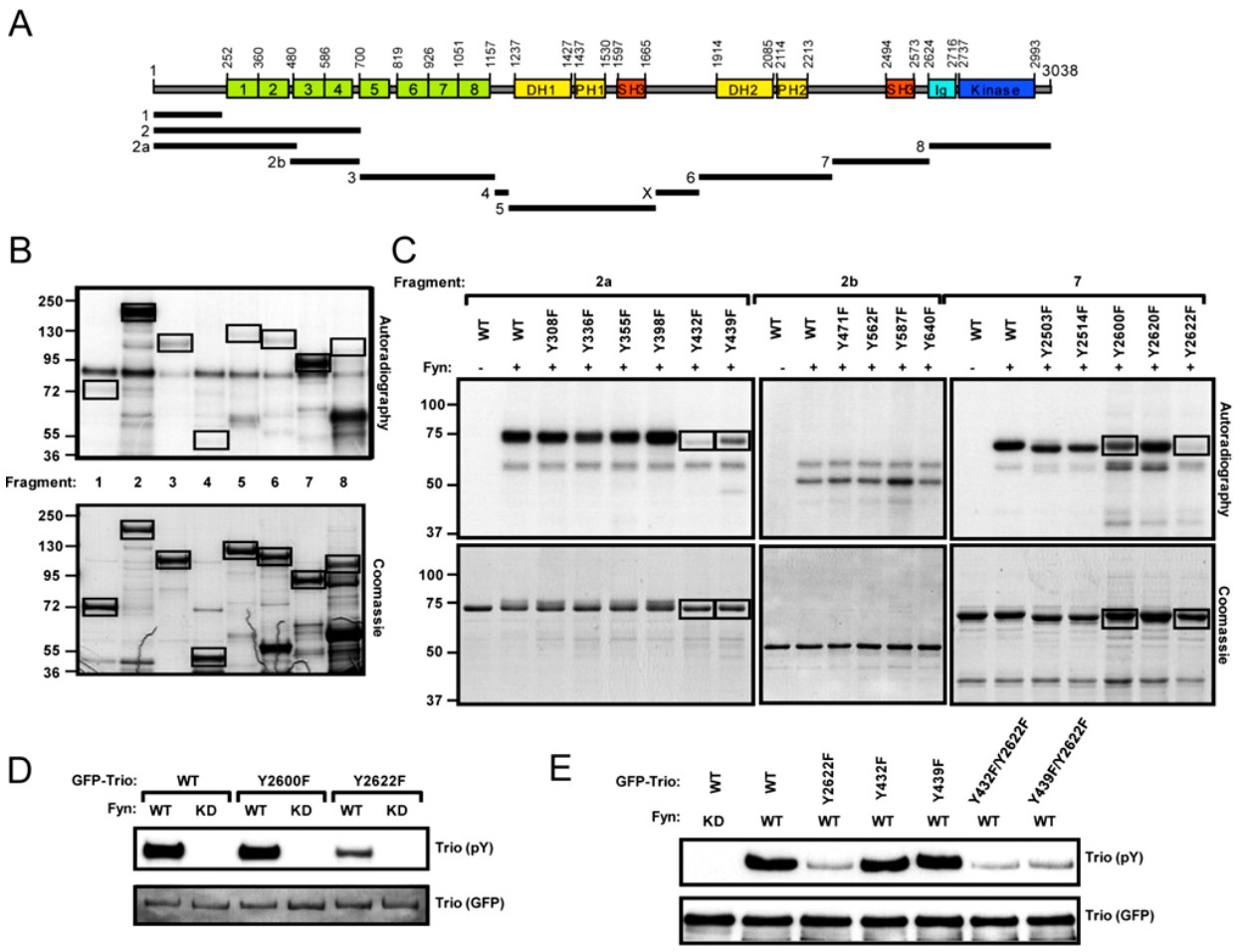
A
1
252
360
480
586
700
819
926
1051
1157
1237
1427
1437
1530
1597
1665
1914
2085
2114
2213
2494
2573
2624
2716
2737
2993
3038
1
2
3
4
5
6
7
8
DH1
PH1
SH3
DH2
PH2
SH3
Ig
Kinase
1
2
2a
2b
3
4
5
X
6
7
8
B
250
130
95
72
55
36
Autoradiography
Fragment: 1 2 3 4 5 6 7 8
Coomassie
C
Fragment:
2a
2b
7
WT
WT
Y308F
Y336F
Y355F
Y398F
Y432F
Y439F
WT
WT
Y471F
Y562F
Y587F
Y640F
WT
WT
Y2503F
Y2514F
Y2600F
Y2620F
Y2622F
Fyn:
100
75
50
37
Autoradiography
Coomassie
D
GFP-Trio:
WT
Y2600F
Y2622F
Fyn:
WT
KD
Trio (pY)
Trio (GFP)
E
GFP-Trio:
WT
WT
Y2622F
Y432F
Y439F
Y432F/Y2622F
Y439F/Y2622F
Fyn:
KD
WT
WT
WT
WT
WT
WT
Trio (pY)
Trio (GFP)

Figure 2.3 – *In vitro* identification of Trio^{Y2622} as the major Fyn phosphorylation site.

(A) Schematic of Trio domain structure and GST-Trio fragment generation plan. Fragment #X does not contain any tyrosine residue and was therefore not included in subsequent analyses. (B) *In vitro* kinase assay. Bacterially expressed GST-Trio fragments were incubated with purified, active Fyn and γ-[^{32}P]-ATP. Phosphorylation states of each fragment were determined by autoradiography (top panel) and compared to total input (coomassie blue staining; lower panel). (C) Single amino acid substitutions of each tyrosine (Y) residue to phenylalanine (F) were introduced into fragments #2a, #2b and #7, and a kinase assay was performed as in B. (D,E) Wild type or point mutant forms of full length GFP-Trio were co-transfected with either wild type (WT) or kinase dead (KD) Fyn in HEK293 cells as indicated. The GFP-Trio proteins were immunoprecipitated from cell lysates. pY-Trio and total GFP-Trio proteins were detected by western blotting using an anti-phosphotyrosine (4G10) antibody and an anti-GFP antibody, respectively.

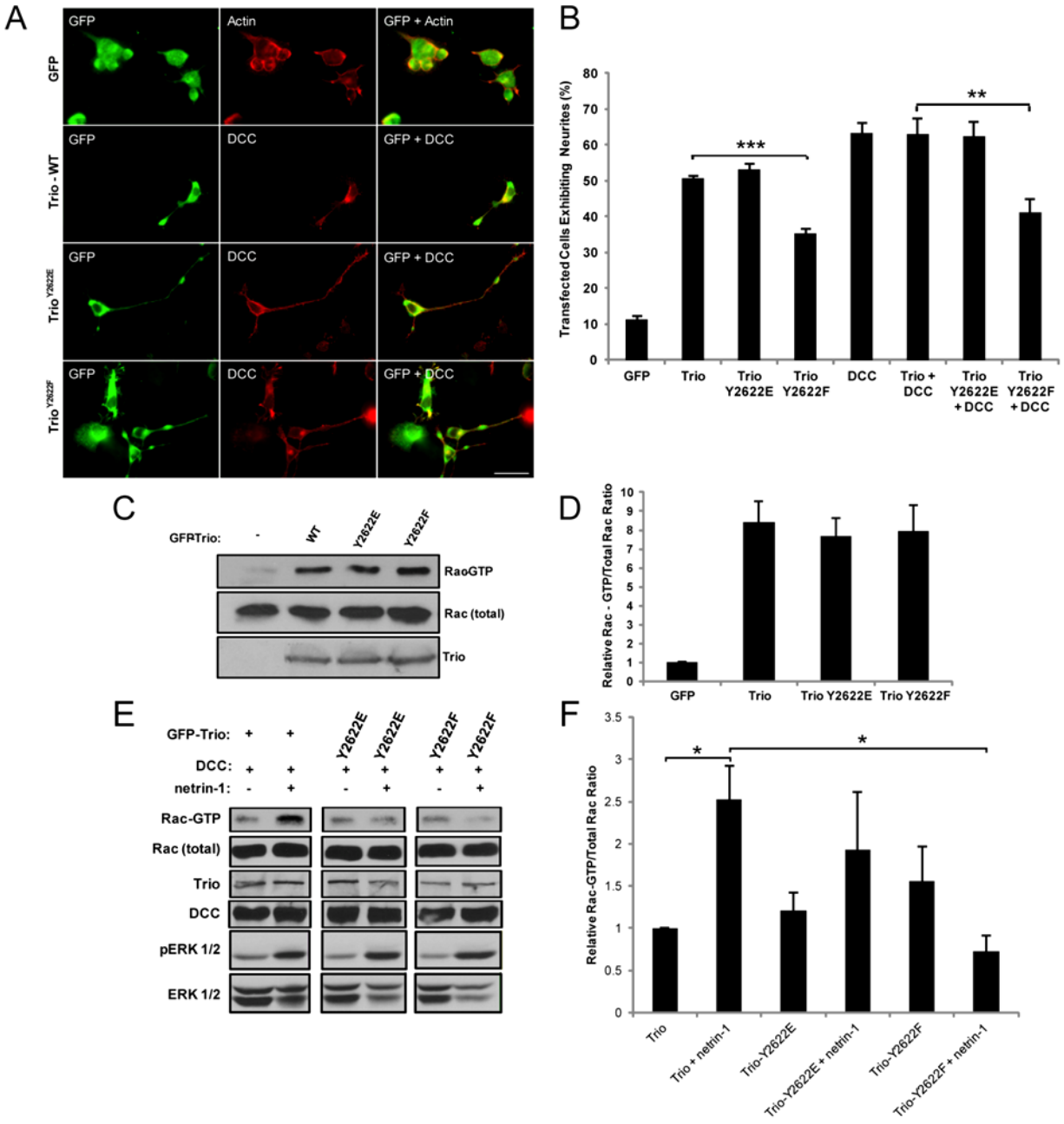
A
GFP
Actin
GFP + Actin
GFP
Trio - WT
GFP
DCC
GFP + DCC
Trio Y2622E
GFP
DCC
GFP + DCC
Trio Y2622F
GFP
DCC
GFP + DCC
B
Transfected Cells Exhibiting Neurites (%)
80
70
60
50
40
30
20
10
0
***
**
GFP
Trio
Trio Y2622E
Trio Y2622F
DCC
Trio + DCC
Trio Y2622E + DCC
Trio Y2622F + DCC
C
GFRTrio:
-
WT
Y2622E
Y2622F
RaoGTP
Rac (total)
Trio
D
Relative Rac - GTP/Total Rac Ratio
10
9
8
7
6
5
4
3
2
1
0
GFP
Trio
Trio Y2622E
Trio Y2622F
E
GFP-Trio:
+
+
Y2622E
Y2622E
Y2622F
Y2622F
DCC:
+
+
+
+
+
+
netrin-1:
-
+
-
+
-
+
Rac-GTP
Rac (total)
Trio
DCC
pERK 1/2
ERK 1/2
F
Relative Rac-GTP/Total Rac Ratio
3.5
3
2.5
2
1.5
1
0.5
0
*
*
Trio
Trio + netrin-1
Trio-Y2622E
Trio-Y2622E + netrin-1
Trio-Y2622F
Trio-Y2622F + netrin-1

Figure 2.4 – Trio^{Y2622} participates in DCC-mediated neurite outgrowth and is required for netrin-1-mediated Rac1 activation.

(A) N1E-115 cells were transfected with pEGFP-Trio, phosphomimetic point mutant pEGFP-Trio^{Y2622E}, or phospho-null point mutant pEGFP-Trio^{Y2622F}, with or without pRK5-DCC. Actin filaments were visualized by indirect immunofluorescence using phalloidin-TRITC, and neurite outgrowth was assessed by fluorescence microscopy. Scale bar, 50μm. (B) Quantification of transfected cells exhibiting neurites from A. Error bars indicate the SEM (n=5, **p<0.005, ***p<0.0001). (C) GTP-loaded Rac1 was pulled down by GST-CRIB from protein lysates of HEK293 cells expressing the indicated GFP-Trio proteins. GTP-bound Rac1 (top panel) and total Rac1 (middle panel) were detected by western blotting. (D) Densitometric ratio of GTP-bound Rac1/Total Rac1 normalized to "GFP". Error bars indicate the SEM (n=7). (E) COS-7 cells expressing the indicated GFP-Trio proteins and DCC were stimulated with netrin-1 for 5 minutes. GTP-loaded Rac1 was pulled down by GST-CRIB. GTP-bound Rac1 (top panel), total Rac1, and the indicated proteins were detected by western blotting. (F) Densitometric ratio of GTP-bound Rac1/Total Rac1 normalized to wild type Trio, unstimulated. Error bars indicate the SEM (n=3, *p<0.02).

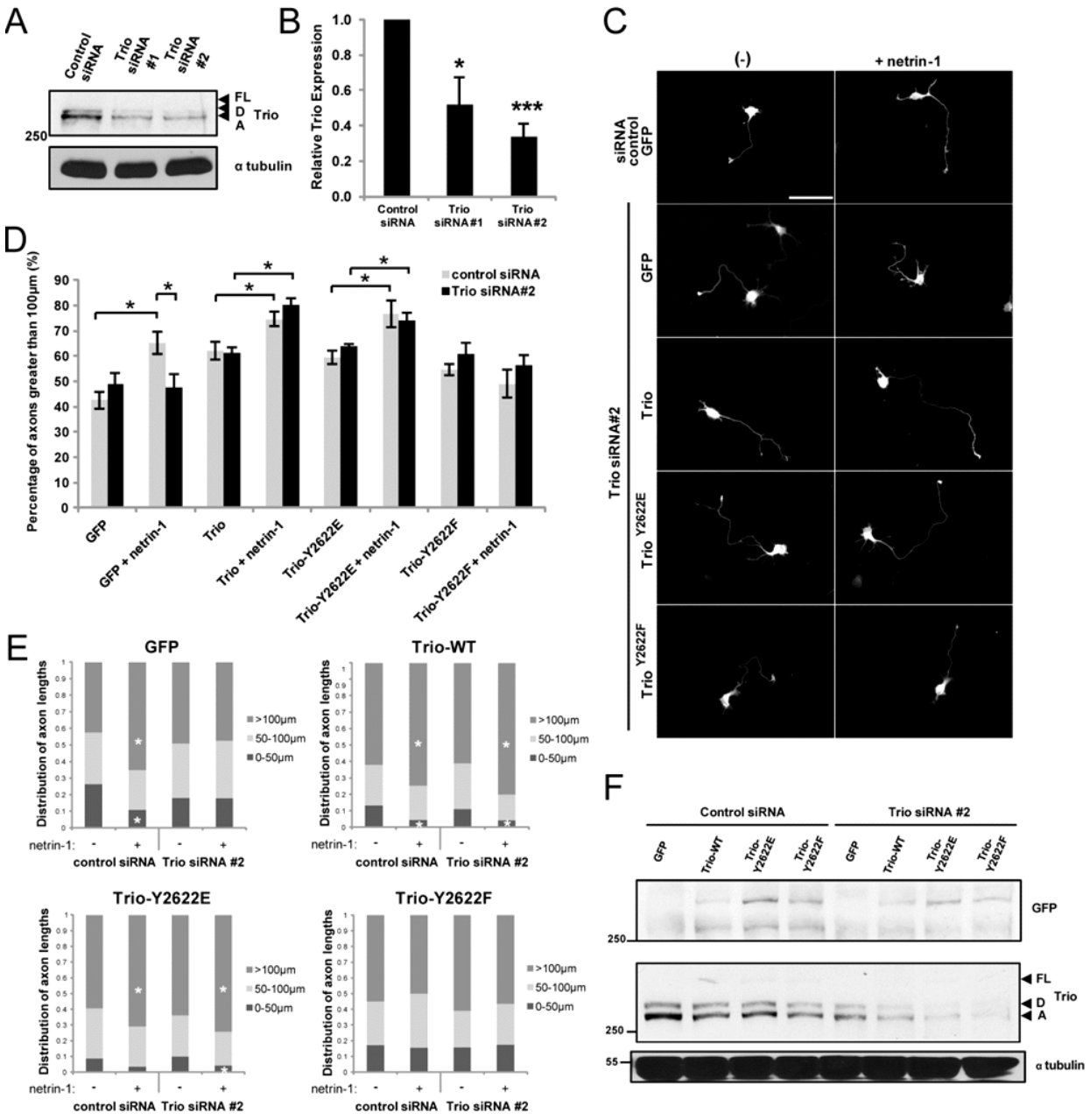
A
Control siRNA
Trio siRNA #1
Trio siRNA #2
FL
D
A
Trio
250
α tubulin
B
Relative Trio Expression
1.0
0.8
0.6
0.4
0.2
0.0
*
***
Control siRNA
Trio siRNA#1
Trio siRNA#2
C
(-)
+ netrin-1
siRNA control GFP
Trio siRNA#2
GFP
Trio
Trio Y2622E
Trio Y2622F
D
Percentage of axons greater than 100μm (%)
control siRNA
Trio siRNA#2
GFP
GFP + netrin-1
Trio
Trio + netrin-1
Trio-Y2622E
Trio-Y2622E + netrin-1
Trio-Y2622F
Trio-Y2622F + netrin-1
E
GFP
Trio-WT
Trio-Y2622E
Trio-Y2622F
Distribution of axon lengths
>100μm
50-100μm
0-50μm
netrin-1:
control siRNA
Trio siRNA #2
F
Control siRNA
Trio siRNA #2
GFP
Trio-WT
Trio-Y2622E
Trio-Y2622F
250
55
FL
D
A
Trio
α tubulin

Figure 2.5 – Trio^{Y2622} phosphorylation is required for netrin-1-mediated cortical axon outgrowth.

(A) Endogenous Trio was silenced in E17 rat cortical neurons by expressing siRNA targeting the 5'-UTR of Trio mRNA, thereby knocking down all neural isoforms of Trio containing the Rac GEF domain. (B) Densitometric analysis of Trio-FL, Trio-D and Trio-A from A. Error bars indicate the SEM (n=4, *p<0.05, ***p<0.001). (C) Dissociated E17 rat cortical neurons were electroporated with Trio and siRNA constructs as indicated, in addition to a GFP-reporter construct. At DIV1 the neurons were stimulated with netrin-1 for 24h before fixation. The axon lengths of GFP-positive neurons were calculated manually using MetaMorph software (>30 neurons/per condition, in duplicate). Scale bar, 55 μm. (D) The percentage of axons in C, measuring greater than 100 μm per condition. Error bars indicate the SEM (n=5, *p<0.05). (E) Distribution of axon lengths of GFP-positive neurons in C (n=5, *p<0.03). (F) Expression of Trio siRNA-resistant GFP-Trio cDNA constructs in cortical neuron cultures at DIV2. GFP-Trio was detected by western blotting using an anti-GFP antibody. Subsequently, total Trio and tubulin levels were detected using appropriate antibodies.

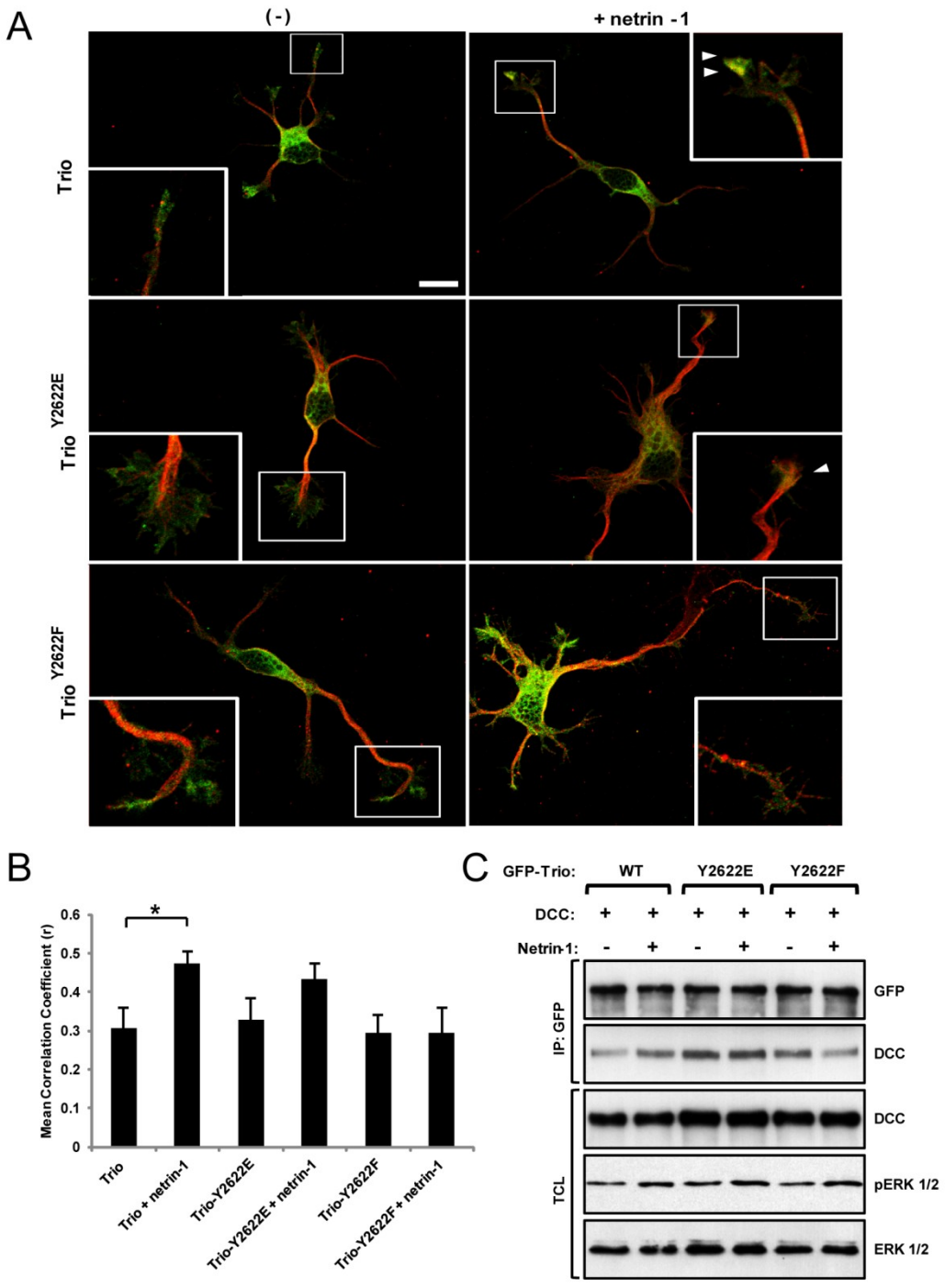
A
(-)
+ netrin -1
Trio
Y2622E Trio
Y2622F Trio
B
Mean Correlation Coefficient (r)
0.6
0.5
0.4
0.3
0.2
0.1
0
*
Trio
Trio + netrin-1
Trio-Y2622E
Trio-Y2622E + netrin-1
Trio-Y2622F
Trio-Y2622F + netrin-1
C
GFP-Trio:
WT
Y2622E
Y2622F
DCC:
Netrin-1:
IP: GFP
GFP
DCC
TCL
DCC
pERK 1/2
ERK 1/2

Figure 2.6 – Trio^{Y2622} phosphorylation is required for netrin-1-mediated Trio/DCC interaction.

(A) Isolated E17 rat cortical neurons were electroporated with the indicated Trio constructs. At DIV1 the neurons were cultured with or without netrin-1 for 5 minutes before fixation. Expression of each protein was assessed by confocal microscopy (green= Trio constructs; red= DCC). Scale bar, 10 μm. (B) The mean Pearson's Correlation Coefficient (r) of green (Trio) and red (DCC) channels within the growth cone was calculated using MetaMorph software. Error bars indicate the SEM (n=4, *$p<0.04$). (C) GFP-Trio was immunoprecipitated (IP) from netrin-1-stimulated COS-7 cells expressing wild type or the indicated point mutants of GFP-Trio and DCC. Co-immunoprecipitation of DCC was detected by western blotting (n=3).

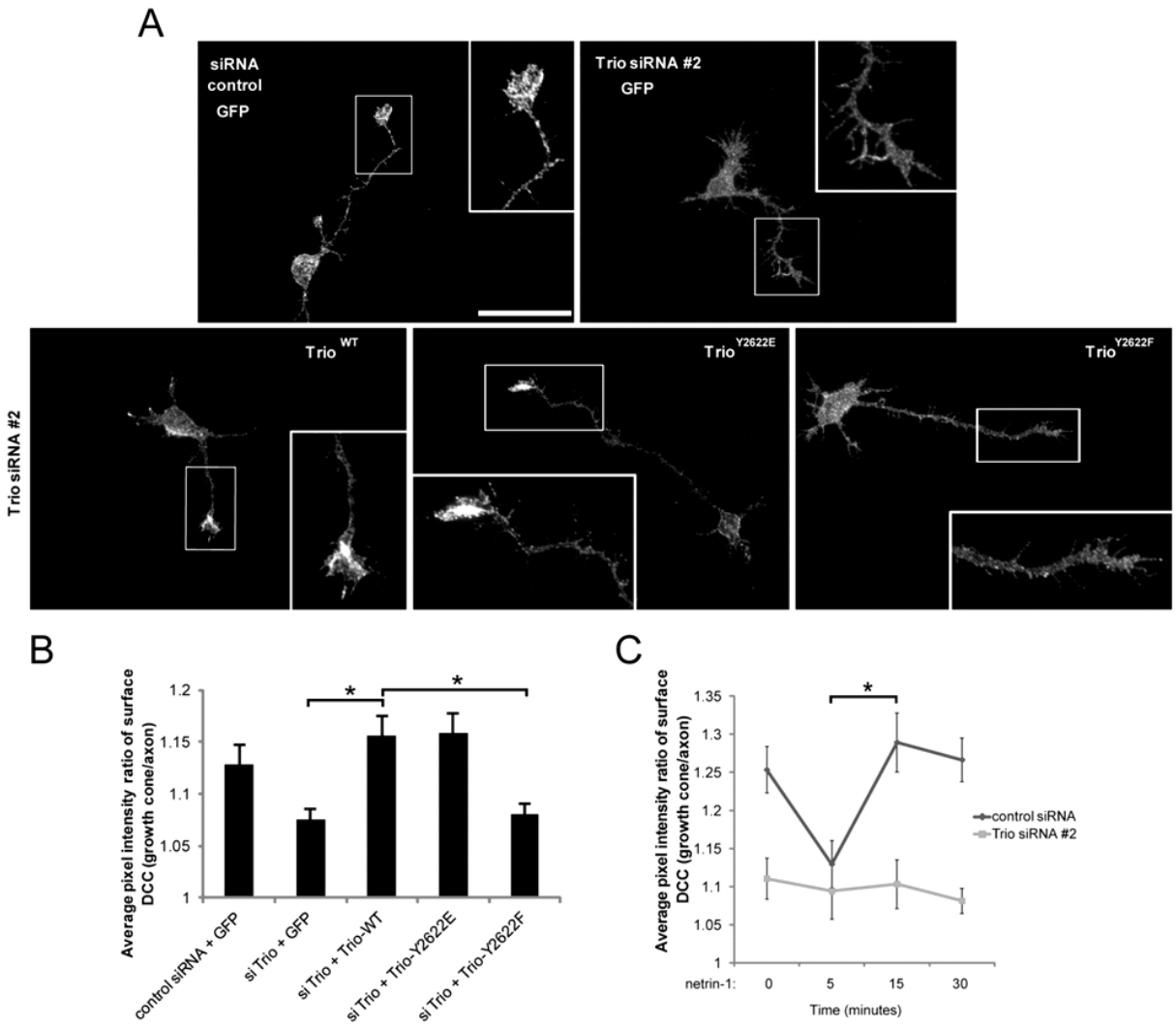
A
siRNA control GFP
Trio siRNA #2 GFP
Trio siRNA #2
Trio WT
Trio Y2622E
Trio Y2622F
B
Average pixel intensity ratio of surface DCC (growth cone/axon)
1.2
1.15
1.1
1.05
1
*
*
control siRNA + GFP
si Trio + GFP
si Trio + Trio-WT
si Trio + Trio-Y2622E
si Trio + Trio-Y2622F
C
Average pixel intensity ratio of surface DCC (growth cone/axon)
1.35
1.3
1.25
1.2
1.15
1.1
1.05
1
*
control siRNA
Trio siRNA #2
netrin-1: 0 5 15 30
Time (minutes)

Figure 2.7 – Trio is required to maintain DCC surface expression at the growth cone.

(A) Dissociated E17 rat cortical neurons were electroporated with the indicated Trio constructs and siRNA#2 in addition to a GFP-reporter construct. At DIV1 the neurons were fixed and the expression of surface DCC was assessed by staining with an antibody recognizing the extracellular domain of DCC in non-permeabilizing conditions, and subsequent fluorescence microscopy (photomicrograph of DCC). Scale bar, 40μm (B) The average pixel intensity ratio of surface DCC expressed at the growth cones relative to axons of each GFP-expressing neuron was calculated using MetaMorph software (15 cells per condition). Error bars indicate the SEM (n=4, 2 replicates each, *$p<0.05$). (C) Dissociated E17 rat cortical neurons were electroporated wtih either control siRNA or Trio siRNA#2 in addition to a GFP-reporter construct. At DIV1 the neurons were stimulated with netrin-1 (250 ng/mL) for the indicated time points, fixed and processed as in A. The average pixel intensity ratio of surface DCC expressed at the growth cones relative to axons of each GFP-expressing neuron was calculated using MetaMorph software (20 cells/condition). Error bars indicate the SEM (n=3, 2 replicates each, *$p<0.05$).

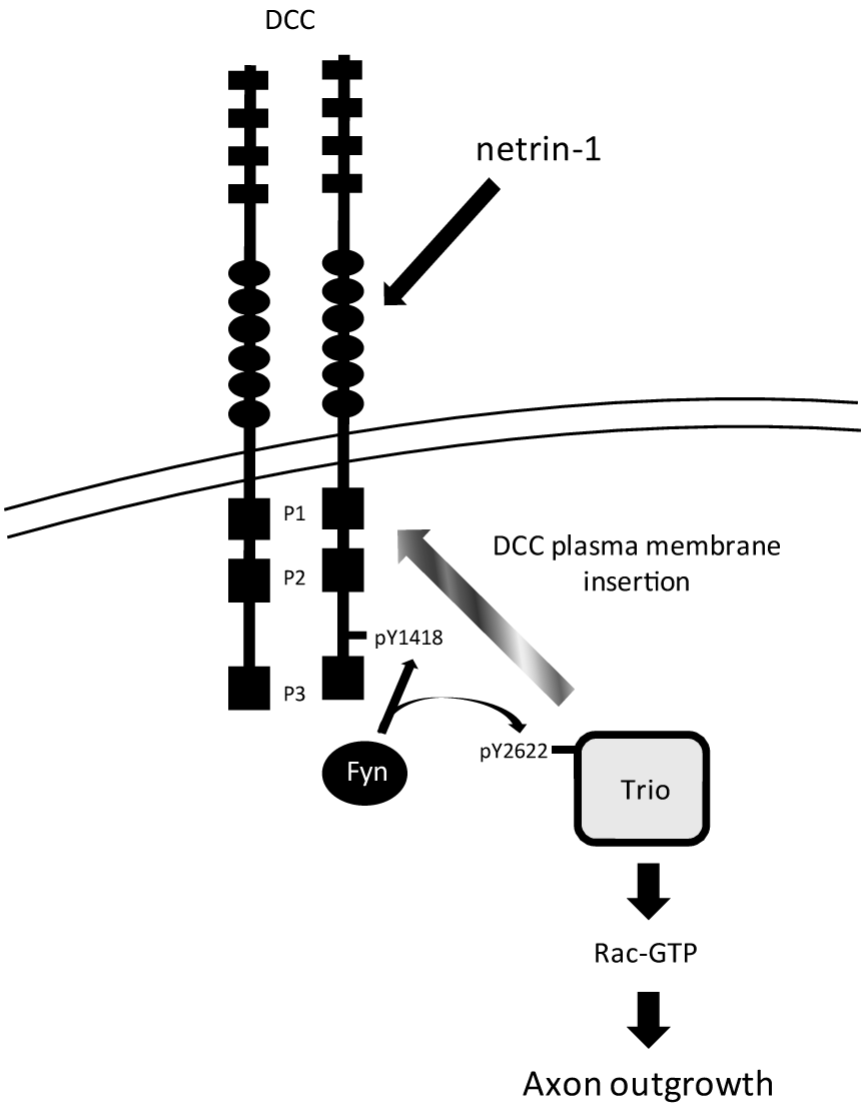
DCC
netrin-1
P1
P2
pY1418
P3
DCC plasma membrane insertion
Fyn
pY2622
Trio
Rac-GTP
Axon outgrowth

Figure 2.8 – Model of Trio regulation during netrin-1/DCC signalling.

Netrin-1/DCC engagement induces a Src-dependent phosphorylation of DCC at Tyr^{1418} ^{460} and Trio at Tyr^{2622}. $Trio^{Y2622}$ is required for both netrin-1-induced activation of Rac1 and enhanced association with DCC. Phosphorylation of Trio at Tyr^{2622} participates in maintaining the level of surface DCC at the growth cone plasma membrane leading to axon outgrowth. Therefore, we propose that $Trio^{Y2622}$ is essential for the proper assembly and stability of the DCC/Trio signalling complex at the cell surface of growth cones in order to mediate netrin-1-induced cortical axon outgrowth.

Chapter 3: Hsc70 chaperone activity underlies Trio GEF function in axon growth and guidance induced by netrin-1

Jonathan DeGeer, Andrew Kaplan, Morgane Morabito, Ursula Stochaj, Timothy E. Kennedy, Anne Debant, Alyson E. Fournier and Nathalie Lamarche-Vane. (2015). In revision, **Journal of Cell Biology**.

Preface to Chapter 3

In addition to phosphorylation, the localized regulation of Rho GEFs may be achieved by association with other proteins. Since Trio is a large protein with many conserved domains, we reasoned that Trio Rac GEF activity may be in part regulated by association with another protein downstream of netrin-1 signaling. Using classical biochemical techniques and mass spectrometric analysis of endogenous Trio from embryonic rat cortices, we identify Hsc70 as a novel binding partner and regulator of Trio. We show that Hsc70 enzymatic activity is required for Trio-dependent functions in cultured cortical neurons. We demonstrate for the first time that a chaperone protein is required to regulate a Rac1 GEF and that chaperone function underlies axon outgrowth and guidance.

Abstract

During development, netrin-1 is both an attractive and repulsive guidance cue, and mediates its attractive function through the receptor Deleted in Colorectal Cancer (DCC). The local activation of Rho GTPases within the extending neuronal growth cone facilitates the dynamic reorganization of the cytoskeleton required to drive axon extension. The Rac1 guanine nucleotide exchange factor (GEF) Trio is essential for netrin-1-induced axon outgrowth and guidance. Here, we identify the molecular chaperone heat shock cognate protein 70 (Hsc70) as a novel Trio regulator. Hsc70 dynamically associates with Trio through Trio's N-terminal and Rac1 GEF domains. While Hsc70 modulates Trio-dependent Rac1 activation, an ATPase-deficient Hsc70 (D10N) abrogates Trio Rac1 GEF activity, and netrin-1-induced Rac1 activation. Furthermore, depletion of Hsc70 abolished netrin-1-mediated cortical axon growth and attraction. These findings demonstrate for the first time that Hsc70 chaperone activity is required for Rac1 activation by Trio and this function underlies netrin-1/DCC-dependent axon outgrowth and guidance.

Introduction

The proper wiring of the central nervous system (CNS) is imperative for normal physiological function and survival. During development, the extension and pathfinding of neurons of the CNS is governed in part by environmental guidance cues [396-398]. Molecular signals initiated by these cues are transduced intracellularly by means of conserved receptors expressed at the distal axon growth cone, ultimately resulting in modulation of the actin cytoskeleton [399]. Netrins constitute a family of axon guidance cues that are required for proper neural specification [443,444,502]. To date, netrin-1 signals through at least four distinct families of transmembrane receptors: the Deleted in Colorectal Cancer (DCC) family (DCC and neogenin), DSCAM, the UNC-5 family, and amyloid precursor protein [437-442]. During development of the spinal cord and cerebral cortex of vertebrates, netrin-1 exerts its attractive functions through the receptor DCC [438,443,447]. In humans, mutations of the *DCC* gene have been associated with congenital mirror movements [456], and small nucleotide polymorphisms within the genes encoding *DCC* and *netrin-1* have been associated with schizophrenia [457], Parkinson's disease and amyotrophic lateral sclerosis [458,459]. Upon netrin-1 stimulation, DCC becomes highly phosphorylated on serine, threonine and tyrosine residues [460]. In particular phosphorylation of rat DCC at Tyr^{1418} by Src family kinases is required for netrin-1-mediated axon outgrowth and guidance in vertebrates [460-462].

Rho family GTPases are molecular switches that have been well characterized as modulators of cytoskeletal dynamics and cellular motility by cycling between an inactive GDP-bound and active GTP-bound state [5]. In the context of axon growth and

pathfinding, the recruitment and localized activation of the Rho GTPases Rac1, Cdc42, and RhoA, are imperative for translating guidance cues into cytoskeletal rearrangements within the extending growth cone [51,399,432,465,489]. Downstream of netrin-1/DCC, Rac1 becomes activated in neurons and drives axonal extension, while RhoA activity is inhibited [244,465-467]. Oversight of Rho GTPase nucleotide cycling is performed by regulatory proteins: guanine nucleotide exchange factors (GEFs) enhance the GTP-bound state [263,503], while GTP hydrolysis is catalyzed by GTPase-activating proteins (GAPs) [8]. Additionally, guanine nucleotide dissociation inhibitors (GDIs) bind to Rho GTPases and restrict them in an inactive state in the cytoplasm, preventing them from associating with their downstream effectors [9]. In recent years, the GEFs DOCK180 and Trio have been shown to mediate Rac1 activation downstream of netrin and DCC in mammalian systems [244,471]. Trio contains two Dbl-homology/pleckstrin-homology (DH-PH) GEF domains (GEFDs) and a serine/threonine kinase domain, for which a substrate has yet to be identified [193]. Trio has activity towards both RhoG and Rac1 via its first GEFD (GEFD1), while the second GEFD (GEFD2) activates RhoA *in vitro* [193,246,247]. Trio is highly enriched in the mammalian brain where five Trio isoforms containing the GEFD1 are generated by alternative-splicing [242]. Trio-null mice die between embryonic day 15.5 (E15.5) and birth and display a general impairment of netrin-1- and DCC-dependent neuronal projections in the spinal cord and brain [243,244]. Specifically in the brain Trio-null embryos lack anterior commissures, and notably DCC-positive projections in the corpus callosum and internal capsule are misguided [244]. We have recently shown that netrin-1 promotes the Src kinase-dependent phosphorylation of Trio^{Y2622} and a concomitant co-association with DCC in cortical growth cones

occurring when Rac1 activation peaks [257]. We also observed that Trio promotes the enrichment of surface DCC at cortical neuronal growth cones in a Trio^{Y2622}-dependent manner [257]. These findings demonstrated the importance of Trio^{Y2622} phosphorylation in the regulation of netrin-1 and DCC-mediated cortical axon outgrowth. Despite these observations, the mechanisms governing Trio localization and activation downstream of netrin-1/DCC are unknown. In this work we provide evidence that the chaperone activity of Hsc70 permits Rac1 activation by Trio in the developing cerebral cortex. In addition, we show that Hsc70 function is required for proper Trio and DCC localization in cortical growth cones treated with netrin-1. We correlate the chaperone-mediated activation of Rac1 by Trio with the regulation of DCC plasma membrane insertion within the growth cones of cortical neurons, and demonstrate Hsc70's requirement for axon outgrowth and guidance induced by netrin-1. In this way we link cytoskeletal proteins with the regulation of an axon guidance receptor and describe a novel function for the chaperone Hsc70 during development.

Results

The molecular chaperone Hsc70 associates with Trio in the developing cerebral cortex

To characterize the molecular mechanisms governing Trio regulation during netrin-1/DCC signaling, we employed a proteomic approach and identified Hsc70 as a novel Trio-associated protein in extracts of netrin-1-treated rat embryonic day 17.5 (E17.5) cerebral cortices. To validate the mass spectrometry result, Trio was immunoprecipitated from cortical tissue extracts and co-immunoprecipitated proteins

were analysed by Western blot. We found that Hsc70 interacted with Trio while the highly homologous chaperone Hsp70 failed to do so (Fig. 3.1A). To determine whether the association between Trio and Hsc70 was netrin-dependent, rat cortices were treated with netrin-1 for 5 to 30 min before harvesting. Trio and Hsc70 co-association in cell extracts peaked 5 min after netrin-1 stimulation, and decreased after 15 and 30 min (Fig. 3.1B, C). FAK was activated (pFAK) after 5 min of netrin-1 treatment and activation was sustained until 30 min of netrin-1 stimulation as reported previously (Fig. 3.1B) [257].

We next investigated the degree of endogenous co-association of Trio and Hsc70 in dissociated cortical neurons by indirect immunofluorescence. Cortical neurons were treated with netrin-1 for the indicated times, fixed and stained with antibodies against Trio and Hsc70 (Fig. 3.1D). Confocal microscopy was performed and the mean Pearson's correlation coefficient (*r*) between Trio and Hsc70 was generated at both cortical growth cones and axon shafts to assess the degree of co-association. By this means, we observed a basal co-localization between Trio and Hsc70 in the cortical growth cones (r=0.50 ± 0.02) (Fig. 3.1D, E). Netrin-1 treatment significantly increased the co-localization of Trio and Hsc70 within growth cones after 5 min (r=0.62 ± 0.02, $p<0.0007$), while the co-localization returned to basal levels after 15 min of netrin-1 treatment (r=0.47 ± 0.02, $p<0.0001$) (Fig. 3.1D, E). The basal co-localization of Hsc70 and Trio in cortical axon shafts was similar to the growth cones (r=0.51 ± 0.02), however netrin-1 application for either 5 or 15 min resulted in no significant modulation of the association (r=0.48 ± 0.03, r=0.42 ± 0.02, $p>0.05$) (Fig. 3.1F, G). In summary we identified Hsc70 as a novel Trio-associated protein in embryonic cortical tissues, and we

demonstrate that the netrin-1-induced co-association occurs preferentially in cortical growth cones versus axons.

Hsc70 facilitates Trio-dependent Rac1 activation and cortical axon outgrowth in a chaperone-dependent manner

To delineate the regions of Trio permitting the association with Hsc70, GFP-Trio deletion mutants were expressed in HEK293 cells and the interaction with Hsc70 was assessed by co-immunoprecipitation (IP) (Fig. 3.2A, B). In this assay, full-length GFP-Trio basally associated with endogenous Hsc70, and the C-terminal truncation of Trio, lacking the RhoA GEF and kinase domains resulting in the Trio 1-1813 fragment, did not reduce the association with Hsc70 relative to immunoprecipitation efficiency (Fig. 3.2B, C). On the contrary, the shorter fragments of Trio comprising the Sec14 domain (Trio 1-232) or GEFD1-SH3 (Trio 1203-1813) were highly associated with Hsc70 (Fig. 3.2B, C). Intriguingly, the intermediate fragment containing the Sec14 domain but lacking the GEFD1-SH3 domain did not associate with Hsc70 in an elevated manner (Fig. 3.2B, C). These results suggest that Hsc70 association with Trio may be mediated in part by the N-terminus and GEFD1 of Trio, though both regions may differentially cooperate to accommodate association in the context of the full length protein.

Since the GEFD1 of Trio associated highly with endogenous Hsc70, we next sought to determine whether Hsc70 modulates the Rac1 GEF activity of Trio. We performed pull down assays with the Cdc42/Rac interactive binding (CRIB) domain of PAK fused to GST to assess the level of active GTP-Rac1 in HEK293 cell extracts [244,468]. As expected, Trio over-expression resulted in a significant increase in Rac1-GTP

levels (p=0.0003), while the expression of Hsc70 had no significant effect on Rac-GTP levels alone (p=0.28) (Fig 3.2D, E). Increasing levels of GFP-Hsc70 co-expression with GFP-Trio resulted in enhanced Trio-dependent Rac-GTP inductionwith low levels of Hsc70 ($p<0.03$), whereas higher levels of Hsc70 expression did not significantly augment Trio-induced Rac activation (p=0.44) (Fig. 3.2D, E). To examine whether Hsc70 chaperone activity is required to modulate the activation of Rac1 by Trio, the dominant negative and chaperone-dead (ATPase-deficient) Hsc70 ^{D10N} was introduced and Rac1-GTP pull-downs were performed. Although GFP-Hsc70 ^{D10N} expression alone had no effect on basal Rac-GTP levels, the co-expression of GFP-Hsc70 ^{D10N} with Trio abolished Trio-dependent Rac1 activation (Fig. 3.2D, E). These results demonstrate that Trio Rac1 GEF activity is regulated by Hsc70 in a chaperone activity-dependent manner.

We have previously reported that exogenous Trio expression in either neuroblastoma cells or dissociated cortical neurons increases neurite or axon lengths in a Rac1 GEF-dependent manner, thereby serving as a readout of Trio function [257]. We applied this model to assess whether Hsc70 functionally regulates Trio-dependent axon outgrowth. Dissociated cortical neurons were electroporated with constructs encoding GFP, and either GFP-Hsc70 or GFP-Hsc70 ^{D10N} alone, or with GFP-Trio. After two days in culture the neurons were fixed, imaged and the average axon lengths of GFP-positive neurons were determined (Fig. 3.2F, G). While expression of GFP-Hsc70 or Trio alone resulted in a significant increase in axon length relative to control cells ($p<0.0001$), co-expression of Hsc70 and Trio did not further enhance average axon lengths relative to Trio-expressing neurons (p=0.97; Fig. 3.2F, G). Axon lengths of GFP-Hsc70 ^{D10N}-

expressing neurons were not significantly different from GFP-expressing neurons, while co-expression of GFP-Hsc70 ^{D10N} with Trio abrogated Trio-dependent enhanced axon extension ($p<0.0001$; Fig. 3.2F, G). To rule out possible down-regulation or degradation of proteins, the expression of GFP-tagged proteins was verified by immunoblotting (Fig. 3.2H). Altogether, these data demonstrate that Rac-GTP induction by Trio is modulated by Hsc70 chaperone activity, which is required for Trio-stimulated axon extension in cortical neurons.

Hsc70 is required for the enrichment of Trio at the growth cone periphery of netrin-1-stimulated cortical neurons

Since Hsc70 is a molecular chaperone, we asked whether it may function to regulate Trio localization within cortical growth cones. To first establish Trio localization dynamics, cortical neurons were treated with netrin-1 for 5 min or left untreated, before fixation and labelling (Fig. 3.3A). Brightfield micrographs of Trio and F-actin expression were acquired for each growth cone, and the intensity of either signal was measured along a 10 μm segment of the distal growth cone (Fig. 3.3A, right panels). Whereas the expression profile of actin increased along the central to peripheral linesegment of untreated growth cones, the intensity of Trio along the segment was less distally pronounced, reflecting a muted spatial enrichment of Trio within the peripheral growth cones relative to F-actin (Fig. 3.3A, B; top panels). Upon netrin-1 treatment, however, the intensity profile of Trio shifted peripherally along the linescan mirroring that of F-actin, reflecting an enrichment of Trio in the peripheral growth cone domain (Fig. 3.3A, B, bottom panels).

We next downregulated endogenous Hsc70 expression in dissociated neurons by electroporation of synthetic siRNA targeting the 5'-UTR of rat Hsc70 along with GFP cDNA as a transfection marker. To verify efficient downregulation, cortical neurons were fixed and immunostained for endogenous Hsc70, and the level of Hsc70 present in GFP-positive neurons versus GFP-negative neurons was assessed by indirect immunofluorescence (Fig. 3.3C, D). In this manner, we observed a 60% reduction in the total level of Hsc70 in GFP-positive neurons relative to non-transfected neurons (Fig. 3.3D). Subsequently, Trio localization was assessed within the growth cones of dissociated cortical neurons electroporated with either control or Hsc70 siRNA, and stimulated with netrin-1 for 5 min. In the absence of netrin-1, Trio localization was largely dispersed throughout the growth cones of control neurons with reduced incidence of compartmentalization in the growth cone periphery (Periphery: 15.17%±4.30) (Fig. 3.3E-G). Similarly, in Hsc70-depleted neurons Trio was largely dispersed throughout the growth cones and a lower proportion displayed a peripheral Trio localization (Periphery: 6.16%±0.32) (Fig. 3.3E, G). Netrin-1 application of 5 min resulted in a significant increase in the proportion of growth cones with peripheral Trio localization (Periphery: 59.25%±5.46, $p<0.001$) (Fig. 3.3E-G). By contrast, Hsc70-depleted cortical neurons displayed no significant change in Trio localization (Periphery: 8.33%±2.08%, $p=0.23$) (Fig. 3.3E, G). The Hsc70-dependent peripheral re-localization of Trio in cortical growth cones treated with netrin-1 complements the finding that Hsc70 ATPase activity is required for Trio-dependent cortical axon outgrowth. It suggests that

impaired localization of Trio to particular sub-cellular structures may contribute to functional deficits caused by Hsc70-deficiency.

Hsc70 associates with a DCC multiprotein signaling complex in the developing cortex stimulated with netrin-1

Since Trio and DCC co-associate in cortical neurons treated with netrin-1 [257], we next examined the interaction between Hsc70 and DCC in cortical tissues. Protein extracts from cerebral cortices treated with netrin-1 were collected, DCC was immunoprecipitated and the level of Hsc70 co-associating was determined by immunoblotting (Fig. 3.4A). Similar to our findings for Trio and Hsc70 interaction, the association of Hsc70 with DCC increased after 5 min of netrin-1 stimulation. However, unlike Trio, DCC remained associated with Hsc70 until after 15 min of treatment (Fig. 3.4A, B). The co-association of Trio and FAK with DCC also increased after 5 min of netrin-1 stimulation and remained elevated until 15 min of netrin-1 treatment (Fig. 3.4A). These results show that Hsc70 is part of a DCC-Trio-FAK signaling complex induced by netrin-1 in cortical tissues.

Since chaperones function in part by regulating protein trafficking and half-life [504], we next investigated whether Hsc70 association with DCC occurs at the plasma membrane or intracellularly. Dissociated cortical neurons were cultured for 2 days before netrin-1 treatment, and subsequently processed according to a surface labelling protocol employing an antibody against the extracellular domain of DCC (Fig. 3.4C) [505]. Following surface DCC isolation from cell extracts, the remaining fraction of intracellular DCC was isolated by immunoprecipitation. In this manner, Hsc70 was found to co-

associate more with surface DCC relative to the intracellular-enriched DCC pool. Moreover, netrin-1 treatment enhanced the co-association (Fig. 3.4C, $p<0.05$). Taken together, these data demonstrate that Hsc70 is associated with DCC signaling complexes in the developing cortex, and Hsc70 association is stronger with surface DCC in response to netrin-1 stimulation.

Hsc70 chaperone activity supports surface DCC enrichment in cortical growth cones

Since Hsc70 preferentially associated with surface DCC in biochemical assays, we next investigated whether Hsc70 influences DCC surface localization in growth cones downstream of netrin-1. To assess this, dissociated cortical neurons expressing GFP-Hsc70 or the ATPase-dead GFP-Hsc70 ^{D10N} were treated with netrin-1 for 15 min and fixed. Following fixation the levels of surface DCC were assessed by indirect immunofluorescence under non-permeabilizing conditions using antibodies against the extracellular domain of DCC (Fig. 3.4D, E). When either GFP-Hsc70 or GFP-Hsc70 ^{D10N} were expressed in untreated cortical neurons, the surface DCC enrichment at the growth cones was not significantly different from neurons expressing GFP alone (Fig. 3.4D, E). After 15 min of netrin-1 treatment of control GFP and GFP-Hsc70-expressing cortical neurons, enrichment of surface DCC intensity at the growth cones was maintained. However the level of surface DCC enrichment in growth cones expressing GFP-Hsc70 ^{D10N} was significantly reduced (Fig. 3.4D, E; $p=0.01$). Intriguingly, the netrin-1-induced activation of FAK and ERK pathways downstream of DCC were uninterrupted in HEK293 cells co-expressing Hsc70^{D10N}, suggesting that the biological function of

Hsc70 chaperone activity likely occurs downstream of these signaling pathways (Fig. 3.4F, G). Taken together, these results support a hypothesis wherein the stabilized enrichment of DCC at the growth cone plasma membrane downstream of netrin-1 requires Hsc70 chaperone activity.

Hsc70 is required for netrin-1-mediated cortical axon outgrowth and Rac1 activation

We next explored the role of Hsc70 in netrin-1-induced axon outgrowth of dissociated cortical neurons. Cortical neurons were electroporated with control or Hsc70 siRNA together with GFP cDNA, and stimulated with either netrin-1 or glutamate for 24h before fixation (Fig. 3.5A, B). While depletion of endogenous Hsc70 did not affect basal cortical axon lengths, netrin-1 treatment was insufficient to stimulate axon extension in these neurons (Fig. 3.5A, B). By contrast, Hsc70-depleted neurons remained responsive to glutamate ($p<0.03$), confirming that Hsc70 depletion does not impair all mechanisms of induced axon outgrowth (Fig. 3.5A, B). To verify the function of Hsc70 in netrin-1-mediated axon outgrowth, siRNA-resistant GFP-Hsc70 or GFP-Hsc70 ^{D10N} were expressed in Hsc70-depleted cortical neurons and stimulated with netrin-1 (Fig. 3.5A, C). Re-expression of Hsc70 was sufficient to restore netrin-1-induced cortical axon extension ($p<0.05$), while expression of the chaperone-dead Hsc70 ^{D10N} did not rescue netrin-1 sensitivity relative to untreated neurons ($p=0.45$) (Fig. 3.5A, C).

To determine whether Hsc70 functions upstream or downstream of Trio during netrin-1-induced axon outgrowth, cortical neurons were depleted of endogenous Hsc70 or Trio (as described [257]), and expression was rescued with siRNA-resistant GFP-Trio or

GFP-Hsc70 cDNAs (Fig. 3.5D). In this context, GFP-Hsc70 over-expression was not sufficient to rescue netrin-1-induced axon extension in Trio-depleted neurons (p=0.75) (Fig. 3.5D, E). Conversely, when neurons were depleted of endogenous Hsc70, the over-expression of GFP-Trio restored the sensitivity of these neurons to netrin-1 and they extended longer axons (p=0.047; Fig. 3.5D, F). These results demonstrate that Hsc70 is specifically required for netrin-1-mediated cortical axon outgrowth by functioning upstream of Trio. This is in agreement with our findings that Hsc70 potentiates Trio-dependent Rac1 activation (Fig. 3.2C), which is a requisite for netrin-1-induced axon extension [244,465].

To examine whether Hsc70 contributes to netrin-1-induced Rac1 activation, we co-expressed either Hsc70 or Hsc70 ^{D10N} with DCC in HEK293 cells. Upon stimulation with netrin-1 for 5 min, we assessed the levels of Rac1-GTP by pull down assays. In these studies, GFP-Hsc70 expression and subsequent netrin-1 treatment led to an activation of Rac1 similar to control cells expressing DCC alone, while expression of Hsc70 ^{D10N} specifically inhibited netrin-1-stimulated Rac1 activation relative to the netrin-1-treated control ($p>0.05$; Fig. 3.5G, H). Therefore Hsc70 chaperone activity is necessary for netrin-1 to stimulate Rac1 activity. We propose that Hsc70 chaperone activity acting upstream of Trio during netrin-1-induced cortical axon extension is essential through its regulation of Trio Rac1 GEF activity.

Hsc70 is required for netrin-1-dependent attraction of embryonic cortical neurons

We have previously reported that Trio-null embryos have defective neural projections within the CNS, notably the netrin-1-dependent ventral projections of

commissural axons and DCC-positive projections of the corpus callosum and internal capsule [244]. In each case, a deficit in axon guidance was observed as the projected fibres were dispersed over a larger area compared to wild type embryos [244]. Since Trio contributes to axon guidance *in vivo* [244], we next evaluated the contribution of Hsc70 to netrin-1-induced chemoattraction of cortical neurons. To assess this proposed function, we employed an *in vitro* axon guidance assay based on the Dunn chamber [506]. E17.5 rat cortical neurons electroporated with control or Hsc70 siRNA together with GFP cDNA were exposed to either vehicle (PBS) or a netrin-1 gradient in the Dunn chamber for at least 90 min at DIV2 (Fig. 3.6A, B). As an internal control, naive cortical neurons (non-electroporated) were also treated as described above. Although the mean turning angles of each PBS-treated condition did not vary significantly ($p>0.2$), netrin-1 induced a robust attractive turning response for either the naive or control siRNA-electroporated neurons resulting in turning angles of 11.9º±4.74º ($p<0.005$) and 10.67º±4.29º ($p<0.02$), respectively (Fig. 3.6B, C). Hsc70-depleted cortical neurons, however, were not attracted to the netrin-1 gradient in the chamber; relative to the PBS controls, as the turning angle was reduced by 6.25º±3.03º ($p>0.07$, Fig. 3.6B, C). Importantly, exposure of neurons to the netrin-1 gradient did not significantly affect the displacement of the growth cones during the imaging period. However, the displacement of the Hsc70-depleted neurons was markedly reduced compared to the control siRNA or naive control neurons (Fig. 3.6D-F). Since some neurons failed to meet the minimum growth cone displacement requirement of 10 μm to be included in the turning angle analysis, the average displacement of all motile growth cones was determined. In this way, the displacement of Hsc70 knock-down neurons was found to be 5.95μm ± 0.94μm

compared to 20.23μm ± 1.52μm for control growth cones (n=74 and 96, respectively; Fig. 6E; left panel). Furthermore, the proportion of growth cones that underwent either temporal retraction, or collapsed all together (negative net displacement) was higher in Hsc70-depleted cortical growth cones (Fig. 6E; middle and right panel). These results emphasise that Hsc70 generally supports axon extension, and is specifically required for netrin-1-dependent chemoattraction *in vitro*.

Discussion

Our data presented here outline a novel function for the molecular chaperone Hsc70 in regulating the Rac1 GEF Trio during netrin-1-mediated cortical axon growth and guidance (summarized in Fig. 3.7). We demonstrate that Hsc70 and Trio associate dynamically downstream of netrin-1 treatment in cortical neurons, and that the function of this association is dependent on Hsc70 chaperone activity. We support this finding with biochemical evidence highlighting that Hsc70 chaperone activity is required for Rac1 activation by Trio. Moreover, we correlate this function with the proper re-localization of Trio and cell surface DCC within cortical growth cones downstream of netrin-1. Hsc70 is a constitutive chaperone that is enriched in the developing CNS, and constitutes 2-3% of total protein of the rat spinal cord [507,508]. Despite being 86% homologous to Hsp70, Hsc70 is preferentially expressed in neurons while Hsp70 is enriched in glial cells in the unstressed mouse embryo [507]. Hsc70 is an ATP-dependent chaperone that carries out various housekeeping chaperone functions; it assists in protein folding, translocation, as well as chaperone-mediated autophagy and prevention of protein aggregation (reviewed in [509]).

Our report is the first to describe Hsc70-mediated regulation of a Rac1 GEF in neurons to date. In earlier studies, Hsc70 was reported to associate with other Rho GEFs including the proto-oncogene Dbl and Plekhg4 [205,510]. Similar to our findings for Trio, Kauppinen *et al.* (2005) demonstrated that the association of proto-Dbl with Hsc70 was mediated by the N-terminus and PH domain of the GEFD of proto-Dbl [510]. In direct contrast to our results, however, Hsc70 was identified as a negative regulator of proto-Dbl-induced RhoA GEF activity [510]. While future studies are required to determine the precise mechanism of Hsc70-mediated regulation of Rho GEFs, our work highlights the exciting possibility that Hsc70 may serve as a universal regulator of Rho GEFs in specific cellular contexts. Elevated Hsc70 expression occurs in various tissues in which Rac1 is known to function, including in the neural tube during embryogenesis and in various types of cancer [507,511,512]. Although Rac1 expression is elevated in primary tumours, and Rac1 activation is required for cancer cell migration and metastasis (reviewed in [513]), the dysregulation of Rac1 and Hsc70 has not yet been linked in any biological system. Currently, pharmacological inhibitors of Hsc70/Hsp70 are being tested as anti-cancer agents and correlate with a function of Hsc70 in regulating Rac1-dependent processes such as cell proliferation and cell migration [514,515].

Since the netrin-1-induced association of Hsc70 with DCC is prolonged in comparison to that with Trio alone, it suggests that Hsc70 may have an additional or downstream function in the DCC signaling complex independent of its regulation of Trio Rac1 GEF activity. The preferential association of Hsc70 with surface DCC further implies that Hsc70 in part regulates surface DCC localization or stability. Indeed we show that Hsc70 chaperone activity is required for the sustained enrichment of surface

DCC in cortical growth cones downstream of netrin-1. Recruitment of DCC to the plasma membrane is important for netrin-1-induced axon guidance in cortical neurons. To date, a few mechanisms have been demonstrated that support netrin-1-induced DCC surface targeting from intracellular pools, including depolarization, activation of protein kinase A, and RhoA inhibition [467,472,516]. We have previously reported that Trio supports the growth cone enrichment of surface DCC downstream of netrin-1 in cortical neurons [257]. The Hsc70 ATPase activity is required for the stabilized enrichment of surface DCC at cortical growth cones treated with netrin-1. Therefore, we postulate that Hsc70 and Trio function by supporting the enrichment of surface DCC or permitting the mobilization of DCC from intracellular pools to the plasma membrane to allow a proper chemoattractive response of growth cones to netrin-1 (Fig. 3.7). Although further studies are required to delineate how Trio and Hsc70 contribute to surface DCC localization, one interesting possibility is local exocytosis of DCC-embedded vesicles. Indeed, axon outgrowth relies on the plasma membrane insertion at the leading edge of the extending growth cone, and downstream of netrin-1 exocytosis of vesicles is instrumental in this process [405,474]. Exocytosis and membrane fusion are mediated by the SNARE complex comprising a v-SNARE such as VAMP-2 (vesicle-associated membrane protein 2) and plasma membrane t-SNAREs, SNAP25 (synaptosomal-associated protein 25) and syntaxin-1 [475]. DCC forms a complex with syntaxin-1 downstream of netrin-1, and in this way induces the local exocytosis of VAMP-2-expressing vesicles during axon outgrowth [405]. Furthermore, the E3 ubiquitin ligase TRIM9 associates directly with both SNAP-25 and DCC, and promotes netrin-1-dependent axon branching in cortical neurons [474]. Interestingly, Hsc70 is closely linked to the exocytotic machinery at synapses by

associating with CSPα (vesicular cysteine-string protein-α) and SNAP25, enabling a SNARE complex formation at the plasma membrane [517]**.** As well, another TRIM protein, TRIM22 has been recently connected to the Hsc70-partner CHIP (carboxyl terminus of Hsc70-interacting protein) [518], suggesting that Hsc70 may contribute in part to DCC-driven exocytosis through a TRIM9/SNAP25-dependent mechanism.

Although some evidence supports the ability for neurons to regenerate and form functional contacts following CNS injury, our knowledge of the cellular mechanisms underlying these processes and treatments for these conditions remain incomplete (reviewed in [519]). Dysfunction of Hsc70 has been implicated in various neurodegenerative disorders including Huntington's, Parkinson's, and Alzheimer's diseases [520-523]. To our knowledge this is the first study to implicate Hsc70 in the regulation of Rac1-dependent cellular processes, raising the possibility that Rac1 dysregulation in neurons may contribute to the pathophysiology of neurodegenerative diseases [51]. Indeed, Hsc70 expression is induced in response to cerebral ischemia, thus supporting a role for Hsc70 in axon regeneration and repair [524,525]. It will be of great interest to investigate whether selectively augmenting Hsc70 chaperone activity will promote nerve re-growth in the context of neurodegeneration.

Materials and methods

DNA constructs and antibodies. GFP-Trio and deletion mutants, GFP-Hsc70, GFP-Hsc70 ^{D10N}, and pRK5-DCC constructs have been described previously [118,244,465,526]. The polyclonal anti-TrioMTP antibody was generated as previously described [257]. Additional antibodies: anti-DCC_{INT} (clone G97-449, BD Biosciences), anti-DCC_{EXT} (clone AF5, Calbiochem), anti-pERK1/2 (pThr202/pThr204) and anti-ERK1/2 (Cell Signaling), anti-pFAK (pY861) and anti-FAK (Invitrogen), anti-GFP (Invitrogen), anti-Hsc70 (clone B-6; Santa Cruz), anti-Hsp70 (Enzo Life Sciences), anti-Rac1 (BD Transduction Laboratories), anti-tubulin (Upstate), anti-rabbit-Alexa-488 and anti-mouse-Cy3 (Molecular Probes).

Cell culture and transfection. HEK293 cells were cultured at 37°C in Dulbecco's modified Eagle's medium (DMEM, Wisent Bioproducts) supplemented with 10% fetal bovine serum (FBS), 2mM L-glutamine, penicillin and streptomycin (Invitrogen) under humidified conditions with 5% CO_2. Cells were transfected with the indicated constructs using linear polyethylenimine (PEI, PolySciences) at a 1:10 ratio (cDNA: PEI) as described previously [257].

Primary cortical neuron culture and electroporation. Cortical neurons from E17.5 rat embryos were dissociated mechanically, and electroporated with cDNA constructs or siRNAs as indicated using the Amaxa Rat Neuron Nucleofector Kit (Lonza). Post-electroporation, neurons were plated on either poly-D-lysine (0.1 mg/ml, Sigma-Aldrich)-coated dishes, or poly-L-lysine (0.1 mg/ml, Sigma-Aldrich)-treated coverslips in 24-well plates at a density of 200,000 cells/well. Neurons were cultured in attachment medium

(DMEM, 10% FBS (Wisent Bioproducts) supplemented with 2mM L-glutamine, penicillin and streptomycin (Invitrogen) under humidified conditions with 5% CO_2. After 1.5h, the medium was replaced with maintenance medium (Neurobasal-A medium (Invitrogen), supplemented with 2% B27 (Invitrogen), 1% L-glutamine, penicillin and streptomycin (Invitrogen)). At DIV1 or DIV2, the neurons were treated for the indicated times with purified recombinant chick myc-netrin-1 (500 ng/ml), which was produced and purified as described previously [444]. Down-regulation of endogenous Hsc70 was achieved by electroporating dissociated E17.5 rat cortical neurons with 150nM synthetic Hsc70 siRNAs designed to target the 5'-UTR of the rat Hsc70 mRNA (5'-UCUGUGUGGUCUCGUCAUCUU-3', Dharmacon/Thermo Scientific) together with 4µg of pmaxGFP vector (Lonza) used as a reporter. Only GFP-expressing neurons were assessed. The siRNA-resistant GFP-Hsc70 or GFP-Hsc70 ^{D10N} plasmids were co-electroporated where indicated, and expression of the exogenous proteins was verified by western blotting (Fig. 3.2G). Similarly, downregulation of Trio was achieved by electroporating 300 nM synthetic Trio siRNA (5'-GAACAUGAUUGACGAGCAUUU-3', Dharmacon Thermo Scientific) as previously described [257].

Cortical tissue culture. Cortical tissues were extracted from E17.5 rat embryos. After light mechanical dissociation, tissues were transferred to a 4-well plate containing pre-warmed maintenance medium and allowed to equilibrate to 37°C. Immediately following netrin-1 stimulation, samples were transferred to ice, collected and processed as described [257].

Mass Spectrometry Analysis. E17.5 rat cortical tissue was treated with 500ng/ml netrin-1 for 5 min, and protein lysates were collected and subsequently probed with anti-Trio antibodies conjugated to Protein-A-Sepharose beads. Antibody-protein complexes were resolved by SDS-PAGE, and proteins were visualized by silver staining. A prominent band of ~65-75 kDa was extracted from the gel and proteins were digested with trypsin and chymotrypsin. Peptide samples underwent mass spectrometric analysis (QTRAP4000 and MALDI-TOF, Genome Innovation Centre, Montreal). Mascot searches of resulting sequences were performed using the UniProt database with a rat filter, and identified 5 peptides corresponding to Hsc70.

Immunoprecipitation and Immunoblotting. Cortical tissues were lysed in buffer containing 20 mM HEPES, pH 7.5, 100 mM NaCl, 10% glycerol, 1% Triton X-100, 20 mM sodium fluoride, 1 mM sodium orthovanadate, 1 mM phenylmethylsulfonyl fluoride (PMSF), and 1 µg/ml aprotinin and leupeptin (Bio Shop). Protein lysates were centrifuged at 10,000 × *g* for 5 min at 4°C to remove insoluble materials. For immunoprecipitation from primary cortical lysates, 1 mg of protein lysate underwent pre-clearing with Protein-A- or -G-Sepharose beads for 1h at 4°C. Supernatants were then incubated for 1h at 4°C with 9 µg of anti-TrioMTP or 1.5 µg of anti-DCC (AF-5) followed by addition of 40 µl Protein-A- or -G-Sepharose beads for 2h (GE Healthcare). Beads were washed a minimum of four times with ice-cold lysis buffer and heated to 95°C in SDS sample buffer. Protein samples were resolved by SDS-PAGE, transferred to nitrocellulose membranes for immunoblotting with the appropriate antibodies, and visualized by enhanced chemiluminescence (ECL; PerkinElmer). For surface and intracellular DCC immunoprecipitations, cortical neurons were treated with or without

500 ng/ml of netrin-1 for 5 min and transferred to ice. Cells were then washed with ice cold PBS containing 1mM magnesium chloride and 0.1mM calcium chloride and then blocked in ice-cold 1% BSA/PBS for 20 min. Following blocking, the cells were incubated with either mouse IgGs or anti-DCC_{EXT} (AF-5) antibodies at 1 µg/ml in ice-cold PBS for 40 min on ice, followed by 3, 5 min washes with cold PBS. Proteins were extracted with RIPA buffer (150 mM NaCl, 50 mM 4-(2-hydroxyethyl)-1-piperazineethanesulfonic acid, pH 7.5, 1% NP-40, 10 mM EDTA, pH 8.0, 0.5% sodium deoxycholate, 0.1% SDS, 20 mM sodium fluoride, 1 mM sodium orthovanadate, 1 mM phenylmethylsulfonyl fluoride (PMSF), and 1 µg/ml aprotinin and leupeptin (Bio Shop)), and protein lysates were centrifuged at 10,000 × *g* for 5 min at 4°C. Surface DCC was isolated by incubation with Protein-G-Sepharose beads for 1h at 4°C. The supernatant corresponding to the intracellular DCC pool was collected for each sample, and immunoprecipitations were subsequently performed with either IgGs or anti-DCC, as described above.

Rac1 activation assay. Transfected HEK293 cells were serum-starved overnight, then lysed in buffer containing 25 mM HEPES, pH 7.5, 1% NP-40, 10 mM $MgCl_2$, 100 mM NaCl, 5% glycerol, 1 mM PMSF, and 1 µg/ml aprotinin and leupeptin (Bio Shop). Protein lysates were centrifuged at 10,000 × *g* for 2 min at 4°C to remove insoluble materials. Endogenous GTP-Rac1 was pulled down by incubating the protein lysates for 30 min at 4°C with the Cdc42/Rac interactive binding domain (CRIB) of mouse PAK3 (amino acids 73-146) fused to GST and coupled to glutathione-sepharose beads. The beads were washed twice with 25 mM HEPES, pH 7.5, 1% NP-40, 30 mM $MgCl_2$, 40 mM NaCl, and 1 mM DTT and resuspended in SDS sample buffer. Protein samples were

resolved by SDS-PAGE and transferred onto nitrocellulose membranes for immunoblotting with the anti-Rac1 antibody. The levels of GTP-bound Rac1 were assessed by densitometry using Quantity One software (Bio-Rad) and normalized to the total amount of GTPases detected in the total cell lysates.

Immunofluorescence, microscopy and Pearson's correlation coefficient. Cortical neurons (DIV1 or 2) were fixed with 3.7% formaldehyde (Sigma-Aldrich) in 20% sucrose/PBS for 30 min at 37°C and permeabilized as described previously [257]. Immunostaining was carried out with the indicated primary antibodies and the respective Cy3 or Alexa-488-conjugated secondary antibodies. To assess protein colocalization, co-immunostained cortical neurons were imaged on a Zeiss LSM510 laser-scanning confocal microscope with a PLAN-Apochromat 63x/1.4 oil immersion objective lens and analyzed with Zen2009 software (Carl Zeiss Microscopy). Quantification of colocalization using Pearson's correlation coefficient (*r*) was performed using MetaMorph software, analyzing more than 15 neurons per condition in at least 3 independent experiments. One way ANOVA statistical analysis was performed, and the data were presented as a mean *r* ± SEM. For axon outgrowth assays, neurons were visualized with an Olympus IX81 motorized inverted microscope using a 40X U PLAN Fluorite oil immersion objective lens. Images were recorded with a CoolSnap 4K camera (Photometrics) and analyzed with Metamorph software (Molecular Devices). For surface DCC detection, cortical neurons remained unpermeabilized, were blocked in 1% BSA/PBS and incubated with anti-DCC_{EXT} in 1% BSA/PBS at 4°C overnight. Cy3-conjugated secondary antibodies were used to label surface DCC. Images were acquired as for the axon outgrowth experiments, and the average pixel intensity of DCC

fluorescence on growth cones and axonal surfaces was measured from acquired images using Metamorph software, employing exclusive thresholding to eliminate background fluorescence.

Axon outgrowth analysis and Dunn chamber assays. To analyze axon outgrowth of primary cortical neurons (2DIV), electroporated (GFP-positive) cells were analyzed for each condition from at least three independent experiments. Axon lengths were measured manually from acquired images with MetaMorph software. One-way ANOVA with Fisher's LSD post-test was used for statistical analysis, and the data were presented as the mean cortical neuron axon length ± SEM. For turning assays, dissociated cortical neurons (2DIV) were plated on coverslips used for Dunn chamber assembly as previously described [506]. Gradients were generated with purified netrin-1 VI-V (200 ng/ml) or buffer containing PBS in the outer well. Cell images were acquired every 3–4 min for at least 90 min on a temperature controlled stage. Neurites of at least 10 µm length were tracked in GFP-expressing neurons. The final position of the growth cone was used to determine the angle turned over 90 min relative to the gradient position. Measurements are presented in rose histograms in bins of 10° with the length of each segment representing the frequency of measurements in percent. Mean turning angle and mean displacement are also represented.

Statistical analysis. Statistical analysis was performed with GraphPad Prism 6. The data are presented as the mean ± the standard error of the mean (SEM).

Acknowledgements

We are grateful to Jerome Boudeau for the anti-Trio antibodies. We thank Min Fu and the imaging core facility of the Research Institute of the McGill University Health Centre (RI-MUHC) for assistance with confocal microscopy. We also thank Line Roy and Daniel Boismenu for their assistance with the mass spectrometry analysis. Funding: This research was supported by Canadian Institute of Health Research (CIHR) Grant MOP-14701 and the Canada Foundation for Innovation-Leaders Opportunity Fund to NLV. N.L.V. is a recipient of a Fonds de la Recherche en Santé du Québec Chercheur-National and a William Dawson Scholar.

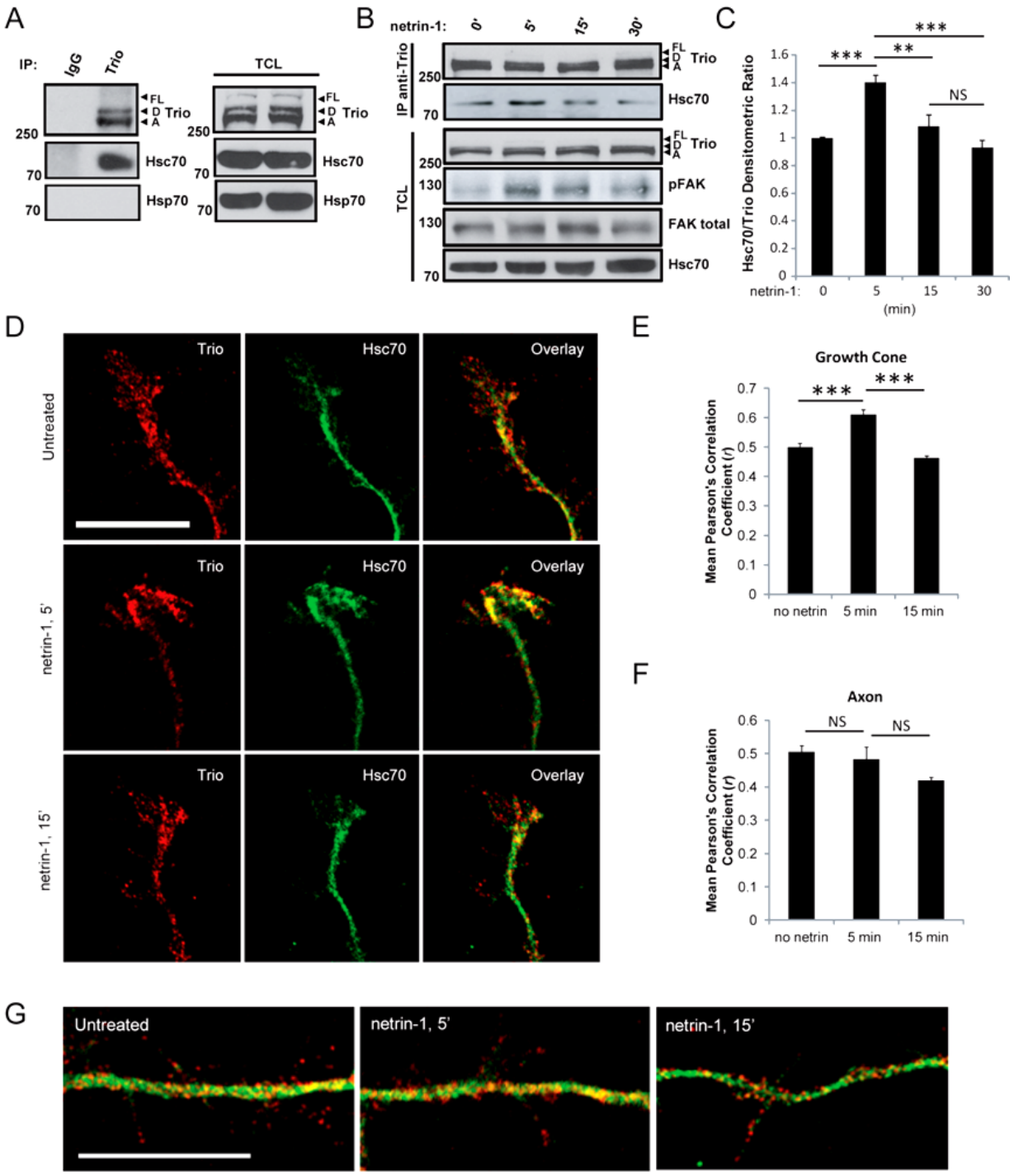
A
IP:
IgG
Trio
TCL
FL
D
A
Trio
250
70
Hsc70
Hsp70
B
netrin-1:
0'
5'
15'
30'
IP anti-Trio
TCL
130
pFAK
FAK total
C
Hsc70/Trio Densitometric Ratio
***
**
NS
netrin-1:
0
5
15
30
(min)
D
Trio
Hsc70
Overlay
Untreated
netrin-1, 5'
netrin-1, 15'
E
Growth Cone
Mean Pearson's Correlation Coefficient (r)
no netrin
5 min
15 min
F
Axon
G
Untreated
netrin-1, 5'
netrin-1, 15'

Figure 3.1 – The molecular chaperone Hsc70 associates with Trio in the developing cerebral cortex

(A) Trio was immunoprecipitated from lysates of isolated E17.5 rat cortices with anti-Trio antibodies or rabbit immunoglobulin G (IgG) as a control. Immunoprecipitated proteins (IP) and total cell lysates (TCL) were resolved by SDS-PAGE and immunoblotted with the indicated antibodies. Trio isoforms: FL= Full length, D = Trio-D, A= Trio-A. (B) Isolated E17.5 rat cortices were stimulated with netrin-1 for the indicated times. Trio isoforms were immunoprecipitated (IP) and Hsc70 co-IP with Trio was assessed by immunoblotting. Netrin-1 stimulation of DCC-induced signaling pathways was assessed by evaluating FAK phosphorylation (Y861) in total cell lysates (TCL). (C) Densitometric analysis of Hsc70 co-association with Trio. Error bars indicate the standard error of the mean (SEM) (n=4; **p<0.01, ***p<0.001; One-way ANOVA, Bonferroni's multiple comparisons test). (D, G) Dissociated E17.5 rat cortical neurons were stimulated with netrin-1 for 5, and 15 min before fixation. Endogenous Trio and Hsc70 localization were assessed by indirect immunofluorescence and confocal microscopy. Scale bar, 2μm. (E, F) The mean Pearson's Correlation Coefficient (*r*) between green (Hsc70) and red (Trio) channels within the growth cone (E) or axon shaft (F) was calculated with Metamorph software. Error bars indicate the SEM (n=3, NS p>0.05, ***p<0.001; One-way ANOVA, Bonferroni's multiple comparisons test).

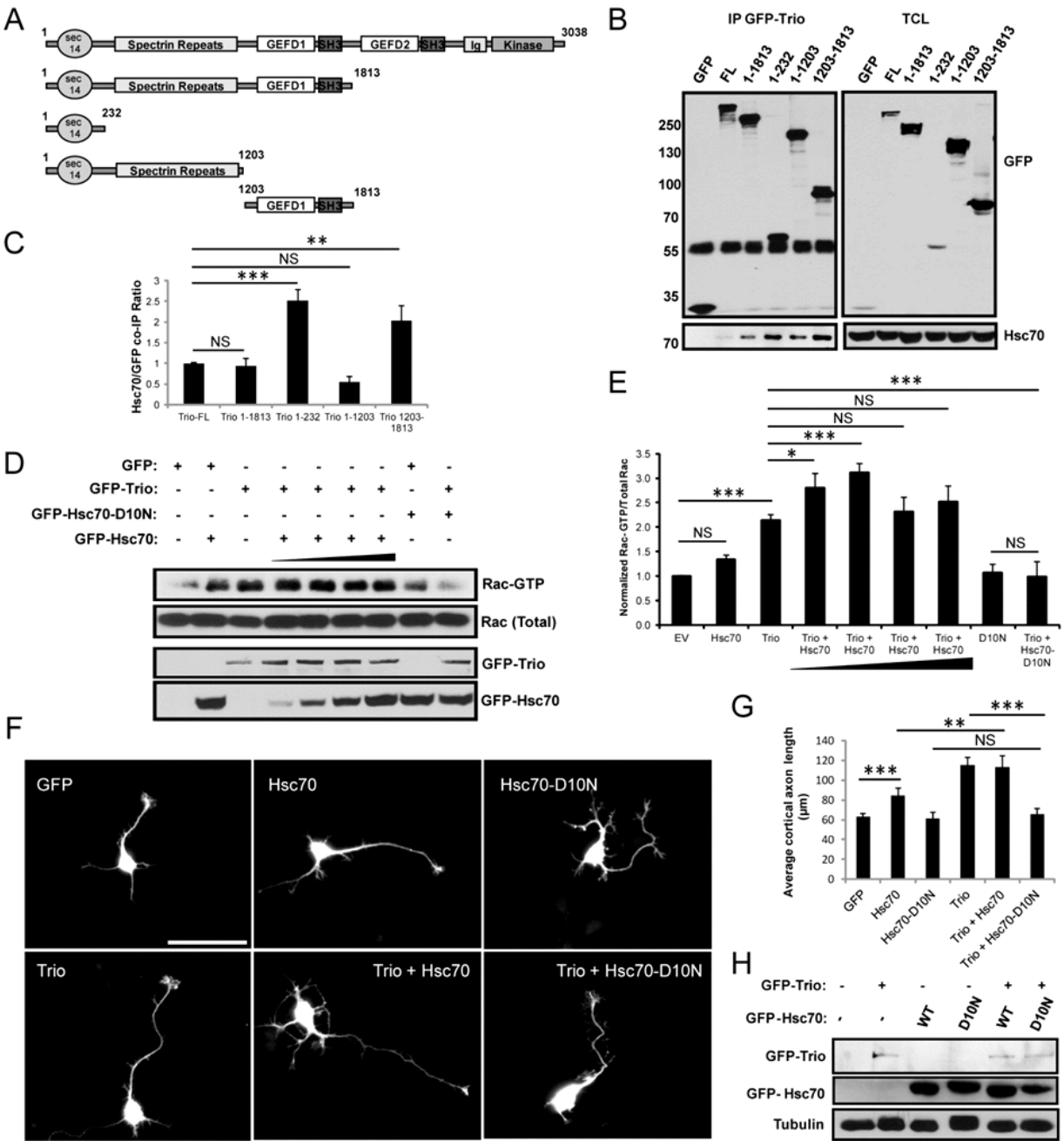
A
Sec 14
Spectrin Repeats
GEFD1
SH3
GEFD2
Ig
Kinase
3038
1813
232
1203
B
IP GFP-Trio
TCL
GFP
FL
1-1813
1-232
1-1203
1203-1813
250
130
100
70
55
35
GFP
Hsc70
C
Hsc70/GFP co-IP Ratio
NS
**
***
Trio-FL
Trio 1-1813
Trio 1-232
Trio 1-1203
Trio 1203-1813
D
GFP:
GFP-Trio:
GFP-Hsc70-D10N:
GFP-Hsc70:
Rac-GTP
Rac (Total)
GFP-Trio
GFP-Hsc70
E
Normalized Rac-GTP/Total Rac
EV
Hsc70
Trio
Trio + Hsc70
D10N
Trio + Hsc70-D10N
F
GFP
Hsc70
Hsc70-D10N
Trio
Trio + Hsc70
Trio + Hsc70-D10N
G
Average cortical axon length (μm)
H
GFP-Trio:
GFP-Hsc70:
WT
D10N
GFP-Trio
GFP- Hsc70
Tubulin

Figure 3.2 – Hsc70 facilitates Trio-dependent Rac1 activation and cortical axon outgrowth in a chaperone-dependent manner

(A) Schematic of Trio domain structure. (B) Trio constructs were transfected into HEK293 cells as indicated. GFP-Trio proteins were immunoprecipitated (IP) from cell lysates and Hsc70 co-IP with Trio was detected by immunoblotting (IB). TCL: total cell lysates. (C) Densitometric analysis of Hsc70 co-associated with GFP-Trio constructs. Error bars indicate the standard error of the mean (SEM) (n=4; NS $p>0.05$, $^{**}p<0.01$, $^{***}p<0.001$; One-way ANOVA, Bonferroni's multiple comparisons test). (D) HEK293 cells were transfected with the indicated constructs, and with increasing amounts of GFP-Hsc70 plasmid. GTP-loaded Rac1 was pulled down from protein lysates by GST-CRIB. GTP-bound Rac1, total Rac1 and the indicated proteins were detected by immunoblotting. (E) Densitometric ratio of GTP-bound Rac1/Total Rac1 normalized to the vector control. Error bars indicate the SEM (n=4, NS $p>0.05$, $^{*}p<0.05$, $^{**}p<0.01$, $^{***}p<0.001$, $^{****}p<0.0001$, One-way ANOVA, Bonferroni's multiple comparisons test). (F) Dissociated E17.5 rat cortical neurons were electroporated with the indicated constructs and a GFP-reporter. Scale bar, 50μm. (G) The average axon lengths of GFP-positive neurons were calculated manually with Metamorph software (>15 neurons/per condition). Error bars indicate the SEM (n=3, NS $p>0.05$, $^{***}p<0.001$, $^{****}p<0.0001$, One-way ANOVA, Bonferroni's multiple comparisons test). (H) Representative protein expression of electroporated constructs in E17.5 cortical neurons from (F).

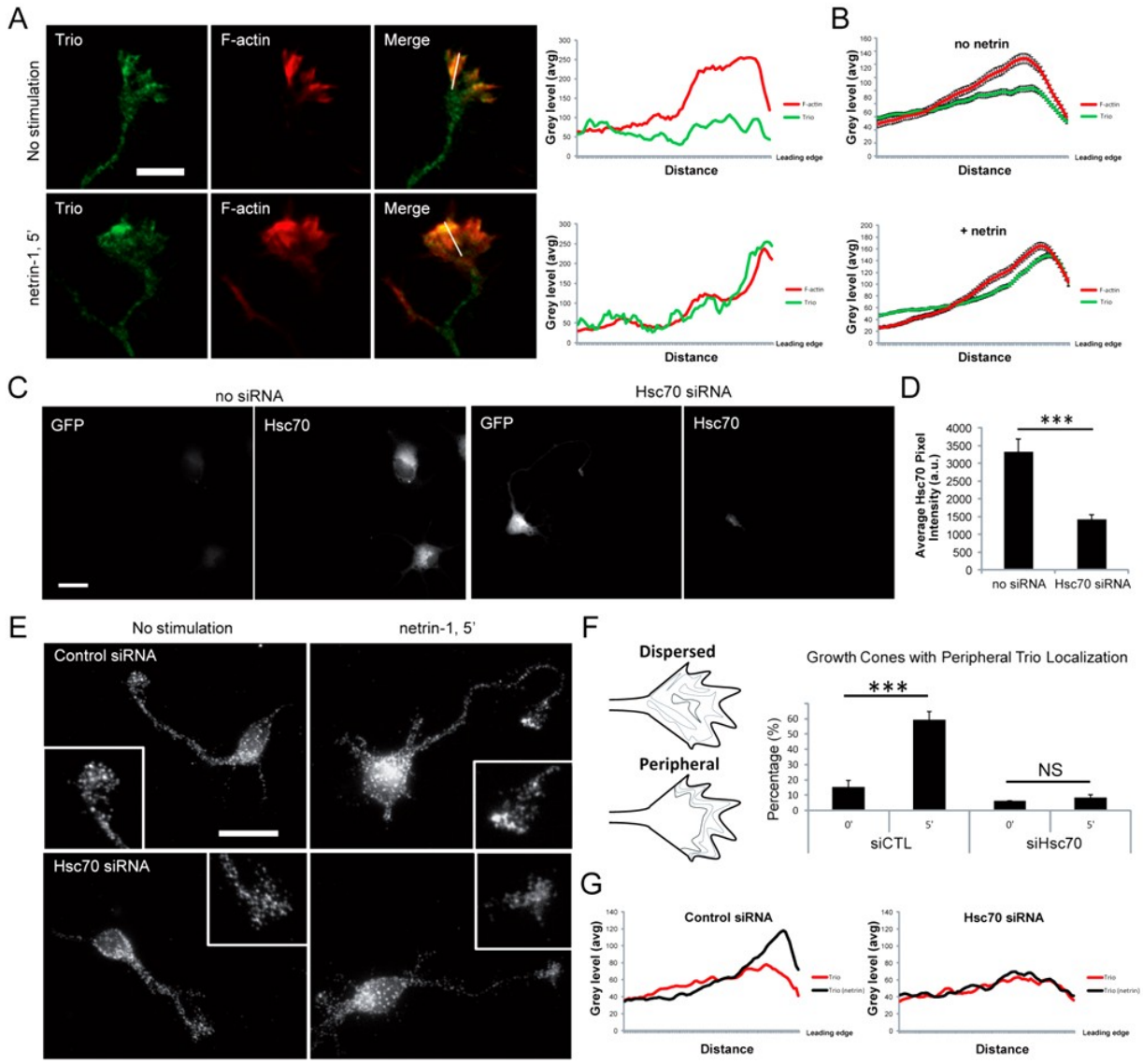
A
Trio
F-actin
Merge
No stimulation
netrin-1, 5'
Grey level (avg)
Distance
Leading edge
F-actin
Trio
B
no netrin
+ netrin
C
no siRNA
Hsc70 siRNA
GFP
Hsc70
D
Average Hsc70 Pixel Intensity (a.u.)
***
no siRNA
Hsc70 siRNA
E
No stimulation
netrin-1, 5'
Control siRNA
Hsc70 siRNA
F
Dispersed
Peripheral
Growth Cones with Peripheral Trio Localization
Percentage (%)
***
NS
0'
5'
siCTL
siHsc70
G
Control siRNA
Hsc70 siRNA
Trio
Trio (netrin)

Figure 3.3 – Hsc70 is required to recruit Trio to the growth cone periphery of netrin-1-stimulated cortical neurons

(A) Dissociated E17.5 rat cortical neurons were left untreated, or stimulated with netrin-1 for 5 min before fixation. Endogenous Trio and F-actin localization were assessed epifluorescence microscopy. Scale bar, 10μm. The intensity of Trio and F-actin fluorescence along a 10μm linescan oriented in the central-to-peripheral axis of each growth cone was calculated using Metamorph software. Right panel: sample of Trio (green) and F-actin (red) pixel intensity plotted against distance from the adjacent micrographs. (B) The mean pixel intensity of Trio (green) and F-actin (red) plotted against distance, without (upper) or with netrin-1 (lower). Error bars indicate the SEM (n>100 growth cones). (C) Dissociated E17.5 rat cortical neurons were electroporated with a GFP-reporter, and Hsc70 siRNA. At 1 DIV, cultures were fixed and levels of endogenous Hsc70 were assessed by indirect immunofluorescence. Scale bar, 15μm. (D) The average pixel intensity of Hsc70 in either GFP-negative or GFP-positive neurons was calculated using Metamorph software. Error bars indicate the SEM (n= 3, GFP-negative neurons=19, GFP-positive neurons= 20, ***$p<0.001$, Unpaired student's t-test). (E) As in (C) dissociated E17.5 rat cortical neurons were electroporated with a GFP-reporter, and control siRNA or Hsc70 siRNA, and left untreated or treated with netrin-1 for 5 min before fixation. Trio localization was assessed by indirect immunofluorescence (>15 neurons/per condition). Scale bar, 15μm. (F) Left: schematic of Trio localization, showing dispersed localization vs. peripheral enrichment. Right: the proportion of electroporated neurons with growth cones harboring a distinct peripheral Trio localization was calculated for each treatment in (E). Error bars indicate the SEM

(n=4, ***p<0.001, Unpaired student's t-test). (G) As in (B), the mean pixel intensity of Trio without (red) and with netrin-1 treatment (black) was calculated along 10 μm linescans oriented in the central-to-peripheral axis of each growth cone from (E) using Metamorph software. Left: control siRNA, Right: Hsc70 siRNA (n>65 growth cones per condition).

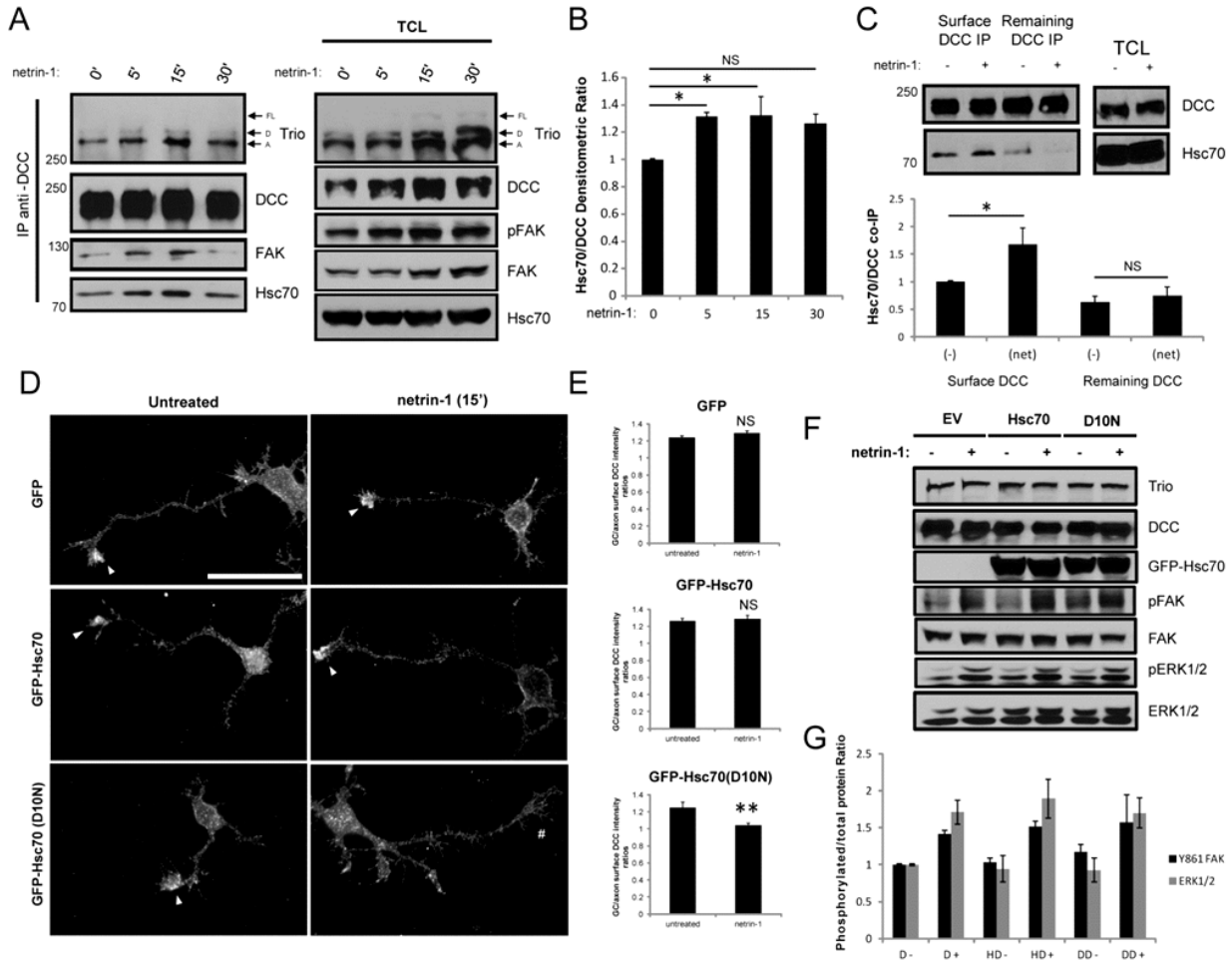
A
TCL
netrin-1:
0'
5'
15'
30'
IP anti-DCC
Trio
DCC
FAK
Hsc70
pFAK
B
Hsc70/DCC Densitometric Ratio
NS
netrin-1: 0 5 15 30
C
Surface DCC IP
Remaining DCC IP
TCL
Hsc70/DCC co-IP
Surface DCC
Remaining DCC
D
Untreated
netrin-1 (15')
GFP
GFP-Hsc70
GFP-Hsc70 (D10N)
E
F
EV
Hsc70
D10N
pERK1/2
ERK1/2
G
Phosphorylated/total protein Ratio
Y861 FAK
ERK1/2

Figure 3.4 – Hsc70 associates with a DCC multiprotein signaling complex in the developing cortex downstream of netrin-1 and supports DCC cell surface localization

(A) Isolated E17.5 rat cortices were stimulated with netrin-1 for the indicated times. DCC was immunoprecipitated (IP) and the level of Trio, FAK and Hsc70 co-IP with DCC was assessed by immunoblotting. (B) Densitometric analysis of Hsc70 co-association with DCC. Error bars indicate the standard error of the mean (SEM) (n=4; NS, $p>0.05$, *$p<0.05$; One-way ANOVA, Dunnett's multiple comparisons test). (C) Cortical neurons were dissociated and treated with netrin-1 at DIV2, followed by surface DCC isolation. Subsequent IP of lysates depleted of surface DCC were performed and the level of Hsc70 co-IP with DCC was assessed by immunoblotting. Lower: densitometric analysis of Hsc70 co-association with either surface or intracellular DCC. Error bars indicate the standard error of the mean (SEM) (n=4; NS, $p>0.05$, *$p<0.05$; Unpaired student's t-test). (D) Isolated E17.5 rat cortical neurons were electroporated with the indicated Hsc70 constructs. At DIV1 the neurons were treated with netrin-1 for 15 min before fixation. Surface DCC was assessed by staining with an extracellular-DCC antibody under non-permeabilizing conditions, and subsequent fluorescence microscopy. Scale bar, 50 μm (▲ denotes enchrichment; # denotes no enrichment). (E) The average pixel intensity ratios of surface DCC at the growth cones relative to axons were calculated using Metamorph software (>15 neurons/per condition). Error bars indicate the SEM (n=4, **$p<0.01$, Unpaired student's t-test). (F) HEK293 cells were transfected with DCC and the indicated Hsc70 constructs, and were treated with netrin-1 for 5 min before lysis. Protein extracts were resolved by SDS-PAGE and the levels of active ERK1/2 and FAK

were assessed by immunoblotting. (G) Densitometric analysis of pERK1/2 and pFAK (Y861) from (F). Error bars indicate the standard error of the mean (SEM) (n=4).

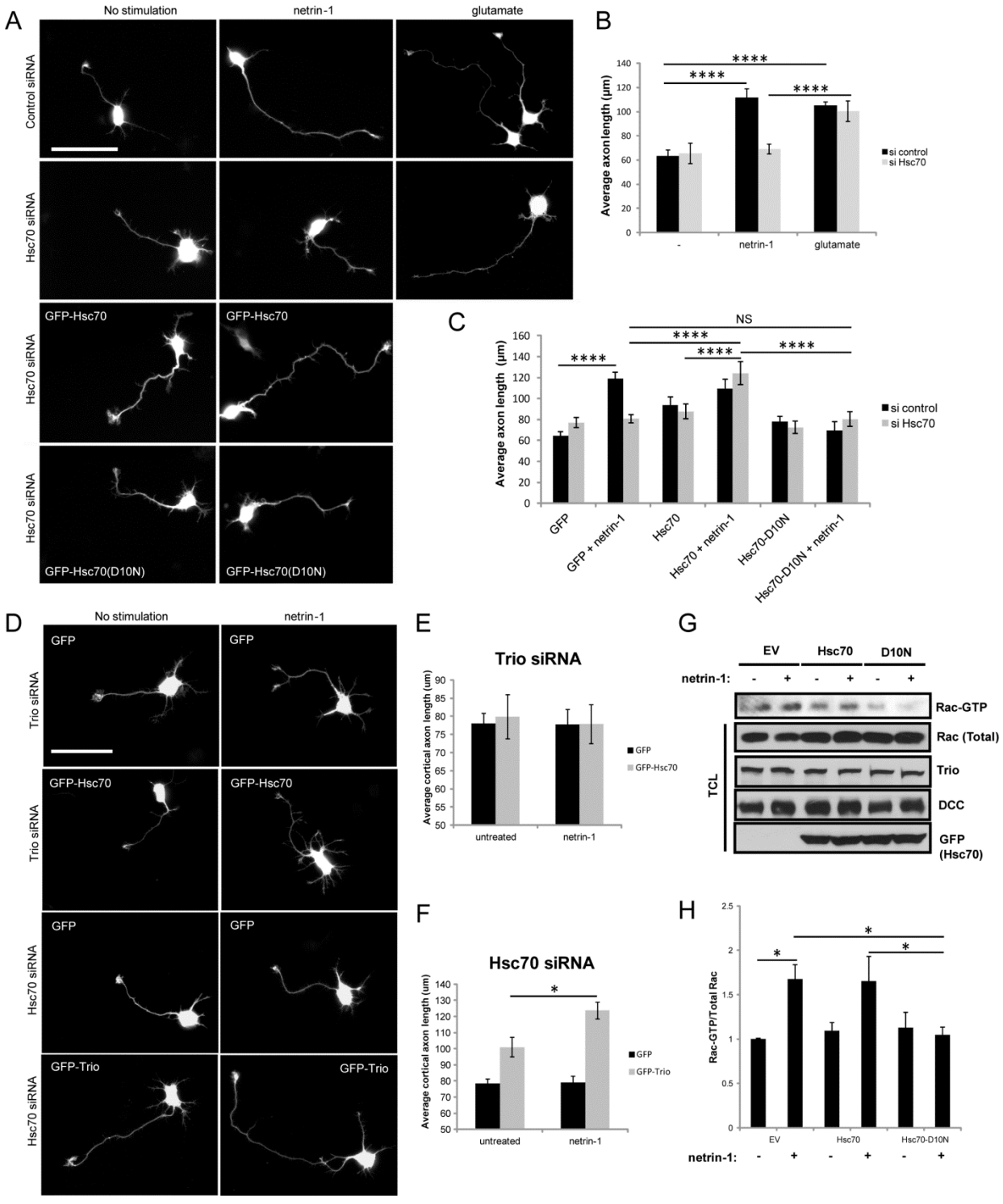
A
No stimulation
netrin-1
glutamate
Control siRNA
Hsc70 siRNA
GFP-Hsc70
GFP-Hsc70(D10N)
B
Average axon length (μm)
si control
si Hsc70
netrin-1
glutamate
C
NS
GFP
GFP + netrin-1
Hsc70
Hsc70 + netrin-1
Hsc70-D10N
Hsc70-D10N + netrin-1
D
Trio siRNA
GFP-Trio
E
Trio siRNA
Average cortical axon length (um)
untreated
F
Hsc70 siRNA
G
EV
Hsc70
D10N
netrin-1:
Rac-GTP
Rac (Total)
Trio
DCC
GFP (Hsc70)
TCL
H
Rac-GTP/Total Rac

Figure 3.5 – Hsc70 is required for netrin-1-mediated cortical axon outgrowth and Rac1 activation

(A) Dissociated E17.5 rat cortical neurons were electroporated with control siRNA or Hsc70 siRNA with a GFP-reporter construct or the indicated GFP constructs. At DIV1, neurons were stimulated with netrin-1 or glutamate for 24h. Scale bar, 50μm. (B, C) The average axon lengths of GFP-positive neurons from (A) were calculated manually using Metamorph software (>15 neurons/per condition). Error bars indicate the SEM (n=3, ****p<0.0001, One way ANOVA, Fisher's LSD post-test). (D) E17.5 rat cortical neurons were depleted of endogenous Trio and Hsc70 by siRNA and re-expressed both with siRNA-resistant Hsc70 and Trio. (E, F) The average axon lengths of GFP-positive neurons were calculated as in (B). Error bars indicate the SEM (n=4, *p<0.05, Unpaired student's t-test). (G) HEK293 cells were transfected with pRK5-DCC with empty vector (EV), GFP-Hsc70 or GFP-Hsc70 ^{D10N}, and stimulated with netrin-1 for 5 min. GTP-loaded Rac1 was pulled down from protein lysates by GST-CRIB. GTP-bound Rac1 (top panel), total Rac1, and the indicated proteins were detected by immunoblotting. TCL = Total cell lysates. (H) Densitometric ratio of GTP-bound Rac1/Total Rac1 normalized to DCC. Error bars indicate the SEM (n=4, *p<0.05, One-way ANOVA, Bonferroni's multiple comparisons test).

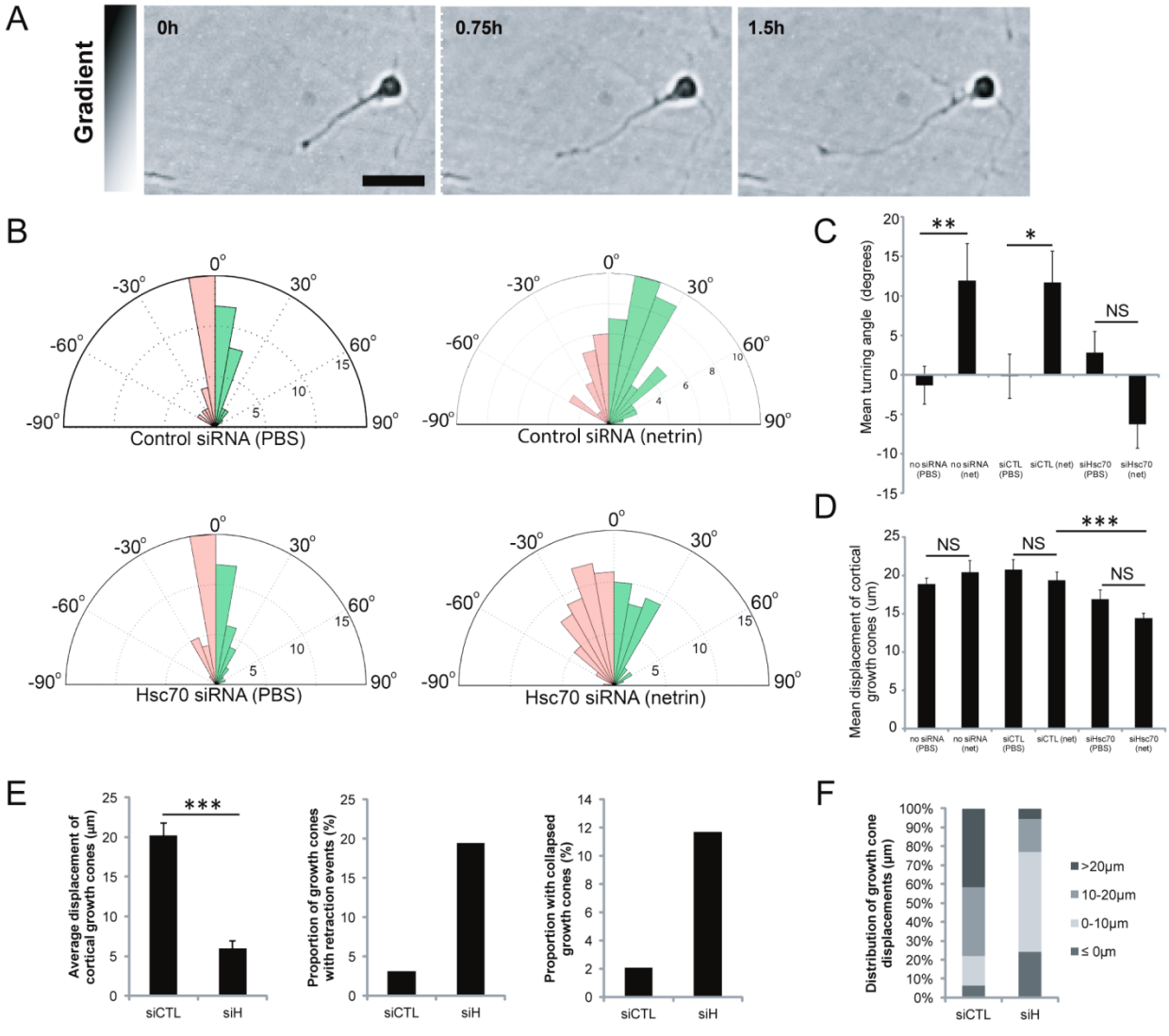
A
Gradient
0h
0.75h
1.5h
B
Control siRNA (PBS)
Control siRNA (netrin)
Hsc70 siRNA (PBS)
Hsc70 siRNA (netrin)
C
Mean turning angle (degrees)
**
*
NS
no siRNA (PBS)
no siRNA (net)
siCTL (PBS)
siCTL (net)
siHsc70 (PBS)
siHsc70 (net)
D
Mean displacement of cortical growth cones (um)
NS
NS
***
NS
E
Average displacement of cortical growth cones (µm)
***
siCTL
siH
Proportion of growth cones with retraction events (%)
Proportion with collapsed growth cones (%)
F
Distribution of growth cone displacements (µm)
>20µm
10-20µm
0-10µm
≤ 0µm

Figure 3.6 – Hsc70 is required for netrin-1-dependent attraction of embryonic cortical neurons

Control (CTL) or Hsc70 siRNA (siHsc70) was electroporated with a GFP-reporter plasmid in E17.5 cortical neurons. At DIV2, neurons were exposed to vehicle PBS or a 200 ng/ml netrin-1 VI-V (net) gradient in Dunn chamber turning assays. (A) Video time-lapse imaging of control neurons exposed to a gradient for 90 min. Scale bar, 20 μm. (B) Mean turning angles for each condition. Error bars indicate the SEM (n>50 axons per condition, NS $p>0.05$, *$p<0.05$, **$p<0.01$, One way ANOVA, Newman-Keuls multiple comparisons test). (C) Rose histograms represent the distribution of turning angles of the cortical neurons in (B). (D) The mean displacement of turning cortical growth cones over the 90 min imaging period. Error bars indicate the SEM (n>50 axons per condition, NS $p>0.05$, ***$p<0.001$, One way ANOVA, Newman-Keuls multiple comparisons test). (E) Left: the mean displacement of all cortical growth cones over the 90-minute imaging period. Error bars indicate the SEM (***$p<0.001$; Unpaired student's t-test). Middle: the proportion of growth cones with at least one retraction event. Right: the proportion of growth cones with net retraction. (F) The distribution of growth cone displacements from (E).

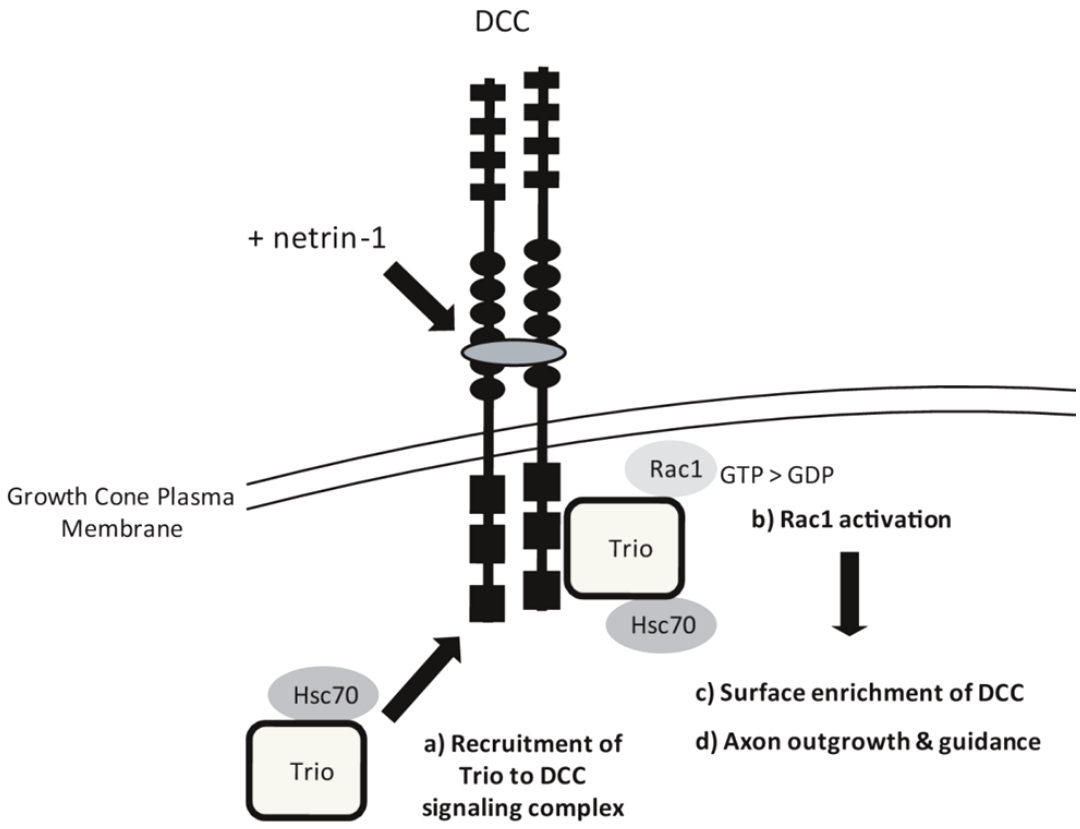
DCC
+ netrin-1
Growth Cone Plasma Membrane
Rac1
GTP > GDP
b) Rac1 activation
Trio
Hsc70
Hsc70
Trio
a) Recruitment of Trio to DCC signaling complex
c) Surface enrichment of DCC
d) Axon outgrowth & guidance

Figure 3.7 – Model of Trio regulation by Hsc70 during netrin-1/DCC signaling

Netrin-1/DCC engagement results in recruitment of Trio and Hsc70 to DCC signaling complexes (A). Hsc70 chaperone activity is required for netrin-1-induced activation of Rac1 (B), surface DCC enrichment at the growth cone plasma membrane (C), and axon outgrowth and guidance downstream of netrin-1 (D). Therefore, we propose that Hsc70-mediated regulation of Trio is essential for the stability of the DCC/Trio signalling complex at the cell surface of growth cones in order to mediate netrin-1-induced cortical axon outgrowth and guidance.

Chapter 4: CdGAP-null mouse generation reveals a role for CdGAP in angiogenesis and central nervous system development

Jonathan DeGeer, Lou Beaulieu-Laroche, Philippe Duquette, Hidetaka Ishii, Vilayphone Luangrath and Nathalie Lamarche-Vane. (2015) In preparation.

Preface to Chapter 4

As master regulators of cytoskeletal dynamics, Rho GTPases are required for such basic processes as cell motility. While ectopic activation of Rho GTPase can lead to deleterious conditions such as invasive carcinoma, during development active Rho GTPases are required for the formation of all tissues and vessels. To date, transgenic mouse models have proven to be invaluable in defining the role and function of Rho GTPases and their regulators *in vivo*. In order to evaluate the function of CdGAP *in vivo*, we have generated a CdGAP germ-line knockout mouse model. Herein we describe the vascular defects present in CdGAP-null embryos and investigate the function of CdGAP during development. We further document the differences between CdGAP null embryonic neurons relative to neurons from wild type littermates and reveal a novel role for CdGAP in regulating crosstalk between the vasculature and neurons.

Abstract

Cdc42 GTPase-activating protein (CdGAP) is a GAP for the well characterized Rho family members Rac1 and Cdc42. Despite being enriched in the adult and post-natal brain tissues, relatively little is known about the function of CdGAP in the CNS. In this study we began by investigating the localization of CdGAP in sub-regions of the embryonic rat brain, revealing an enrichment of CdGAP in the developing hippocampus. Generation of CdGAP-null mice revealed vascular deficits in E15.5 embryos including hemorrhaging of superficial vasculature and severe edema, resulting in 50 percent embryonic or perinatal lethality. We further assessed the brains of CdGAP-null mice and observed that the meninges surrounding the CNS were hypovascularized, indicating that loss of CdGAP may affect neuronal function. CdGAP-null dissociated cortical neurons displayed distinct gross morphological differences relative to those from wild type littermates. Additionally, VEGF treatment induced a rapid upregulation of CdGAP expression in dissociated cortical neurons; and CdGAP-deficient neurons failed to extend ectopic primary neurites in response to VEGF. In summary we demonstrate that CdGAP is a novel regulator of angiogenesis *in vivo* and implicate its function in neurons downstream of neuronal VEGF signaling.

Introduction

The proper wiring of the central nervous system (CNS) is imperative for normal physiological function and survival, and as such is a tightly regulated process. The mammalian CNS is composed of billions of neurons which undergo a conserved program of polarization, growth and maturation. Rho family GTPases are molecular switches that have been well characterized as modulators of cytoskeletal dynamics and cellular motility by cycling between an inactive GDP-bound and active GTP-bound state[5]. The Rho family of small GTPases are important regulators of cytoskeletal dynamics thathave been implicated in neuronal development including: axon specification, axon outgrowth and guidance, migration, synaptogenesis and synaptic plasticity [375,527,528]. In the context of axon growth and pathfinding, the recruitment and localized activation of the Rho GTPases Rac1, Cdc42, and RhoA, are imperative for translating guidance cues into cytoskeletal rearrangements within the extending growth cone [51,399,432,465,489]. Oversight of Rho GTPase nucleotide cycling is performed by regulatory proteins: guanine nucleotide exchange factors (GEFs) enhance the GTP-bound state [263,503], while GTP hydrolysis is catalyzed by GTPase-activating proteins (GAPs) [8]. Cdc42 GTPase-activating protein (CdGAP) is a member of the latter family and its GAP activity is directed toward Rac1 and Cdc42 [354]. CdGAP is composed of a PBR and a GAP domain at the N-terminal region, a basic-rich (BR) stretch in the central region, a proline rich domain (PRD) and a C-terminal region [355]. CdGAP overexpression in diverse cell lines was previously shown to reduce cell spreading and lamellipodia formation [356,357].

Although CdGAP becomes upregulated downstream of growth factor treatment, little is known about its function *in vivo* [359]. We have shown that CdGAP is required for TGFβ and Neu/ErbB2-mediated breast cancer cell migration and invasion [529]. Also, gain-of-function mutations of CdGAP in humans have been linked to Adams-Oliver syndrome, a developmental disorder characterized by *cutis aplasia* and terminal limb defects [364]. CdGAP is highly phosphorylated on serine and threonine residues [355]. Notably, ERK1/2 and GSK-3 protein kinases phosphorylate threonine-776 in the PRD domain of CdGAP resulting in down-regulation of its GAP activity [355,361]. Additionally, the endocytic scaffolding protein intersectin was shown to interact with CdGAP through its SH3D domain, thereby inhibiting its GAP activity [356,362]. Finally, CdGAP binding to phosphatidylinositol 3,4,5-trisphosphate through a stretch of N-terminal polybasic residues is required for its membrane recruitment downstream of PDGF [363]. Together these data have demonstrated that CdGAP functions downstream of growth factors to regulate cell motility and migration in various biological contexts.

Although CdGAP is expressed in the fetal human brain [530], its precise function in the nervous system is completely unknown. In this study we combined both *in vitro* approaches and a CdGAP-null mouse model to investigate the function of CdGAP in the developing brain. We observed that CdGAP is expressed in various sub-regions of embryonic rat brains, and notably enriched in the hippocampus. Analysis of CdGAP-null embryos revealed a striking, incompletely penetrant defect in angiogenesis, resulting in 50 percent late embryonic or perinatal lethality. Subsequent analysis of neurons of CdGAP knockout embryos versus wild type littermates revealed many differences in cytoskeletal architecture. VEGF is a neurotrophic factor expressed by neurons,

endothelial and glial cells in the CNS [531]. Intriguingly, VEGF treatment of dissociated cortical neurons resulted in an upregulation of CdGAP expression. Furthermore, VEGF-treatment of CdGAP-null cortical neurons failed to induce ectopic neurites, thereby supporting a function of CdGAP in VEGF-dependent signaling in dissociated cortical neurons. These results are the first to indicate that CdGAP functions in the developing CNS and vasculature, and lay the groundwork for future studies to reveal the mechanisms of CdGAP action.

Materials and methods

Primary cortical neuron culture. Cortices and hippocampi of embryonic E17.5 rat or E15.5 mouse brains were extracted, trypsinized and lightly triturated. Dissociated neurons were plated on either poly-D-lysine (0.1 mg/ml, Sigma-Aldrich)-coated dishes for protein extraction, or poly-L-lysine (0.1 mg/ml, Sigma-Aldrich)-treated coverslips in 24-well plates at a density of 75,000 cells/well for imaging experiments. Neurons were maintained in attachment medium (DMEM, 10% FBS (Wisent Bioproducts) supplemented with 2mM L-glutamine, penicillin and streptomycin (Invitrogen)) under humidified conditions with 5% CO_2. After 1.5 hours, the medium was replaced with maintenance medium (Neurobasal-A medium (Invitrogen), supplemented with 2% B27 (Invitrogen), 1% L-glutamine, penicillin and streptomycin (Invitrogen)).

Protein lysis and immunoblotting. Proteins from neuronal tissues or dissociated neurons were extracted with ristocetin-induced platelet agglutination (RIPA) buffer (150

mM NaCl, 50 mM 4-(2-hydroxyethyl)-1-piperazineethanesulfonic acid, pH 7.5, 1% NP-40, 10 mM EDTA, pH 8.0, 0.5% sodium deoxycholate, 0.1% SDS, 20 mM sodium fluoride, 1 mM sodium orthovanadate, 1 mM phenylmethylsulfonyl fluoride (PMSF), and 1 µg/mL aprotinin and leupeptin (Bio Shop)). Lysates were centrifuged at 10,000 × *g* for 5 minutes at 4°C to remove insoluble materials. Protein samples were resolved by SDS-PAGE, transferred to nitrocellulose membrane for immunoblotting with the appropriate antibodies, and visualized by enhanced chemiluminescence (ECL; PerkinElmer). Antibodies used for western blot analysis: anti-CdGAP (Sigma-Aldrich), anti-Glyceraldehyde 3-phosphate dehydrogenase (GAPDH; Millipore) and anti-alpha tubulin (Sigma-Aldrich).

Generation of CdGAP fl/fl and CdGAP -/- mice and Genotyping. For targeting CdGAP, a single loxP site containing an engineered EcoRV site was inserted 177bp 5' of exon 1 and a loxP/FRT flanked Neo cassette containing and engineered Spe1 site, was inserted 270bp 3' of exon 1. CdGAP fl/fl mice were generated from a mixed 129SVEV/C57BL6 hybrid genetic background. CdGAP -/- mice were bred by first crossing CdGAP fl/fl mice with mice expressing Cre recombinase under the Meox2 promoter (a gift from N. Saidah, IRCM), which is active as early as embryonic day 5 in epiblast-derived tissues. Meox2-Cre^{-}; CdGAP $^{fl/-}$ mice were intercrossed to generate Meox2-Cre^{-}; CdGAP $^{-/-}$ used in the study. Meox2-Cre^{-}; CdGAP $^{fl/fl}$ were used as controls. For genotyping, mouse tail samples were lysed overnight at 55°C in direct tail lysis buffer (Viagen) supplemented with 60ug of proteinase K. Samples were then heated to 85°C for 2 minutes to inactivate the proteinase K, and crude lysates were cleared by

centrifugation. These samples were subject to PCR analysis for genotyping. Deletion of exon 1 was assessed by PCR in PCR buffer (Zmtech) supplemented with 0.5mM $MgCl_2$, 0.2mM dNTPs, 1uM primers flanking exon 1, and 0.04% DMSO; 1.56 units of Taq polymerase (Gentech) was used per reaction. Presence of the 5'LoxP site thus confirming the floxed gene was determined by PCR analysis as above, but with the addition of 0.5mM $MgCl_2$ to the reaction.

Immunofluorescence, microscopy. Cortical neurons were fixed with 3.7% formaldehyde (Sigma-Aldrich) in 20% sucrose/PBS for 30 minutes at 37°C and permeabilized as described previously [257]. Cells were then blocked for 30min with PBS containing 1% bovine serum albumin (BSA), and immunostaining was carried out using anti-MAP2 (Clone HM-2; Sigma-Aldrich) and Alexa-488-conjugated anti-mouse IgG (Invitrogen). Rhodamine-conjugated phalloidin (Sigma-Aldrich) was used to visualize actin filaments. Cells were examined with an Olympus IX81 motorized inverted microscope using the 40X U PLAN Fluorite oil objective lenses. Images were recorded with a CoolSnap 4K camera (Photometrics) and analyzed with the Metamorph software (Molecular Devices).

Tissue fixation and staining. E15.5 embryos were dissected and briefly visualized under dissection microscope (Zeiss Stemi 2000-C) while pictures were taken using a Zeiss Axiocam MRc camera. Embryos were then fixed in 4% PFA in PBS overnight at $4^{o}C$. The next day embryos were washed 3 times with PBS and either cryoprotected in 30% sucrose at $4^{o}C$ for 3 days and sectioned. Cryoprotected embryos were then

embedded in OCT compound and snap frozen in 2-methyl butane at -30^{o}C and stored at -80^{o}C until sectioning. 14 μm thick tissue sections were prepared and then processed following a standard H&E protocol before mounting with Permount (Fisher). Sections were visualized using a Zeiss Imager M2 upright microscope and images obtained with a Zeiss AxioCam ICc5 camera.

Cytoskeletal measurements. To analyze axon length, width, growth cone area, branching and filopodia density of primary cortical neurons (1-4DIV), at least 30 cells were analyzed per embryo for each genotype from at least three independent experiments. A branch was defined as an actin projection longer than 10 μm, while a filopodium was defined as an actin projection shorter than 10 μm emanating from the primary cortical axons. Measurements were obtained manually from acquired images with MetaMorph software. The results are presented as the mean for each genotype ±SEM.

VEGF treatments, neuritogenesis. At DIV1, cortical neurons were either left untreated or treated with 50 ng/mL recombinant human VEGF-165 (R&D Systems). At DIV4, neurons were either lysed for immunoblotting analysis or fixed at DIV4 and stained for MAP2 to visualize primary neurites. The number of neurites per soma were counted manually, with a minimum of 30 cells being analyzed per condition. The average number of neurites per soma was determined for each embryo and the data are presented as the mean for each genotype in each condition ±SEM.

Statistical analysis. Two-tailed independent student t-tests were used to analyze the data concerning axon length, axon width, growth cone area, axonal branching and filopodia density. Two-way ANOVA followed by Bonferroni simple effect analysis was used to analyze VEGF-induced neuritogenesis data. Statistical analysis was performed with GraphPad Prism 6. The data are presented as the mean ± the standard error of the mean (SEM).

Results

CdGAP is expressed in the brain and is enriched in the hippocampus in E17.5 rat

To investigate the function of CdGAP in the developing brain, we first attempted to verify its expression in the embryonic rat brain and determine in which sub-regions it is enriched. We collected tissue samples from the sub-regions of E17.5 rat brains (Fig. 4.1A), resolved crude lysates by SDS-PAGE, and CdGAP expression was assessed by immunoblotting. Expression of CdGAP in the olfactory bulb, cortex, cerebellum and midbrain was strong, but notably CdGAP was most highly enriched in hippocampal tissues (Fig. 4.1B). To pinpoint a window of function of CdGAP in neurons, we next sought to determine whether CdGAP expression varied over a time course during which neuronal polarization, neurite outgrowth or synapse formation occur. Dissociated rat cortical and hippocampal neuons were cultured over a period of two weeks and protein lysates were collected at intervals and resolved by SDS-PAGE. In this way, Western blotting revealed that CdGAP expression levels increased similarly in both cortical and hippocampal cultures relative to GAPDH and stabilized after one week relative to GAPDH levels (Fig. 4.1C, D). These results demonstrate that CdGAP is expressed

throughout the embryonic rat brain, and while CdGAP is enriched in hippocampal tissues, its dynamic expression in dissociated hippocampal neurons is indistinguishable from that in dissociated cortical neurons.

CdGAP -/- mice exhibit incompletely penetrant embryonic lethality, edema, and vascular defects.

To explore the importance of CdGAP *in vivo* during embryonic development, we generated conditional floxed exon 1 allele to remove the ATG start codon of the CdGAP gene (Fig. 4.2A). Conditional CdGAPfl/fl mouse were crossed with mice expressing Cre recombinase under the Meox2 promoter, which is active as early as embryonic day 5 in epiblast-derived tissues. To eliminate the possibility of non-specific effects caused by Meox2-Cre recombinase expression, heterozygous $CdGAP^{fl/-}$;Meox2-Cre- were intercrossed to generate $CdGAP^{-/-}$ as assessed by PCR (Fig. 4.2B). The complete absence of CdGAP expression in $CdGAP^{-/-}$ mice was confirmed by western blotting of protein lysates of lung, brain, and heart tissues compared to those isolated from CdGAPfl/fl mice (Fig. 4.2C). These analyses indicated the successful generation of CdGAP-depleted mice. While the offspring of $CdGAP^{-/+}$ intercrosses at E15.5 revealed a Mendelian ratio of genotypes (CdGAP-null: 22%, heterozygote: 54%, wild-type: 24%), the proportion of CdGAP-null pups at P21 reduced to half of those expected (CdGAP-null: 14%, heterozygote: 59%, wild-type: 27%; Fig. 4.2D). Therefore, the complete loss of CdGAP expression leads to incompletely penetrant embryonic lethality.

Furthermore, we observed general vascular defects in 89% of CdGAP-null embryos at E15.5, including multifocal progressive hemorrhages of varying severity

from ruptured blood vessels (white *), and dorsal subcutaneous edema (black *) in 73% and 77% of CdGAP-null embryos, respectively (Fig. 4.3 A, B). In addition to these superficial defects, the livers of CdGAP-null embryos were relatively pale in colour compared to littermate controls (Fig. 4.3A, B), and a reduction in vascularization was clearly apparent in the brains dissected from E15.5 CdGAP $^{-/-}$ embryos (Fig. 4.3A-C). In addition, H/E staining of transverse sections of E15.5 CdGAP-null embryonic torsos revealed the severity of the dorsal edema, and the infiltration of red blood cells into subcutaneous regions compared to control embryos, which may account for the lethality of some pups (Fig. 4.3D). Taken together these results indicate that CdGAP supports general vascular maintenance during embryonic development.

CdGAP$^{-/-}$ hippocampal neurons undergo polarization normally *in vitro*

Since CdGAP deletion in mice resulted in hypovascularized meninges lining the embryonic brains, we next investigated the morphology of dissociated neurons from CdGAP-null embryos relative to litter mate controls. We began by asking whether CdGAP deficiency affects hippocampal neuronal polarization, a process that is known to implicate Cdc42 and Rac1 activity [532]. Dissociated hippocampal neurons from wild type and CdGAP-null embryos were maintained in culture for one or two days before fixation, after which actin filaments were stained with Rhodamine-conjugated phalloidin and assessed blindly by fluorescence microscopy (Fig. 4.4A, B). The neurons were classified according to established polarization stages: Stage 1 (only lamellipodia and small actin-rich microspikes emanating from the cell body), Stage 2 (primary neurites are present but there is no defined polarity), and Stage 3 (neuron is polarized with a

primary, immature axon) [376]. Under these conditions, CdGAP-null hippocampal neurons underwent the first three stages of polarization indistinguishably from littermate control hippocampal neurons (Fig. 4.4A, B). These results indicate that loss of CdGAP expression does not affect the intrinsic program of hippocampal neuronal polarization *in vitro*.

CdGAP-null cortical axons have abnormal cytoarchitecture at DIV2

Since CdGAP regulates Rac1 and Cdc42, which contribute to axon outgrowth by dynamic regulation of the actin cytoskeleton [533], we next examined whether CdGAP deficiency affected the axon length of cortical neurons. Dissociated cortical neurons were maintained for two days before fixation and staining with Rhodamine-conjugated Phalloidin. To our intrigue, the axons of CdGAP-null cortical neurons were significantly shorter compared to the axons of littermate control cortical neurons with an average length of 86.28 μm ± 4.03 versus 101.53 μm ± 5.59, respectively (Fig. 4.5A, B; $p<0.05$). Furthermore, we observed that the average thickness of CdGAP-null cortical axons were significantly larger at DIV2 relative to control cortical neurons at 4.49 μm ± 0.41 versus 2.52 μm ± 0.28, respectively (Fig. 4.5C, D; $p<0.01$). In addition to abnormal axon sizes, the most-striking feature of CdGAP-null cortical neurons was the enlargement of the growth cones (Fig. 4.6A, B). Relative to $CdGAP^{fl/fl}$ control cortical growth cones, the average surface area occupied by CdGAP-null cortical growth cones was two times larger (204.78 μm^2 ± 26.14 versus 95.95 μm^2 ± 30.35, $p<0.05$) and the growth cones often exhibited an unusual shape (Fig. 4.6C). Taken together, these results indicate that

CdGAP contributes to the cytoarchitecture of embryonic cortical neurons *in vitro*, and its deficiency negatively influences axon extension.

Since Rac1 and Cdc42 also contribute to axon branching and filopodia formation [533-535], we next focused on whether CdGAP-null cortical neurons presented abnormal numbers of filopodia or branches along the primary axon at DIV2. Intriguingly CdGAP-null cortical neurons had more filopodia at DIV2, at 3.1 filopodia per 20 μm of axon compared to 2.3 filopodia per 20 μm of control cortical axons (Fig. 4.6D, E; $p<0.05$). To verify that these cytoskeletal differences were not transient, we also assessed the abundance of filopodia at DIV4 only to find that the disparity was even larger, with CdGAP-null cortical axons having 4.7 filopodia per 20 μm of axon compared to 2.2 filopodia per 20 μm of control cortical axons (data not shown). In addition to increased axonal filopodia, CdGAP-null cortical neurons also had a relatively high incidence of axon branching with a frequency of 1.17 branches ± 0.15 per cortical axon, versus 0.43 branches ± 0.13 per cortical axon of CdGAP fl/fl neurons (Fig. 4.6F, G; $p<0.01$). When expressed as a percentage, 61.2% ± 3.9 of CdGAP-null cortical neurons had at least one branch, while only 28.6% ± 7.8 of control cortical neurons possessed one or more branches (Fig. 4.6F, H; $p<0.001$). These results indicate that CdGAP contributes to the cytoskeletal organization of cortical neurons, and that loss of CdGAP expression results in supernumerary filopodia and ectopic branching along the primary axon of cortical neurons relative to wild type neurons from littermate controls.

CdGAP$^{-/-}$ cortical neurons are unresponsive to VEGF mediated neuritogenesis

Since the brains of E15.5 embryos of CdGAP-null mice were pale in colour, and the meninges surrounding the brain had a noticeably disorganized vasculature (Fig. 4.3A, C), we next asked whether CdGAP could function downstream of the well characterized vascular endothelial growth factor (VEGF) in cortical neurons. To this means, cortices were isolated from E17.5 rat embryos and the tissue was incubated with VEGF for 30 min and 1 hr at 37ºC before protein extraction. Protein lysates were resolved by SDS-PAGE and CdGAP expression was assessed by immunoblotting. In this way, we observed that CdGAP expression in the cortical tissue was readily upregulated relative to α-tubulin levels within one hour of VEGF application, while phospho-ERK1/2 immunoblotting validated the efficacy of VEGF treatment (Fig. 4.7A). Since cortical tissues contain many cell types, we next asked whether exogenous VEGF application would augment CdGAP expression in dissociated cortical neurons. To test this hypothesis, rat cortical neuons were isolated and cultured for one day before addition of VEGF. Following 24 hours of VEGF incubation, protein lysates were collected, resolved by SDS-PAGE and Western blotting was performed. In this way we observed that CdGAP levels were upregulated at the protein level with VEGF treatment, while the levels of the VEGF receptor VEGF-R2 were also upregulated relative to α – tubulin (Fig. 4.7B). Taken together, VEGF treatment of the embryonic cortex and dissociated cortical neurons results in upregulation of CdGAP.

Previous reports have indicated that VEGF induces neuritogenesis of dissociated primary cortical neurons *in vitro*[531]. To determine whether CdGAP was required for this phenomenon, cortical neurons of E15.5 CdGAP$^{-/-}$ and wild type control embryos were dissociated and treated with VEGF at DIV1 for 3 days before fixation. Using antibodies

against the dendritic marker MAP2, we immunostained and assessed the number of primary neurites emanating from the cell soma of each neuron per embryo (Fig. 4.7C, D). Both control and CdGAP-deficient cortical neurons had on average 7 primary neurites without treatment (Fig. 4.7C, D). However, while VEGF treatment resulted in an increase in primary neurites of CdGAP fl/fl and fl/- cortical neurons to 8.4 and 7.5, respectively (p=0.02; p=0.06), VEGF-treatment failed to induce primary neuritogenesis of CdGAP-null cortical neurons (p=0.95; Fig. 4.7C, D). We next asked whether this result was due to the downregulation of VEGF-R2, the VEGF receptor required for induced neuritogenesis in cortical neurons. Protein lysates extracted from $CdGAP^{fl/fl}$, $CdGAP^{fl/-}$ and CdGAP-null cortical neurons were resolved by SDS-PAGE and the levels of CdGAP and VEGF-R2 were determined by immunoblotting (Fig. 4.7E). As expected, CdGAP was only expressed in wild type and heterozygote neurons, while VEGF-R2 expression was similar in extracts from all three genotypes when compared to GAPDH and α-tubulin (Fig. 4.7E). Taken together, these data suggest that CdGAP plays an important role in VEGF signaling in cortical neurons.

Discussion

Until now, the function of CdGAP in the brain has been virtually unexplored. In this study, we demonstrate that CdGAP is well expressed in the developing rat brain. Although CdGAP was enriched in hippocampal tissues, the indistinguishable upregulation of CdGAP in both dissociated hippocampal and cortical neurons with days in culture suggests a general role of CdGAP in functionally diverse populations of neurons. Since CdGAP expression is low during the first three days in culture, it would

imply that the major role of CdGAP in neurons likely follows early cellular events *in vitro*, such as polarization and axon outgrowth. Indeed, we assessed the ability of CdGAP-null neurons to polarize, a process known to involve regulation of both Rac1 and Cdc42 [532]. Since CdGAP$^{-/-}$ neurons failed to display differences in polarization relative to wild-type littermates, we conclude that CdGAP is not a major contributor to neuronal polarization *in vitro*.

In contrast to CdGAP being dispensable for polarization, we observed that CdGAP deficiency affects the cytoskeletal architecture of dissociated cortical neurons at DIV1 and 2 despite low CdGAP expression. Since CdGAP is a GAP protein for Rac1 and Cdc42, many of these observations may be in part explained by a differential regulation of these Rho GTPases. Rac1 and Cdc42 support axon outgrowth and growth cone protrusion by driving lamellipodia and filopodia formation, respectively at the axon tip [533,536]. Rac1 has also been implicated in axonal branching while Cdc42 promotes filopodia formation along the axon [534,535]. In the context of CdGAP-deficient cortical neurons, loss of a Rac1/Cdc42 GAP protein may result in enhanced axon outgrowth, axonal branching and filopodia formation by via enhanced local Rac1 and Cdc42 activation. Indeed, increased incidence of branching and elevated filopodial density were observed along axons of CdGAP-null cortical neurons, however the reduced axon lengths relative to wild-type littermates suggests that CdGAP may have GAP-independent functions in dissociated neurons or that CdGAP deficiency impairs axon extension indirectly. In the future, rescue of CdGAP deficiency with expression of GAP-dead CdGAP in cortical neurons will help to determine whether loss of GAP activity is causative in altering the cytoarchitecture of CdGAP-null cortical neurons.

While larger growth cones of CdGAP-null cortical neurons may be explained by deregulation of Rac1 or Cdc42 activity, an additional hypothesis is that CdGAP ablation alters cell adhesion and thereby favours enlarged growth cones and thicker axons in 2D space. Indeed, CdGAP has been shown to localize to focal adhesions[357], and down-regulation of CdGAP leads to upregulation of E-cadherin resulting in enhanced cell-to-cell junctions and reduced motility of breast cancer cells[529]. More recently, CdGAP was shown to influence cell migration U2OS osteosarcoma cells by regulating adhesion maturation dynamics, but in this study the depletion of CdGAP resulted in decreased half-life of adhesions resulting in more motile cells[537]. Since the depletion of CdGAP results in different effects on adhesion dynamics in various cell types, it is not possible to speculate whether the larger axon widths and enlarged growth cone surface area of CdGAP-null cortical neurons may result from dysregulated adhesion complexes. Furthermore, cortical neurons are a heterogeneous population of cells, and not all $CdGAP^{-/-}$ neurons exhibited the same defects, therefore further study is required to assess which subtype of cortical neurons are most affected by CdGAP deficiency.

The generation of CdGAP-null mice revealed a novel function of CdGAP in angiogenesis. Angiogenesis is the formation of new blood vessels from pre-existing ones, and a major driver of angiogenesis is the trophic factor, VEGF [538]. CdGAP-deficient embryos displayed defective vascularization at E15.5, and by P21 the survival rate of CdGAP knockout pups was roughly half of that expected. Although some knockout pups survive into adulthood, the long term effects of CdGAP deficiency remain unknown. The hypovascularized CNS exhibited by CdGAP-null embryos begs the

following questions: Is CdGAP implicated in VEGF-dependent signaling, and does loss of CdGAP affect neural function *in vivo*?

To date CdGAP has been shown to play a role downstream of several growth factor pathways such as TGFβ and PDGF.[363,529] Here we show that downstream of VEGF treatment, CdGAP expression is upregulated in cortical tissue and neurons. VEGF has been extensively studied in various systems including the nervous system where it is implicated in neurodevelopment and neurodegeneration via various pleiotropic mechanisms [539,540]. Considering that VEGF is secreted by various cell types including neurons [541], investigating VEGF signaling *in vivo* remains a difficult task. In this study, we explored the requirement for CdGAP during VEGF-induced neuritogenesis. In this context, our observation that CdGAP-null cortical neurons remained unresponsive to VEGF treatment independently of VEGFR2 down-regulation, suggests that CdGAP acts downstream of VEGFR2 in mediating VEGF-induced neuritogenesis in cortical neurons. These results are in support that CdGAP is implicated in VEGF-dependent signaling, but further studies will be required to delineate the precise mechanism of CdGAP participation in VEGF signaling. Furthermore, since CdGAP expression in dissociated neurons peaks at the time when neurons begin to form synaptic connections in culture [542], further study is needed to determine whether CdGAP contributes to functional, mature neuronal networks. This first investigation of CdGAP in the nervous system unveils several defects caused by CdGAP deficiency and insights to the function of CdGAP in neurons.

Acknowledgements

This research was supported by Canadian Institute of Health Research (CIHR) Grant MOP-14701 and the Canada Foundation for Innovation-Leaders Opportunity Fund to NLV. N.L.V. is a recipient of a Fonds de la Recherche en Santé du Québec Chercheur-National and a William Dawson Scholar.

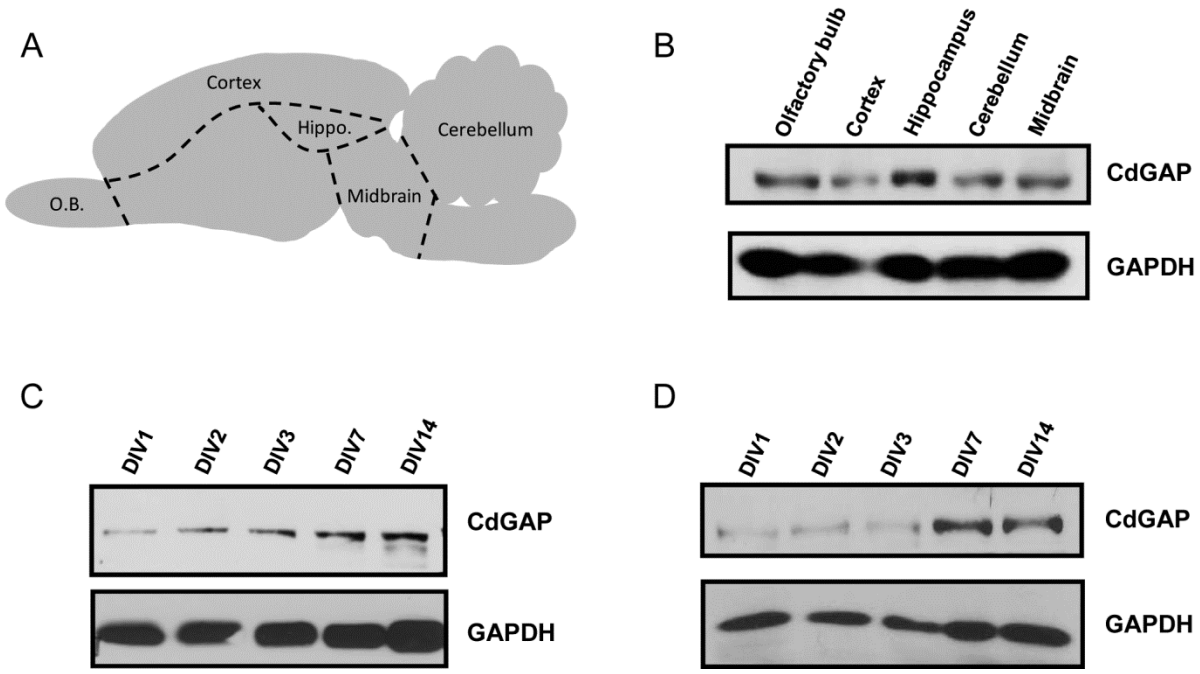
A
Cortex
Hippo.
Cerebellum
O.B.
Midbrain
B
Olfactory bulb
Cortex
Hippocampus
Cerebellum
Midbrain
CdGAP
GAPDH
C
DIV1
DIV2
DIV3
DIV7
DIV14
CdGAP
GAPDH
D
DIV1
DIV2
DIV3
DIV7
DIV14
CdGAP
GAPDH

Figure 4.1 – CdGAP expression in the developing rodent brain

(A) Schematic of the subregions of embryonic rat brain. (B) Brains were isolated from E17.5 rats and the olfactory bulb, cerebral cortex, hippocampi, midbrain and cerebellum were separated. Protein extracts were resolved by SDS-PAGE and immunoblotted with the indicated antibodies. (C) Dissociated E17.5 rat hippocampal neurons were maintained *in vitro* up to two weeks. CdGAP and GAPDH protein levels from cell extracts were determined by immunoblotting. (D) CdGAP expression in dissociated cortical neurons was assessed as in (C).

A

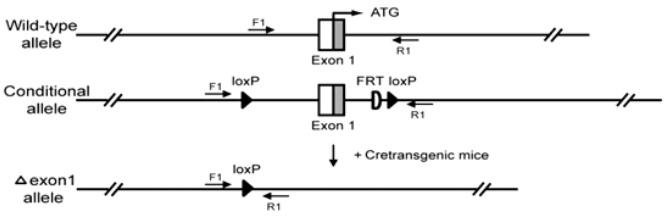

B

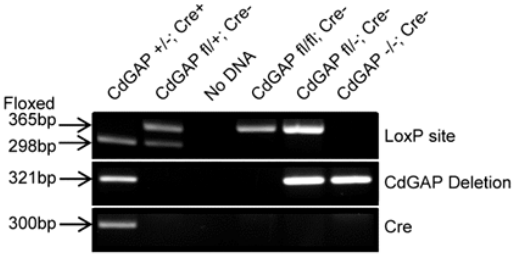

C

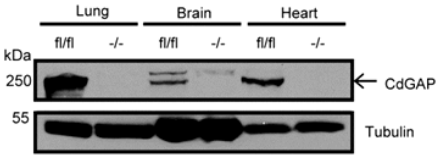

D

Genotypes of offsprings from CdGAP fl/- intercrosses

Age	CdGAPfl/fl	CdGAPfl/-	CdGAP-/-
E15.5	24% (23)	54% (52)	22% (21)
P21	27% (98)	59% (214)	14% (51)

Figure 4.2 – Generation of CdGAP-null mouse model reveals incompletely penetrant embryonic lethality

(A) Schematic drawing of the targeting strategy for the production of *CdGAP* conditional floxed (fl) mice. Primers (F1 and R1) for PCR assessment of *CdGAP* exon1 deletion (Δexon1). (B) CdGAP -/- mice were generated by crossing CdGAP fl/fl mice with mice expressing Cre recombinase under the Meox2 promoter. Samples for PCR were prepared from Cre negative, CdGAP fl/fl, CdGAP fl/- and CdGAP -/- mouse tails. Δexon1 allele-specific (321 bp) bands indicate deletion of *CdGAP* exon 1. (C) Western blot analysis of CdGAP expression was performed using lung, brain and heart tissue lysates from CdGAP fl/fl and CdGAP-null mice. Tubulin was used as a protein loading control. CdGAP expression was absent in all tissues derived from knockout animals. (D) Breeding table from heterozygous intercrosses show that CdGAP$^{-/-}$ were not born at the expected Mendelian ratio, and CdGAP-null embryos exhibited 44% embryonic/perinatal lethality. The numbers of embryos (E.15.5) or born mice (P21) assessed are indicated in parenthesis.

A

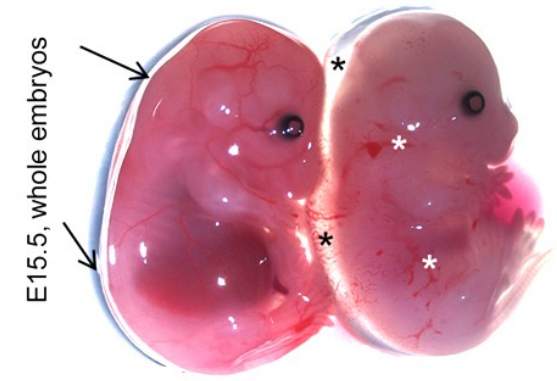

B

Phenotypes of CdGAP-/- embryos (E15.5)

	CdGAPfl/fl	CdGAPfl/-	CdGAP-/-
Vascular Defects	0 (17)	20 (30)	89 (26)
Edema	0 (17)	0 (30)	77 (26)
Superficial Bleeding	0 (17)	3 (30)	73 (26)
Pale liver	0 (17)	3 (30)	65 (23)
Pale meninges	0 (5)	7 (14)	93 (14)

C

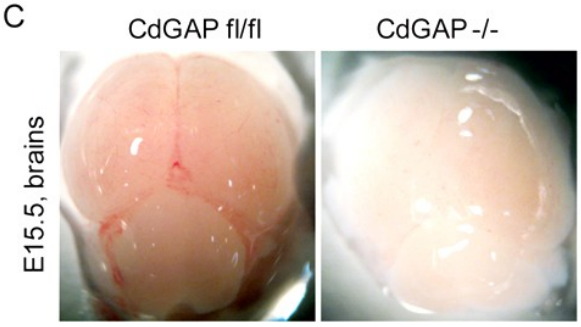

D

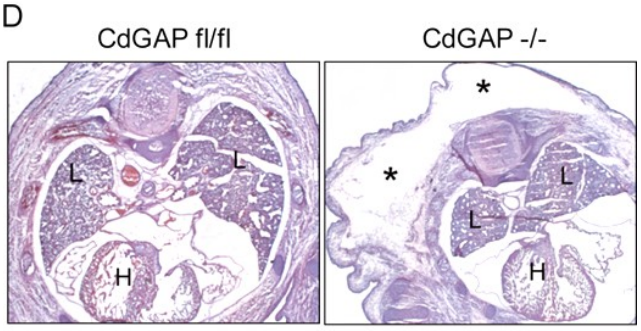

Figure 4.3 – CdGAP$^{-/-}$ mice exhibit subcutaneous edema, and vascular defects

(A) E15.5 CdGAP-null whole embryos displayed vascular defects with subcutaneous edema (*) and various degrees of subcutaneous hemorrhage (white asterisks). (B) The proportion of embryos exhibiting each major phenotype. The total number of embryos analyzed per genotype is indicated in parenthesis. (C) Reduced vascularization of the meninges surrounding the brains of CdGAP-null embryos relative to littermate controls. (D) H&E staining of transverse sections of E15.5 CdGAP fl/fl and -/- embryonic torsos revealing subcutaneous edema (*). L, lung; H, heart.

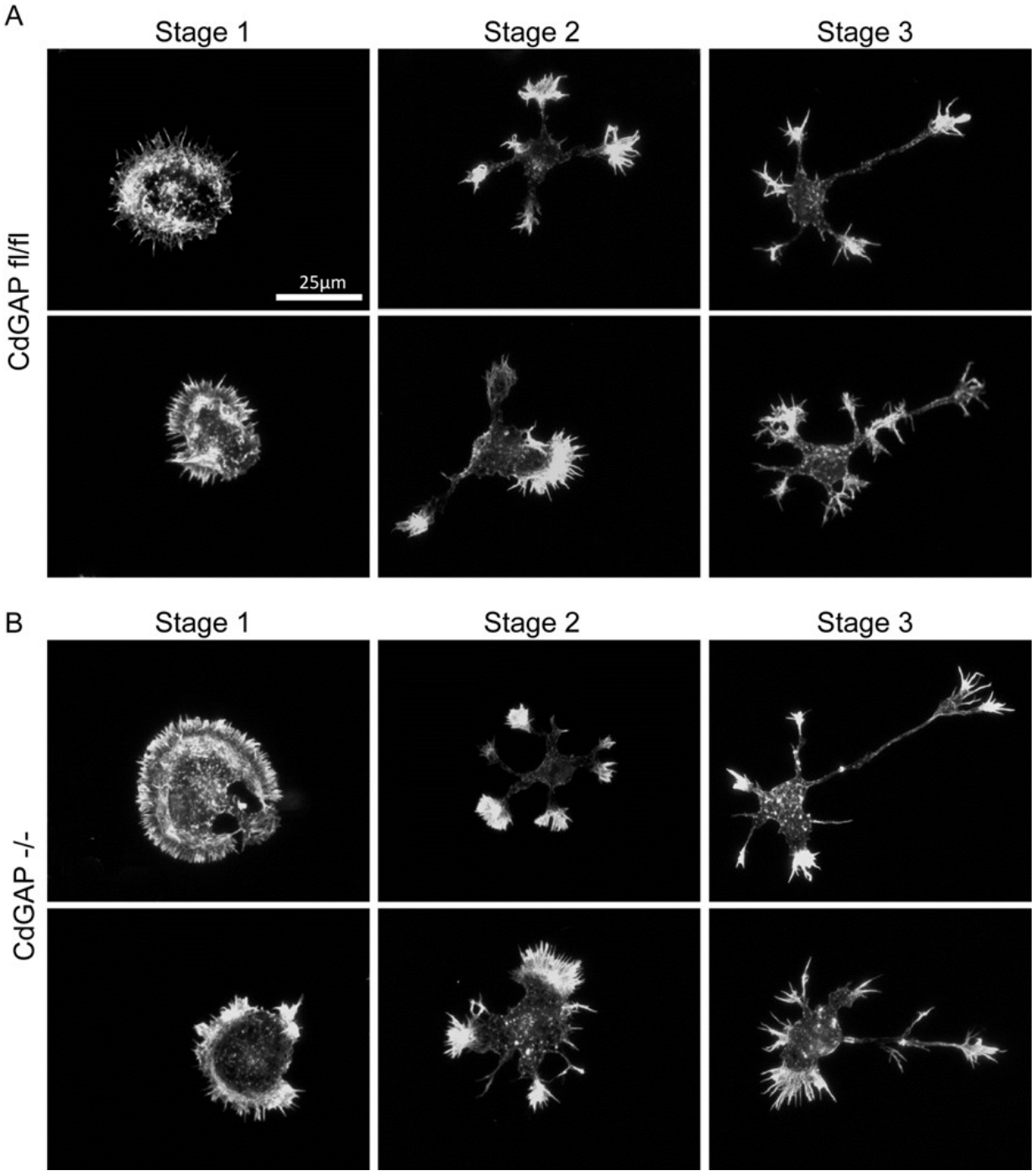
A
Stage 1
Stage 2
Stage 3
CdGAP fl/fl
25µm
B
Stage 1
Stage 2
Stage 3
CdGAP -/-

Figure 4.4 – CdGAP deficiency does not impair hippocampal neuron polarization Dissociated E15.5 hippocampal neurons were fixed after one or two days and stained with Rhodamine-conjugated phalloidin to visualize actin filaments. Representative micrographs of (A) wild-type and (B) CdGAP $^{-/-}$ neurons undergoing stages 1 through 3 of polarization.

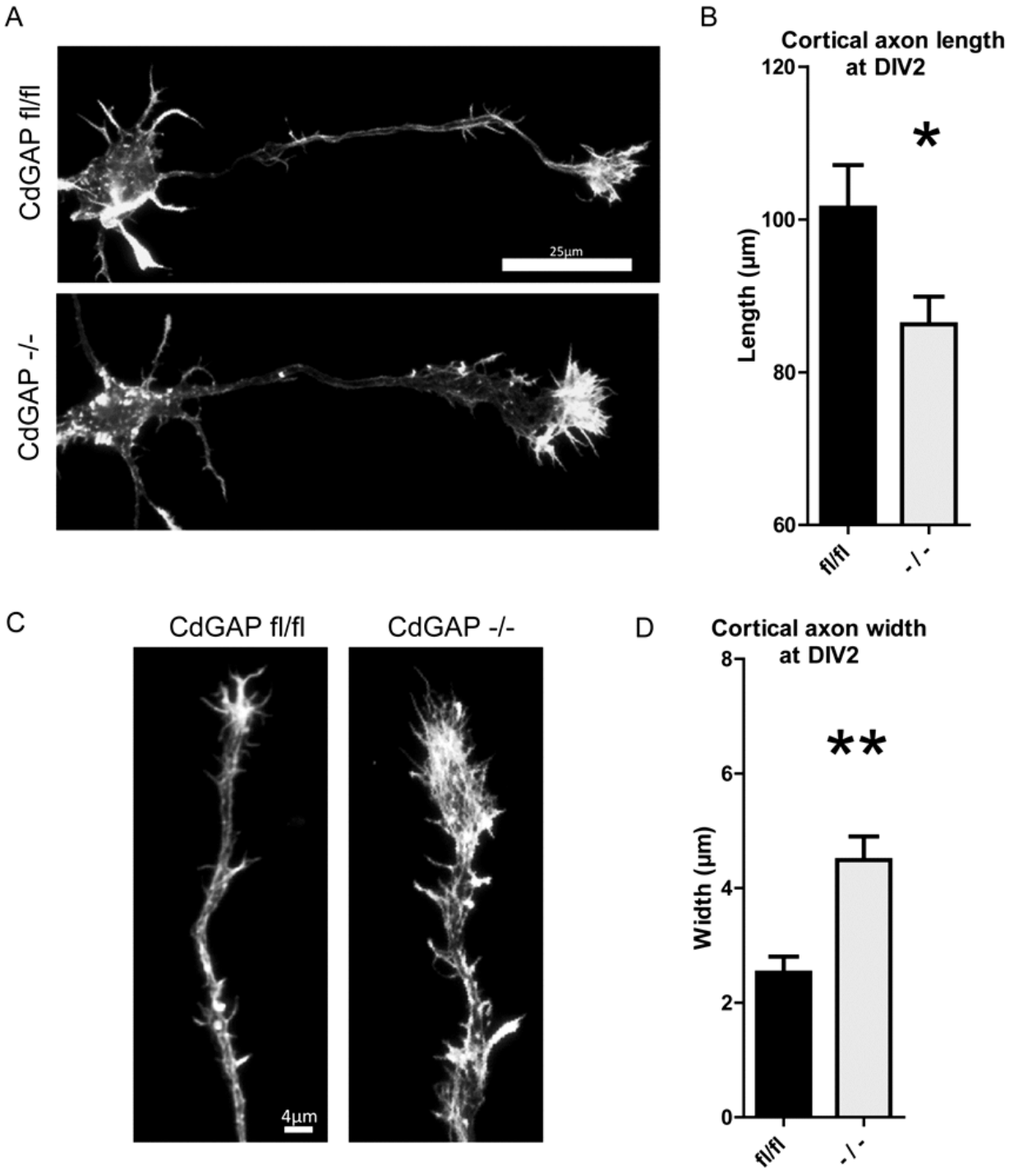
A
CdGAP fl/fl
CdGAP -/-
25µm
B
Cortical axon length at DIV2
120
100
80
60
Length (µm)
*
fl/fl
-/-
C
CdGAP fl/fl
CdGAP -/-
4µm
D
Cortical axon width at DIV2
8
6
4
2
0
Width (µm)
**
fl/fl
-/-

Figure 4.5 – Mean length of CdGAP -null cortical neurons is reduced at DIV2, width is increased

Dissociated E15.5 mouse cortical neurons were fixed after two days and stained with Rhodamine-conjugated phalloidin to visualize actin filaments. (A, C) Representative images of whole cell or enlarged axons are shown from $CdGAP^{fl/fl}$ and $CdGAP^{-/-}$ cortical neurons. (B, D) The mean lengths and widths of cortical axons were measured. Error bars indicate the SEM (n>30 axons per embryo (fl/fl= 5, -/-=10), length: *p<0.05; width: **p<0.01, Unpaired student t-test).

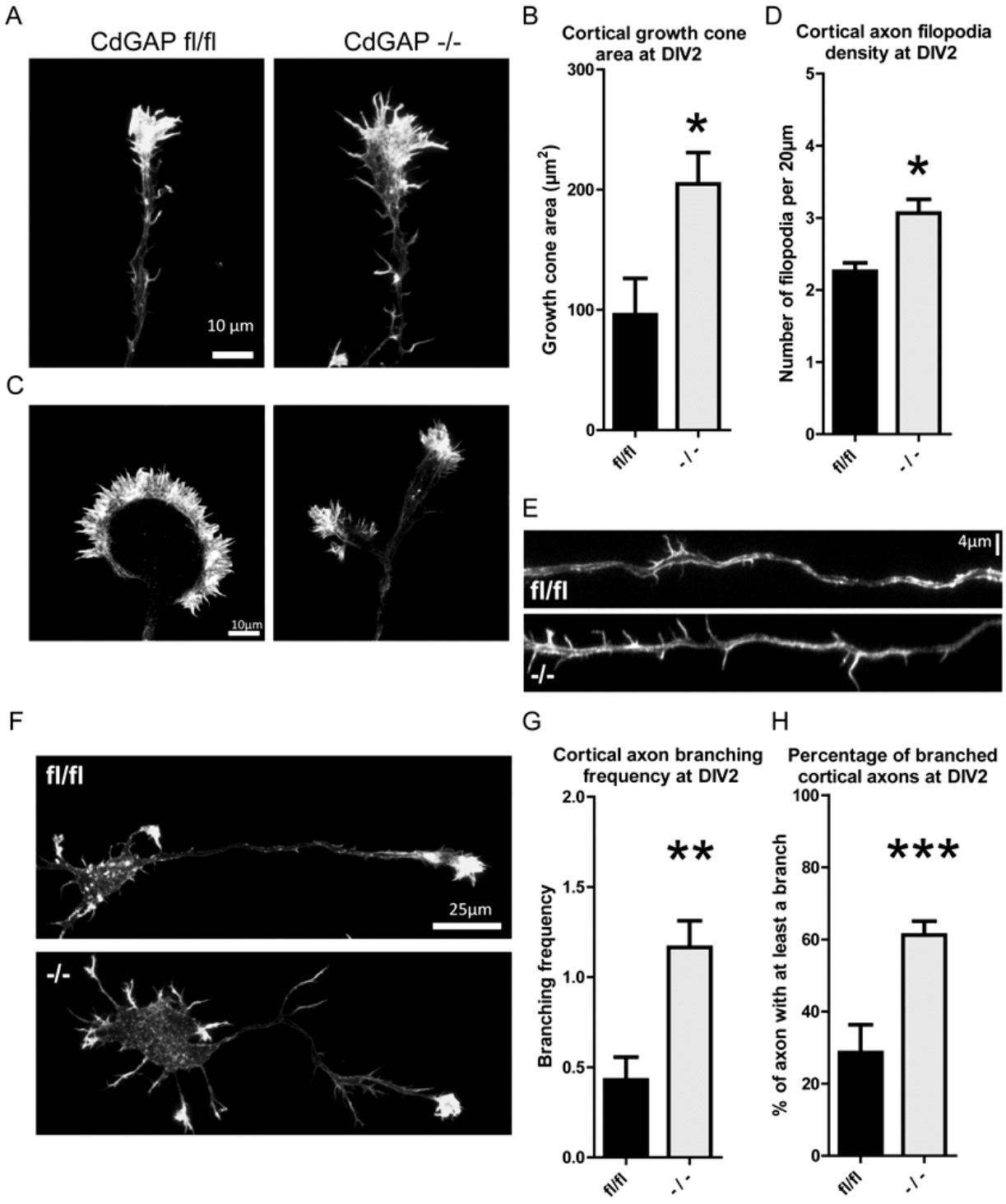
A
CdGAP fl/fl
CdGAP -/-
10 µm
B
Cortical growth cone area at DIV2
Growth cone area (µm²)
300
200
100
0
*
fl/fl
-/-
D
Cortical axon filopodia density at DIV2
Number of filopodia per 20µm
5
4
3
2
1
0
*
fl/fl
-/-
C
10µm
E
4µm
fl/fl
-/-
F
fl/fl
25µm
-/-
G
Cortical axon branching frequency at DIV2
Branching frequency
2.0
1.5
1.0
0.5
0.0
**
fl/fl
-/-
H
Percentage of branched cortical axons at DIV2
% of axon with at least a branch
100
80
60
40
20
0
***
fl/fl
-/-

Figure 4.6 – CdGAP-deficient cortical neurons have larger growth cones, and more axonal filopodia and branching

Dissociated E15.5 mouse cortical neurons were fixed at DIV2 and stained with Rhodamine-conjugated phalloidin to visualize actin filaments. (A, E, F) Representative images of growth cones, axons and full cells are shown for each genotype. (B) Average growth cone surface area for each embryo per genotype. Error bars indicate the SEM (n>30 axons per embryo (fl/fl= 5, -/-=10), *p<0.05, Unpaired student t-test). (C) Various CdGAP-null cortical neurons with oddly shaped growth cones. (D, G, H) The mean axonal filopodia density, primary axon branching frequency and percentage of axons with at least one branch observed per embryo. Error bars indicate the SEM (n>30 axons per embryo (fl/fl= 5, -/-=10), *p<0.05, **p<0.01, ***p<0.001, Unpaired student t-test).

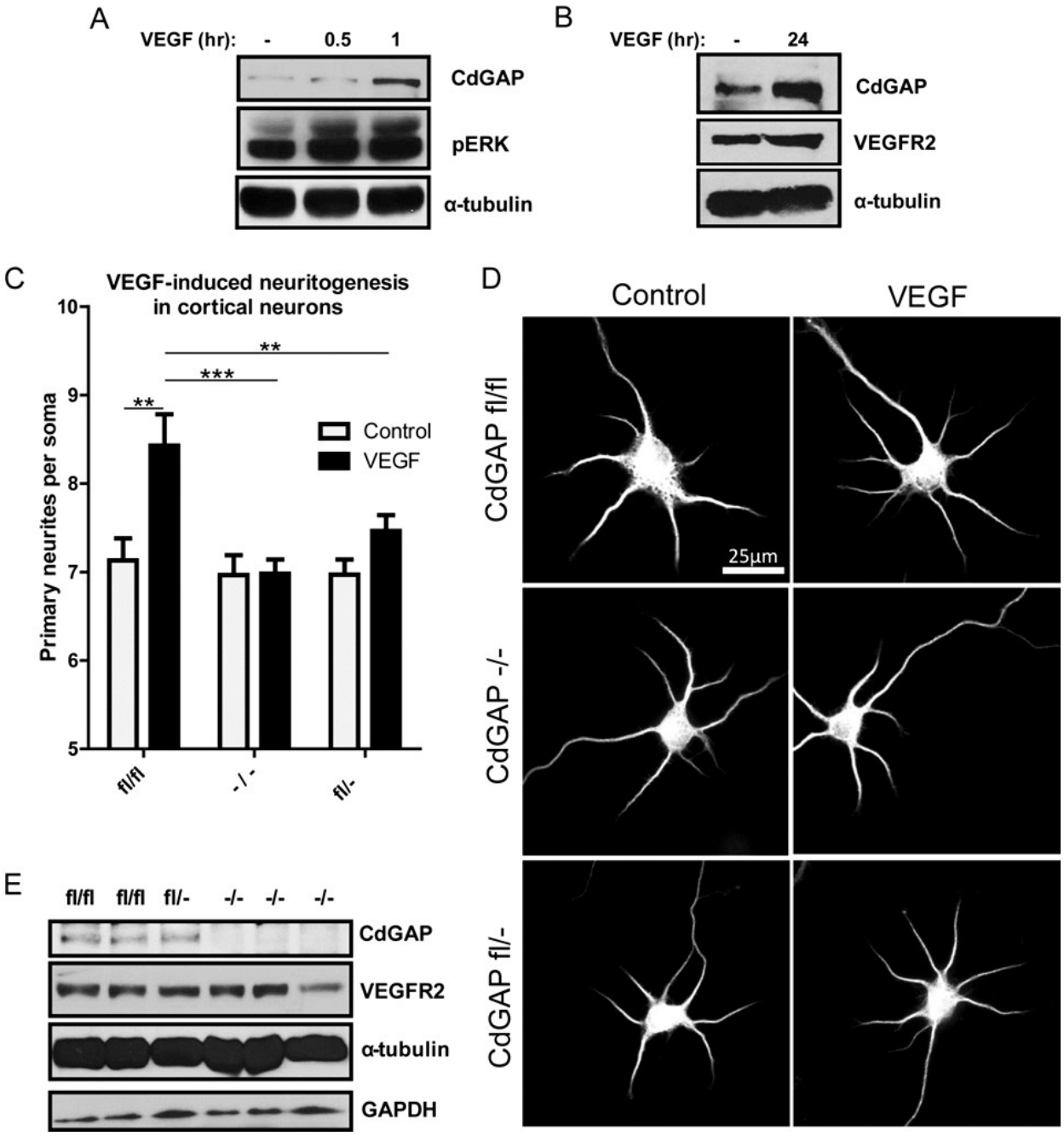
A
VEGF (hr): - 0.5 1
CdGAP
pERK
α-tubulin
B
VEGF (hr): - 24
CdGAP
VEGFR2
α-tubulin
C
VEGF-induced neuritogenesis in cortical neurons
Primary neurites per soma
10
9
8
7
6
5
**
***
**
Control
VEGF
fl/fl
-/-
fl/-
D
Control
VEGF
CdGAP fl/fl
CdGAP -/-
CdGAP fl/-
25μm
E
fl/fl fl/fl fl/- -/- -/- -/-
CdGAP
VEGFR2
α-tubulin
GAPDH

Figure 4.7 – CdGAP expression is induced by VEGF treatment of cortical neurons and is required for VEGF-induced neuritogenesis

(A) Isolated E17.5 rat cortical tissues were incubated with 50 ng/mL of VEGF for the indicated times. Protein extracts were resolved by SDS-PAGE and immunoblotted with the indicated antibodies. Efficacy of VEGF treatment was verified by assessing ERK 1/2 phosphorylation. (B) Dissociated E17.5 cortical neurons were treated with 50 ng/mL of VEGF for 24 hours at DIV3 before lysis. Protein extracts were resolved by SDS-PAGE and immunoblotted with the indicated antibodies. (C, D) Dissociated E15.5 mouse cortical neurons were incubated with VEGF (50 ng/mL) at DIV1 for 3 days. Immunocytochemistry was performed with anti-MAP2 antibodies, and the mean primary neurites per soma were calculated. Error bars indicate the SEM (n>30 axons per embryo (fl/fl= 5, -/-=10, fl/-=14), **p<0.01, ***p<0.001, Two-way ANOVA, Bonferroni test). (E) Protein extracts from cortical neurons of each genotype at DIV4 were resolved by SDS-PAGE and immunoblotted with the indicated antibodies.

Chapter 5: General Discussion and Conclusions

5.1 Major Findings

5.1.1 Tyrosine phosphorylation of Trio

This study was the first to demonstrate that Trio is tyrosine phosphorylated in either cultured cells or in tissues *ex vivo*, despite its identification via direct binding with the LAR transmembrane tyrosine phosphatase [193]. Before this study, it was assumed that Trio and DCC were constitutively associated [244], however we show that Trio is recruited to DCC signaling complexes upon netrin-1 treatment and is directly phosphorylated at its C-terminus by the Src-kinase Fyn at tyrosine-2622. We further confirm that the netrin-1-induced axon outgrowth and activation of Rac1 by Trio requires this modification. Furthermore, we show for the first time that Trio regulates DCC surface expression at the growth cones of neurons—a phenomenon that was also dependent on tyrosine-2622. Together, these findings support a hypothesis whereby phosphorylation regulates both Trio localization and activation in neurons.

5.1.2 Hsc70 chaperone activity regulates Trio GEF function

Next, we demonstrated for the first time that the activity of a molecular chaperone protein is required for directed axon outgrowth in response to a guidance cue. We show that Hsc70 is required for the localized regulation of Trio Rac1 GEF activity in cortical growth cones, and implicate its function in regulating DCC signaling complex formation downstream of netrin-1. We further confirm functionally that Hsc70 is an upstream modulator of Trio during netrin-1-induced axon outgrowth. Together, this work supports a novel hypothesis whereby molecular chaperones are regulators of GEF-dependent Rac1 activation.

5.1.3 CdGAP is required for angiogenesis and contributes to cortex development

In this work we describe for the first time that CdGAP is involved in blood vessel biology, and implicate its function in the regulation of the cytoarchitecture of developing cortical neurons. We demonstrate that in the developing brain, CdGAP expression is enriched in the hippocampus. We further show that absence of CdGAP results in an altered structure of the actin cytoskeleton in CdGAP-null cortical neurons. We also demonstrate the requirement of CdGAP in neuronal VEGF signaling for the first time.

5.2 Regulation of Trio by phosphorylation

We have shown that in neurons, the induced activation of Rac1 by Trio requires phosphorylation at tyrosine-2622 by Fyn. Since Trio is ubiquitously expressed and upregulated during invasive carcinomas [241], it is possible that Src-mediated regulation of Trio can occur in a pathological setting. It may be of potential interest to investigate whether tyrosine-2622 is required for Trio-induced cell migration in cancer cells, or whether cells constitutively expressing the Y2662F mutation impair metastasis or tumor growth upon tail-vein injection into nude mice versus cell expressing wild type Trio. In the developing cerebral cortex, the most abundant Trio isoform, Trio-A, lacks tyrosine-2622 altogether. Since Trio-A becomes phosphorylated in a Src-dependent manner, additional residues of Trio are likely phosphorylated by Src family kinases during netin-1-induced axon outgrowth. *In vitro* kinase assays with recombinant Fyn and Trio fragments revealed tyrosine-432 and tyrosine-921 as *in vitro* Fyn phospho-sites (Fig. 2.3). Although these sites were ignored because tyrosine to phenylalanine point mutation failed to reduce the Fyn-dependent net phosphorylation of Trio, in the shorter

neural isoforms these residues may be the primary target of Src family kinases and directly regulate Trio Rac1 GEF activity. These putative sites are contained within the Spectrin repeat domain of Trio and may contribute to Trio regulation by potentiating the binding of an SH2-domain containing protein yet to be identified in this system. Introduction of phospho-mimicking or phospho-null point mutations at tyrosine-432 and -921 in truncated Trio proteins lacking the C-terminus may be a good first method to determine whether these sites regulate Trio Rac1 GEF activity directly.

Despite being identified as a serine phospho-protein, whether serine phosphorylation regulates Trio function *in vivo* has yet to be reported. By [^{32}P]-orthophosphate labelling of embryonic rat cortices *ex vivo*, isolated Trio was found to be phosphorylated, while netrin-1-treatment enhanced this in a DCC-dependent manner (Fig. 5.1A). Since full-length Trio is expressed at relatively weak levels compared to Trio-A and Trio-D in these tissues, it emphasizes the degree at which Trio is phosphorylated in this experimental context. Similarly, Trio extracted from N1E-115 cells was found to be phosphorylated, while DCC co-expression augmented this (Fig. 5.1B). Subsequent phospho-amino acid analysis by 2D thin layer chromatography revealed that Trio was mainly serine phosphorylated under these conditions (Fig. 5.1C). In further support of this, mass spectrometry of Trio peptides isolated from N1E-115 cells co-expressing DCC revealed serine-1665, -1720, -2400, -2418 and -2572 as phosphorylated (Table 5.1; Fig. 5.1D). Together this data supports the original finding that Trio is highly serine phosphorylated, and provides the context that Trio may be regulated by serine phosphorylation *in vivo* downstream of DCC.

A

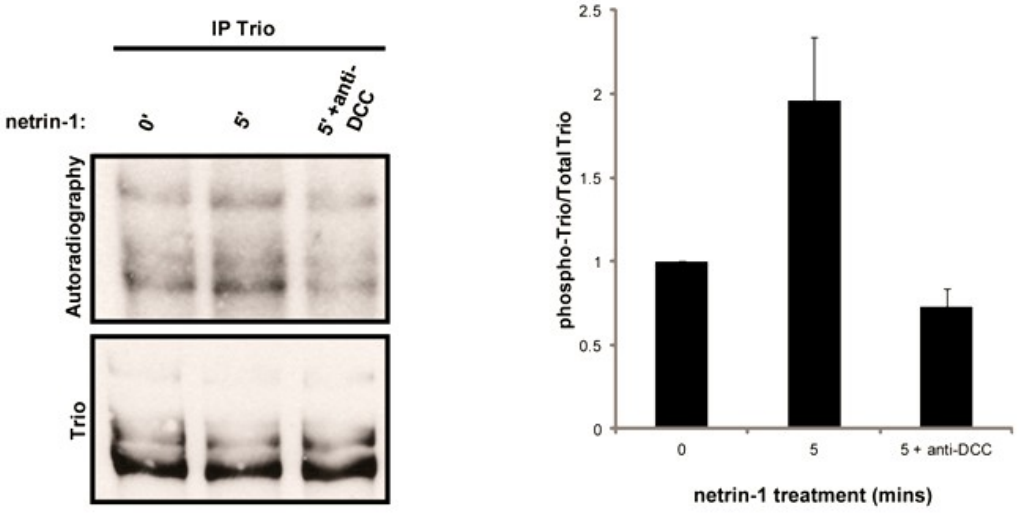
IP Trio
netrin-1:
0'
5'
5'+anti-DCC
Autoradiography
Trio
phospho-Trio/Total Trio
2.5
2
1.5
1
0.5
0
0
5
5 + anti-DCC
netrin-1 treatment (mins)

B

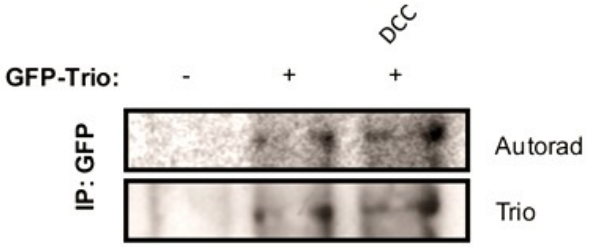
DCC
GFP-Trio:
-
+
+
IP: GFP
Autorad
Trio

C

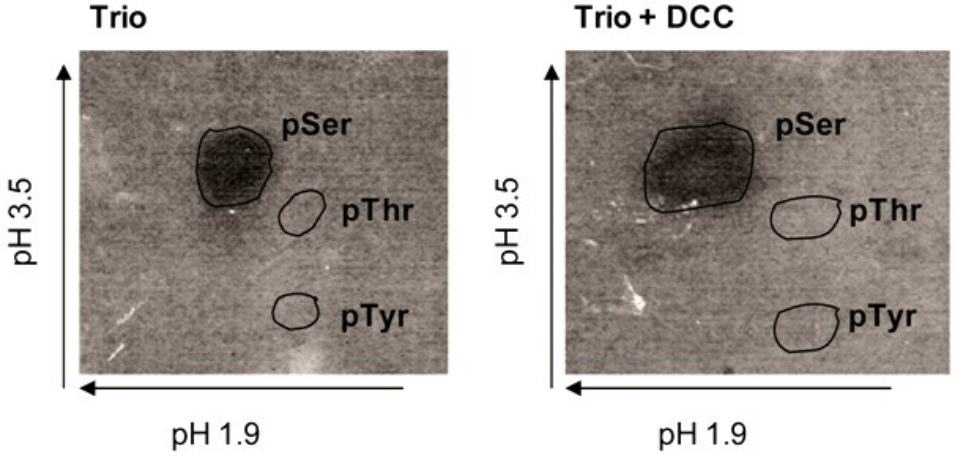
Trio
Trio + DCC
pSer
pThr
pTyr
pH 3.5
pH 1.9

D

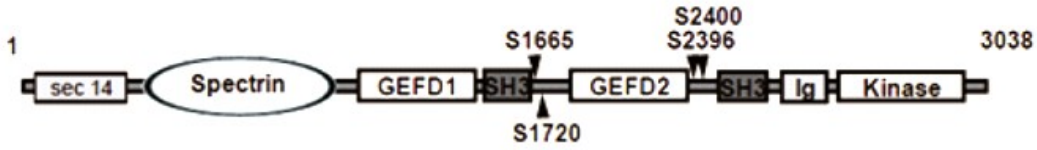
1
3038
S2400
S2396
S1665
S1720
sec 14
Spectrin
GEFD1
SH3
GEFD2
SH3
Ig
Kinase

Figure 5.1 – Trio is predominantly serine phosphorylated with netrin-1/DCC

(A) Trio was immunoprecipitated from lysates of isolated E17.5 rat cortices that had been incubated with [^{32}P]-orthophosphate and treated with netrin-1, in the absence or presence of DCC function blocking antibodies. Immunoprecipitated proteins (IP) and total cell lysates (TCL) were resolved by SDS-PAGE and immunoblotted with the indicated antibodies. Densitometry of phospho-Trio vs. Total Trio was performed. Error bars indicate the SEM. (B) GFP-Trio was immunoprecipitated (IP) from extracts of [^{32}P]-orthophosphate-treated N1E-115 neuroblastoma cells transfected with eGFP-Trio and pRK5-DCC. Proteins were resolved by SDS-PAGE and phospho- and total Trio were visualized by autoradiography (upper panel) or western blotting with anti-GFP antibodies (lower panel). (C) Bands corresponding to Trio from (B) were excised and acid hydrolyzed. 2D thin layer chromatography was performed, and the phosphorylated amino acids from each sample were revealed by autoradiography. (D) Schematic of Trio linear domain structure with phospho-sites identified by LC-MS/MS analysis following phosphopeptide enrichment of isolated GFP-Trio peptides digested with trypsin.

Table 5.1 – Mass spectrometry analysis of Trio phosphopeptides.

GFP-Trio samples were extracted from N1E-115 cells expressing either GFP-Trio alone or GFP-Trio with DCC. Isolated Trio was trypsin-digested and peptides underwent phosphopeptide enrichement on a Sepharose-Al^{3+} resin followed by MALDI-TOF analysis. Phospho-peptide sequences were identified by MASCOT searches using the UniProt database (human filter). Two phosphopeptides identified are near the SH3 domain following GEFD1, while the others are concentrated in the C-terminal domain following the GEFD2. These data confirm our previous findings that Trio is serine phosphorylated with DCC co-expression.

Expression Condition	Fragment position (amino acid #)	Peptide Fragment(S)	Site(s)
Trio alone	2391 – 2412	R.AGAA**S**PLNSPLSSAVPSLGK.E	**S2396**
Trio + DCC	1663 – 1676	R.S**S**MEMEGIFNHK.D	**S1665**
	1716 – 1724	K.WLT**S**PVR.R	**S1720**
	2391 – 2412	R.AGAA**S**PLNSPLSSAVPSLGK.E	**S2396**
	2391 – 2412	R.AGAA**S**PLN**S**PLSSAVPSLGK.E	**S2400**
	2411 – 2423	K.EPFPPS**S**PLQK.G	**S2418**
	2569 – 2579	K.ST**S**WHTALR.L	**S2572**

There are many highly scored putative kinases that are predicted to phosphorylate Trio at these specific sites (Table 5.2). Common putative kinases for the phosphopeptides containing an “SP” motif include members of the CDK/MAPK/GSK/CDK-like (CMGC) kinase family, namely: JNK, p38MAPK, ERK, Cdk-family members, and GSK3 with a high score (Table 5.2). Since all of these kinases are related to either Rho GTPase activation and/or regulation of the actin cytoskeleton, it will be of great interest to validate whether Trio is a phospho-substrate, and is regulated by their kinase activity. Intriguingly, serine-1665 is a putative target of Pak1, which associates with Trio in neurons treated with netrin-1 (Fig. 5.2A). By *in vitro* kinase assay, Pak1 extracted from N1E-115 cells robustly phosphorylated Trio (Fig. 5.2B). In correlation with this active Pak1 (CA-Pak) expression with Trio enhances the total phosphorylation of Trio similarly to DCC co-expression, as determined by ProQ Diamond phospho-protein stain relative to total silver-stained Trio (Fig. 5.2C). Expression of wild type Pak (WT-Pak) was not sufficient to augment Trio total phosphorylation in this manner, nor impair the DCC-enhanced phosphorylation (Fig. 5.2B). Intriguingly, the highest predicted Pak1 consensus sites in Trio (serine-1230 and serine-1726; Table 5.3) are contained within predicted trypsin-cleaved peptides that are too small for MS/MS identification in a proteomics screen. As such, their exclusion from our proteomics screen would not exclude them as putative Pak phosphorylation sites. These preliminary data suggest that Trio is mainly serine phosphorylated by (potentially) various putative kinases, and Pak1 is a viable and particularly logical candidate. Future work should focus on the importance of these phosphorylation sites in the regulation of Trio localization and enzymatic function.

Table 5.2 – GPS 2.1-predicted kinases of Trio phosphopeptides. Amino acid sequences of Trio phosphopeptides were analyzed by GPS 2.1 software for high threshold kinase prediction. Putative kinases with the highest scores are indicated.

Site	Trio Phosphopeptide	Kinase	Score/Cutoff
S1665	**R.S<u>S</u>MEMEGIFNHK.D**	CK2β GRK-4 Pak1	9/6.5 8.333/5 7.071/5.05
S1720	**K.WLT<u>S</u>PVR.R**	JNK p38MAPK Cdk1 VRK mTOR GRK-1	16.472/15.889 11.667/10.667 10.216/4.072 8.75/5.75 7.467/5.8 7/3.75
S2396	**RAGAA<u>S</u>PLNSPLSSAVPSLGKE**	JNK p38MAPK Cdk1 ERK DYRK Cdk6 Akt2	16.361/15.889 13/10.667 9.716/3.095 8.368/7.747 7.167/5.083 7/5.25 6.25/5.75
S2400	**RAGAASPLN<u>S</u>PLSSAVPSLGKE**	JNK p38MAPK Cdk6 mTOR Cdk1 ERK GRK-1 GSK3	16.361/15.889 11/10.667 10/5.25 8.6/5.8 8.187/4.072 7.452/6.557 7.25/3.75 6.667/4
S2418	**KEPFPPS<u>S</u>PLQKG**	JNK p38MAPK Cdk4 ERK Cdk5 CMGC GSK3	17.444/15.889 14/10.667 11.923/5.077 11.241/7.747 10.684/9.158 7.798/5.352 6/4
2572	**KST<u>S</u>WHTALRL**	CAMK	6.394/6.03

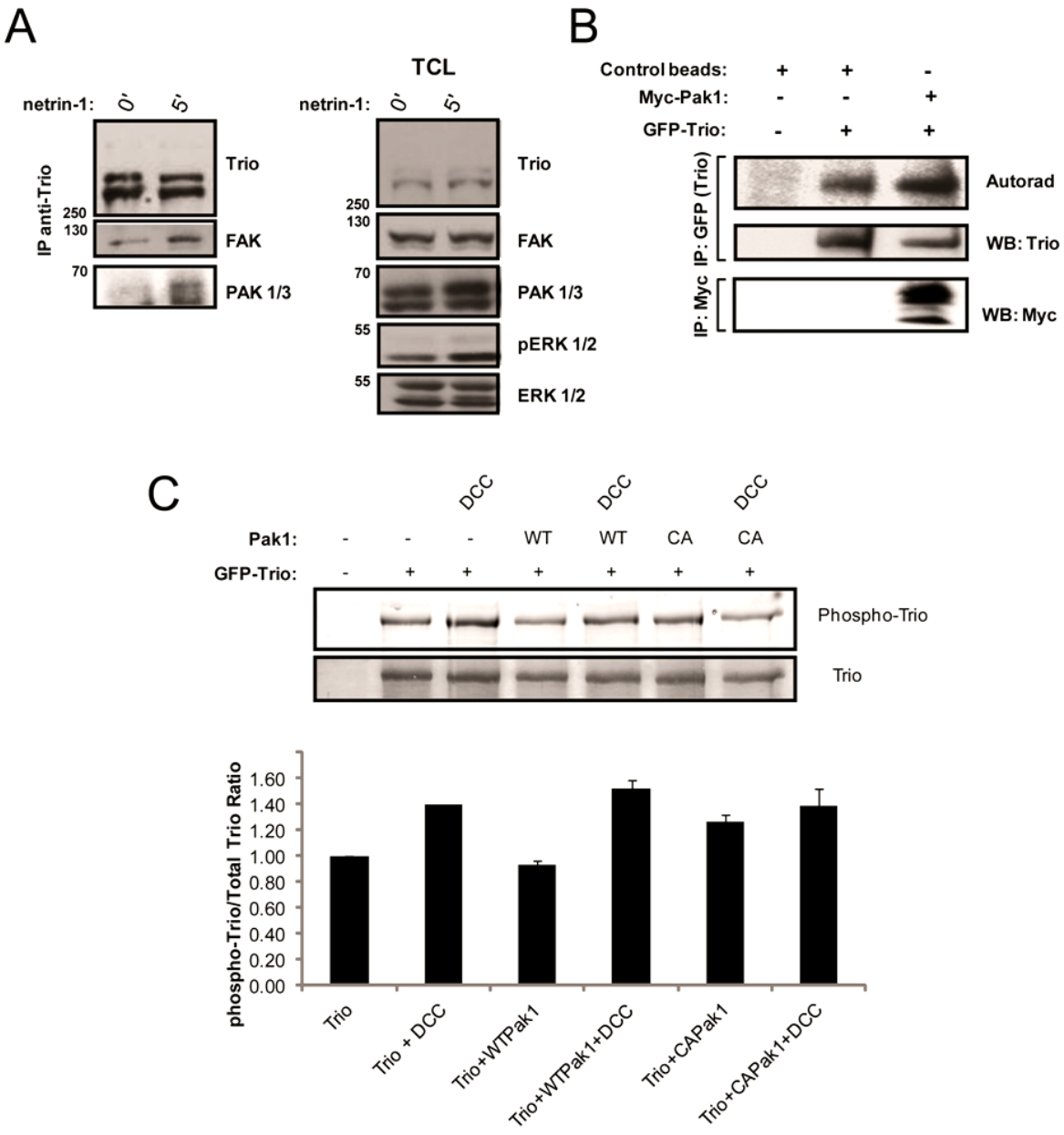
A
TCL
netrin-1: 0' 5'
IP anti-Trio
Trio
FAK
PAK 1/3
250
130
70
55
pERK 1/2
ERK 1/2
B
Control beads: + + -
Myc-Pak1: - - +
GFP-Trio: - + +
IP: GFP (Trio)
Autorad
WB: Trio
IP: Myc
WB: Myc
C
DCC
Pak1: - - - WT WT CA CA
GFP-Trio: - + + + + + +
Phospho-Trio
Trio
phospho-Trio/Total Trio Ratio
0.00
0.20
0.40
0.60
0.80
1.00
1.20
1.40
1.60
Trio
Trio + DCC
Trio+WTPak1
Trio+WTPak1+DCC
Trio+CAPak1
Trio+CAPak1+DCC

Figure 5.2 – Pak1 associates with Trio and potentiates Trio phosphorylation

(A) Trio isoforms were immunoprecipitated from lysates of isolated E17.5 rat cortices treated with netrin-1. Co-association of the kinases FAK and Pak1 were assessed by immunoblotting. Netrin-1 stimulation of DCC-induced signaling pathways was assessed by evaluating pERK1/2 activation in total cell lysates (TCL). (B) GFP-Trio and Myc-Pak1 were immunoprecipitated from extracts of N1E-115 neuroblastoma cells. GFP-Trio was incubated at 30C with either control beads or Pak1-enriched beads in the presence of γ-[^{32}P]-ATP. Phosphorylated and total proteins were visualized by autoradiography and western blotting with the indicated antibodies. (C) GFP-Trio was immunoprecipitated (IP) from extracts of N1E-115 neuroblastoma cells transfected with GFP-Trio, pRK5-DCC, Myc-Pak1 (wild type, WT) or constitutively active (CA) Myc-Pak1 (L107F), as indicated. Proteins were resolved by SDS-PAGE and phospho- and total Trio were visualized in-gel using ProQ Diamond phospho-protein reagent and silver staining, respectively. Densitometry of phospho-Trio vs. Total Trio was performed. Error bars indicate the SEM.

Table 5.3 – GPS 2.1 predicted Pak1 consensus sites in human Trio. The amino acid sequence of human Trio was entered into GPS 2.1 phosphosite prediction software and a search was performed for Pak1 phospho targets. 23 putative serine phosphorylation sites were identified, including serine-1665. Additional high score putative Pak1 sites include serine-1230, -1726 and -2981.

Trio amino acid sequence	Pak1 sites (in Trio)	Score (cutoff 4.375)
VIVDMRGSKWDSIKP	74	4.429
ESFPKKNSGSGNADL	238	4.821
LIQQLRDSAISSNKT	682	4.714
LKYLHRNSVNMPGMV	1033	5.857
RMEKYRTSLEKALGI	1182	4.821
LNEEKRKSARRKEFI	**1230**	**8.286**
KIVLKASSIENKQDW	1516	4.893
ISIASRTSQNTLDSD	1586	5.429
CIAHSRSSMEMEGIF	**1665**	**6.821**
TSPVRRLSSGKADGH	**1726**	**7.429**
KSREVRKSADAGSQK	1750	5.321
GTLSKSSSSGMQSCG	1790	4.429
SQDDKASSRLLVRPT	1833	4.393
ALEDRPSSLLVDQGD	1870	4.536
DEMEERKSSSLKRRH	1905	6.25
EMEERKSSSLKRRHY	1906	6.464
MEERKSSSLKRRHYV	1907	4.75
LKYSKKASLDTSELE	2063	5.571
STSRSRPSRIPQPVR	2280	4.857
PAKDARASLGTLPLG	2381	6
ALRLRKKSEKKDKDG	2583	5.643
LENGYRKSREGLSNK	2603	5.25
EDPAKRPSAALALQE	2981	6.821

5.3 Regulation of the actin cytoskeleton by Hsc70

The idea that Hsc70 is associated with the actin cytoskeleton has been noted, but is not often cited. In 1984 it was reported that a 70 kDa chaperone protein could be enriched at the leading edge of unstressed and motile primary fibroblasts, particularly to actin-containing microfilaments [543]. Although this observed localization of Hsc70 has been documented, little is known about how Hsc70 functions at the leading edge of a migrating cell, notably whether it acts upstream or downstream of Rac1. Hsc70 localized to the periphery of fibroblasts treated with serum, namely to actin-rich lamellipodia structures (Fig. 5.3A). Since Rac activation is required for lamellipodia induction, it is difficult to say whether this localization is due to Rac activation or a consequence. Ectopically expressed Hsc70 localized to and induced membrane ruffles in the absence of serum (Fig. 5.3B). Intriguingly, dominant negative Hsc70 (D10N)-expressing cells lacked ectopic ruffles without serum, but GFP-D10N localized to actin structures (Fig. 5.3C). These data indicate that while Hsc70 recruitment to actin structures is chaperone independent, its function at these sites may be ATPase-dependent. By performing time-lapse imaging, serum treatment induced large membrane ruffles/lamellipodia in vector control or wild type Hsc70-expressing COS7 cells, while Hsc70-D10N-expressing cells had smaller, though dynamic, membrane ruffles which serum failed to augment (Fig. 5.3D). In addition to exhibiting larger membrane ruffles, serum increased the duration of continuous ruffling in vector control and Hsc70-expressing cells, while having no effect on D10N-expressing cells (data not shown). Although these findings are consistent with Hsc70 supporting Rac-dependent actin structures, they do not preclude that Hsc70 acts downstream of Rac1.

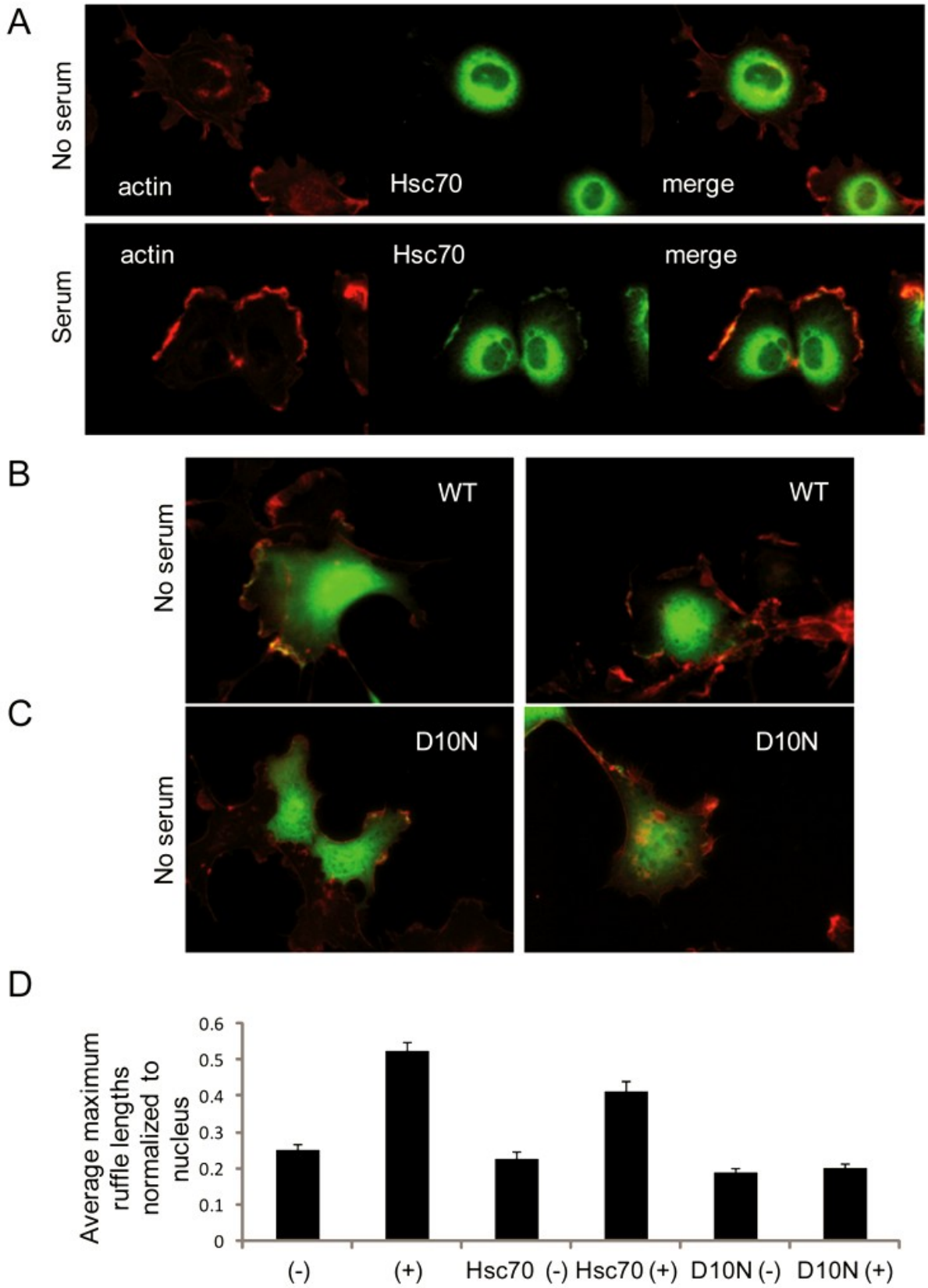
A
No serum
actin
Hsc70
merge
Serum
actin
Hsc70
merge
B
No serum
WT
WT
C
No serum
D10N
D10N
D
Average maximum ruffle lengths normalized to nucleus
0.6
0.5
0.4
0.3
0.2
0.1
0
(-)
(+)
Hsc70 (-)
Hsc70 (+)
D10N (-)
D10N (+)

Figure 5.3 – Hsc70 localizes to actin structures and regulates lamellipodia induction

Serum-starved COS7 cells were cultured on poly-L-lysine coated cover slips and treated with serum for 15 minutes before fixation. (A) Endogenous Hsc70 was visualized by indirect immunofluorescence using a monoclonal antibody. (B) GFP-Hsc70 or (C) GFP-Hsc70(D10N) localization was determined by fluorescence microscopy. In all cases, actin filaments were stained with Rhodamine-conjugated phalloidin. (D) Timelapse microscopy of serum-starved COS7 cells expressing either GFP, GFP-Hsc70 or GFP-Hsc70(D10N) was performed. The average maximum membrane ruffles/lamellipodia lengths were measured and normalized to the nuclear diameter of each cell.

Intriguingly, the structure of the ATPase domain of Hsc70 as determined by X-ray crystallography has a high similarity to actin, despite sharing very little sequence identity [544]. Further study revealed that Hsc70 from *Dictyostelium discoideum* interacts with the heterodimeric actin-binding protein cap32/34 via its ATPase domain, and promotes the actin-capping activity of this complex *in vitro* [545]. In mammalian cardiomyocytes, Hsc70 associates directly with the capping protein (CP) subunit CapZβ1 and promotes its binding to F-actin *in vitro* [546]. While actin capping proteins are essential for cell migration both *in vitro* and *in vivo* [547] and CP supports lamellipodia formation [548], the contribution of Hsc70 to these processes has not been described. In cells, the activity of CP is antagonized by Ena/VASP, which binds the barbed ends of F-actin and promotes actin polymerization. Ena/VASP proteins can cooperate with the WAVE complex to regulate the actin cytoskeleton downstream of Rac1 activation [549,550]. Therefore, though speculative, Hsc70 may regulate actin dynamics by both directly binding to and activating actin capping proteins, and by recruiting Dbl family Rac1 GEFs like Trio to the tips of actin structures, promoting local Rac1 activation and downstream activation of WAVE and Ena/VASP. In addition to this, it will be of considerable interest to determine whether Hsc70-dependent regulation of Rac1 is involved in other biological systems including cancer progression, tumour invasion, or whether modulation of Hsc70 activity will support nerve regeneration *in vivo*.

5.4 **CdGAP regulation in the nervous system**

The CdGAP-null mouse has proven to be an important tool for studying the function of CdGAP *in vivo.* Indeed many new questions have now arisen regarding the

contribution of CdGAP to the development of the vascular system and the nervous system. Particularly the severe vascular phenotypes documented in this thesis indicate a somewhat unforeseen importance of CdGAP during development. Outside of the work that has been presented in this thesis, in collaboration with colleagues, we have studied the requirement for CdGAP during VEGF-induced signaling in endothelial cells. CdGAP is required both *in vitro* and *ex vivo* for VEGF-dependent models of angiogenesis, while it is not required for vasculogenesis [551].

We have previously reported that CdGAP depletion in breast cancer explants results in decreased cell proliferation [360]. In the adult brain the dendate gyrus region of the hippocampus is the site of neuronal progenitor proliferation [552]. The finding that CdGAP is enriched in the developing hippocampus may indeed indicate that CdGAP is involved in neural proliferation. This hypothesis is supported by the fact that growth factor treatment induces the upregulation of CdGAP expression [359]. In adult mice, CdGAP mRNA is enriched in the dendate gyrus of the hippocampus (Allen Brain Atlas). To assess whether CdGAP contributes to neural proliferation, histological sections of the dendate gyrus of both embryos and adult CdGAP-null mice can be probed with antibodies for Ki-67, which is a strong proliferative marker for adult neurogenesis [553]. Studies have reported that exercise and housing rodents in an enriched environment increases neuronal proliferation of the hippocampus [554,555]. As such, differences in neural proliferation between CdGAP-null and wild type mice may be more pronounced by first subjecting the adult mice to a fitness or enrichment regimen. There is a considerable amount of crosstalk between neurogenesis and angiogenesis in the brain, and VEGF acting by its receptor VEGF-R2 is instrumental in both processes [556]. The

hypovascularized supportive tissue surrounding CdGAP-null brains indicate that CdGAP supports neural vascularisation *in vivo*. In the context of the fitness paradigm, exercise-induced neurogenesis correlates with an increased cerebral blood volume at the dendate gyrus [557]. VEGF is an important regulator of neural proliferation within the hippocampus, particularly by activating MEK/ERK and PI3K/Akt signaling pathways [558]. Since we have implicated CdGAP function in both endothelial and neuronal VEGF signaling *ex vivo*, it raises the exciting prospect that CdGAP is a key regulator of VEGF-induced neurogenesis *in vivo.* To assess this, CdGAP-null mice will be subjected to various behavioural paradigms including those testing learning, memory, motor and coordination (gate, climbing).

In addition to the hippocampus, CdGAP mRNA is most highly enriched in the Purkinje cell layer of the adult cerebellum, and to a lesser extent, the granule cell layer (Allen Brain Atlas). It may be of interest to determine whether CdGAP is enriched in the adult cerebellum at the protein level, and to investigate whether loss of CdGAP disrupts the structure or function of the cerebellum. Since the cerebellum is an important centre for coordinating motor signals, the tonality of CdGAP-null skeletal muscle could be assessed. Preliminary assessments indicate that CdGAP-null mice have a reduced tendency of climbing on their hind legs (moving in the Z-axis), which may be directly due to defects in the cerebellum. Further studies will be required to confirm this finding.

Despite CdGAP being enriched in the hippocampus, dissociated hippocampal neurons expressed similar levels of CdGAP as dissociated cortical neurons (Fig. 4.1). Although CdGAP-null neurons polarize normally and form synapses (data not shown),

electrophysiological assessments will need to be performed to confirm whether these neuronal connections are functional and similar to wild-type neurons. The defects in cytoarchitecture of cortical neurons we reported are certainly perplexing. The strikingly large CdGAP-null cortical growth cones are the most obvious abnormality. These growth cones appear to have an expanded, disorganized microtubule core relative to neurons from littermate controls. It is possible that dysregulation of microtubules may be a key effect of CdGAP-loss in neurons. As such it may be of interest to assess the degree of acetylation or tyrosination of microtubules of these CdGAP-null neurons relative to control neurons. Interestingly, type II histone deacetylases HDAC5 and 6 deacetylate tubulin, and HDAC inhibitors promote neurite outgrowth and axonal regeneration (reviewd in [559]). It will be of interest to determine which genes are selectively regulated in CdGAP-null neurons relative to control neurons by RNA deep sequencing, with an emphasis on regulators of the actin cytoskeleton. In addition to this, identifying novel binding partners of CdGAP extracted from neurons via a proteomics screen may be of potential interest. To date, lack of effective antibodies for mouse CdGAP limits the efficiency for extracting endogenous CdGAP from neurons. Since this may be in part caused by the epitope of CdGAP being masked by other protein(s), interactors of CdGAP may be pulled down from neuronal extracts using purified, recombinant CdGAP domains and identified by mass spectrometry.

5.5 Conclusion

The generation of genetic animal models of Rho GTPases and regulators has profoundly expedited our discovery of their fine-tuned functions during nervous system

development and maintenance. This thesis has provided some insights into the localized regulation of the Rho GEF Trio in neurons and has implicated CdGAP function during embryogenesis *in vivo* for the first time. Using a combination of techniques and model systems, we demonstrate that Trio is regulated by phosphorylation and association with a molecular chaperone. We describe an important role for CdGAP in vascular development and implicate CdGAP in neuronal function. Further study is required to better characterize the regulation of Trio and CdGAP in neurons and to determine their specific contribution to neuronal health and/or diseases. Ultimately, we hope these studies will contribute to revealing new mechanisms and targets to treat various pathologies including metastatic cancers and neurodegeneration where dysregulation of Rho GEF or GAP proteins are reported.

REFERENCES

1 Rowbury, R. Robert Hooke, 1635-1703. *Sci Prog* **95**, 238-254 (2012).

2 Fred, E. B. Antony van Leeuwenhoek: On the three-hundredth anniversary of his birth. *J Bacteriol* **25**, iv.2-iv.18 (1933).

3 Madaule, P. & Axel, R. A novel ras-related gene family. *Cell* **41**, 31-40 (1985).

4 Rojas, A. M., Fuentes, G., Rausell, A. & Valencia, A. The Ras protein superfamily: Evolutionary tree and role of conserved amino acids. *J Cell Biol* **196**, 189-201 (2012).

5 Jaffe, A. B. & Hall, A. Rho GTPases: Biochemistry and Biology. *Ann. Rev. Cell Dev. Biol.* **21**, 247-269 (2005).

6 Vega, F. M. & Ridley, A. J. SnapShot: Rho family GTPases. *Cell* **129**, 1430 (2007).

7 Zheng, Y. Dbl family guanine nucleotide exchange factors. *Trends Biochem Sci* **26**, 724-732 (2001).

8 Tcherkezian, J. & Lamarche-Vane, N. Current knowledge of the large RhoGAP family of proteins *Biol. Cell* **99**, 67-86 (2007).

9 Olofsson, B. Rho guanine dissociation inhibitors: pivotal molecules in cellular signalling. *Cell Signal* **11**, 545-554 (1999).

10 Vetter, I. R. & Wittinghofer, A. The guanine nucleotide-binding switch in three dimensions. *Science* **294**, 1299-1304 (2001).

11 Valencia, A., Chardin, P., Wittinghofer, A. & Sander, C. The ras protein family: evolutionary tree and role of conserved amino acids. *Biochemistry* **30**, 4637-4648 (1991).

12 Ihara, K. *et al.* Crystal structure of human RhoA in a dominantly active form complexed with a GTP analogue. *J Biol Chem* **273**, 9656-9666 (1998).

13 Hirshberg, M., Stockley, R. W., Dodson, G. & Webb, M. R. The crystal structure of human rac1, a member of the rho-family complexed with a GTP analogue. *Nat Struct Biol* **4**, 147-152 (1997).

14 Hakoshima, T., Shimizu, T. & Maesaki, R. Structural basis of the Rho GTPase signaling. *J Biochem* **134**, 327-331 (2003).

15 Roberts, P. J. *et al.* Rho family GTPase modification and dependence on CAAX motif-signaled posttranslational modification. *J Biol Chem* **283**, 25150-25163 (2008).

16 Reid, T. S., Terry, K. L., Casey, P. J. & Beese, L. S. Crystallographic analysis of CaaX prenyltransferases complexed with substrates defines rules of protein substrate selectivity. *J Mol Biol* **343**, 417-433 (2004).

17 Ashby, M. N. CaaX converting enzymes. *Curr Opin Lipidol* **9**, 99-102 (1998).

18 Boyartchuk, V. L., Ashby, M. N. & Rine, J. Modulation of Ras and a-factor function by carboxyl-terminal proteolysis. *Science* **275**, 1796-1800 (1997).

19 Hrycyna, C. A., Sapperstein, S. K., Clarke, S. & Michaelis, S. The Saccharomyces cerevisiae STE14 gene encodes a methyltransferase that mediates C-terminal methylation of a-factor and RAS proteins. *Embo J* **10**, 1699-1709 (1991).

20 Mitin, N., Roberts, P. J., Chenette, E. J. & Der, C. J. Posttranslational lipid modification of Rho family small GTPases. *Methods in Molecular Biology* **827**, 87-95 (2012).
21 Navarro-Lérida, I. *et al.* A palmitoylation switch mechanism regulates Rac1 function and membrane organization. *Embo J* **31**, 534-551 (2012).
22 Burnett, G. & Kennedy, E. P. The enzymatic phosphorylation or proteins. *J Biol Chem* **211**, 969-980 (1954).
23 Lang, P. *et al.* Protein kinase A phosphorylation of RhoA mediates the morphological and functional effects of cyclic AMP in cytotoxic lymphocytes. *EMBO J* **15**, 510-519 (1996).
24 Sauzeau, V. *et al.* Cyclic GMP-dependent protein kinase signaling pathway inhibits RhoA-induced Ca2+ sensitization of contraction in vascular smooth muscle. *J Biol Chem* **275**, 21722-21729 (2000).
25 Ellerbroek, S. M., Wennerberg, K. & Burridge, K. Serine phosphorylation negatively regulates RhoA in vivo. *J Biol Chem* **278**, 19023-19031 (2003).
26 Tu, S., Wu, W. J., Wang, J. & Cerione, R. A. Epidermal growth factor-dependent regulation of Cdc42 is mediated by the Src tyrosine kinase. *J Biol Chem* **278**, 49293-49300 (2003).
27 Kwon, T., Kwon, D. Y., Chun, J., Kim, J. H. & Kang, S. S. Akt protein kinase inhibits Rac1-GTP binding through phosphorylation at serine 71 of Rac1. *J Biol Chem* **275**, 423-428 (2000).
28 Popovic, D., Vucic, D. & Dikic, I. Ubiquitination in disease pathogenesis and treatment. *Nat Med* **20**, 1242-1253 (2014).
29 Kovacic, H. N., Irani, K. & Goldschmidt-Clermont, P. J. Redox regulation of human Rac1 stability by the proteasome in human aortic endothelial cells. *J Biol Chem* **276**, 45856-45861 (2001).
30 Visvikis, O. *et al.* Activated Rac1, but not the tumorigenic variant Rac1b, is ubiquitinated on Lys 147 through a JNK-regulated process. *FEBS J* **275**, 386-396 (2008).
31 Lynch, E. A., Stall, J., Schmidt, G., Chavrier, P. & D`Souza-Schorey, C. Proteasome-mediated degradation of Rac1-GTP during epithelial cell scattering. *Mol Biol Cell* **17**, 2236-2242 (2006).
32 Torrino, S. *et al.* The E3 ubiquitin-ligase HACE1 catalyzes the ubiquitylation of active Rac1. *Dev Cell* **21**, 959-965 (2011).
33 Wang, H. R. *et al.* Regulation of cell polarity and protrusion formation by targeting RhoA for degradation. *Science* **302**, 1775-1779 (2003).
34 Chen, Y. *et al.* Cullin mediates degradation of RhoA through evolutionarily conserved BTB adaptors to control actin cytoskeleton structure and cell movement. *Mol Cell* **35**, 841-855 (2009).
35 Wilkins, A., Ping, Q. & Carpenter, C. L. RhoBTB2 is a substrate of the mammalian Cul3 ubiquitin ligase complex. *Genes Dev* **18**, 856-861 (2004).
36 Geiss-Friedlander, R. & Melchoir, F. Concepts in sumoylation: a decade on. *Nat Rev Mol Cell Biol* **8**, 947-956 (2007).
37 Muller, S., Hoege, C., Pyrowolakis, G. & Jentsch, S. SUMO, ubiquitin's mysterious cousin. *Nat Rev Mol Cell Biol* **2**, 202-210 (2001).

38 Castillo-Lluva, S. *et al.* SUMOylation of the GTPase Rac1 is required for optimal cell migration. *Nat Cell Biol* **12**, 1078-1085 (2010).
39 Ridley, A. J. & Hall, A. The small GTP-binding protein rho regulates the assembly of focal adhesions and actin stress fibers in response to growth factors. *Cell* **70**, 389-399 (1992).
40 Ridley, A. J., Paterson, H. F., Johnston, C. L., Diekmann, D. & Hall, A. The small GTP-binding protein rac regulates growth factor-induced membrane ruffling. *Cell* **70**, 401-410 (1992).
41 Nobes, C. D. & Hall, A. Rho, Rac and Cdc42 GTPases regulate the assembly of multimolecular focal complexes associated with actin stress fibers, lamellipodia and filopodia. *Cell* **81**, 53-62 (1995).
42 Wheeler, A. P. & Ridley, A. J. Why three Rho proteins? RhoA, RhoB, RhoC, and cell motility. *Experimental Cell Research* **301**, 43-49 (2004).
43 Aktories, K. & Just, I. Clostridial Rho-inhibiting protein toxins. *Curr Top Microbiol Immunol* **291**, 113-145 (2005).
44 Allal, C. *et al.* RhoA prenylation is required for promotion of cell growth and transformation and cytoskeleton organization but not for induction of serum response element transcription. *J Biol Chem* **275**, 31001-31008 (2000).
45 Stamatakis, K., Cernuda-Morollón, E., Hernández-Perera, O. & Pérez-Sala, D. Isoprenylation of RhoB is necessary for its degradation. A novel determinant in the complex regulation of RhoB expression by the mevalonate pathway. *J Biol Chem* **277**, 49389-49396 (2002).
46 Wennerberg, K. & Der, C. J. Rho-family GTPases: it's not only Rac and Rho (and I like it). *J Cell Sci* **117**, 1301-1312 (2004).
47 Adamson, P., Paterson, H. F. & Hall, A. Intracellular localization of the P21rho proteins. *J Cell Biol* **119**, 617-627 (1992).
48 Garcia-Mata, R., Boulter, E. & Burridge, K. The 'invisible hand': regulation of RHO GTPases by RHOGDIs. *Nat Rev Mol Cell Biol* **12**, 493-504 (2011).
49 Wherlock, M., Gampel, A., Futter, C. & Mellor, H. Farnesyltransferase inhibitors disrupt EGF receptor traffic through modulation of the RhoB GTPase. *J Cell Sci* **117**, 3221-3231 (2004).
50 Ridley, A. J. RhoA, RhoB and RhoC have different roles in cancer cell migration. *J Microsc* **251**, 242-249 (2013).
51 DeGeer, J. & Lamarche-Vane, N. Rho GTPases in neurodegeneration diseases. *Experimental Cell Research* **319**, 2384-2394 (2013).
52 Ridley, A. J. & Hall, A. Distinct patterns of actin organization regulated by the small GTP-binding proteins Rac and Rho. *Cold Spring Harb Symp Quant Biol* **57**, 661-671 (1992).
53 Paterson, H. F. *et al.* Microinjection of recombinant p21rho induces rapid changes in cell morphology. *J Cell Biol* **111**, 1001-1007 (1990).
54 Kaibuchi, K., Kuroda, S. & Amano, M. Regulation of the cytoskeleton and cell adhesion by the Rho family GTPases in mammalian cells. *Annu Rev Biochem* **68**, 459-486 (1999).
55 Etienne-Manneville, S. & Hall, A. Rho GTPases in cell biology. *Nature* **420**, 629-635 (2002).

56 Amano, M. *et al.* Phosphorylation and activation of myosin by Rho-associated kinase (Rho-kinase). *J Biol Chem* **271**, 20246-20249 (1996).
57 Kimura, K. *et al.* Regulation of myosin phosphatase by rho and rho-associated kinase (rho-kinase). *Science* **273**, 245-248 (1996).
58 Riento, K. & Ridley, A. J. Rocks: multifunctional kinases in cell behaviour. *Nat Rev Mol Cell Biol* **4**, 446-456 (2003).
59 Maekawa, M. *et al.* Signaling from Rho to the actin cytoskeleton through protein kinases ROCK and LIM-kinase. *Science* **285**, 895-898 (1999).
60 Ohashi, K. *et al.* Rho-associated kinase ROCK activates LIM-kinase 1 by phosphorylation at threonine 508 within the activation loop. *J Biol Chem* **275**, 3577-3582 (2000).
61 Palazzo, A. F., Cook, T. A., Alberts, A. S. & Gundersen, G. G. mDia mediates Rho-regulated formation and orientation of stable microtubules. *Nat Cell Biol* **3**, 723-729 (2001).
62 Watanabe, N. *et al.* p140mDia, a mammalian homolog of Drosophila diaphanous, is a target protein for Rho small GTPase and is a ligand for profilin. *EMBO J* **16**, 3044-3056 (1997).
63 Watanabe, N., Kato, T., Fujita, A., Ishizaki, T. & Narumiya, S. Cooperation between mDia1 and ROCK in Rho-induced actin reorganization. *Nat Cell Biol* **1**, 136-143 (1999).
64 Wallar, B. J. & Alberts, A. S. The formins: active scaffolds that remodel the cytoskeleton. *Trends Cell Biol* **13**, 435-446 (2003).
65 Piekny, A., Werner, M. & Glotzer, M. Cytokinesis: welcome to the Rho zone. *Trends Cell Biol* **15**, 651-658 (2005).
66 Lammers, M., Meyer, S., Kühlmann, D. & Wittinghofer, A. Specifity of interactions between mDia isoforms and Rho proteins. *J Biol Chem* **283**, 35236-35246 (2008).
67 Pertz, O., Hodgson, L., Klemke, R. L. & Hahn, K. M. Spatiotemporal dynamics of RhoA activity in migrating cells. *Nature* **440**, 1069-1072 (2006).
68 Broussard, J. A., Webb, D. J. & Kaverina, I. Asymmetric focal adhesion disassembly in motile cells. *Curr Opin Cell Biol* **20**, 85-90 (2008).
69 Ridley, A. J. Life at the leading edge. *Cell* **145**, 1012-1022 (2011).
70 Sahai, E., Garcia-Medina, R., Pouysségur, J. & Vial, E. Smurf1 regulates tumor cell plasticity and motility through degradation of RhoA leading to localized inhibition of contractility. *J Cell Biol* **176**, 35-42 (2007).
71 Horiiuchi, A. *et al.* Up-regulation of small GTPases, RhoA and RhoC, is associated with tumor progression in ovarian carcinoma. *Lab Invest* **83**, 861-870 (2003).
72 Vega, F. a. R., AJ. Rho GTPases in cancer cell biology. *FEBS Lett* **582**, 2093-2101 (2008).
73 Croft, D. R. *et al.* Conditional ROCK activation in vivo induces tumor cell dissemination and angiogenesis. *Cancer Res* **64**, 8994-9001 (2004).
74 Hakem, A. *et al.* RhoC is dispensable for embryogenesis and tumor initiation but essential for metastasis. *Genes Dev* **19**, 1974-1979 (2005).
75 Liu, A. X., Rane, N., Liu, J. P. & Prendergast, G. C. RhoB is dispensable for mouse development, but it modifies susceptibility to tumor formation as well as

cell adhesion and growth factor signaling in transformed cells. *Mol Cell Biol* **21**, 6906-6912 (2001).
76 Hill, C. S., Wynne, J. & Treisman, R. The Rho family GTPases RhoA, Rac1, and CDC42Hs regulate transcriptional activation by SRF. *Cell* **81**, 1159-1170 (1995).
77 Perona, R. *et al.* Activation of the nuclear factor-kappaB by Rho, CDC42, and Rac-1 proteins. *Genes Dev* **11**, 463-475 (1997).
78 Zalcman, G. *et al.* Regulation of Ras-related RhoB protein expression during the cell cycle. *Oncogene* **10**, 1935-1945 (1995).
79 Adini, I., Rabinovitz, I., SUn, J. F., Prendergast, G. C. & Benjamin, L. E. RhoB controls Akt trafficking and stage-specific survival of endothelial cells during vascular development. *Genes Dev* **17**, 2721-2732 (2003).
80 Gampel, A., Parker, P. J. & Mellor, H. Regulation of epidermal growth factor receptor traffic by the small GTPase rhoB. *Curr Biol* **9**, 955-958 (1999).
81 Huang, M., Duhadaway, J. B., Prendergast, G. C. & Laury-Kleintop, L. D. RhoB regulates PDGFR-beta trafficking and signaling in vascular smooth muscle cells. *Arterioscler Thromb Vasc Biol* **27**, 2597-2605 (2007).
82 Kazerounian, S. *et al.* RhoB differentially controls Akt function in tumor cells and stromal endothelial cells during breast tumorigenesis. *Cancer Res* **73**, 50-61 (2013).
83 Didsbury, J., Weber, R. F., Bokoch, G. M., Evans, T. & Snyderman, R. *rac*, a Novel *ras*-related Family of Proteins that are Botulinum Toxin Substrates. *J. Biol. Chem.* **264**, 16378-16382 (1989).
84 Jordan, P., Brazão, R., Boavida, M. G., Gespach, C. & Chastre, E. Cloning of a novel human Rac1b splice variant with increased expression in colorectal tumors. *Oncogene* **18**, 6835-6839 (1999).
85 Matos, P., Collard, J. G. & Jordan, P. Tumor-related alternatively spliced Rac1b is not regulated by Rho-GDP dissociation inhibitors and exhibits selective downstream signaling. *J Biol Chem* **278**, 50442-50448 (2003).
86 Corbetta, S. *et al.* Generation and characterization of Rac3 knockout mice. *Mol. Cell Biol.* **25**, 5763-5776 (2005).
87 Vincent, S., Jeanteur, P. & Fort, P. Growth-regulated expression of rhoG, a new member of the ras homolog gene family. *Mol Cell Biol* **12**, 3138-3148 (1992).
88 Hordijk, P. L. Regulation of NADPH oxidases: the role of Rac proteins. *Circ Res* **98**, 453-462 (2006).
89 Qiu, R.-G., Chen, J., Kirn, D., McCormick, R. & Symons, M. An essential role for Rac in Ras transformation. *Nature* **374**, 457-459 (1995).
90 Lamarche, N., Tapon, N., Stowers, L., Burbelo, P.D., Aspenstrom, P., Bridges, T., Chant, J. and Hall, A. Rac and Cdc42 induce actin polymerization and G1 cell cycle progression independently of p65PAK and the JNK/SAPK MAP kinase cascade. *Cell* **87**, 519-529 (1996).
91 Kaufmann, N., Wills, Z.P., and Van Vactor, D. Drosophila Rac1 controls motor axon guidance. *Development* **125**, 453-461 (1998).
92 Manser, E., Leung, T., Salihuddin, H., Zhao, Z. S. & Lim, L. A brain serine/threonine protein kinase activated by Cdc42 and Rac1. *Nature* **367**, 40-46 (1994).

93 Edwards, D. C., Sanders, L. C., Bokoch, G. M. & Gill, G. N. Activation of LIM-kinase by Pak1 couples Rac/Cdc42 GTPase signalling to actin cytoskeletal dynamics. *Nat Cell Biol* **1**, 253-259 (1999).
94 Yang, N. *et al.* Cofilin phosphorylation by LIM-kinase 1 and its role in Rac-mediated actin reorganization. *Nature* **393**, 809-812 (1998).
95 Goeckeler, Z. M. *et al.* Phosphorylation of myosin light chain kinase by p21-activated kinase PAK2. *J Biol Chem* **275**, 18366-18374 (2000).
96 Sanders, L. C., Matsumura, F., Bokoch, G. M. & de Lanerolle, P. Inhibition of myosin light chain kinase by p21-activated kinase. *Science* **283**, 2083-2085 (1999).
97 Eblen, S. T., Slack, J. K., Weber, M. J. & Catling, A. D. Rac-PAK signaling stimulates extracellular signal-regulated kinase (ERK) activation by regulating formation of MEK1-ERK complexes. *Mol Cell Biol* **22**, 6023-6033 (2002).
98 Zhang, S. *et al.* Rho family GTPases regulate p38 mitogen-activated protein kinase through the downstream mediator Pak1. *J Biol Chem* **270**, 23934-23936 (1995).
99 Bagrodia, S., Derijard, B., Davis, R. J. & Cerione, R. A. Cdc42 and PAK-mediated signaling leads to Jun kinase and p38 mitogen-activated protein kinase activation. *J Biol Chem* **270**, 27995-27998 (1995).
100 Rohatgi, R. *et al.* The interaction between N-WASP and the Arp2/3 complex links Cdc42- dependent signals to actin assembly. *Cell* **97**, 221-231 (1999).
101 Tomasevic, N. *et al.* Differential regulation of WASP and N-WASP by Cdc42, Rac1, Nck, and PI(4,5)P2. *Biochemistry* **46**, 3494-3502 (2007).
102 Machesky, L. M. *et al.* Scar, a WASp-related protein, activates nucleation of actin filaments by the Arp2/3 complex. *Proc Natl Acad Sci U S A* **96**, 3739-3744 (1999).
103 Pollitt, A. Y. & Insall, R. H. WASP and SCAR/WAVE proteins: the drivers of actin assembly. *J Cell Sci* **122**, 2575-2578 (2009).
104 Lebensohn, A. M. & Kirschner, M. W. Activation of the WAVE complex by coincident signals controls actin assembly. *Mol Cell* **36**, 512-524 (2009).
105 Derivery, E. & Gautreau, A. Generation of branched actin networks: assembly and regulation of the N-WASP and WAVE molecular machines. *Bioessays* **32**, 119-131 (2010).
106 Matos, P. & Jordan, P. Expression of Rac1b stimulates NF-kappaB-mediated cell survival and G1/S progression. *Experimental Cell Research* **305**, 292-299 (2005).
107 Schnelzer, A. *et al.* Rac1 in human breast cancer: overexpression, mutation analysis, and characterization of a new isoform, Rac1b. *Oncogene* **19**, 3013-3020 (2000).
108 Zhou, C. *et al.* The Rac1 splice form Rac1b promotes K-ras-induced lung tumorigenesis. *Oncogene* **32**, 903-909 (2013).
109 Knaus, U. G., Wang, Y., Reilly, A. M., Warnock, D. & Jackson, J. H. Structural requirements for PAK activation by Rac GTPases. *J Biol Chem* **273**, 21512-21518 (1998).
110 Abraham, M. T. *et al.* Motility-related proteins as markers for head and neck squamous cell cancer. *Laryngoscope* **111**, 1285-1289 (2001).

111 Roberts, A. W. *et al.* Deficiency of the hematopoietic cell-specific rho family GTPase Rac2 is characterized by abnormalities in neutrophil function and host defense. *Immunity* **10**, 183-196 (1999).
112 Wheeler, A. P. *et al.* Rac1 and Rac2 regulate macrophage morphology but are not essential for migration. *J Cell Sci* **119**, 2749-2757 (2006).
113 Sugihara, K. *et al.* Rac1 is required for the formation of three germ layers during gastrulation. *Oncogene* **17**, 3427-3433 (1998).
114 Haataja, L., Groffen, J. & Heisterkamp, N. Characterization of RAC3, a novel member of the Rho family. *J Biol Chem* **272**, 20384-20388 (1997).
115 Haataja, L., Kaartinen, V., Groffen, J. & Heisterkamp, N. The small GTPase Rac3 interacts with the integrin-binding protein CIB and promotes integrin alpha(IIb)beta(3)-mediated adhesion and spreading. *J Biol Chem* **277**, 8321-8328 (2002).
116 Joyce, P. L. & Cox, A. D. Rac1 and Rac3 are targets for geranylgeranyltransferase I inhibitor-mediated inhibition of signaling, transformation, and membrane ruffling. *Cancer Res* **63**, 7959-7967 (2003).
117 Keller, P. J., Gable, C. M., Wing, M. R. & Cox, A. D. Rac3-mediated transformation requires multiple effector pathways. *Cancer Res* **65**, 9883-9890 (2005).
118 Estrach, S. *et al.* The Human Rho-GEF trio and its target GTPase RhoG are involved in the NGF pathway, leading to neurite outgrowth. *Curr Biol*, 307-312 (2002).
119 Katoh, H. *et al.* Small GTPase RhoG is a key regulator for neurite outgrowth in PC12 cells. *Mol Cell Biol* **20**, 7378-7387 (2000).
120 Fujimoto, S., Negishi, M. & Katoh, H. RhoG promotes neural progenitor cell proliferation in mouse cerebral cortex. *Mol Biol Cell* **20**, 4941-4950 (2009).
121 Murga, C., Zohar, M., Teramoto, H. & Gutkind, J. S. Rac1 and RhoG promote cell survival by the activation of PI3K and Akt, independently of their ability to stimulate JNK and NF-kappaB. *Oncogene* **21**, 207-216 (2002).
122 Ellerbroek, S. M. *et al.* SGEF, a RhoG guanine nucleotide exchange factor that stimulates macropinocytosis. *Mol Biol Cell* **15**, 3309-3319 (2004).
123 Gauthier-Rouviere, C. *et al.* RhoG GTPase controls a pathway that independently activates Rac1 and Cdc42Hs. *Mol Biol Cell* **9**, 1379-1394 (1998).
124 Katoh, H. & Negishi, M. RhoG activates Rac1 by direct interaction with the Dock180-binding protein Elmo. *Nature* **424**, 461-464 (2003).
125 Vigorito, E. *et al.* RhoG regulates gene expression and the actin cytoskeleton in lymphocytes. *Oncogene* **22**, 330-342 (2003).
126 Shinjo, K. *et al.* Molecular cloning of the gene for the human placental GTP-binding protein Gp (G25K): identification of this GTP-binding protein as the human homolog of the yeast cell-division-cycle protein CDC42. *Proc Natl Acad Sci* **87**, 9853-9857 (1990).
127 Munemitsu, S. *et al.* Molecular cloning and expression of a G25K cDNA, the human homolog of the yeast cell cycle gene CDC42. *Mol Cell Biol* **10**, 5977-5982 (1990).
128 Marks, P. W. & Kwiatkowski, D. J. Genomic organization and chromosomal location of murine Cdc42. *Genomics* **38**, 13-18 (1996).

129 Chen, F. *et al.* Cdc42 is required for PIP2-induced actin polymerization and early development but not for cell viability. *Curr Biol* **10**, 758-765 (2000).
130 Tanabe, K. *et al.* The small GTP-binding protein TC10 promotes nerve elongation in neuronal cells, and its expression is induced during nerve regeneration in rats. *J Neurosci* **20**, 4138-4144 (2000).
131 Abe, T., Kato, M., Miki, H., Takenawa, T. & Endo, T. Small GTPase Tc10 and its homologue RhoT induce N-WASP-mediated long process formation and neurite outgrowth. *J Cell Sci* **116**, 155-168 (2003).
132 Vignal, E. *et al.* Characterization of TCL, a new GTPase of the Rho family related to TC10 and Cdc42. *J Biol Chem* **275**, 36457-36464 (2000).
133 Wilson, E. *et al.* RhoJ interacts with the GIT-PIX complex and regulates focal adhesion disassembly. *J Cell Sci* **127**, 3039-3051 (2014).
134 Arias-Romero, L. E. & Chernoff, J. Targeting Cdc42 in cancer. *Expert Opin. Ther. Targets* **17**, 1263-1273 (2013).
135 Chou, M. M., Masuda-Robens, J. M. & Gupta, M. L. Cdc42 promotes G1 progression through p70 S6 kinase-mediated induction of cyclin E expression. *J Biol Chem* **278**, 35241-35247 (2003).
136 Wirth, A. *et al.* Dual lipidation of the brain-specific Cdc42 isoform regulates its functional properties. *Biochem J* **456**, 311-322 (2013).
137 Kang, R. *et al.* Neural palmitoyl-proteomics reveals dynamic synaptic palmitoylation. *Nature* **456**, 904-909 (2008).
138 Neudauer, C. L., Joberty, G., Tatsis, N. & Macara, I. G. Distinct cellular effects and interactions of the Rho-family GTPase TC10. *Curr Biol* **21**, 1151-1161 (1998).
139 De Toledo, M. *et al.* The GTP/GDP cycling of rho GTPase TCL is an essential regulator of the early endocytic pathway. *Mol Biol Cell* **14**, 4846-4856 (2003).
140 Hemsath, L., Dvorsky, R., Fiegen, D., Carlier, M. F. & Ahmadian, M. R. An electrostatic steering mechanism of Cdc42 recognition by Wiskott-Aldrich syndrome proteins. *Mol Cell* **20**, 313-324 (2005).
141 Pollard, T. D. & Borisy, G. G. Cellular motility driven by assembly and disassembly of actin filaments. *Cell* **112**, 453-465 (2003).
142 Peng, J., Wallar, B. J., Flanders, A., Swiatek, P. J. & Alberts, A. S. Disruption of the Diaphanous-related formin Drf1 gene encoding mDia1 reveals a role for Drf3 as an effector for Cdc42. *Curr Biol* **13**, 534-545 (2003).
143 Cory, G. O. & Cullen, P. J. Membrane curvature: the power of bananas, zeppelins and boomerangs. *Curr Biol* **17**, R455-R457 (2007).
144 Johnson, D. I. & Pringle, J. R. Molecular characterization of CDC42, a Saccharomyces cerevisiae gene involved in the development of cell polarity. *J Cell Biol* **111**, 143-152 (1990).
145 Ohno, S. Intercellular junctions and cellular polarity: the PAR-aPKC complex, a conserved core cassette playing fundamental roles in cell polarity. *Curr Opin Cell Biol* **13**, 641-648 (2001).
146 Macara, I. G. Parsing the polarity code. *Nat Rev Mol Cell Biol* **5**, 220-231 (2004).
147 Etienne-Manneville, S. Cdc42 - the centre of polarity. *J Cell Sci* **117**, 1291-1300 (2004).

148 Martin-Belmonte, F. *et al.* PTEN-mediated apical segregation of phosphoinositides controls epithelial morphogenesis through Cdc42. *Cell* **128**, 383-397 (2007).
149 Pegtel, D. M. *et al.* The Par-Tiam1 complex controls persistent migration by stabilizing microtubule-dependent front-rear polarity. *Curr Biol* **17**, 1623-1634 (2007).
150 Nishimura, T. *et al.* PAR-6-PAR-3 mediates Cdc42-induced Rac activation through the Rac GEFs STEF/Tiam1. *Nat Cell Biol* **7**, 270-277 (2005).
151 Olson, M. F., Ashworth, A. & Hall, A. An essential role for Rho, Rac, and Cdc42 GTPases in cell cycle progression through G1. *Science* **269**, 1270-1272 (1995).
152 Bauerfeld, C. P., Hershenson, M. B. & Page, K. Cdc42, but not RhoA, regulates cyclin D1 expression in bovine tracheal myocytes. *Am J Physiol Lung Cell Mol Physiol* **280**, L974-L982 (2001).
153 Yasuda, S. *et al.* Cdc42 and mDia3 regulate microtubule attachment to kinetochores. *Nature* **428**, 767-771 (2004).
154 Yasuda, S. *et al.* An essential role of Cdc42-like GTPases in mitosis of HeLa cells. *FEBS Lett* **580**, 3375-3380 (2006).
155 Qiu, R. G., Abo, A., McCormick, F. & Symons, M. Cdc42 regulates anchorage-independent growth and is necessary for Ras transformation. *Mol Cell Biol* **17**, 3449-3458 (1997).
156 Murphy, G. A. *et al.* Cellular functions of TC10, a Rho family GTPase: regulation of morphology, signal transduction and cell growth. *Oncogene* **18**, 3831-3845 (1999).
157 Côté, J. F., Motoyama, A. B., Bush, J. A. & Vuori, K. A novel and evolutionarily conserved PtdIns(3,4,5)P3-binding domain is necessary for DOCK180 signalling. *Nat Cell Biol* **7**, 797-807 (2005).
158 Rossman, K. L., Der, C. J. & Sondek, J. GEF means go: turning on RHO GTPases with guanine nucleotide-exchange factors. *Nat Rev Mol Cell Biol* **6**, 167-180 (2005).
159 Koyano, Y. *et al.* Molecular Cloning and Characterization of CDEP, a Novel Human Protein Containing the Ezrin-like Domain of the Band 4.1 Superfamily and the Dbl Homology Domain of Rho Guanine Nucleotide Exchange Factors. *Biochem Biophys Res Commun* **241**, 369-375 (1997).
160 Cheadle, L. & Biederer, T. The novel synaptogenic protein Farp1 links postsynaptic cytoskeletal dynamics and transsynaptic organization. *J Cell Biol* **199**, 985-1001 (2012).
161 Miyamoto, Y., Yamauchi, J. & Itoh, H. Src kinase regulates the activation of a novel FGD-1-related Cdc42 guanine nucleotide exchange factor in the signaling pathway from the endothelin A receptor to JNK. *J Biol Chem* **278**, 29890-29900 (2003).
162 Kubo, T. *et al.* A novel FERM domain including guanine nucleotide exchange factor is involved in Rac signaling and regulates neurite remodeling. *J Neurosci* **22**, 8504-8513 (2002).
163 Chuang, T. H. *et al.* Abr and Bcr are multifunctional regulators of the Rho GTP-binding protein family. *Proc Natl Acad Sci* **92**, 10282-10286 (1995).

164 Topp, J. D., Gray, N. W., Gerard, R. D. & Horazdovsky, B. F. Alsin is a Rab5 and Rac1 guanine nucleotide exchange factor. *J Biol Chem* **279**, 24612-24623 (2004).
165 Hart, M. J. *et al.* Identification of a novel guanine nucleotide exchange factor for the Rho GTPase. *J Biol Chem* **271**, 25452-25458 (1996).
166 Ren, Y., Li, R., Zheng, Y. & Busch, H. Cloning and characterization of GEF-H1, a microtubule-associated guanine nucleotide exchange factor for Rac and Rho GTPases. *J Biol Chem* **273**, 34954-34960 (1998).
167 Arthur, W. T., Ellerbroek, S. M., Der, C. J., Burridge, K. & Wennerberg, K. XPLN, a guanine nucleotide exchange factor for RhoA and RhoB, but not RhoC. *J Biol Chem* **277**, 42964-42972 (2002).
168 Kawasaki, Y. *et al.* Asef, a link between the tumor suppressor APC and G-protein signaling. *Science* **289**, 1194-1197 (2000).
169 Gotthardt, K. & Ahmadian, M. R. Asef is a Cdc42-specific guanine nucleotide exchange factor. *Biol Chem* **388**, 67-71 (2007).
170 Kawasaki, Y. *et al.* Identification and characterization of Asef2, a guanine–nucleotide exchange factor specific for Rac1 and Cdc42. *Oncogene* **26**, 7620-7627 (2007).
171 Wang, Z. *et al.* Regulation of Immature Dendritic Cell Migration by RhoA Guanine Nucleotide Exchange Factor Arhgef5. *J Biol Chem* **284**, 28599-28606 (2009).
172 Xie, X., Chang, S. W., Tatsumoto, T., Chan, A. M. L. & Miki, T. TIM, a Dbl-related protein, regulates cell shape and cytoskeletal organization in a Rho-dependent manner. *Cellular signalling* **17**, 461-471 (2005).
173 Manser, E. *et al.* PAK Kinases Are Directly Coupled to the PIX Family of Nucleotide Exchange Factors. *Mol Cell* **1**, 183-192 (1998).
174 Alberts, A. S. & Treisman, J. E. Activation of RhoA and SAPK/JNK signalling pathways by the RhoA-specific exchange factor mNET1. *EMBO J* **17**, 4075-4085 (1995).
175 Srougi, M. C. & Burridge, K. The nuclear guanine nucleotide exchange factors Ect2 and Net1 regulate RhoB-mediated cell death after DNA damage. *PLoS One* **6**, e17108 (2011).
176 Reid, T., Bathoorn, A., Ahmadian, M. R. & Collard, J. G. Identification and characterization of hPEM-2, a guanine nucleotide exchange factor specific for Cdc42. *J Biol Chem* **274** (1999).
177 Mohl, M., Winkler, S., Wieland, T. & Lutz, S. Gef10--the third member of a Rho-specific guanine nucleotide exchange factor subfamily with unusual protein architecture. *Naunyn Schmiedebergs Arch Pharmacol.* **373**, 333-341 (2006).
178 Winkler, S., Mohl, M., Wieland, T. & Lutz, S. GrinchGEF--a novel Rho-specific guanine nucleotide exchange factor. *Biochem Biophys Res Commun* **335**, 1280-1286 (2005).
179 Fukuhara, S., Murga, C., Zohar, M., Igishi, I. & Gutkind, J. S. A novel PDZ domain containing guanine nucleotide exchange factor links heterotrimeric G proteins to Rho. *J Biol Chem* **274**, 5868-5879 (1999).
180 Jaiswal, M. *et al.* Mechanistic Insights into Specificity, Activity, and Regulatory Elements of the Regulator of G-protein Signaling (RGS)-containing Rho-specific

Guanine Nucleotide Exchange Factors (GEFs) p115, PDZ-RhoGEF (PRG), and Leukemia-associated RhoGEF (LARG). *J Biol Chem* **286**, 18202-18212 (2011).
181 Fukuhara, S., Chikumi, H. & Gutkind, J. S. Leukemia-associated Rho guanine nucleotide exchange factor (LARG) links heterotrimeric G proteins of the G12 family to Rho. *FEBS Lett* **485**, 183-188 (2000).
182 Zheng, Y., Olson, M. F., Hall, A., Cerione, R. A. & Toksoz, D. Direct involvement of the small GTP-binding protein Rho in lbc oncogene function. *J Biol Chem* **270**, 9031-9034 (1995).
183 Whitehead, I. P. *et al.* Dependence of Dbl and Dbs Transformation on MEK and NF-κB Activation. *Mol Cell Biol* **19**, 7759-7770 (1999).
184 Ogita, H. *et al.* EphA4-mediated Rho activation via Vsm-RhoGEF expressed specifically in vascular smooth muscle cells. *Circ Res* **93** (2003).
185 Hiramoto-Yamaki, N. *et al.* Ephexin4 and EphA2 mediate cell migration through a RhoG-dependent mechanism. *J Cell Biol* **190**, 461-477 (2010).
186 Rümenapp, U., Freichel-Blomquist, A., Wittinghofer, A., Jakobs, K. H. & Wieland, T. A mammalian Rho-specific guanine-nucleotide exchange factor (p164-RhoGEF) without a pleckstrin homology domain. *Biochem J* **366**, 721-728 (2002).
187 Mitin, N., Rossman, K. L. & Der, C. J. Identification of a Novel Actin-Binding Domain within the Rho Guanine Nucleotide Exchange Factor TEM4. *PLoS One* **7**, e41876 (2012).
188 Niu, J., Profirovic, J., Pan, H., Vaiskunaite, R. & Voyno-Yasenetskaya, T. G Protein betagamma subunits stimulate p114RhoGEF, a guanine nucleotide exchange factor for RhoA and Rac1: regulation of cell shape and reactive oxygen species production. *Circ Res* **93**, 848-856 (2003).
189 Blomquist, A. *et al.* Identification and characterization of a novel Rho-specific guanine nucleotide exchange factor. *Biochem J* **352 Pt 2**, 319-325 (2000).
190 Wang, Y. *et al.* WGEF is a novel RhoGEF expressed in intestine, liver, heart, and kidney. *Biochem Biophys Res Commun* **324**, 1053-1058 (2004).
191 Hart, M. J., Eva, A., Evans, T., Aaronson, S. A. & Cerione, R. A. Catalysis of guanine nucleotide exchange on the CDC42Hs protein by the dbl oncogene product. *Nature* **354**, 311-314 (1991).
192 Zheng, Y., Hart, M. J. & Cerione, R. A. Guanine nucelotide exchange catalyzed by *dbl* oncogene product. *Methods Enzymol* **256**, 77-84 (1995).
193 Debant, A. *et al.* The multidomain protein Trio binds the LAR transmembrane tyrosine phosphatase, contains a protein kinase domain, and has separate rac-specific and rho-specific guanine nucleotide exchange factor domains. *Proc Natl Acad Sci U S A* **93**, 5466-5471 (1996).
194 Colomer, V. *et al.* Huntingtin-associated protein 1 (HAP1) binds to a Trio-like polypeptide, with a rac1 guanine nucleotide exchange factor domain. *Hum Mol Genet* **6**, 1519-1525 (1997).
195 May, V., Schiller, M. R., Eipper, B. A. & Mains, R. E. Kalirin Dbl-homology guanine nucleotide exchange factor 1 domain initiates new axon outgrowths via RhoG-mediated mechanisms. *J Neurosci* **22**, 6980-6990 (2002).
196 Ma, X. M., Huang, J., Wang, Y., Eipper, B. A. & Mains, R. E. Kalirin, a multifunctional Rho guanine nucleotide exchange factor, is necessary for

maintenance of hippocampal pyramidal neuron dendrites and dendritic spines. *J Neurosci* **23**, 10593-10603 (2003).
197 Souchet, M. *et al.* Human p63RhoGEF, a novel RhoA-specific guanine nucleotide exchange factor, is localized in cardiac sarcomere. *J Cell Sci* **115**, 629-640 (2002).
198 Guo, X. *et al.* A Rac/Cdc42-specific exchange factor, GEFT, induces cell proliferation, transformation, and migration. *J Biol Chem* **278**, 13207-13215 (2003).
199 Shamah, S. M. *et al.* EphA receptors regulate growth cone dynamics through the novel guanine nucleotide exchange factor ephexin. *Cell* **105**, 233-244 (2001).
200 Ford-Speelman, D. L., Roche, J. A., Bowman, A. L. & Bloch, R. J. The rho-guanine nucleotide exchange factor domain of obscurin activates rhoA signaling in skeletal muscle. *Mol Biol Cell* **20**, 3905-3917 (2009).
201 Tatsumoto, T., Xie, X., Blumenthal, R., Okamoto, I. & Miki, T. Human Ect2 Is an Exchange Factor for Rho Gtpases, Phosphorylated in G2/M Phases, and Involved in Cytokinesis. *J Cell Biol* **147**, 921-928 (1999).
202 Curtis, C. *et al.* Scambio, a novel guanine nucleotide exchange factor for Rho. *Mol Cancer* **3**, 10 (2004).
203 Sun, Y. J. *et al.* Solo/Trio8, a membrane-associated short isoform of Trio, modulates endosome dynamics and neurite elongation. *Mol Cell Biol* **26**, 6923-6935 (2006).
204 Ueda, H. *et al.* Heterotrimeric G protein betagamma subunits stimulate FLJ00018, a guanine nucleotide exchange factor for Rac1 and Cdc42. *J Biol Chem* **283**, 1946-1953 (2008).
205 Gupta, M. *et al.* Plekhg4 is a novel Dbl family guanine nucleotide exchange factor protein for rho family GTPases. *J Biol Chem* **288**, 14522-14530 (2013).
206 De Toledo, M., Coulon, V., Schmidt, S., Fort, P. & Blangy, A. The gene for a new brain specific RhoA exchange factor maps to the highly unstable chromosomal region 1p36.2-1p36.3. *Oncogene* **20**, 7307-7317 (2001).
207 Wu, D., Asiedu, M., Adelstein, R. S. & Wei, Q. A Novel Guanine Nucleotide Exchange Factor MyoGEF is Required for Cytokinesis. *Cell Cycle* **5**, 1234-1239 (2006).
208 D'Angelo, R. *et al.* Interaction of ezrin with the novel guanine nucleotide exchange factor PLEKHG6 promotes RhoG-dependent apical cytoskeleton rearrangements in epithelial cells. *Mol Biol Cell* **18**, 4780-4793 (2007).
209 Wu, D., Asiedu, M. & Wei, Q. Myosin-interacting guanine exchange factor (MyoGEF) regulates the invasion activity of MDA-MB-231 breast cancer cells through activation of RhoA and RhoC. *Oncogene* **28**, 2219-2230 (2009).
210 Zheng, Y. *et al.* The faciogenital dysplasia gene product FGD1 functions as a Cdc42Hs-specific guanine-nucleotide exchange factor. *J Biol Chem* **271**, 33169-33172 (1996).
211 Huber, C., Martensson, A., Bokoch, G. M., Nemazee, D. & Gavin, A. L. FGD2, a CDC42-specific Exchange Factor Expressed by Antigen-presenting Cells, Localizes to Early Endosomes and Active Membrane Ruffles. *J Biol Chem* **283**, 34002-34012 (2008).

212 Pasteris, N. G., Nagata, K., Hall, A. & Gorski, J. L. Isolation, characterization, and mapping of the mouse Fgd3 gene, a new Faciogenital Dysplasia (FGD1; Aarskog Syndrome) gene homologue. *Gene* **242**, 237-247 (2000).
213 Ono, Y. *et al.* Two actions of frabin: direct activation of Cdc42 and indirect activation of Rac. *Oncogene* **19**, 3050-3058 (2000).
214 Kurogane, Y. *et al.* FGD5 Mediates Proangiogenic Action of Vascular Endothelial Growth Factor in Human Vascular Endothelial Cells. *Artheriosclerosis, Thrombosis, and Vascular Biology* **32**, 988-996 (2012).
215 Steenblock, C. *et al.* The Cdc42 guanine nucleotide exchange factor FGD6 coordinates cell polarity and endosomal membrane recycling in osteoclasts. *J Biol Chem* **289**, 18347-18359 (2014).
216 Hussain, N. K. *et al.* Endocytic protein intersectin-l regulates actin assembly via Cdc42 and N-WASP. *Nat Cell Biol* **3**, 927-932 (2001).
217 McGavin, M. K. H. *et al.* The Intersectin 2 Adaptor Links Wiskott Aldrich Syndrome Protein (WASp)-mediated Actin Polymerization to T Cell Antigen Receptor Endocytosis. *J Exp Med* **194**, 1777-1787 (2001).
218 Welch, H. C. *et al.* P-Rex1, a PtdIns(3,4,5)P3- and Gbetagamma-regulated guanine-nucleotide exchange factor for Rac. *Cell* **108**, 809-821 (2002).
219 Rosenfeldt, H., Vázquez-Prado, J. & Gutkind, J. S. P-Rex2, a novel PI-3-kinase sensitive Rac exchange factor. *FEBS Lett* **572**, 167-171 (2004).
220 Kiyono, M., Satoh, T. & Kaziro, Y. G protein βγ subunit-dependent Rac-guanine nucleotide exchange activity of Ras-GRF1/CDC25(Mm). *Proc Natl Acad Sci* **96**, 4826-4831 (1999).
221 Fan, W., Koch, C. A., de Hoog, C. L., Fam, N. P. & Moran, M. F. The exchange factor Ras-GRF2 activates Ras-dependent and Rac-dependent mitogen-activated protein kinase pathways. *Curr Biol* **8**, 935-938 (1998).
222 Nimnual, A. S., Yatsula, B. A. & Bar-Sagi, D. Coupling of Ras and Rac guanosine triphosphatases through the Ras exchanger Sos. *Science* **279**, 560-563 (1998).
223 Michiels, F., Habets, G. G., Stam, J. C., van, d. K. R. A. & Collard, J. G. A role for Rac in Tiam1-induced membrane ruffling and invasion. *Nature* **375**, 338-340 (1995).
224 Hoshino, M. *et al.* Identification of the *stef* gene that encodes a novel guanine nucleotide exchange factor specific for Rac1. *J Biol Chem* **274**, 17837-17844 (1999).
225 Han, J. *et al.* Lck regulates Vav activation of members of the Rho family of GTPases. *Mol Cell Biol* **17**, 1346-1353 (1997).
226 Crespo, P., Schuebel, K. E., Ostrom, A. A., Gutkind, J. S. & Bustelo, X. R. Phosphotyrosine-dependent activation of Rac-1 GDP/GTP exchange by the vav proto-oncogene product. *Nature* **18**, 169-172 (1997).
227 Schuebel, K. E., Movilla, N., Rosa, J. L. & Bustelo, X. R. Phosphorylation-dependent and constitutive activation of Rho proteins by wild-type and oncogenic Vav-2. *EMBO J* **17**, 6427-6766 (1998).
228 Movilla, N. & Bustelo, X. R. Biological and regulatory properties of Vav-3, a new member of the Vav family of oncoproteins. *Mol Cell Biol* **19**, 7870-7885 (1999).

229 Zeng, L. *et al.* Vav3 mediates receptor protein tyrosine kinase signaling, regulates GTPase activity, modulates cell morphology, and induces cell transformation. *Mol Cell Biol* **20**, 9212-9224 (2000).
230 Salazar, M. A. *et al.* Tuba, a novel protein containing bin/amphiphysin/Rvs and Dbl homology domains, links dynamin to regulation of the actin cytoskeleton. *J Biol Chem* **278**, 49031-49043 (2003).
231 Whitehead, I. P., Campbell, S., Rossman, K. L. & Der, C. J. Dbl family proteins. *Biochim. Biophys. Acta* **1332**, 1-23 (1997).
232 Soisson, S. M., Nimnual, A. S., Uy, M., Bar-Sagi, D. & Kuriyan, J. Crystal Structure of the Dbl and Pleckstrin Homology Domains from the Human Son of Sevenless Protein. *Cell* **95**, 259-268 (1998).
233 Liu, X. *et al.* NMR structure and mutagenesis of the N-terminal Dbl homology domain of the nucleotide exchange factor Trio. *Cell* **95**, 269-277 (1998).
234 Rossman, K. L. & Campbell, S. L. Bacterial expressed DH and DH/PH domains. *Methods Enzymol* **325**, 25-38 (2000).
235 Kristelly, R., Gao, G. & Tesmer, J. J. Structural determinants of RhoA binding and nucleotide exchange in leukemia-associated Rho guanine-nucleotide exchange factor. *J Biol Chem* **279**, 47352-47362 (2004).
236 Chhatriwala, M. K., Betts, L., Worthylake, D. K. & Sondek, J. The DH and PH domains of Trio coordinately engage Rho GTPases for their efficient activation. *J Mol Biol* **368**, 1307-1320 (2007).
237 Rossman, K. L. *et al.* A crystallographyic view of interactions between Dbs and Cdc42: PH domain-assisted guanine nucleotide exchange. *EMBO J* **21**, 1315-1326 (2002).
238 Harlan, J. E., Hajduk, P. J., Yoon, H. S. & Fesik, S. W. Pleckstrin homology domains bind to phosphatidylinositol-4,5-bisphosphate. *Nature* **371**, 168-170 (1994).
239 Snyder, J. T. *et al.* Quantitative analysis of the effect of phosphoinositide interactions on the function of Dbl family proteins. *J Biol Chem* **276** (2001).
240 Alam, M. R. *et al.* Kalirin, a cytosolic protein with spectrin-like and GDP/GTP exchange factor-like domains that interacts with peptidylglycine alpha-amidating monooxygenase, an integral membrane peptideprocessing enzyme. *J Biol Chem* **272**, 12667-12675 (1997).
241 Schmidt, S. & Debant, A. Function and regulation of the Rho guanine nucleotide exchange factor Trio. *Small GTPases* **5**, 1-10 (2014).
242 Portales-Casamar, E., Briancon-Marjollet, A., Fromont, S., Triboulet, R., and Debant, A. Identification of novel neuronal isoforms of the Rho-GEF Trio. *Biol. Cell* **98**, 183-193 (2006).
243 O'Brien, S. P. *et al.* Skeletal muscle deformity and neuronal disorder in Trio exchange factor-deficient mouse embryos. *Proc Natl Acad Sci* **97**, 12074-12078 (2000).
244 Briancon-Marjollet, A. *et al.* Trio mediates netrin-1-induced Rac1 activation in axon outgrowth and guidance. *Mol. Cell Biol.* **28**, 2314-2323 (2008).
245 Cahill, M. *et al.* Kalirin regulates cortical spine morphogenesis and disease-related behavioral phenotypes. *Proc Natl Acad Sci U S A* **106**, 13058-13063 (2009).

246 Bellanger, J.-M. *et al.* The two guanine nucleotide exchange factor domains of Trio link the Rac1 and the RhoA pathways in vivo. *Oncogene* **16**, 147-152 (1998).
247 Blangy, A. *et al.* TrioGEF1 controls Rac- and Cdc42-dependent cell structures through the direct activation of rhoG. *J Cell Sci* **113**, 729-739 (2000).
248 Yoshizuka, N. *et al.* An alternative transcript derived from the trio locus encodes a guanosine nucleotide exchange factor with mouse cell-transforming potential. *J Biol Chem* **279** (2004).
249 Bellanger, J.-M. *et al.* The Rac1- and RhoG-specific GEF domain of Trio targets filamin to remodel cytoskeletal actin. *Nat Cell Biol* **2**, 888-892 (2000).
250 Seipel, K., O'Brien, S. P., Iannotti, E., Medley, Q. G. & Streuli, M. Tara, a novel F-actin binding protein, associates with the Trio guanine nucleotide exchange factor and regulates actin cytoskeletal organization. *J Cell Sci* **114**, 389-399 (2001).
251 Yano, T. *et al.* Tara up-regulates E-cadherin transcription by binding to the Trio RhoGEF and inhibiting Rac signaling. *J Cell Biol* **193**, 319-332 (2011).
252 Charrasse, S. *et al.* M-cadherin activates Rac1 GTPase through the Rho-GEF trio during myoblast fusion. *Mol Biol Cell* **18**, 1734-1743 (2007).
253 Cannet, A., Schmidt, S., Delaval, B. & Debant, A. Identification of a mitotic Rac-GEF, Trio, that counteracts MgcRacGAP function during cytokinesis. *Mol Biol Cell* **25**, 4063-4071 (2014).
254 van Haren, J. *et al.* Dynamic microtubules catalyze formation of navigator-TRIO complexes to regulate neurite extension. *Curr Biol* **24**, 1778-1785 (2014).
255 Chen, S. Y., Huang, P. H. & Cheng, H. J. Disrupted-in-Schizophrenia 1-mediated axon guidance involves TRIO-RAC-PAK small GTPase pathway signaling. *Proc Natl Acad Sci U S A* **108**, 5861-5866 (2011).
256 Neubrand, V. E., Thomas, C., Schmidt, S., Debant, A. & Schiavo, G. Kidins220/ARMS regulates Rac1-dependent neurite outgrowth by direct interaction with the RhoGEF Trio. *J Cell Sci* **123**, 2111-2123 (2010).
257 DeGeer, J. *et al.* Tyrosine phosphorylation of the rho guanine nucleotide exchange factor Trio regulates Netrin-1/DCC-mediated cortical axon outgrowth. *Mol Cell Biol* **33**, 739-751 (2013).
258 Forsthoefel, D. J., Liebl, E. C., Kolodziej, P. A. & Seeger, M. A. The Abelson tyrosine kinase, the Trio GEF and Enabled interact with the Netrin receptor Frazzled in Drosophila. *Development* **132**, 1983-1994 (2005).
259 Liebl, E. *et al.* Dosage-sensitive, reciprocal genetic interactions between the Abl tyrosine kinase and the putative GEF trio reveal trio's role in axon pathfinding. *Neuron* **26**, 107-118 (2000).
260 Schmidt, S. & Debant, A. TRIO (triple functional domain (PTPRF interacting)). *Atlas Genet Cytogenet Oncol Haematol* **15**, 490-498 (2011).
261 Fortin, S. P. *et al.* Cdc42 and the guanine nucleotide exchange factors Ect2 and trio mediate Fn14-induced migration and invasion of glioblastoma cells. *Mol Cancer Res* **10**, 958-968 (2012).
262 Namekata, K., Kimura, A., Kawamura, K., Harada, C. & Harada, T. Dock GEFs and their therapeutic potential: neuroprotection and axon regeneration. *Prog Retin Eye Res* **43**, 1-16 (2014).

263 Laurin, M. & Côté, J. F. Insights into the biological functions of Dock family guanine nucleotide exchange factors. *Genes & Dev.* **28**, 533-547 (2014).
264 Premkumar, L. *et al.* Structural basis of membrane targeting by the Dock180 family of Rho family guanine nucleotide exchange factors (Rho-GEFs). *J Biol Chem* **285**, 13211-13222 (2010).
265 Jungmichel, S. *et al.* Specificity and commonality of the phosphoinositide-binding proteome analyzed by quantitative mass spectrometry. *Cell Reports* (2014).
266 Kiyokawa, E. *et al.* Activation of Rac1 by a Crk SH3-binding protein, DOCK180. *Genes Dev* **12**, 3331-3336 (1998).
267 Nishihara, H. *et al.* DOCK2 associates with CrkL and regulates Rac1 in human leukemia cell lines. *Blood* **100**, 3968-3974 (2002).
268 Nishihara, H. *et al.* DOCK2 mediates T cell receptor-induced activation of Rac2 and IL-2 transcription. *Biochem Biophys Res Commun* **296**, 716-720 (2002).
269 Namekata, K., Enokido, Y., Iwasawa, K. & Kimura, H. MOCA induces membrane spreading by activating Rac1. *J Biol Chem* **279**, 14331-14337 (2004).
270 Lu, M. *et al.* A steric-inhibition model for regulation of nucleotide exchange via the Dock180 family of GEFs. *Curr Biol* **15**, 371-377 (2005).
271 Omi, N. *et al.* Mutation of Dock5, a member of the guanine exchange factor Dock180 superfamily, in the rupture of lens cataract mouse. *Exp Eye Res* **86**, 828-834 (2008).
272 Miyamoto, Y., Yamauchi, J., Sanbe, A. & Tanoue, A. Dock6, a Dock-C subfamily guanine nucleotide exchanger, has the dual specificity for Rac1 and Cdc42 and regulates neurite outgrowth. *Experimental Cell Research* **313**, 791-804 (2007).
273 Watabe-Uchida, M., John, K. A., Janas, J. A., Newey, S. E. & Van Aelst, L. The Rac activator Dock7 regulates neuronal polarity through local phosphorylation of stathmin/Op18. *Neuron* **51**, 727-739 (2006).
274 Zhou, Y., Johnson, J. L., Cerione, R. A. & Erickson, J. W. Prenylation and membrane localization of Cdc42 are essential for activation by DOCK7. *Biochemistry* **52**, 4354-4363 (2013).
275 Harada, Y. *et al.* DOCK8 is a Cdc42 activator critical for interstitial dendritic cell migration during immune responses. *Blood* **119**, 4451-4461 (2012).
276 Meller, N., Irani-Tehrani, M., Kiosses, W. B., Del Pozo, M. A. & Schwartz, M. A. Zizimin1, a novel Cdc42 activator, reveals a new GEF domain for Rho proteins. *Nat Cell Biol* **4**, 639-647 (2002).
277 Gadea, G., Sanz-Moreno, V., Self, A., Godi, A. & Marshall, C. J. DOCK10-mediated Cdc42 activation is necessary for amoeboid invasion of melanoma cells. *Curr Biol* **18**, 1456-1465 (2008).
278 Nishikimi, A. *et al.* Zizimin2: a novel, DOCK180-related Cdc42 guanine nucleotide exchange factor expressed predominantly in lymphocytes. *579* (2005).
279 Shinohara, M. *et al.* SWAP-70 is a guanine-nucleotide-exchange factor that mediates signalling of membrane ruffling. *Nature* **416**, 759-763 (2002).
280 Gupta, S. *et al.* T cell receptor engagement leads to the recruitment of IBP, a novel guanine nucleotide exchange factor, to the immunological synapse. *J Biol Chem* **278**, 43541-43549 (2003).

281 Mavrakis, K. J., McKinlay, K. J., Jones, P. & Sablitzky, F. DEF6, a novel PH-DH-like domain protein, is an upstream activator of the Rho GTPases Rac1, Cdc42, and RhoA. *Experimental Cell Research* **294**, 335-344 (2004).
282 Hamel, B. *et al.* SmgGDS Is a Guanine Nucleotide Exchange Factor That Specifically Activates RhoA and RhoC. *J Biol Chem* **286**, 12141-12148 (2011).
283 Mahankali, M., Peng, H. J., Henkels, K. M., Dinauer, M. C. & Gomez-Cambronero, J. Phospholipase D2 (PLD2) is a guanine nucleotide exchange factor (GEF) for the GTPase Rac2. *Proc Natl Acad Sci U S A* **108**, 19617-19622 (2011).
284 Jeon, H. *et al.* Phospholipase D2 induces stress fiber formation through mediating nucleotide exchange for RhoA. *Cell Signal* **23**, 1320-1326 (2011).
285 Namekata, K. *et al.* Dock3 induces axonal outgrowth by stimulating membrane recruitment of the WAVE complex. *PNAS* **107**, 7586-7591 (2010).
286 Côté, J. F. & Vuori, K. Identification of an evolutionarily conserved superfamily of DOCK180-related proteins with guanine nucleotide exchange activity. *J Cell Sci* **115**, 4901-4913 (2002).
287 Kulkarni, K., Yang, J., Zhang, Z. & Barford, D. Multiple factors confer specific Cdc42 and Rac protein activation by dedicator of cytokinesis (DOCK) nucleotide exchange factors. *J Biol Chem* **286**, 25341-25351 (2011).
288 Brugnera, E. *et al.* Unconventional Rac-GEF activity is mediated through the Dock180–ELMO complex. *Nat Cell Biol* **4**, 572-582 (2002).
289 Meller, N., Irani-Tehrani, M., Ratnikov, B. I., Paschal, B. M. & Schwartz, M. A. The novel Cdc42 guanine nucleotide exchange factor, zizimin1, dimerizes via the Cdc42-binding CZH2 domain. *J Biol Chem* **279**, 37470-37476 (2004).
290 Terasawa, M. *et al.* Dimerization of DOCK2 is essential for DOCK2-mediated Rac activation and lymphocyte migration. *PLoS One* **7**, e46277 (2012).
291 Patel, M., Pelletier, A. & Côté, J. F. Opening up on ELMO regulation: new insights into the control of Rac signaling by the DOCK180/ELMO complex. *Small GTPases* **2**, 268-275 (2011).
292 Peng, H.-J. *et al.* The dual effect of Rac2 on phospholipase D2 regulation that explains both the onset and termination of chemotaxis. *Mol Cell Biol* **31**, 2227-2240 (2011).
293 Bos, J. L., Rehmann, H. & Wittinghofer, A. GEFs and GAPs: critical elements in the control of small G proteins. *Cell* **129**, 865-877 (2007).
294 Barfod, E. T. *et al.* Cloning and expression of a human CDC42 GTPase-activating protein reveals a functional SH3-binding domain. *J Biol Chem* **268**, 26059-26062 (1993).
295 Lancaster, C. A. *et al.* Characterization of rhoGAP. A GTPase-activating protein for rho-related small GTPases. *J Biol Chem* **269**, 1137-1142 (1994).
296 Kozma, R., Ahmed, S., Best, A. & Lim, L. The GTPase-activating protein n-chimaerin cooperates with Rac1 and Cdc42Hs to induce the formation of lamellipodia and filopodia. *Mol. Cell. Biol.* **16**, 5069-5080 (1996).
297 Leung, T., How, B. E., Manser, E. & Lim, L. Germ cell beta-chimaerin, a new GTPase-activating protein for p21rac, is specifically expressed during the acrosomal assembly stage in rat testis. *J Biol Chem* **268**, 3813-3816 (1993).

298 Tribioli, C. *et al.* An X chromosome-linked gene encoding a protein with characteristics of a rhoGAP predominantly expressed in hematopoietic cells. *Proc Natl Acad Sci U S A* **93**, 695-699 (1996).
299 Burbelo, P. D., Finegold, A. A., Kozak, C. A., Yamada, Y. & Takami, H. Cloning, genomic organization and chromosomal assignment of the mouse p190-B gene. *yes* **1443**, 203-210 (1998).
300 Burbelo, P. D. *et al.* p190-B, a new member of the Rho GAP family, and Rho are induced to cluster after integrin cross-linking. *J Biol Chem* **270**, 30919-30926 (1995).
301 Ochocka, A. M., Grden, M., Sakowicz-Burkiewicz, M., Szutowicz, A. & Pawelczyk, T. Regulation of phospholipase C-delta1 by ARGHAP6, a GTPase-activating protein for RhoA: possible role for enhanced activity of phospholipase C in hypertension. *Int J Biochem Cell Biol* **40**, 2264-2273 (2008).
302 Prakash, S. K. *et al.* Functional analysis of ARHGAP6, a novel GTPase-activating protein for RhoA. *Hum Mol Genet* **9**, 477-488 (2000).
303 Shang, X., Zhou, Y. T. & Low, B. C. Concerted regulation of cell dynamics by BNIP-2 and Cdc42GAP homology/Sec14p-like, proline-rich, and GTPase-activating protein domains of a novel Rho GTPase-activating protein, BPGAP1. *J Biol Chem* **278**, 45903-45914 (2003).
304 Furukawa, Y. *et al.* Isolation of a novel human gene, ARHGAP9, encoding a rho-GTPase activating protein. *Biochem Biophys Res Commun* **284**, 643-649 (2001).
305 Ren, X. R. *et al.* Regulation of CDC42 GTPase by proline-rich tyrosine kinase 2 interacting with PSGAP, a novel pleckstrin homology and Src homology 3 domain containing rhoGAP protein. *J Cell Biol* **152**, 971-984 (2001).
306 Zanin, E. *et al.* A conserved RhoGAP limits M phase contractility and coordinates with microtubule asters to confine RhoA during cytokinesis. *Dev Cell* **26**, 496-510 (2013).
307 Florio, M. *et al.* Human-specific gene ARHGAP11B promotes basal progenitor amplification and neocortex expansion. *Science* **347**, 1465-1470 (2015).
308 Gentile, A. *et al.* Met-driven invasive growth involves transcriptional regulation of Arhgap12. *Oncogene* **27**, 5590-5598 (2008).
309 Wong, K. *et al.* Signal transduction in neuronal migration: roles of GTPase activating proteins and the small GTPase Cdc42 in the Slit-Robo pathway. *Cell* **107**, 209-221 (2001).
310 Endris, V. *et al.* The novel Rho-GTPase activating gene MEGAP/ srGAP3 has a putative role in severe mental retardation. *Proc Natl Acad Sci U S A* **99**, 11754-11759 (2002).
311 Seoh, M. L., Ng, C. H., Yong, J., Lim, L. & Leung, T. ArhGAP15, a novel human RacGAP protein with GTPase binding property. *FEBS Lett* **539**, 131-137 (2003).
312 Harada, A. *et al.* Nadrin, a novel neuron-specific GTPase-activating protein involved in regulated exocytosis. *J Biol Chem* **275**, 36885-36891 (2000).
313 Richnau, N. & Aspenstrom, P. Rich, a rho GTPase-activating protein domain-containing protein involved in signaling by Cdc42 and Rac1. *J Biol Chem* **276**, 35060-35070 (2001).
314 Maeda, M. *et al.* ARHGAP18, a GTPase-activating protein for RhoA, controls cell shape, spreading, and motility. *Mol Biol Cell* **22**, 3840-3852 (2011).

315 David, M. D., Petit, D. & Bertoglio, J. The RhoGAP ARHGAP19 controls cytokinesis and chromosome segregation in T lymphocytes. *J Cell Sci* **127**, 400-410 (2014).
316 Lazarini, M. *et al.* ARHGAP21 is a RhoGAP for RhoA and RhoC with a role in proliferation and migration of prostate adenocarcinoma cells. *yes* **1832**, 365-374 (2013).
317 Sanz-Moreno, V. *et al.* Rac activation and inactivation control plasticity of tumor cell movement. *Cell* **135**, 510-523 (2008).
318 Ohta, Y., Hartwig, J. H. & Stossel, T. P. FilGAP, a Rho- and ROCK-regulated GAP for Rac binds filamin A to control actin remodelling. *Nat Cell Biol* **8**, 803-814 (2006).
319 Csépányi-Kömi, R., Sirokmány, G., Geiszt, M. & Ligeti, E. ARHGAP25, a novel Rac GTPase-activating protein, regulates phagocytosis in human neutrophilic granulocytes. *Blood* **119**, 573-582 (2012).
320 Taylor, J. M., Macklem, M. M. & Parsons, J. T. Cytoskeletal changes induced by GRAF, the GTPase regulator associated with focal adhesion kinase, are mediated by Rho. *J Cell Sci* **112**, 231-242 (1999).
321 Sakakibara, T., Nemoto, Y., Nukiwa, T. & Takeshima, H. Identification and characterization of a novel Rho GTPase activating protein implicated in receptor-mediated endocytosis. *FEBS Lett* **566**, 294-300 (2004).
322 Yeung, C. Y. *et al.* Arhgap28 is a RhoGAP that inactivates RhoA and downregulates stress fibers. *PLoS One* **9**, e107036 (2014).
323 Saras, J. *et al.* A novel GTPase-activating protein for Rho interacts with a PDZ domain of the protein-tyrosine phosphatase PTPL1. *J Biol Chem* **272**, 24333-24338 (1997).
324 Naji, L., Pacholsky, D. & Aspenstrom, P. ARHGAP30 is a Wrch-1-interacting protein involved in actin dynamics and cell adhesion. *Biochem Biophys Res Commun* **409**, 96-102 (2011).
325 Lamarche-Vane, N. a. H., A. CdGAP, a novel proline-rich GTPase-activating protein for Cdc42 and Rac. *Journal of Biological Chemistry* (1998).
326 Okabe, T. *et al.* RICS, a novel GTPase-activating protein for Cdc42 and Rac1, is involved in the beta-catenin-N-cadherin and N-methyl-D-aspartate receptor signaling. *J Biol Chem* **278**, 9920-9927 (2003).
327 Chiang, S. H. *et al.* TCGAP, a multidomain Rho GTPase-activating protein involved in insulin-stimulated glucose transport. *Embo J* **22**, 2679-2691 (2003).
328 Guerrier, S. *et al.* The F-BAR domain of srGAP2 induces membrane protrusions required for neuronal migration and morphogenesis. *Cell* **138**, 990-1004 (2009).
329 Ridley, A. J. *et al.* Rho family GTPase activating proteins p190, bcr and rhoGAP show distinct specificities *in vitro* and *in vivo*. *EMBO J* **12**, 5151-5160 (1993).
330 Rack, P. G. *et al.* Arhgap36-dependent activation of Gli transcription factors. *Proc Natl Acad Sci U S A* **111**, 11061-11066 (2014).
331 Lundstrom, A. *et al.* Vilse, a conserved Rac/Cdc42 GAP mediating Robo repulsion in tracheal cells and axons. *Genes Dev* **18**, 2161-2171 (2004).
332 Billuart, P. *et al.* Oligophrenin-1 encodes a rhoGAP protein involved in X-linked mental retardation. *Nature* **392**, 923-926 (1998).

333 Bai, X. *et al.* The smooth muscle-selective RhoGAP GRAF3 is a critical regulator of vascular tone and hypertension. *Nat Commun* **4**, 2910 (2013).
334 Cicchetti, P., Ridley, A. J., Zheng, Y., Cerione, R. A. & Baltimore, D. 3BP-1, an SH3 domain binding protein, has GAP activity for Rac and inhibits growth factor-induced membrane ruffling in fibroblasts. *Embo J* **14**, 3127-3135 (1995).
335 de Kreuk, B.-J. *et al.* The human minor histocompatibility antigen1 is a RhoGAP. *PLoS One* **8**, e73962 (2013).
336 Aresta, S., de Tand-Heim, M. F., Beranger, F. & de Gunzburg, J. A novel Rho GTPase-activating-protein interacts with Gem, a member of the Ras superfamily of GTPases. *Biochem J* **367**, 57-65 (2002).
337 Kawai, K., Kiyota, M., Seike, J., Deki, Y. & Yagisawa, H. START-GAP3/DLC3 is a GAP for RhoA and Cdc42 and is localized in focal adhesions regulating cell morphology. *Biochem Biophys Res Commun* **364**, 783-789 (2007).
338 Lahoz, A. & Hall, A. DLC1: a significant GAP in the cancer genome. *Genes Dev* **22**, 1724-1730 (2008).
339 Ching, Y. P. *et al.* Deleted in liver cancer (DLC) 2 encodes a RhoGAP protein with growth suppressor function and is underexpressed in hepatocellular carcinoma. *J Biol Chem* **278**, 10824-10830 (2003).
340 Touré, A. *et al.* MgcRacGAP, a new human GTPase-activating protein for Rac and Cdc42 similar to Drosophila rotundRacGAP gene product, is expressed in male germ cells. *J Biol Chem* **273**, 6019-6023 (1998).
341 Miura, K. *et al.* ARAP1: a point of convergence for Arf and Rho signaling. *Mol Cell* **9**, 109-119 (2002).
342 Yoon, H. Y. *et al.* ARAP2 effects on the actin cytoskeleton are dependent on Arf6-specific GTPase-activating-protein activity and binding to RhoA-GTP. *J Cell Sci* **119**, 4650-4666 (2006).
343 Krugmann, S., Williams, R., Stephens, L. & Hawkins, P. T. ARAP3 is a PI3K- and rap-regulated GAP for RhoA. *Curr Biol* **14**, 1380-1384 (2004).
344 Diekmann, D. *et al.* Bcr encodes a GTPase-activating protein for p21rac. *Nature* **351**, 400-402 (1991).
345 Reinhard, J. *et al.* A novel type of myosin implicated in signalling by rho family GTPases. *EMBO J* **14**, 697-704 (1995).
346 Jullien-Flores, V. *et al.* Bridging Ral GTPase to Rho pathways. RLIP76, a Ral effector with CDC42/Rac GTPase-activating protein activity. *J Biol Chem* **270**, 22473-22477 (1995).
347 Hart, M. J., Callow, M. G., Souza, B. & Polakis, P. IQGAP1, a calmodulin-binding protein with a rasGAP-related domain, is a potential effector for cdc42Hs. *EMBO J* **15**, 2997-3005 (1996).
348 Kuroda, S. *et al.* Identification of IQGAP as a putative target for the small GTPases, Cdc42 and Rac1. *J Biol Chem* **271**, 23363-23367 (1996).
349 Brill, S. *et al.* The ras GTPase-activating-protein-related human protein IQGAP2 harbors a potential actin binding domain and interacts with calmodulin and rho family GTPases. *Mol Cell Biol* **16**, 4869-4878 (1996).
350 Wang, S. *et al.* IQGAP3, a novel effector of Rac1 and Cdc42, regulates neurite outgrowth. *J Cell Sci* **120**, 567-577 (2007).

351 Faucherre, A. *et al.* Lowe syndrome protein OCRL1 interacts with Rac GTPase in the trans-Golgi network. *Hum Mol Genet* **12**, 2449-2456 (2003).
352 Rittinger, K., Walker, P. A., Eccleston, J. F., Smerdon, S. J. & Gamblin, S. J. Structure at 1.65 A of RhoA and its GTPase-activating protein in complex with a transition-state analogue. *Nature* **389**, 758-762 (1997).
353 Kandpal, R. P. Rho GTPase activating proteins in cancer phenotypes. *Curr Protein and Pept Sci* **7**, 355-365 (2006).
354 Lamarche-Vane, N. & Hall, A. CdGAP, a novel proline-rich GTPase-activating protein for Cdc42 and Rac. *The Journal of biological chemistry* **273**, 29172-29177 (1998).
355 Tcherkezian, J., Danek, E. I., Jenna, S., Triki, I. & Lamarche-Vane, N. Extracellular signal-regulated kinase 1 interacts with and phosphorylates CdGAP at an important regulatory site. *Mol Cell Biol* **25**, 6314-6329 (2005).
356 Jenna, S. *et al.* The activity of the GTPase-activating protein CdGAP is regulated by the endocytic protein intersectin. *J Biol Chem* **277**, 6366-6373 (2002).
357 LaLonde, D. P., Grubinger, M., Lamarche-Vane, N. & Turner, C. E. CdGAP associates with actopaxin to regulate integrin-dependent changes in cell morphology and motility. *Current biology : CB* **16**, 1375-1385, doi:10.1016/j.cub.2006.05.057 (2006).
358 Lalonde, D., Grubinger, M., Lamarche-Vane, N., and Turner, CE. CdGAP associates with actopaxin to regulate integrin-dependent changes in cell morphology and motility. *Curr Biol* **16**, 1-11 (2006).
359 Danek, E. I., Tcherkezian, J., Meriane, M., Triki, I., and Lamarche-Vane, N. Glycogen synthase kinase-3 phosphorylates CdGAP at a consensus ERK1 regulatory site. *J. Biol. Chem.* **282**, 3624-3631 (2007).
360 He, Y. *et al.* CdGAP is required for transforming growth factor beta- and Neu/ErbB-2-induced breast cancer cell motility and invasion. *Oncogene* **30**, 1032-1045 (2011).
361 Danek, E. I., Tcherkezian, J., Triki, I., Meriane, M. & Lamarche-Vane, N. Glycogen synthase kinase-3 phosphorylates CdGAP at a consensus ERK 1 regulatory site. *The Journal of biological chemistry* **282**, 3624-3631, doi:10.1074/jbc.M610073200 (2007).
362 Primeau, M., Ben Djoudi Ouadda, A. & Lamarche-Vane, N. Cdc42 GTPase-activating protein (CdGAP) interacts with the SH3D domain of Intersectin through a novel basic-rich motif. *FEBS letters* **585**, 847-853, doi:10.1016/j.febslet.2011.02.022 (2011).
363 Karimzadeh, F., Primeau, M., Mountassif, D., Rouiller, I. & Lamarche-Vane, N. A stretch of polybasic residues mediates Cdc42 GTPase-activating protein (CdGAP) binding to phosphatidylinositol 3,4,5-trisphosphate and regulates its GAP activity. *The Journal of biological chemistry* **287**, 19610-19621, doi:10.1074/jbc.M112.344606 (2012).
364 Southgate, L. *et al.* Gain-of-function mutations of ARHGAP31, a Cdc42/Rac1 GTPase regulator, cause syndromic cutis aplasia and limb anomalies. *American journal of human genetics* **88**, 574-585, doi:10.1016/j.ajhg.2011.04.013 (2011).

365 Isrie, M., Wuyts, W., Van Esch, H. & Devriendt, K. Isolated terminal limb reduction defects: extending the clinical spectrum of Adams-Oliver syndrome and ARHGAP31 mutations. *Am J Med Genet A* **164A**, 1576-1579 (2014).
366 Southgate, L., Machado, RD., Snape, KM, Primeau, M. et al. . Gain-of-function mutations of ARHGAP31,a Cdc42/Rac1 GTPase regulator, cause syndromic cutis aplasia and limb anomalies. *Am. J. Hum. Gen.* **88**, 574-585 (2011).
367 Swartz, E. N., Sanatani, S., Sandor, G. G. & Schreiber, R. A. Vascular abnormalities in Adams-Oliver syndrome: cause or effect? *Am J Med Genet* **82**, 49-52 (1999).
368 van Buul, J. D., Geerts, D. & Huveneers, S. Rho GAPs and GEFs: Controling switches in endothelial cell adhesion. *Cell Adh Migr* **8** (2014).
369 DerMardirossian, C. & Bokoch, G. M. GDIs: central regulatory molecules in Rho GTPase activation. *Trends Cell Biol* **15**, 356-363 (2005).
370 Fukumoto, Y. *et al.* Molecular cloning and characterization of a novel type of regulatory protein (GDI) for the rho proteins, ras p21-like small GTP-binding proteins. *Oncogene* **5**, 1321-1328 (1990).
371 Leonard, D. *et al.* The identification and characterization of a GDP-dissociation inhibitor (GDI) for the CDC42Hs protein. *J Biol Chem* **267**, 22860-22868 (1992).
372 Lelias, J. M. *et al.* cDNA cloning of a human mRNA preferentially expressed in hematopoietic cells and with homology to a GDP-dissociation inhibitor for the rho GTP-binding proteins. *Proc Natl Acad Sci U S A* **90**, 1479-1483 (1993).
373 Brunet, N., Morin, A. & Olofsson, B. RhoGDI-3 regulates RhoG and targets this protein to the Golgi complex through its unique N-terminal domain. *Traffic* **3**, 342-357 (2002).
374 Zalcman, G. *et al.* RhoGDI-3 is a new GDP dissociation inhibitor (GDI). Identification of a non-cytosolic GDI protein interacting with the small GTP-binding proteins RhoB and RhoG. *J Biol Chem* **271**, 30366-30374 (1996).
375 Govek, E. E., Newey, S. E. & Van Aelst, L. The role of the Rho GTPases in neuronal development. *Genes Dev* **19**, 1-49 (2005).
376 Dotti, C. G., Sullivan, C. A. & Banker, G. A. The establishment of polarity by hippocampal neurons in culture. *J Neurosci* **8**, 1454-1468 (1988).
377 Kishi, M., Pan, Y. A., Crump, J. G. & Sanes, J. R. Mammalian SAD kinases are required for neuronal polarization. *Science* **307**, 929-932 (2005).
378 Shi, S. H., Jan, L. Y. & Jan, Y. N. Hippocampal neuronal polarity specified by spatially localized mPar3/mPar6 and PI 3-kinase activity. *Cell* **112**, 63-75 (2003).
379 Craig, A. M. & Banker, G. Neuronal polarity. *Annu Rev Neurosci* **17**, 267-310 (1994).
380 Prasad, B. C. & Clark, S. G. Wnt signaling establishes anteroposterior neuronal polarity and requires retromer in C. elegans. *Dev* **133**, 1757-1766 (2006).
381 Adler, C. E., Fetter, R. D. & Bargmann, C. I. UNC-6/Netrin induces neuronal asymmetry and defines the site of axon formation. *Nat Neurosci* **9**, 511-518 (2006).
382 Polleux, F., Giger, R. J., Ginty, D. D., Kolodkin, A. L. & Ghosh, A. Patterning of cortical efferent projections by semaphorin-neuropilin interactions. *Science* **282**, 1904-1906 (1998).

383 Polleux, F., Morrow, T. & Ghosh, A. Semaphorin 3A is a chemoattractant for cortical apical dendrites. *Nature* **404**, 567-573 (2000).
384 Esch, T., Lemmon, V. & Banker, G. Local presentation of substrate molecules directs axon specification by cultured hippocampal neurons. *J Neurosci* **19**, 6417-6426 (1999).
385 Wiggin, G. R., Fawcett, J. P. & Pawson, T. Polarity proteins in axon specification and synaptogenesis. *Dev Cell* **8**, 803-816 (2005).
386 Kunda, P., Paglini, G., Quiroga, S., Kosik, K. & Caceres, A. Evidence for the involvement of Tiam1 in axon formation. *J Neurosci* **21**, 2361-2372 (2001).
387 Jiang, H., Guo, W., Liang, X. & Rao, Y. Both the establishment and the maintenance of neuronal polarity require active mechanisms: critical roles of GSK-3beta and its upstream regulators. *Cell* **120**, 123-135 (2005).
388 Yoshimura, T. *et al.* GSK-3beta regulates phosphorylation of CRMP-2 and neuronal polarity. *Cell* **120**, 137-149 (2005).
389 Inagaki, N. *et al.* CRMP-2 induces axons in cultured hippocampal neurons. *Nat Neurosci* **4**, 781-782 (2001).
390 Arimura, N. & Kaibuchi, K. Key regulators in neuronal polarity. *Neuron* **48**, 881-884 (2005).
391 Barnes, A. P. *et al.* LKB1 and SAD kinases define a pathway required for the polarization of cortical neurons. *Cell* **129**, 549-563 (2007).
392 Kemphues, K. J., Priess, J. R., Morton, D. G. & Cheng, N. S. Identification of genes required for cytoplasmic localization in early C. elegans embryos. *Cell* **52**, 311-320 (1988).
393 Shelly, M., Cancedda, L., Heilshorn, S., Sumbre, G. & Poo, M. M. LKB1/STRAD promotes axon initiation during neuronal polarization. *Cell* **129**, 565-577 (2007).
394 Chang, C. *et al.* MIG-10/lamellipodin and AGE-1/PI3K promote axon guidance and outgrowth in response to slit and netrin. *Curr Biol* **16**, 854-862 (2006).
395 Polleux, F. & Snider, W. Initiating and Growing an Axon. *Cold Spring Harb Perspect Biol* **2**, a001925 (2010).
396 Guan, K. L. & Rao, Y. Signalling mechanisms mediating neuronal responses to guidance cues. *Nat Rev Neurosci* **4**, 941-956 (2003).
397 Huber, A. B., Kolodkin, A. L., Ginty, D. D. & Cloutier, J. F. Signaling at the growth cone: ligand-receptor complexes and the control of axon growth and guidance. *Annu Rev Neurosci* **26**, 509-563 (2003).
398 Tessier-Lavigne, M. & Goodman, C. S. The molecular biology of axon guidance. *Science* **274**, 1123-1133 (1996).
399 Lowery, L. A. & Van Vactor, D. The trip of the tip: understanding the growth cone machinery. *Nat Rev Mol Cell Biol* **10**, 332-343 (2009).
400 Baas, P. W. & Buster, D. W. Slow axonal transport and the genesis of neuronal morphology. *J Neurobiol* **58**, 3-17 (2004).
401 Hall, A. & Lalli, G. Rho and Ras GTPases in axon growth, guidance and branching. *Cold Spring Harb Perspect Biol* **2**, a001818 (2010).
402 Dent, E. a. G., FB. Cytoskeletal dynamics and transport in growth cone motility and axon guidance. *Neuron* **40**, 209-227 (2003).
403 Hirokawa, N. & Takemura, R. Molecular motors in neuronal development, intracellular transport and diseases. *Curr Opin Neurobiol* **14**, 564-573 (2004).

404 Maday, S., Twelvetrees, A. E., Moughamian, A. J. & Holzbaur, E. L. Axonal transport: cargo-specific mechanisms of motility and regulation. *Neuron* **84**, 292-309 (2014).
405 Cotrufo, T. *et al.* A signaling mechanism coupling netrin-1/deleted in colorectal cancer chemoattraction to SNARE-mediated exocytosis in axonal growth cones. *J Neurosci* **31**, 14463-14480 (2011).
406 Sarner, S., Kozma, R., Ahmed, S. & Lim, L. Phosphatidylinositol 3-kinase, Cdc42, and Rac1 act downstream of Ras in integrin-dependent neurite outgrowth in N1E-115 neuroblastoma cells. *Mol Cell Biol* **20**, 158-172 (2000).
407 Yamaguchi, Y., Katoh, H., Yasui, H., Mori, K. & Negishi, M. RhoA inhibits the nerve growth factor-induced Rac1 activation through Rho-associated kinase-dependent pathway. *J Biol Chem* **276**, 18977-18983 (2001).
408 Talens-Visconti, R., Peris, B., Guerri, C. & Guasch, R. M. RhoE stimulates neurite-like outgrowth in PC12 cells through inhibition of the RhoA/ROCK-I signalling. *J Neurochem* **112**, 1074-1087 (2010).
409 Ehler, E., van Leeuwen, F., Collard, J. G. & Salinas, P. C. Expression of Tiam-1 in the developing brain suggests a role for the Tiam-1-Rac signaling pathway in cell migration and neurite outgrowth. *Mol Cell Neurosci* **9**, 1-12 (1997).
410 Matsuo, N., Hoshino, M., Yoshizawa, M. & Nabeshima, Y. Characterization of STEF, a guanine nucleotide exchange factor for Rac1, required for neurite growth. *J Biol Chem* **277**, 2860-2868 (2002).
411 Za, L. *et al.* βPIX controls cell motility and neurite extension by regulating the distribution of GIT1. *J Cell Sci* **119**, 2654-2666 (2006).
412 Bryan, B. *et al.* GEFT, a Rho-family guanine nucleotide exchange factor, regulates neurite outgrowth and dendritic spine formation. *J Biol Chem* **279**, 45824-45832 (2004).
413 Aoki, K., Nakamura, T., Fujikawa, K. & Matsuda, M. Local phosphatidylinositol 3,4,5-trisphosphate accumulation recruits Vav2 and Vav3 to activate Rac1/Cdc42 and initiate neurite outgrowth in nerve growth factor-stimulated PC12 cells. *Mol Biol Cell* **16**, 2207-2217 (2005).
414 Baldassa, S., Gnesutta, N., Fascio, U., Sturani, E. & Zippel, R. SCLIP, a microtubule-destabilizing factor, interacts with RasGRF1 and inhibits its ability to promote Rac activation and neurite outgrowth. *J Biol Chem* **282**, 2333-2345 (2007).
415 Tudor, E. L. *et al.* ALS2/Alsin regulates Rac-PAK signaling and neurite outgrowth. *J Biol Chem* **280**, 34735-34740 (2005).
416 Irie, F. & Yamaguchi, Y. EphB receptors regulate dendritic spine development via intersectin, Cdc42 and N-WASP. *Nat Neurosci* **5**, 1117-1118 (2002).
417 Xiao, Y. *et al.* The atypical guanine nucleotide exchange factor Dock4 regulates neurite differentiation through modulation of Rac1 GTPase and actin dynamics. *J Biol Chem* **288**, 20034-20045 (2013).
418 Beg, A. A., Sommer, J. E., Martin, J. H. & Scheiffele, P. alpha2-Chimaerin is an essential EphA4 effector in the assembly of neuronal locomotor circuits. *Neuron* **55**, 768-778 (2007).

419 Hall, C. *et al.* alpha2-chimaerin, a Cdc42/Rac1 regulator, is selectively expressed in the rat embryonic nervous system and is involved in neuritogenesis in N1E-115 neuroblastoma cells. *J Neurosci* **21**, 5191-5202 (2001).
420 Ip, J. P. K. *et al.* α2-chimaerin controls neuronal migration and functioning of the cerebral cortex through CRMP-2. *Nat Neurosci* **15**, 39-47 (2012).
421 Katoh, H., Aoki, J., Ichikawa, A. & Negishi, M. p160 RhoA-binding kinase ROKalpha induces neurite retraction. *J Biol Chem* **273**, 2489-2492 (1998).
422 Furuta, B. *et al.* Identification and functional characterization of nadrin variants, a novel family of GTPase activating protein for rho GTPases. *J Neurochem* **82**, 1018-1028 (2002).
423 Brouns, M. R., Matheson, S. F. & Settleman, J. p190 RhoGAP is the principal Src substrate in brain and regulates axon outgrowth, guidance and fasciculation. *Nat Cell Biol* **3**, 361-367 (2001).
424 Nakamura, T. *et al.* Grit, a GTPase-activating protein for the Rho family, regulates neurite extension through association with the TrkA receptor and N-Shc and CrkL/Crk adapter molecules. *Mol Cell Biol* **22**, 8721-8734 (2002).
425 Moon, S. Y., Zang, H. & Zheng, Y. Characterization of a brain-specific Rho GTPase-activating protein, p200RhoGAP. *J Biol Chem* **278**, 4151-4159 (2003).
426 Daniels, R. H., Hall, P. S. & Bokoch, G. M. Membrane targeting of p21-activated kinase 1 (PAK1) induces neurite outgrowth from PC12 cells. *EMBO J* **17**, 754-764 (1998).
427 Dan, C., Nath, N., Liberto, M. & Minden, A. PAK5, a new brain-specific kinase, promotes neurite outgrowth in N1E-115 cells. *Mol Cell Biol* **22**, 567-577 (2002).
428 Banzai, Y., Miki, H., Yamaguchi, H. & Takenawa, T. Essential role of neural Wiskott-Aldrich syndrome protein in neurite extension in PC12 cells and rat hippocampal primary culture cells. *J Biol Chem* **275**, 11987-11992 (2000).
429 Chen, X. Q., Tan, I., Leung, T. & Lim, L. The myotonic dystrophy kinase-related Cdc42-binding kinase is involved in the regulation of neurite outgrowth in PC12 cells. *J Biol Chem* **274**, 19901-19905 (1999).
430 Fujita, A. *et al.* GTP hydrolysis of TC10 promotes neurite outgrowth through exocytic fusion of Rab11- and L1-containing vesicles by releasing exocyst component Exo70. *PLoS One* **8**, e79689 (2013).
431 Zuo, X. *et al.* Exo70 interacts with the Arp2/3 complex and regulates cell migration. *Nat Cell Biol* **8**, 1383-1388 (2006).
432 Barallobre, M. J., Pascual, M., Del Rio, J.A., and Soriano, E. The netrin family of guidance factors: emphasis on netrin-1 signalling. *Brain Res Reviews* **49**, 22-47 (2005).
433 Serafini, T. *et al.* The netrins define a family of axon outgrowth-promoting proteins homologous to C. elegans UNC-6. *Cell* **78**, 409-424 (1994).
434 Ishii, N., Wadsworth, W. G., Stern, B. D., Culotti, J. G. & Hedgecock, E. M. UNC-6, a laminin-related protein, guides cell and pioneer axon migrations in C. elegans. *Neuron* **9**, 873-881 (1992).
435 Rajasekharan, S. & Kennedy, T. E. The netrin protein family. *Genome Biology* **10**, 239 (2009).
436 Colamarino, S. A. & Tessier Lavigne, M. The axonal chemoattractant netrin-1 is also a chemorepellent for trochlear motor axons. *Cell* **81**, 621-629 (1995).

437 Ackerman, S. L. *et al.* The mouse rostral cerebellar malformation gene encodes an UNC-5-like protein. *Nature* **866**, 838-842 (1997).
438 Keino-Masu, K. *et al.* Deleted in colorectal cancer (DCC) encodes a netrin receptor. *Cell* **87**, 175-185 (1996).
439 Leonardo, E. D. *et al.* Vertebrate homologues of C.elegans UNC-5 are candidate netrin receptors. *Nature* **386**, 833-838 (1997).
440 Liu, G. *et al.* DSCAM functions as a netrin receptor in commissural axon pathfinding. *Proc Natl Acad Sci* **106**, 2951-2956 (2009).
441 Ly, A. *et al.* DSCAM is a netrin receptor that collaborates with DCC in mediating turning responses to netrin-1. *Cell* **133**, 1241-1254 (2008).
442 Rama, N. *et al.* Amyloid precursor protein regulates netrin-1-mediated commissural axon outgrowth. *J Biol Chem* **287**, 30014-30023 (2012).
443 Kennedy, T. E., Serafini, T., de la Torre, J. R. & Tessier-Lavigne, M. Netrins are diffusible chemotropic factors for commissural axons in the embryonic spinal cord. *Cell* **78**, 425-435 (1994).
444 Serafini, T. *et al.* Netrin-1 is required for commissural axon guidance in the developing vertebrate nervous system. *Cell* **87**, 1001-1014 (1996).
445 Fazeli, A., Dickinson, S.L., Hermiston, M.L., Tighe, R.V., Steen, R.G., Small, C.G., Stoeckli, E.T., Keino-Masu, K., Masu, M., Rayburn, H., Simons, J., Bronson, R.T., Gordon, J.I., Tessier-Lavigne, M. and Weinberg, R.A. Phenotype of mice lacking functional Deleted in colorectal cancer (DCC) gene. *Nature* **386**, 796-803 (1997).
446 Xu, K. *et al.* Structures of netrin-1 bound to two receptors provide insight into its axon guidance mechanism. *Science* **344**, 1275-1279 (2014).
447 Richards, L. J., Koester, S. E., Tuttle, R. & O'Leary, D. D. M. Directed growth of early cortical axons is influenced by a chemoattractant released from an intermediate target *J Neurosci* **17**, 2445-2458 (1997).
448 Stein, E., Zou, Y, Poo, M., and Tessier-Lavigne, M. Binding of DCC by netrin-1 to mediate axon guidance independent of adenosine A2B receptor activation. *Science* **291**, 1976-1982 (2001).
449 Moore, S. W., Tessier-Lavigne, M. & Kennedy, T. E. Netrins and their receptors. *Adv Exp Med Biol* **621**, 17-31 (2007).
450 Cho, K. R. *et al.* The DCC gene: structural analysis and mutations in colorectal carcinomas. *Genomics* **19**, 525-531 (1994).
451 Finci, L. I. *et al.* The crystal structure of netrin-1 in complex with DCC reveals the bifunctionality of netrin-1 as a guidance cue. *Neuron* **83**, 839-849 (2014).
452 Hong, K. *et al.* A ligand-gated association between cytoplasmic domains of UNC5 and DCC family receptors converts netrin-induced growth cone attraction to repulsion. *Cell* **97**, 927-941 (1999).
453 Fearon, E. R. *et al.* Identification of a chromosome 18q gene that is altered in colorectal cancers. *Science* **247**, 49-56 (1990).
454 Mehlen, P. *et al.* The DCC gene product induces apoptosis by a mechanism requiring receptor proteolysis. *Nature* **395**, 801-804 (1998).
455 Geisbrecht, B. V., Dowd, K. A., Barfield, R. W., Longo, P. A. & Leahy, D. J. Netrin binds discrete subdomains of DCC and UNC5 and mediates interactions between DCC and heparin. *J Biol Chem* **278**, 32561-32568 (2003).

456 Srour, M. *et al.* Mutations in DCC cause congenital mirror movements. *Science* **328**, 592 (2010).
457 Grant, A., Fathalli, F., Rouleau, G. A., Joober, R. & Flores, C. Association between schizophrenia and genetic variation in DCC: A case–control study. *Schizophrenia Res* **137**, 26-31 (2012).
458 Lin, L., Lesnick, TG, Maraganore, DM. and Isacson. Axon guidance and synaptic maintenance: preclinical markers for neurodegenerative disease and therapeutics. *T.in neurosciences* **32**, 142-149 (2009).
459 Lesnick, T. G. *et al.* Beyond Parkinson Disease: Amyotrophic Lateral Sclerosis and the Axon Guidance Pathway. *PLoS One* **3**, e1449 (2008).
460 Meriane, M. *et al.* Phosphorylation of DCC by Fyn mediates Netrin-1 signaling in growth cone guidance. *J Cell Biol* **167**, 687-698 (2004).
461 Li, W. *et al.* Activation of FAK and Src are receptor-proximal events required for netrin signaling. *Nat Neurosci* **7**, 1213-1221 (2004).
462 Liu, G. *et al.* Netrin requires focal adhesion kinase and Src family kinases for axon outgrowth and attraction. *Nat Neurosci* **7**, 1222-1232 (2004).
463 Forcet, C. *et al.* Netrin-1-mediated axon outgrowth requires deleted in colorectal cancer-dependent MAPK activation. *Nature* **417**, 443-447 (2002).
464 Ma, W. *et al.* Phosphorylation of DCC by ERK2 is facilitated by direct docking of the receptor P1 domain to the kinase. *Structure* **18**, 1502-1511 (2010).
465 Li, X., Saint-Cyr-Proulx, E., Aktories, K. & Lamarche-Vane, N. Rac1 and Cdc42 but not RhoA or Rho kinase activities are required for neurite outgrowth induced by the Netrin-1 receptor DCC (deleted in colorectal cancer) in N1E-115 neuroblastoma cells. *J Biol Chem* **277**, 15207-15214 (2002).
466 Shekarabi, M. & Kennedy, T. E. The netrin-1 receptor DCC promotes filopodia formation and cell spreading by activating Cdc42 and Rac1. *Mol Cell Neurosci* **19**, 1-17 (2002).
467 Moore, S. W. *et al.* Rho inhibition recruits DCC to the neuronal plasma membrane and enhances axon chemoattractionn to netrin1. *Dev* **135**, 2855-2864 (2008).
468 Picard, M. *et al.* Spatial and temporal regulation of the small GTPases RhoA and Rac1 by the netrin-1 receptor UNC5a during neurite outgrowth. *Cellular signalling* **21**, 1961-1973 (2009).
469 Antoine-Bertrand, J., Ghogha, A., Bedford, FK., and Lamarche-Vane, N. A role of Ezrin/Radixin/Moesin phosphorylation in netrin-1/DCC-mediated axon outgrowth. *Mol Biol Cell* (2011).
470 Li, X. *et al.* The adaptor protein Nck-1 couples the netrin-1 receptor DCC (deleted in colorectal cancer) to the activation of the small GTPase Rac1 through an atypical mechanism. *J Biol Chem* **277**, 37788-37797 (2002).
471 Li, X., Gao, X., Liu, G., Xiong, W., Wu, J. and Rao, Y. Netrin signal transduction and the guanine nucleotide exchange factor DOCK180 in attractive signaling. *Nature Neurosci.* **11**, 28-35 (2008).
472 Bouchard, J.-F. *et al.* Protein kinase A activation promotes plasma membrane insertion of DCC from an intracellular pool: A novel mechanism regulating commissural axon extension. *J Neurosci* **24**, 3040-3050 (2004).

473 Deming, P. B. *et al.* Anchoring of protein kinase A by ERM (ezrin-radixin-moesin) proteins is required for proper netrin signaling through DCC (Deleted in Colorectal Cancer). *J Biol Chem* **290**, 5783-5796 (2015).
474 Winkle, C. C. *et al.* A novel Netrin-1–sensitive mechanism promotes local SNARE-mediated exocytosis during axon branching. *J Cell Biol* **205**, 217-232 (2014).
475 Südhof, T. C. & Rothman, J. E. Membrane fusion: grappling with SNARE and SM proteins. *Science* **323**, 474-477 (2009).
476 Atwal, J. K. *et al.* PirB is a Functional Receptor for Myelin Inhibitors of Axonal Regeneration. *Sci Rep* **322**, 967-970 (2008).
477 Wang, K. C., Kim, J. A., Sivasankaran, R., Segal, R. & He, Z. P75 interacts with the Nogo receptor as a co-receptor for Nogo, MAG and OMgp. *Nature* **420**, 74-78 (2002).
478 Park, J. B. *et al.* A TNF receptor family member, TROY, is a coreceptor with Nogo receptor in mediating the inhibitory activity of myelin inhibitors. *Neuron* **45**, 345-351 (2005).
479 Singh, K. K. *et al.* Developmental axon pruning mediated by BDNF-p75NTR-dependent axon degeneration. *Nat Neurosci* **11**, 649-658 (2008).
480 Park, K. J., Grosso, C. A., Aubert, I., Kaplan, D. R. & Miller, F. D. p75NTR-dependent, myelin-mediated axonal degeneration regulates neural connectivity in the adult brain. *Nat Neurosci* **13**, 559-566 (2010).
481 Yamashita, T. & Tohyama, M. The p75 receptor acts as a displacement factor that releases Rho from Rho-GDI. *Nat Neurosci* **6**, 461-467 (2003).
482 Harrington, A. W. *et al.* The role of Kalirin9 in p75/nogo receptor-mediated RhoA activation in cerebellar granule neurons. *J Biol Chem* **283**, 24690-24697 (2008).
483 Niederöst, B., Oertle, T., Fritsche, J., McKinney, R. A. & Bandtlow, C. E. Nogo-A and myelin-associated glycoprotein mediate neurite growth inhibition by antagonistic regulation of RhoA and Rac1. *J Neurosci* **22**, 10368-10376 (2002).
484 Fournier, A. E., Takizawa, B. T. & Strittmatter, S. M. Rho Kinase Inhibition Enhances Axonal Regeneration in the Injured CNS. *J Neurosci* **23**, 1416-1423 (2003).
485 Borisoff, J. F. *et al.* Suppression of Rho-kinase activity promotes axonal growth on inhibitory CNS substrates. *Mol Cell Neurosci* **22**, 405-416 (2003).
486 Schulz, A. *et al.* Merlin isoform 2 in neurofibromatosis type 2-associated polyneuropathy. *Nat Neurosci* **16**, 426-433 (2013).
487 Fry, E. J., Ho, C. & David, S. A role for Nogo receptor in macrophage clearance from injured peripheral nerve. *Neuron* **53**, 649-662 (2007).
488 Jung, J. *et al.* Actin polymerization is essential for myelin sheath fragmentation during Wallerian degeneration. *J Neurosci* **31**, 2009-2015 (2011).
489 Antoine-Bertrand, J., Villemure, J. F. & Lamarche-Vane, N. Implication of Rho GTPases in Neurodegenerative Diseases. *Curr Drug Targets* **12**, 1202-1215 (2011).
490 O'Donnell, M., Chance, RK. and Bashaw, GJ. Axon growth and guidance: receptor regulation and signal transduction. *Ann.Rev.Neurosci.* **32**, 383-412 (2009).

491 Bateman, J. & Van Vactor, D. The Trio family of guanine-nucleotide-exchange factors: regulators of axon guidance. *J Cell Sci* **114**, 1973-1980 (2001).
492 Tcherkezian, J., Brittis, P. A., Thomas, F., Roux, P. P. & Flanagan, J. G. Transmembrane receptor DCC associates with protein synthesis machinery and regulates translation. *Cell* **141**, 632-644 (2010).
493 Levy-Strumpf, N. & Culotti, J. G. VAB-8, UNC-73, and MIG-2 regulate axon polarity and cell migration functions of UNC-40 in *C. elegans*. *Nat Neurosci* (2007).
494 Watari-Goshima, N., Ogura, K., Wolf, F. W., Goshima, Y. & Garriga, G. *C. elegans* VAB-8 and UNC-73 regulate the SAX-3 receptor to direct cell and growth-cone migrations. *Nat Neurosci* **10**, 169-176 (2007).
495 Egea, J. & Klein, R. Bidirectional Eph-ephrin signaling during axon guidance. *Trends in Cell Biology* **17**, 230-238 (2007).
496 Sahin, M. *et al.* Eph-dependent tyrosine phosphorylation of ephexin1 modulates growth cone collapse. *Neuron* **46**, 191-204 (2005).
497 Cowan, C. W. *et al.* Vav family GEFs link activated Ephs to endocytosis and axon guidance. *Neuron* **46**, 205-217 (2005).
498 Tolias, K. F. *et al.* The Rac1 guanine nucleotide exchange factor Tiam1 mediates EphB receptor-dependent dendritic spine development. *Proc Natl Acad Sci* **104**, 7265-7270 (2007).
499 Shi, L. *et al.* alpha2-Chimaerin interacts with EphA4 and regulates EphA4-dependent growth cone collapse. *Proc Natl Acad Sci* **104**, 16347-16352 (2007).
500 Demarco, R. S., Struckhoff, E. C. & Lundquist, E. A. The Rac GTP exchange factor TIAM-1 acts with Cdc-42 and the guidance receptor UNC-40/DCC in neuronal protrusion and axon guidance. *PLoS Genetics* **8**, 1-18 (2012).
501 Moran, M. F., Polakis, P., McCormick, F., Pawson, T. & Ellis, C. Protein-tyrosine kinases regulate the phosphorylation, protein interactions, subcellular distribution, and activity of p21ras GTPase-activating protein. *Mol Cell Biol* **11**, 1804-1812 (1991).
502 Bashaw, G. J. & Klein, R. Signaling from Axon Guidance Receptors. *Cold Spring Harb Perspect Biol* **2**, a001941 (2010).
503 Cook, D. R., Rossman, K. L. & Der, C. J. Rho guanine nucleotide exchange factors: regulators of Rho GTPase activity in development and disease. *Oncogene* **33**, 4021-4035 (2014).
504 Hartl, F. U., Bracher, A. & Hayer-Hartl, M. Molecular chaperones in protein folding and proteostasis. *Nature* **475**, 324-332 (2011).
505 Kim, T. H. *et al.* Netrin induces down-regulation of its receptor, Deleted in Colorectal Cancer, through the ubiquitin–proteasome pathway in the embryonic cortical neuron. *J Neurochem* **95**, 1-8 (2005).
506 Yam, P. T., Langlois, S. D., Morin, S. & Charron, F. Sonic Hedgehog guides axons through a noncanonical, Src-family-kinase-dependent signaling pathway. *Neuron* **62**, 349-362 (2009).
507 Loones, M. T., Chang, Y. & Morange, M. The distribution of heat shock proteins in the nervous system of the unstressed mouse embryo suggests a role in neuronal and non-neuronal differentiation. *Cell Stress Chaperones* **5**, 291-305 (2000).

508 Aquino, D. A., Klipfel, A. A., Brosnan, C. F. & Norton, W. T. The 70-kDa heat shock cognate protein (HSC70) is a major constituent of the central nervous system and is up-regulated only at the mRNA level in acute experimental autoimmune encephalomyelitis. *J Neurochem* **61**, 1340-1348 (1993).
509 Daugaard, M., Rohde, M. & Jäättelä, M. The heat shock protein 70 family: Highly homologous proteins with overlapping and distinct functions. *FEBS Lett* **581**, 3702-3710 (2007).
510 Kauppinen, K. P., Duan, F., Wels, J. I. & Manor, D. Regulation of the Dbl proto-oncogene by heat shock cognate protein 70 (Hsc70). *J Biol Chem* **280**, 21638-21644 (2005).
511 Rohde, M. *et al.* Members of the heat-shock protein 70 family promote cancer cell growth by distinct mechanisms. *Genes & Dev.* **19**, 570-582 (2005).
512 Duquette, P. M. & Lamarche-Vane, N. Rho GTPases in embryonic development. *Small GTPases* **e29716** (2014).
513 Bid, H. K., Roberts, R. D., Manchanda, P. K. & Houghton, P. J. RAC1: an emerging therapeutic option for targeting cancer angiogenesis and metastasis. *Mol Cancer Ther* **12**, 1925-1934 (2013).
514 Balaburski, G. M. *et al.* A modified HSP70 inhibitor shows broad activity as an anticancer agent. *Mol Cancer Res* **11**, 219-229 (2013).
515 Kaiser, M. *et al.* Antileukemic activity of the HSP70 inhibitor pifithrin-μ in acute leukemia. *Blood Cancer* **1**, e28 (2011).
516 Bouchard, J.-F., Horn, K., Stroh, T. & Kennedy, T. E. Depolarization recruits DCC to the plasma membrane of embryonic cortical neurons and enhances axon extension in response to netrin-1. *J Neurochem* **107**, 398-417 (2008).
517 Sharma, M., Burré, J. & Südhof, T. C. CSPα promotes SNARE-complex assembly by chaperoning SNAP-25 during synaptic activity. *Nat Cell Biol* **13**, 30-39 (2011).
518 Gao, B. *et al.* Inhibition of histone deacetylase activity suppresses IFN-γ induction of tripartite motif 22 via CHIP-mediated proteasomal degradation of IRF-1. *J Immunol* **191**, 464-471 (2013).
519 Mar, F. M., Bonni, A. & Sousa, M. M. Cell intrinsic control of axon regeneration. *EMBO Rep* **15**, 254-263 (2014).
520 Koga, H. *et al.* Constitutive upregulation of chaperone-mediated autophagy in Huntington's disease. *J Neurosci* **31**, 18492-18505 (2011).
521 Pemberton, S. & Melki, R. The interaction of Hsc70 protein with fibrillar α-Synuclein and its therapeutic potential in Parkinson's disease. *Commun Integr Biol* **5**, 94-95 (2012).
522 Turturici, G., Sconzo, G. & Geraci, F. Hsp70 and Its Molecular Role in Nervous System Diseases. *Biochem Res Int* **2011**, 618127 (2011).
523 Shimura, H., Schwartz, D., Gygi, S. P. & Kosik, K. S. CHIP-Hsc70 complex ubiquitinates phosphorylated tau and enhances cell survival. *J Biol Chem* **279**, 4869-4876 (2004).
524 Muranyi, M., He, Q. P., Fong, K. S. & Li, P. A. Induction of heat shock proteins by hyperglycemic cerebral ischemia. *Brain Res Mol Brain Res* **139**, 80-87 (2005).
525 Chen, A., Liao, W. P., Lu, Q., Wong, W. S. & Wong, P. T. Upregulation of dihydropyrimidinase-related protein 2, spectrin alpha II chain, heat shock cognate

protein 70 pseudogene 1 and tropomodulin 2 after focal cerebral ischemia in rats--a proteomics approach. *Neurochem Int* **50**, 1078-1086 (2007).

526 Bański, P. *et al.* Nucleolar targeting of the chaperone hsc70 is regulated by stress, cell signaling, and a composite targeting signal which is controlled by autoinhibition. *J Biol Chem* **285**, 21858-21867 (2010).

527 Govek, E. E., Hatten, M. E. & Van Aelst, L. The role of Rho GTPase proteins in CNS neuronal migration. *Dev Neurobiol* **71**, 528-553 (2011).

528 Arimura, N. & Kaibuchi, K. Neuronal polarity: from extracellular signals to intracellular mechanisms. *Nat Rev Neurosci* **8**, 194-205 (2007).

529 He, Y. *et al.* CdGAP is required for transforming growth factor beta- and Neu/ErbB-2-induced breast cancer cell motility and invasion. *Oncogene* **30**, 1032-1045, doi:10.1038/onc.2010.477 (2011).

530 Tcherkezian, J., Triki, I., Stenne, R., Danek, E. I. & Lamarche-Vane, N. The human orthologue of CdGAP is a phosphoprotein and a GTPase-activating protein for Cdc42 and Rac1 but not RhoA. *Biology of the cell / under the auspices of the European Cell Biology Organization* **98**, 445-456, doi:10.1042/BC20050101 (2006).

531 Rosenstein, J. M., Mani, N., Khaibullina, A. & Krum, J. M. Neurotrophic effects of vascular endothelial growth factor on organotypic cortical explants and primary cortical neurons. *J Neurosci* **23**, 11036-11044 (2003).

532 Tahirovic, S. & Bradke, F. Neuronal polarity. *Cold Spring Harbor perspectives in biology* **1**, a001644, doi:10.1101/cshperspect.a001644 (2009).

533 Bromberg, K. D., Iyengar, R. & He, J. C. Regulation of neurite outgrowth by G(i/o) signaling pathways. *Frontiers in bioscience : a journal and virtual library* **13**, 4544-4557 (2008).

534 Spillane, M. & Gallo, G. Involvement of Rho-family GTPases in axon branching. *Small GTPases* **5**, e27974, doi:10.4161/sgtp.27974 (2014).

535 Meyer, G. & Feldman, E. L. Signaling mechanisms that regulate actin-based motility processes in the nervous system. *Journal of neurochemistry* **83**, 490-503 (2002).

536 Gomez, T. M. & Letourneau, P. C. Actin dynamics in growth cone motility and navigation. *Journal of neurochemistry* **129**, 221-234, doi:10.1111/jnc.12506 (2014).

537 Wormer, D., Deakin, N. O. & Turner, C. E. CdGAP regulates cell migration and adhesion dynamics in two-and three-dimensional matrix environments. *Cytoskeleton (Hoboken, N.J.)* **69**, 644-658, doi:10.1002/cm.21057 (2012).

538 Kajdaniuk, D., Marek, B., Borgiel-Marek, H. & Kos-Kudla, B. Vascular endothelial growth factor (VEGF) - part 1: in physiology and pathophysiology. *Endokrynologia Polska* **62**, 444-455 (2011).

539 Carmeliet, P. & Ruiz de Almodovar, C. VEGF ligands and receptors: implications in neurodevelopment and neurodegeneration. *Cellular and molecular life sciences : CMLS* **70**, 1763-1778, doi:10.1007/s00018-013-1283-7 (2013).

540 Miyamoto, N. *et al.* Crosstalk between cerebral endothelium and oligodendrocyte. *Cellular and molecular life sciences : CMLS* **71**, 1055-1066, doi:10.1007/s00018-013-1488-9 (2014).

541 Schiera, G. *et al.* Neurons produce FGF2 and VEGF and secrete them at least in part by shedding extracellular vesicles. *Journal of cellular and molecular medicine* **11**, 1384-1394, doi:10.1111/j.1582-4934.2007.00100.x (2007).
542 Ichikawa, M., Muramoto, K., Kobayashi, K., Kawahara, M. & Kuroda, Y. Formation and maturation of synapses in primary cultures of rat cerebral cortical cells: an electron microscopic study. *Neuroscience research* **16**, 95-103 (1993).
543 LaThangue, N. B. A major heat-shock protein defined by a monoclonal antibody. *Embo J* **3**, 1871-1879 (1984).
544 Flaherty, K. M., McKay, D. B., Kabsch, W. & Holmes, K. C. Similarity of the three-dimensional structures of actin and the ATPase fragment of a 70-kDa heat shock cognate protein. *Proc Natl Acad Sci U S A* **88**, 5041-5045 (1991).
545 Haus, U. *et al.* The heat shock cognate protein from Dictyostelium affects actin polymerization through interaction with the actin-binding protein cap32/34. *Embo J* **12**, 3763-3771 (1993).
546 Hishiya, A., Kitazawa, T. & Takayama, S. BAG3 and Hsc70 interact with actin capping protein CapZ to maintain myofibrillar integrity under mechanical stress. *Circ Res* **107**, 1220-1231 (2010).
547 Sinnar, S. A., Antoku, S., Saffin, J. M., Cooper, J. A. & Halpain, S. Capping protein is essential for cell migration in vivo and for filopodial morphology and dynamics. *Mol Biol Cell* **25**, 2152-2160 (2014).
548 Mejillano, M. R. *et al.* Lamellipodial versus filopodial mode of the actin nanomachinery: pivotal role of the filament barbed end. *Cell* **118**, 363-373 (2004).
549 Chen, X. J. *et al.* Ena/VASP proteins cooperate with the WAVE complex to regulate the actin cytoskeleton. *Dev Cell* **30**, 569-584 (2014).
550 Havrylenko, S. *et al.* WAVE binds Ena/VASP for enhanced Arp2/3 complex-based actin assembly. *Mol Biol Cell* **26**, 55-65 (2015).
551 Caron, C. *et al.* CdGAP/ARHGAP31 is a critical regulator of vascular development and VEGF-mediated angiogenesis. *In preparation.* (2015).
552 Kuhn, H. G., Dickinson-Anson, H. & Gage, F. H. Neurogenesis in the dentate gyrus of the adult rat: age-related decrease of neuronal progenitor proliferation. *J Neurosci* **16**, 2027-2033 (1996).
553 Kee, N., Sivalingam, S., Boonstra, R. & Wojtowicz, J. M. The utility of Ki-67 and BrdU as proliferative markers of adult neurogenesis. *J Neurosci Methods* **115**, 97-105 (2002).
554 van Praag, H., Kempermann, G. & Gage, F. H. Running increases cell proliferation and neurogenesis in the adult mouse dentate gyrus. *Nat Neurosci* **2**, 266-270 (1999).
555 Kempermann, G., Kuhn, H. G. & Gage, F. H. More hippocampal neurons in adult mice living in an enriched environment. *Nature* **386**, 493-495 (1997).
556 Louissaint, A., Rao, S., Leventhal, C. & Goldman, S. A. Coordinated interaction of neurogenesis and angiogenesis in the adult songbird brain. *Neuron* **34**, 945-960 (2002).
557 Pereira, A. C. *et al.* An in vivo correlate of exercise-induced neurogenesis in the adult dentate gyrus. *Proc Natl Acad Sci U S A* **104**, 5638-5643 (2007).

558 Fournier, N. M., Lee, B., Banasr, M., Elsayed, M. & Duman, R. S. Vascular endothelial growth factor regulates adult hippocampal cell proliferation through MEK/ERK- and PI3K/Akt-dependent signaling. *Neuropharmacology* **63**, 642-652 (2012).
559 Tang, B. L. Class II HDACs and neuronal regeneration. *J Cell Biochem* **115**, 1225-1233 (2014).

Appendix: Rho GTPases in neurodegeneration diseases

Jonathan DeGeer and Nathalie Lamarche-Vane. (2013). **Experimental Cell Research** 319(15): 2384-2394.

Abstract

Rho GTPases are molecular switches that modulate multiple intracellular signaling processes by means of various effector proteins. As a result, Rho GTPase activities are tightly spatiotemporally regulated in order to ensure homeostasis within the cell. Though the roles of Rho GTPases during neural development have been well documented, their participation during neurodegeneration has been far less characterized. Herein we discuss our current knowledge of the role and function of Rho GTPases and regulators during neurodegeneration, and highlight their potential as targets for therapeutic intervention in common neurodegenerative disorders.

Introduction

Rho GTPases

Small G proteins of the Rho family are evolutionarily conserved regulators of cytoskeletal dynamics, functioning during the earliest stages of embryonic development and supporting life thereafter. The Rho family of GTPases are encoded by 20 genes and act as molecular switches, cycling between inactive GDP-bound and active GTP-bound states, thereby regulating downstream pathways via effector proteins (1). The 20 Rho GTPases have been sub-classified into various families based on sequence homology: Rac (Rac1-3, RhoG), Rho (RhoA-C), Cdc42 (Cdc42, TC10, TCL, Chp/Wrch2, Wrch1), Rnd (Rnd1-2, Rnd3/RhoE), RhoD (RhoD, Rif/RhoF), RhoBTB (RhoBTB1-2) and RhoH (2). Oversight of Rho GTPase nucleotide cycling is performed by regulatory proteins: guanine nucleotide exchange factors **(**GEFs) enhance the GTP-bound state, while GTP hydrolysis is catalyzed by GTPase-activating proteins (GAPs) (3, 4). Additionally, guanine nucleotide dissociation inhibitors (GDIs) bind to some Rho GTPases and restrict them in an inactive state in the cytoplasm, preventing them from associating with their downstream effectors (5). Whereas RhoGAPs are characterized by a trademark “RhoGAP” domain (reviewed in ref. 4), RhoGEFs are subdivided into two families: the Dbl-homology domain-containing family and the non-classical DOCK family. GEFs of the former group contain a characteristic Dbl-homology (DH) domain directly followed by a Plekstrin homology (PH) domain, which interact with GDP-bound substrates and promote membrane localization, respectively (3). The DOCK family of GEFs have two characteristic DOCK homology regions (DHR) termed DHR1 and DHR2, which are involved in phospho-lipid association and GEF activity, respectively

(6). The localized modulation of Rho GTPases by GEFs, GAPs and GDIs varies from cell type to cell type and thus presents a complex network of regulatory mechanisms. Furthermore, given the significant role of GEFs and GAPs in modulating Rho GTPases, mutations in the functional domains of these proteins can lead to dysregulation of GTPase signaling pathways.

Of the Rho GTPases identified, the best characterized are Rac1, Cdc42 and RhoA. Earliest studies in murine fibroblast cultures highlighted the fundamental role of these GTPases in mediating cytoskeletal rearrangements: stress fiber and focal adhesion formation by RhoA, lamellipodia and membrane ruffles by Rac1 and filopodia and actin microspikes by Cdc42 (7-9). Well known effectors downstream of active Rac1 and Cdc42 are the p21-activated kinase (PAK) family of serine/threonine kinases. When bound to Rac-GTP or Cdc42-GTP, PAKs overcome autoinhibition, modulate the actin cytoskeleton by Lin-11, Isl-1, and Mec-3 (LIM) domain-containing kinases, which phosphorylate and inhibit the actin filament depolymerizing factor cofilin leading to F-actin stabilization (10, 11). A direct target of PAK kinase activity downstream of active Rac1 and Cdc42 is myosin light chain kinase (MLCK), which leads to reduced phosphorylation and activity of its target, myosin II regulatory light chain, a molecular motor involved in actin cytoskeletal dynamics (12). In addition to targeting LIMK and MLCK, PAKs also link Rac1/Cdc42 to various signaling pathways including the mitogen-activated protein kinase (MAPK), the c-Jun-NH2-terminal kinase (JNK) and p38 MAPK pathways (13-16). Important downstream effectors of active Cdc42 and Rac1, thereby linking these GTPases to actin polymerization, are the Wiskott-Aldrich-syndrome family scaffold proteins: Wiskott-Aldrich-syndrome Protein (WASP) and WAVE proteins (17).

WASP and WAVE associate with the actin cytoskeleton via the Arp 2/3 actin nucleation complex. Direct association of GTP-Cdc42 with WASP results in activation of WASP *in vitro*, and promotes association with the Arp2/3 complex which nucleates new actin filaments (18). Downstream of active Rac1, activation of the WAVE family members occurs indirectly, by release of an inhibitory WAVE complex (refer to (19) for a more comprehensive review).

Downstream of RhoA, activity of the Rho-kinase (ROCK) family and Diaphanous formin subfamily (Dia) are stimulated. Rho-kinases are serine/threonine kinases that contribute to cytoskeletal rearrangements by promoting the phosphorylation and activation of MLC, and inactivation of MLC phosphatase (20). In a similar mechanism to PAKs, ROCK also contributes to F-actin dynamics by phosphorylating LIMK, which phosphorylates and inactivates the actin depolymerisation factor cofilin (21, 22). Mammalian Dia proteins (mDia) are effectors of RhoA that bind to and nucleate actin filaments, while they also contribute to microtubule stabilization at the leading edge during cell migration downstream of RhoA (23).

Rho GTPases in nerve injury

An accumulating body of evidence has supported an indispensable role for Rho GTPases in nerve cell function, from neuronal specification and polarization to axon guidance, survival and nerve growth (reviewed in (24)). In the context of axon growth and pathfinding, for example, the recruitment and localized activation of the Rho GTPases Rac1, Cdc42, and RhoA, are imperative for translating extracellular cues into cytoskeletal rearrangements within the extending growth cone (25-27). In recent years,

molecular mechanisms implicated in neurodegeneration have been investigated and thus far have highlighted many signaling pathways, including those involving Rho GTPases.

In the injured CNS, regeneration of neural tracts is impeded by formation of astroglial scars and the expression of inhibitory myelin-associated molecules: Nogo, myelin-associated glycoprotein (MAG), oligodendrocyte-myelin glycoprotein (OMgp). Nogo, MAG and OMpg bind to and signal through the neuronal Nogo family receptors (NgR) or the paired immunoglobulin receptor B (28, 29). Additionally, NgR-mediated signaling by myelin-associated molecules occurs via the partnering with either p75 neurotrophin receptor (p75NTR) or the orphan receptor TROY (28-30). p75NTR has been previously implicated in local neurodegeneration, where under physiological conditions p75NTR-expressing sympathetic neurons undergo a neurotrophin-dependent myelin-mediated degeneration program (31). In this context, p75NTR binds to and sequesters RhoGDI downstream of BDNF during axon pruning, leading to elevation of active RhoA (32, 33). In addition, the Rac1 and RhoA GEF Kalirin-9 competes with RhoGDI for binding to p75NTR in cerebellar granule neurons downstream of MAG, suggesting an interplay between these GTPase regulators underlies the RhoA-mediated inhibitory functions of myelin-associated molecules downstream of p75NTR (34). Further evidence showing that Nogo-A-mediated activation of RhoA antagonizes Rac1 activity during neurite growth inhibition indicates cross-talk between GTPase signaling pathways occurs during inhibition of nerve growth due to injury (35).

In accordance with the finding that RhoA is activated during local axon pruning and degeneration, inhibition of the RhoA effector ROCK has been shown to promote

neuronal growth on inhibitory substrates in culture and promote nerve regeneration and locomotor recovery *in vivo* (36, 37). In addition to its role in nerve growth, RhoA regulation is also important in peripheral nerve axon integrity. In a recent study, Schulz and colleagues identified that RhoA/ROCK act downstream of the cytoskeletal protein merlin isoform 2 (merlin-iso2), which was required for the maintenance of peripheral axon integrity (38). Axonal merlin-iso2, which is closely associated with neurofilaments, acts as a scaffold tethering both p190RhoGAP and RhoGDI, leading to local RhoA regulation (38). Intriguingly, a patient-derived mutation of merlin at C784T resulted in impaired sequestering of RhoGDI resulting in reduced RhoA activity and programmed axonal atrophy, clinically manifesting as severe neuropathy (38).

In response to axonal transection, molecular mechanisms within the proximal axon are stimulated by the extracellular environment, the sum of which lead to demyelination, axonal die-back and distal axonal clearance typical of Wallerian type degeneration. During peripheral nerve injury a subtype of activated macrophages synthesize *de novo* NgR1 and NgR2, which promote the clearance of macrophages and signals termination of inflammation via myelin-dependent RhoA activation and repulsion (39). Furthermore during demyelination, myelin undergoes fragmentation as Schwann cells dedifferentiate. The injury-induced demyelination leads to Rac1-dependent modulation of actin dynamics within the Schwann cell (40). Together these few examples demonstrate the implication of Rho GTPase signaling in response to nerve injury.

Rho GTPases in neurodegenerative diseases

Whether in response to an intrinsic program or a traumatic injury, the loss of functional connections within the nervous system can lead to severe detrimental consequences. Loss of active neural connections and induction of axon degeneration are characteristic of many neurodegenerative diseases. Though the mechanisms of neurodegeneration are not fully understood, recent findings indicate that Rho GTPases are key components of neuronal cell degeneration pathways**.** The remainder of this review will focus on the Rho GTPase pathways implicated in specific neurodegenerative disorders (summarized in Table 1).

Amyotrophic Lateral Sclerosis (ALS)

ALS is a neurodegenerative disorder which is characterized by the preferential loss of upper and lower motor neural networks within the brainstem and spinal cord of affected patients. During progression of ALS, motor neuron loss results in weakness of skeletal muscles, leading to atrophy and death due to paralysis of the respiratory muscles (for review see (41)). Though classical inherited ALS results from mutations in the gene encoding superoxide dismutase 1 resulting in a gain-of-function (42), additional mutations in the *ALS2* gene encoding the Rab5 and RacGEF, Alsin, were correlated with a severe primary lateral sclerosis with juvenile onset (43). Since a patient-derived mutation of Alsin led to reduced protein stability and expression, the study of ALS2 loss-of-function mice was assessed (44). In this context, the lower motor neurons appeared to be relatively intact compared to lower motor neurons of the classical ALS mouse model (carrying the superoxide dismutase 1 mutation) suggesting

that loss of Alsin leads to a condition distinct from ALS (43). From these studies, it was proposed that axon degeneration in the ALS2 mouse model may be due to the role of Alsin in vesicular trafficking and/or neurite extension via Rab5 and/or Rac1 activation, respectively (45, 46), or by protecting cells from SOD1-mediated toxicity via Rac1/PI3K/Akt pathway (47).

Since the majority of ALS cases are sporadically occurring, efforts have been made to elucidate the contribution of epigenetic regulation to disease onset. Recently, Figueroa-Romero and colleagues assessed loci-specific alterations in methylation in post-mortem spontaneous ALS spinal cords (48). To this means, they identified many genes differentially methylated, including loci encoding the RhoGEF ARHGEF16 and RhoGAP srGAP1. Since ARHGEF16 was found to be hyper-methylated and down-regulated in patients with sporadic ALS, it is attractive to speculate that a reduction of GEF activity towards its substrates Rac1 and Cdc42 is implicated in the ALS pathology (49, 50). Conversely, srGAP1 was hypo-methylated and up-regulated in this screen, which may contribute to sporadic ALS by increasing the hydrolysis of its target GTPases: Cdc42 and RhoA (51). In summary, these initial studies suggest a reduction in Rho GTPase activation may be associated with sporadic ALS.

Alzheimer's Disease (AD)

AD is a progressive age-associated neurodegenerative disease characterized by cognitive decline and dementia. AD onset corresponds with an accumulation of extracellular neuritic plaques rich in amyloid-β (Aβ), intracellular neurofibrillary tangles rich in hyperphosphorylated Tau, and loss of dendritic spines and synaptic function (for

review see (52)). Accumulating evidence supports a role for Rho GTPases in various aspects of AD progression. In general RhoA levels were found to be reduced in AD brains, while remaining RhoA co-localized with hyperphosphorylated Tau in neurofibrillary tangles (53). Moreover, RhoA expression was decreased within synapses and increased in degenerating neurites of Aβ precursor protein over-expressing transgenic mouse brains, while localization of Rac1, Cdc42 or PAKs remained unaffected (53). Further observation that Aβ production by the secretase-dependent cleavage of amyloid precursor protein was enhanced by the activity of RhoA/ROCK highlights the importance of RhoA regulation in AD (54). In this study, the production of the pro-fibrillary Aβ42 fragment was reduced by treatment with non-steroidal anti-inflammatory drugs, which counter RhoA/ROCK activity *in vivo* (54).

RhoA has been extensively studied in neuronal development, where its activation promotes growth cone collapse and axon retraction (25). Similarly, the addition of Aβ to cultured human neuroblastoma cells resulted in shorter neurite lengths, via RhoA activation and reduced active Rac1 levels (55). In addition, application of Aβ correlated with an increase in the alternatively spliced variant of collapsin response mediator protein-2 (CRMP-2), CRMP-2A, and enhanced its inhibitory threonine phosphorylation (55). Expression of active Rac1 or application of the ROCK inhibitor Y27632 reduced CRMP-2A phosphorylation, which enhanced its association with tubulin (55).

Rho GTPases are activated when membrane bound, a process that is mediated in part by addition of a prenyl moiety (56). Intriguingly, the addition of the isoprenoid geranylgeranyl pyrophosphate to cells leading to RhoA activation, resulted in increased levels of Aβ peptides which are known to accumulate in neuritic plaques in AD (54).

More recently, exogenous application of Aβ42 to neurons resulted in impaired prenylation of Rab and Ras GTPases by inducing cholesterol sequestration (57). This finding raises the possibility that a negative feedback mechanism exists to down-regulate GTPase activation (potentially towards RhoA), when excessive Aβ levels are generated (57). In a recent study, Cook and colleagues reported hyper-activation of the *Drosophila melanogaster* orthologue of RhoA, Rho1, in progressive and age-dependent neurodegeneration in flies lacking AMP-activated protein kinase (AMPK) γ-subunit (58). In this model, loss of AMPK-mediated repression of hydroxyl-methylglutaryl-CoA reductase, the rate limiting enzyme in isoprenoid synthesis, led to enhanced prenylation of Rho1. Though no deleterious effects during nervous system development were observed in this model, dysregulation of Rho1 reduced neuronal integrity in adulthood, in part due to decreased capacity for degrading elevated active Rho1 (58). Taken together, dysregulation of RhoA by aberrant isoprenylation may contribute to the pathogenesis of AD and neurodegeneration.

Proteosomal dysfunction and poly-ubiquitinated protein aggregates are a common theme in neurodegenerative diseases including AD (reviewed in (59)). BARGIN (BGIN) is a brain-specific RhoGAP splice variant that has been implicated in AD by its colocalization with poly-ubiquitin aggregates of neurofibrillary tangles (60). BGIN associated with poly-ubiquitinated proteins via its phosphatase domain, mediating its distribution to membranous fractions where it locally inactivated Rac1 and augmented reactive oxygen species generation via the Nox1 complex (60). This study correlates with previous work showing that Rac1 effectors PAK1 and PAK3 have reduced expression and activity in human AD brains, thereby impairing actin remodeling

via cofilin in dendritic spines (61). Though a global reduction of Rac1 activation occurs in AD brains, studies have implicated Rac1 activation in early stages of AD. For example, Aβ42 addition to hippocampal cultures enhanced cytoskeletal dynamics by increasing activation of Rac1 and Cdc42, as well as up-regulating the Rac GEF Tiam1 (62). This work provides a mechanism whereby Aβ-induced cell stress may promote aberrant F-actin aggregation in early AD via Rac1 and Cdc42 activation (62).

Impaired dendritic spine maintenance, leading to loss of synaptic function is a key contributor to the cognitive deficits elicited during AD progression. The RacGEF Kalirin-7 is an essential component of mature excitatory synapses that is down-regulated in AD hippocampal tissues (63). Furthermore, Kalirin-7 was found to associate with inducible nitric oxide synthase (iNOS) and down-regulate its enzymatic activity (63). Intriguingly, increased NOS has been correlated with brain lesions during AD development, and thus the loss of Kalirin-7 in AD patients may further augment iNOS activity thereby promoting AD pathology (63, 64).

Reduction in cortical thickness is a hallmark of AD and recently the Cdc42 GAP, NOMA-GAP has been shown to regulate cortical thickness and cortical neuron dendritic branching during development (65). Suppression of NOMA-GAP led to hyperactivated Cdc42 and oversimplification of dendritic arborization in the neocortex of NOMA-GAP knockout mice, which was partially rescued by reduction of Cdc42 levels or expression of active cofilin (65). Though NOMA-GAP is not required for early neuronal development, NOMA-GAP is necessary in NGF-simulated signaling pathways, which are reduced in age-related neurodegeneration such as AD (66, 67). While a functional

link has yet to be made, it is an attractive hypothesis that NOMA-GAP is affected during the progression of AD.

Activation of pro-apoptotic caspases in the cortex and hippocampus has been associated with neurodegeneration characteristic of AD (68). Intriguingly, RhoB levels are induced by neurotrauma, which have been shown to be inversely correlated to cell survival (69, 70). Furthermore, the finding that RhoB modulates the expression of genes related to AD susceptibility support a function of RhoB in neurodegeneration (71). Indeed, cortico-hippocampal neurons lacking RhoB expression exhibited increased survival, reduced DNA fragmentation and caspase 3 and 9 activation induced by staurosporine (72). These data highlight RhoB as a potential therapeutic target, whereby diminishing its activity may impair apoptosis during AD progression.

Mutation of the γ-secretase intramembrane protease complex member, presenilin 1, is causative for early onset familial AD, due to a resulting increase in production of aggregate-prone Aβ42 by amyloid precursor protein cleavage (73). Expression of the Rac1 GEF Dock3, which associates with presenilin 1, was found to be reduced in AD brains (73). Dock3 promotes neurite outgrowth of hippocampal neurons downstream of brain-derived neurotrophic factor (BDNF) via complex formation with Fyn and WAVE proteins at the plasma membrane (74). Since Dock3 interacts with and inhibits GSK3β downstream of BDNF, thereby promoting axon branching and microtubule assembly by CRMP2, these functions of Dock3 would be suppressed in the AD brain (75). Additional links of Dock3 to AD include its ability to regulate metabolism of APP (76), its presence in AD tangles and regulation of tau phosphorylation (77). Furthermore, Dock3 knockout mice present with impaired sensorimotor function and

central axonal dystrophy related to reduced inhibition of cofilin (78). Most recently, Dock3 was reported to associate with glutamate-receptor subunit NR2D, which is a target of the AD drug, metamine (79). Association of Dock3 to the C-terminal tail of NR2D protected neurons from excitotoxicity by reducing the surface expression of NR2D (79). Taken together, Dock3 is a major player in the regulation of pathways associated with AD, and emphasizes the significance of Rac1 regulation during neuronal maintenance.

In summary the pathogenesis of AD elicits the participation of many Rho GTPases, their regulators and effectors. It still remains unclear how the interplay between these multiple signalling pathways contribute to the pathogenesis of the disease.

Huntington's Disease (HD)

HD is a progressive, inherited neurodegenerative disorder characterized by behavioural, cognitive and psychological dysfunction, ultimately leading to death. The pathology of HD is caused by the addition of polyglutamine expansions to the protein huntingtin (Htt), leading to toxic aggregation of Htt, subsequent loss of medium spiny neurons within the striatum, and altered dendritic spine shape and density (for review see (80)). An early link between HD and Rho GTPase regulation was the identification that the Trio-like RacGEF Kalirin-7 interacts with Huntington associated protein-1 (HAP-1) (81). Kalirin-7 plays a key role in neuronal spine formation and synapse dynamics (reviewed in (82)) and notably reduction of Kalirin-7 results in loss of dendritic complexity in the medium spiny neurons of the striatum (82), an effect that is dependent

on its Rac1 GEF activity (83). Since degeneration of the cerebellum often occurs at the early stages of HD, identifying proteins involved in cerebellar maintenance may potentially be of therapeutic interest to treat cerebellum-associated HD symptoms. Recently the RacGEF Trio has been shown to regulate the migration and morphogenesis of granule cells in the developing cerebellum (84). Neural-specific knockout of Trio resulted in defective cerebella, which contained misguided neurons and downregulation of active Rac1, RhoA and Cdc42 (84). Although a direct link with Trio and HD has not yet been made, its high level of homology to Kalirin and reported implication in cerebellar maintenance may make it a formidable candidate protein warranting further investigation.

In HD, nuclear localization of the transcription repressor, Repressor Element 1 Silencing Transcription (REST) Factor, contributes to mRNA dysregulation. Johnson and colleagues identified miR-132 as a substrate of REST in the brain (85). Intriguingly, miR-132 repressed the expression of the Rho/Rac/Cdc42 GAP, p250GAP and thereby promoted neurite outgrowth of cultured cortical neurons in response to neurotrophins (86). In human HD cortices, there is a reduction of miR-132 expression, and consequent upregulation of p250GAP mRNA which may prevent neurite growth and sprouting in the HD pathology (85).

Further implication of Rho GTPase effectors in the pathogenesis of HD include Cdc42-interacting protein 4 (CIP4) which associates with Htt. Neuronal CIP4 accumulated with neuropathological severity in the neostriatum of HD patients and partially colocalized with ubiquitin-positive aggregates, while overexpression of CIP4 induced cell death of striatal neurons (87). CIP4 is a Cdc42 effector protein that

interacts with WASP and is involved in cytoskeletal organization (88). Since CIP4 may be involved in the binding of WASP to microtubules, accumulation of CIP4 may interfere with Cdc42/WASP-dependent pathways (88).

Some studies have shown that inhibition of the RhoA effector, ROCK is of therapeutic benefit in HD models. Application of Y-27632 reduced Htt aggregation in cultured cells and reduced Htt-mediated neurodegeneration in *Drosophila* (89). Furthermore, the actin-binding factor, profilin which interacts with Htt is a direct target of ROCK1 (90). Expression of profilin reduced aggregation of polyglutamine-expanded Htt, while phosphorylation of profilin by ROCK1 at Ser-137 impaired association of profilin and Htt (90). Since the depletion of profilin blocked the inhibitory effects of Y-27632 on Htt aggregation, it is hypothesized that ROCK1 controls polyglutamine protein aggregation and may be of therapeutic interest for treating the progression of HD (90). Additional work has revealed the contribution of microtubule dynamics to survival in the mutant Htt-expressing striatal neuronal model. Application of microtubule destabilizers promoted survival in mutant Htt cells, in a pathway involving the RhoA GEF, GEF-H1 and downstream ROCK signaling which led to activation of pro-survival ERK, but not in control cells (91). In summary, the activities of various Rho GTPases, regulators and effectors have been implicated in HD pathology, many of which may be the target for designing future therapeutics to prevent HD progression.

Parkinson's Disease (PD)

PD is a progressive neurodegenerative disorder arising from loss of dopaminergic neurons from the *substantia nigra* region of the midbrain, leading to progressive

cognitive and locomotor impairments (92). Affected neurons present characteristic cytoplasmic inclusions, termed Lewy bodies, which are composed of protein aggregates containing α-synuclein (93). Accumulation of α-synuclein aggregates may occur with age due to reduced clearance capacity, or due to an inherited mutation. Synphilin-1 can form small storage compartments “aggresomes” either alone, or in association with α-synuclein—which store misfolded proteins when clearance mechanisms are overwhelmed (94). Rho GTPases and regulators are increasingly being demonstrated to function alongside major players in PD pathology. A recent study characterized a direct interaction between Kalirin-7 and synphilin-1 (95). Kalirin-7 expression increased the susceptibility of synphilin-1 inclusion Lewy bodies to be degraded, though this function was found to be independent of its Rac GEF activity (95).

The most common genetic cause of familial late-onset PD has been linked to mutations in leucine-rich repeat kinase 2 (LRRK2). Chan and colleagues identified that LRRK interacts with endogenous Rac1, and to a lesser extent Cdc42 (96). LRRK2 potentiated Rac1 activation in a kinase-dependent manner and modulated Rac1 cellular localization. The PD associated G2019S mutant of LRRK2 was no longer able to bind Rac1, leading to neurite retraction (96).

The role of microglia which supports neuronal health is imperative for the normal functioning of neural networks. During neuronal injury microglia become activated and recruited to the damage site, where they can release various factors and phagocytose cellular debris. In a recent study by Barcia *et al*, the induction of PD by the dopaminergic neurotoxin MPTP activated microglia and recruited them to affected neurons (97). Interestingly, this effect was mediated by ROCK activity, and coincided

with a ROCK-dependent upregulation of Cdc42 *in vivo*, providing another link between Rho GTPase regulation and the pathology of PD (97).

Glaucoma

Glaucoma is the leading cause of blindness, resulting from progressive loss of retinal ganglion cell (RGC) axon integrity, arising from injury of the optic nerve head. Until recently no genetic model for glaucoma had been identified, and thus studies have relied on inducing injury to the optic nerve head in order to study molecular pathways of RGC degeneration. In 2010 Fujikawa and colleagues reported that deficiency of the RhoGEFs Vav2 and Vav3 leads to a condition likened to glaucoma (98). Vav2 and Vav3 double knockout mice presented with early onset iridocorneal angle changes, elevated intraocular pressure with subsequent selective loss of retinal ganglion cells and optic nerve head cupping (98). Interestingly, a genome-wide screening of glaucoma susceptibility loci in a Japanese study identified *VAV2* and *VAV3* as candidates (98). Although Vav2 and Vav3 have GEF activity towards RhoA, RhoB, and RhoG, these studies did not investigate the specific contribution of Vav GEF activity to prevention of glaucoma (99). In another study, EphB2 or EphB3 KO mice were subjected to laser-induced ocular hypertension, an experimental model for glaucoma; these mice exhibited a more severe case of axonal degeneration (100). Intriguingly, they observed Vav2 phosphorylation and upregulation (and potential activation) in the optic nerve head after ocular hypertension induction, whereas EphB-deficient mice showed reduced Vav2 phosphorylation suggesting that it may be important for induced glaucoma (100). The apparent activation of Vav2 in this study promoting glaucoma varying from the knock-

out study hints at a differential requirement of Vav2 and Vav3 in various tissues affected during glaucoma (100).

In a different study, the RhoGEF Dock3 has been implicated in a neuroprotective role following optic nerve crush. The authors demonstrated that Dock3 is required for BDNF-TrkB signaling in RGCs, leading to Rac1 activation via recruitment of Dock3/WAVE1 complex to the plasma membrane during nerve extension (74). Furthermore since transgenic mice expressing ectopic levels of Dock3 exhibited enhanced optic nerve regeneration following injury (74), Dock3 may be a potential therapeutic targets to prevent degeneration of RGC axons during glaucoma.

Taken together, various Rho GTPases and regulators may contribute to the initiation of glaucoma, though further work will be required to characterize the specific function of each protein in this system.

Charcot-Marie-Tooth Disease (CMTD)

CMTD encompasses many genetically heterogeneous, inherited neuromuscular disorders of motor and sensory neural networks (101). The major clinical manifestations of CMTD are progressive muscle weakness, atrophy, paralysis and distal sensory loss. There are two subtypes of CMTD, the first is characterized by enhanced demyelination ultimately resulting in lower nerve conduction velocities (NCVs), and the second is characterized by an axonal phenotype, whereby the NCVs are not affected but the amplitude of motor and sensory action potentials and signs of axonal degeneration (102). Recent studies have implicated the activity and regulation of Rho GTPases in myelination and axon maintenance, and have been linked to some forms of CMTD. The

first indication that Rho GTPases function in myelination of motor neurons were derived from studies on a family which presented with slowed NCVs, but not severe motor neuropathies. Mutations were found in the gene encoding ARHGEF10, which is a RhoA GEF highly expressed in the peripheral nervous system (103). Further study revealed that inherited mutations localized in the N-terminal region of ARHGEF10 protein resulted in a constitutively active RhoA GEF activity, leading to elevated active RhoA levels in peripheral nerves (104). This work indicates that erroneously elevated RhoA activation in Schwann cells is detrimental to neural transmission by reducing myelination of peripheral nerves.

In another case, Stendel and colleagues (2007) report that the autosomal recessive demyelinating form of CMTD (CMT4H) involves the disruption of a Cdc42 GEF, frabin/FGD4. Mutation of frabin induced demyelination of peripheral nerves, leading to reduced NCVs and thinly myelinated axons (105). Since expression of frabin in Schwann cells resulted in increased formation of filopodia and lamellipodia, it is hypothesized that Cdc42 activity is required for proper myelination of peripheral nerves. Subsequent studies of frabin/FGD4 knockout mice revealed that dysregulated myelination occurs both in early peripheral nerve development and at later stages (106). Using an inducible Schwann cell-specific knock out model of Frabin, they demonstrated that Frabin is required for accurate myelin maintenance post-development independently of the axon/neuronal expression, and the reduced myelin maintenance correlated with reduced active Cdc42 levels and impaired endocytosis (106). Taken together these studies highlight the critical role of Cdc42 in myelin maintenance and homeostasis of Schwann cells in the peripheral nervous system.

In the context of lower motor neuron diseases, mutation in the Pleckstrin homology domain-containing family G member 5 gene *PLEKHG5,* has been implicated in a severe form of the disease with childhood onset. Studies have linked PLEKHG5/Syx expression to activation of nuclear factor κB (NFκB), and mutation of PLEKHG5 in its RhoA GEF domain impaired NFκB signaling pathways (107). Rho GTPases have been shown to activate the NFκB signaling pathway, and while this activation has not been demonstrated to be neuroprotective, inhibition of NFκB leads to apoptosis of neurons (108, 109). Thus reduced RhoA activation downstream of PLEKHG5 may impede NFκB-mediated neuroprotection and thereby contribute to the neurodegeneration observed in the lower motor neuron disease patients.

The constitutively active Rho GTPase RhoE/Rnd3 is well expressed in the central nervous system and has been shown to participate in neurite outgrowth in PC12 cells by negatively regulating RhoA/ROCK1 (110). Intriguingly, RhoE-deficient mice present with severe motor neuron deficits and delayed neuromuscular maturation, lacking the peroneal nerve completely (111). Despite the involvement of RhoE in muscle maturation, its interaction with brain-specific PLEKHG5/Syx further implicate it in motor neuron diseases (112). RhoE modulates the actin cytoskeleton by antagonizing RhoA signaling by activation of p190RhoGAP (113) and/or by directly binding to ROCK1 and activating MLC phosphatase, resulting in increased phosphorylated and inactivated cofilin (114, 115). These studies suggest that RhoE/Rnd3 participates in motor neuron maintenance through inhibition of the RhoA/ROCK pathway.

Overall, these studies demonstrate the direct implication of RhoA/Cdc42 regulatory pathways in the pathogenesis of CMTD and lower motor neuron diseases.

Concluding Remarks

The generation of genetic animal models of Rho GTPases and regulators has profoundly expedited our discovery of their fine-tuned functions during nervous system development and maintenance. The additional use of animal disease models has further reinforced the importance of Rho GTPase signaling pathways in the pathogenesis of neurodegeneration. With increased studies of the large numbers of Rho GTPase regulators, more than 80 human GEFs and 70 human GAPs, we expect our knowledge of these protein signaling pathways to increase and reveal novel targets for therapeutic intervention. Ultimately, we hope these studies will promote the development of individualized therapies to treat these terrible incapacitating diseases, and in coming years reduce the number of people affected by neurodegeneration.

Acknowledgments

NLV is a William Dawson Chair and FRSQ Chercheur National. This work was supported by grants from CIHR MOP -14701. JD was supported by an FRSQ Master's Training Award. We acknowledge the limited scope of this review and apologize that we were unable to reference more works related to this field.

Table 1: Summary of Rho GTPases, regulators and effectors implicated in neurodegeneration disorders

	Name	Modulation	Effector(s)	Associated Pathology/Setting
GTPases	Cdc42	▲▼	CIP4	AD, HD, PD, CMTD4H (62, 65, 87, 97, 106)
	Rac1	▼▲		nerve injury, early AD, PD, HD, optic nerve regeneration (35, 55, 62, 74, 82, 96)
	RhoA	▼▲	ROCK	nerve injury, AD, degeneration, HD, PD, CMTD, lower motor neuron disease (35-37, 53, 54, 58,
	RhoB	▲		89, 104, 107, 116)
	RhoE/Rnd3	▲	▼RhoA/ROCK	neurotrauma, *AD* (69, 71, 72)
				motor neuron maintenance (111, 114)
GEFs	Alsin	▼	Rab5, Rac1	ALS/Upper motor neuron disease (43)
	ARHGEF10	▲	RhoA	peripheral nerve disease (103)
	ARHGEF16	▼	Rac1, Cdc42	*sporadic ALS* (48)
	Dock3	▼	Rac1	AD, optic nerve regeneration (73-76, 79)
	Frabin/FGD4	▼	Cdc42	CMTD4H (105)
	GEF-H1	n.d.	RhoA	HD (91)
	PLEKHG5/Syx	▼	RhoA	Lower motor neuron disease (107)
	Kalirin 7	▼	Rac1	AD, HD, PD (63, 81, 95)
	Kalirin 9	n.d.	RhoA, Rac1	Nerve injury/axon pruning (34)
	Tiam1	▲	Rac1	AD (62)
	Trio	n.d.	RhoA,Rac1, RhoG	cerebellum maintenance, *HD* (84)
	Vav2/Vav3	n.d.	RhoA/B/G	Glaucoma (98)
GAPs	BARGIN	▲	Rac1	AD (60)
	NOMA-GAP	▼	Cdc42	Cortical thickness, *AD* (65)
	p250GAP	▲	RhoA, Rac, Cdc42	HD (86)
	p190RhoGAP	n.d.	RhoA	Injury/axon pruning (38)
	srGAP1	▲	Cdc42, RhoA	*sporadic ALS* (48)
GDIs	RhoGDI	▼	RhoA	Injury/axon pruning (33)
Effectors/ Regulators	CIP4	▲	WASP	HD (87)
	LRRK2	▼	Rac1, Cdc42	PD (96)
	Merlin-iso2	n.d.	RhoGDI,	Severe neuropathy (38)
	miR-132	▼	p190RhoGAP	HD cortex (85)
	ROCK	▲▼	p250GAP	AD, HD, PD (54, 90, 97)
	PAK1 & PAK3	▼	cofilin	AD brain (61)

▲ upregulation of expression or activity
▼downregulation of expression or activity
n.d. = not yet determined
italics = direct link has yet to be confirmed

References

1. Jaffe AB, Hall A. Rho GTPases: Biochemistry and Biology. Ann Rev Cell Dev Biol. 2005;21:247-69.
2. Vega FM, Ridley AJ. SnapShot: Rho family GTPases. Cell. 2007;129:1430.
3. Zheng Y. Dbl family guanine nucleotide exchange factors. Trends Biochem Sci. 2001;26:724-32.
4. Tcherkezian J, Lamarche-Vane N. Current knowledge of the large RhoGAP family of proteins Biol Cell. 2007;99:67-86.
5. Olofsson B. Rho guanine dissociation inhibitors: pivotal molecules in cellular signalling. Cell Signal. 1999;11:545-54.
6. Côté JF, Motoyama AB, Bush JA, Vuori K. A novel and evolutionarily conserved PtdIns(3,4,5)P3-binding domain is necessary for DOCK180 signalling. Nat Cell Biol. 2005;7:797-807.
7. Ridley AJ, Hall A. The small GTP-binding protein rho regulates the assembly of focal adhesions and actin stress fibers in response to growth factors. Cell. 1992;70:389-99.
8. Ridley AJ, Paterson HF, Johnston CL, Diekmann D, Hall A. The small GTP-binding protein rac regulates growth factor-induced membrane ruffling. Cell. 1992;70:401-10.
9. Nobes CD, Hall A. Rho, Rac and Cdc42 GTPases regulate the assembly of multimolecular focal complexes associated with actin stress fibers, lamellipodia and filopodia. Cell. 1995;81:53-62.
10. Edwards DC, Sanders LC, Bokoch GM, Gill GN. Activation of LIM-kinase by Pak1 couples Rac/Cdc42 GTPase signalling to actin cytoskeletal dynamics. Nat Cell Biol. 1999;1:253-9.
11. Yang N, Higuchi O, Ohashi K, Nagata K, Wada A, Kangawa K, et al. Cofilin phosphorylation by LIM-kinase 1 and its role in Rac-mediated actin reorganization. Nature. 1998;393:809-12.
12. Sanders LC, Matsumura F, Bokoch GM, de Lanerolle P. Inhibition of myosin light chain kinase by p21-activated kinase. Science. 1999;283:2083-5.
13. Eblen ST, Slack JK, Weber MJ, Catling AD. Rac-PAK signaling stimulates extracellular signal-regulated kinase (ERK) activation by regulating formation of MEK1-ERK complexes. Mol Cell Biol. 2002;22:6023-33.
14. Zhang S, Han J, Sells MA, Chernoff J, Knaus UG, Ulevitch RJ, et al. Rho family GTPases regulate p38 mitogen-activated protein kinase through the downstream mediator Pak1. J Biol Chem. 1995;270:23934-6.
15. Bagrodia S, Derijard B, Davis RJ, Cerione RA. Cdc42 and PAK-mediated signaling leads to Jun kinase and p38 mitogen-activated protein kinase activation. J Biol Chem. 1995;270:27995-8.
16. Lamarche N, Tapon, N., Stowers, L., Burbelo, P.D., Aspenstrom, P., Bridges, T., Chant, J. and Hall, A. Rac and Cdc42 induce actin polymerization and G1 cell cycle progression independently of p65PAK and the JNK/SAPK MAP kinase cascade. Cell. 1996;87:519-29.

17. Rohatgi R, Ma L, Miki H, Lopez M, Kirchhausen T, Takenawa T, et al. The interaction between N-WASP and the Arp2/3 complex links Cdc42- dependent signals to actin assembly. Cell. 1999;97:221-31.
18. Machesky LM, Mullins RD, Higgs HN, Kaiser DA, Blanchoin L, May RC, et al. Scar, a WASp-related protein, activates nucleation of actin filaments by the Arp2/3 complex. Proc Natl Acad Sci U S A. 1999;96:3739-44.
19. Pollitt AY, Insall RH. WASP and SCAR/WAVE proteins: the drivers of actin assembly. J Cell Sci. 2009;122:2575-8.
20. Kimura K, Ito M, Amano M, Chihara K, Fukata Y, Nakafuku M, et al. Regulation of myosin phosphatase by rho and rho-associated kinase (rho-kinase). Science. 1996;273:245-8.
21. Maekawa M, Ishizaki T, Boku S, Watanabe N, Fujita A, Iwamatsu A, et al. Signaling from Rho to the actin cytoskeleton through protein kinases ROCK and LIM-kinase. Science. 1999;285:895-8.
22. Ohashi K, Nagata K, Maekawa M, Ishizaki T, Narumiya S, Mizuno K. Rho-associated kinase ROCK activates LIM-kinase 1 by phosphorylation at threonine 508 within the activation loop. J Biol Chem. 2000;275:3577-82.
23. Palazzo AF, Cook TA, Alberts AS, Gundersen GG. mDia mediates Rho-regulated formation and orientation of stable microtubules. Nat Cell Biol. 2001;3:723-9.
24. Govek EE, Newey SE, Van Aelst L. The role of the Rho GTPases in neuronal development. Genes Dev. 2005;19:1-49.
25. Lowery LA, Van Vactor D. The trip of the tip: understanding the growth cone machinery. Nat Rev Mol Cell Biol. 2009;10:332-43.
26. Li X, Saint-Cyr-Proulx E, Aktories K, Lamarche-Vane N. Rac1 and Cdc42 but not RhoA or Rho kinase activities are required for neurite outgrowth induced by the Netrin-1 receptor DCC (deleted in colorectal cancer) in N1E-115 neuroblastoma cells. J Biol Chem. 2002;277:15207-14.
27. Antoine-Bertrand J, Villemure JF, Lamarche-Vane N. Implication of Rho GTPases in Neurodegenerative Diseases. Curr Drug Targets. 2011;12:1202-15.
28. Atwal JK, Pinkston-Gosse J, Syken J, Stawicki S, Wu Y, Shatz C, et al. PirB is a Functional Receptor for Myelin Inhibitors of Axonal Regeneration. Sci Rep. 2008;322:967-70.
29. Wang KC, Kim JA, Sivasankaran R, Segal R, He Z. P75 interacts with the Nogo receptor as a co-receptor for Nogo, MAG and OMgp. Nature. 2002;420:74-8.
30. Park JB, Yiu G, Kaneko S, Wang J, Chang J, He XL, et al. A TNF receptor family member, TROY, is a coreceptor with Nogo receptor in mediating the inhibitory activity of myelin inhibitors. Neuron. 2005;45:345-51.
31. Singh KK, Park KJ, Hong EJ, Kramer BM, Greenberg ME, Kaplan DR, et al. Developmental axon pruning mediated by BDNF-p75NTR-dependent axon degeneration. Nat Neurosci. 2008;11:649-58.
32. Park KJ, Grosso CA, Aubert I, Kaplan DR, Miller FD. p75NTR-dependent, myelin-mediated axonal degeneration regulates neural connectivity in the adult brain. Nat Neurosci. 2010;13:559-66.
33. Yamashita T, Tohyama M. The p75 receptor acts as a displacement factor that releases Rho from Rho-GDI. Nat Neurosci. 2003;6:461-7.

34. Harrington AW, Li QM, Tep C, Park JB, He Z, Yoon SO. The role of Kalirin9 in p75/nogo receptor-mediated RhoA activation in cerebellar granule neurons. J Biol Chem. 2008;283:24690-7.
35. Niederöst B, Oertle T, Fritsche J, McKinney RA, Bandtlow CE. Nogo-A and myelin-associated glycoprotein mediate neurite growth inhibition by antagonistic regulation of RhoA and Rac1. J Neurosci. 2002;22:10368-76.
36. Fournier AE, Takizawa BT, Strittmatter SM. Rho Kinase Inhibition Enhances Axonal Regeneration in the Injured CNS. J Neurosci. 2003;23:1416-23.
37. Borisoff JF, Chan CC, Hiebert GW, Oschipok L, Robertson GS, Zamboni R, et al. Suppression of Rho-kinase activity promotes axonal growth on inhibitory CNS substrates. Mol Cell Neurosci. 2003;22:405-16.
38. Schulz A, Baader SL, Niwa-Kawakita M, Jung MJ, Bauer R, Garcia C, et al. Merlin isoform 2 in neurofibromatosis type 2-associated polyneuropathy. Nat Neurosci. 2013;16:426-33.
39. Fry EJ, Ho C, David S. A role for Nogo receptor in macrophage clearance from injured peripheral nerve. Neuron. 2007;53:649-62.
40. Jung J, Cai W, Lee HK, Pellegatta M, Shin YK, Jang SY, et al. Actin polymerization is essential for myelin sheath fragmentation during Wallerian degeneration. J Neurosci. 2011;31:2009-15.
41. Bruijn LI, Miller TM, Cleveland DW. Unraveling the mechanisms involved in motor neuron degeneration in ALS. Annu Rev Neurosci. 2004;27:723-49.
42. Rosen DR, Siddique T, Patterson D, Figlewicz DA, Sapp P, Hentati A, et al. Mutations in Cu/Zn superoxide dismutase gene are associated with familial amyotrophic lateral sclerosis. Nature. 1993;362:59-62.
43. Yamanaka K, Miller TM, McAlonis-Downes M, Chun SJ, Cleveland DW. Progressive spinal axonal degeneration and slowness in ALS2-deficient mice. Ann Neurol. 2006;60:95-104.
44. Yamanaka K, Vande Velde C, Eymard-Pierre E, Bertini E, Boespflug-Tanguy O, Cleveland DW. Unstable mutants in the peripheral endosomal membrane component ALS2 cause early-onset motor neuron disease. Proc Natl Acad Sci. 2003;100:16041-6.
45. Otomo A, Hadano S, Okada T, Mizumura H, Kunita R, Nishijima H, et al. ALS2, a novel guanine nucleotide exchange factor for the small GTPase Rab5, is implicated in endosomal dynamics. Hum Mol Genet. 2003;12:1671-87.
46. Tudor EL, Perkinton MS, Schmidt A, Ackerley S, Brownlees J, Jacobsen NJ, et al. ALS2/Alsin regulates Rac-PAK signaling and neurite outgrowth. J Biol Chem. 2005;280:34735-40.
47. Kanekura K, Hashimoto Y, Kita Y, Sasabe J, Aiso S, Nishimoto I, et al. A Rac1/phosphatidylinositol 3-kinase/Akt3 anti-apoptotic pathway, triggered by AlsinLF, the product of the ALS2 gene, antagonizes Cu/Zn-superoxide dismutase (SOD1) mutant-induced motoneuronal cell death. J Biol Chem. 2005;280:4532-43.
48. Figueroa-Romero C, Hur J, Bender DE, Delaney CE, Cataldo MD, Smith AL, et al. Identification of epigenetically altered genes in sporadic amyotrophic lateral sclerosis. PLoS One. 2012;7:e52672.
49. Blanke S, Jäckle H. Novel guanine nucleotide exchange factor GEFmeso of Drosophila melanogaster interacts with Ral and Rho GTPase Cdc42. Faseb J. 2006;20:683-91.

50. Oliver AW, He X, Borthwick K, Donne AJ, Hampson L, Hampson IN. The HPV16 E6 binding protein Tip-1 interacts with ARHGEF16, which activates Cdc42. Br J Cancer. 2011;104:324-31.
51. Wong K, Ren XR, Huang YZ, Xie Y, Liu G, Saito H, et al. Signal transduction in neuronal migration: roles of GTPase activating proteins and the small GTPase Cdc42 in the Slit-Robo pathway. Cell. 2001;107:209-21.
52. Lansbury PT, Lashuel HA. A century-old debate on protein aggregation and neurodegeneration enters the clinic. Nature. 2006;443:774-9.
53. Huesa G, Baltrons MA, Gómez-Ramos P, Morán A, García A, Hidalgo J, et al. Altered distribution of RhoA in Alzheimer's disease and AbetaPP overexpressing mice. J Alzheimers Dis. 2010;19:37-56.
54. Zhou Y, Su Y, Li B, Liu F, Ryder JW, Wu X, et al. Nonsteroidal anti-inflammatory drugs can lower amyloidogenic Abeta42 by inhibiting Rho. Science. 2003;302:1215-7.
55. Petratos S LQ, George AJ, Hou X, Kerr ML, Unabia SE, Hatzinisiriou I, Maksel D, Aguilar MI, Small DH. The beta-amyloid protein of Alzheimer's disease increases neuronal CRMP-2 phosphorylation by a Rho-GTP mechanism. Brain. 2008;131:90-108.
56. Adamson P, Marshall CJ, Hall A, Tilbrook PA. Post-translational modifications of p21rho proteins. J Biol Chem. 1992;267:20033-8.
57. Mohamed A, Saavedra L, Di Pardo A, Sipione S, Posse de Chaves E. β-amyloid inhibits protein prenylation and induces cholesterol sequestration by impairing SREBP-2 cleavage. J Neurosci. 2012;32:6490-500.
58. Cook M, Mani P, Wentzell J, Kretzschmar D. Increased RhoA Prenylation in the loechrig (loe) Mutant Leads to Progressive Neurodegeneration. PLoS One. 2012;7:e44440.
59. Alves-Rodrigues A, Gregori L, Figueiredo-Pereira ME. Ubiquitin, cellular inclusions and their role in neurodegeneration. Trends Neurosci. 1998;21:516-20.
60. Huang TY, Michael S, Xu T, Sarkeshik A, Moresco JJ, Yates JR, et al. A novel Rac1 GAP splice variant relays poly-Ub accumulation signals to mediate Rac1 inactivation. Mol Biol Cell. 2012;24:194-209.
61. Zhao L, Ma QL, Calon F, Harris-White ME, Yang F, Lim GP, et al. Role of p21-activated kinase pathway defects in the cognitive deficits of Alzheimer disease. Nat Neurosci. 2006;9:234-42.
62. Mendoza-Naranjo A, Gonzalez-Billault C, Maccioni RB. Abeta 1-42 stimulates actin polymerization in hippocampal neurons through Rac1 and Cdc42 Rho GTPases. J Cell Sci. 2007;120:279-88.
63. Youn H, Ji I, Ji H, Markesbery W, Ji T. Under-expression of Kalirin-7 Increases iNOS Activity in Cultured Cells and Correlates to Elevated iNOS Activity in Alzheimer’s Disease Hippocampus. J Alzheimers Dis. 2007;12:271-81.
64. Aliev G, Palacios HH, Lipsitt AE, Fischbach K, Lamb BT, Obrenovich ME, et al. Nitric oxide as an initiator of brain lesions during the development of Alzheimer disease. Neurotox Res. 2009;16:293-305.
65. Rosario M, Schuster S, Juttner R, Parthasarathy S, Tarabykin V, Birchmeier W. Neocortical dendritic complexity is controlled during development by NOMA-GAP-dependent inhibition of Cdc42 and activation of cofilin Genes & Dev. 2012;26:1743-57.

66. Rosario M, Franke R, Bednarski C, Birchmeier W. The neurite outgrowth multiadaptor RhoGAP, NOMA-GAP, regulates neurite extension through SHP2 and Cdc42. J Cell Biol. 2007;178:503-16.
67. Capsoni S, Ugolini G, Comparini A, Ruberti F, Berardi N, Cattaneo A. Alzheimer-like neurodegeneration in aged antinerve growth factor transgenic mice. PNAS. 2000;97:6826-31.
68. Gervais FG, Xu D, Robertson GS, Vaillancourt JP, Zhu Y, Huang J, et al. Involvement of caspases in proteolytic cleavage of Alzheimer's amyloid-beta precursor protein and amyloidogenic A beta peptide formation. Cell. 1999;97:395-406.
69. Brabeck C, Beschorner R, Conrad S, Mittelbronn M, Bekure K, Meyermann R, et al. Lesional expression of RhoA and RhoB following traumatic brain injury in humans. J Neurotrauma. 2004;21:697-706.
70. Trapp T, Korhonen L, Besselmann M, Martinez R, Mercer EA, Lindholm D. Transgenic mice overexpressing XIAP in neurons show better outcome after transient cerebral ischemia. Mol Cell Neurosci. 2003;23:302-13.
71. Kamasani U, Prendergast GC. Genetic response to DNA damage: proapoptotic targets of RhoB include modules for p53 response and susceptibility to Alzheimer's disease. Cancer Biol Ther. 2005;4:282-8.
72. Barberan S, McNair K, Iqbal K, Smith NC, Prendergast GC, Stone TW, et al. Altered apoptotic responses in neurons lacking RhoB GTPase. Eur J Neurosci. 2011;34:1737-46.
73. Kashiwa A, Yoshida H, Lee S, Paladino T, Liu Y, Chen Q, et al. Isolation and characterization of novel presenilin binding protein. J Neurochem. 2000;75:109-16.
74. Namekata K, Harada C, Taya C, Guo X, Kimura H, Parada LF, et al. Dock3 induces axonal outgrowth by stimulating membrane recruitment of the WAVE complex. PNAS. 2010;107:7586-91.
75. Namekata K, Harada C, Guo X, Kimura A, Kittaka D, Watanabe H, et al. Dock3 stimulates axonal outgrowth via GSK-3β-mediated microtubule assembly. J Neurosci. 2012;32:264-74.
76. Chen Q, Kimura H, Schubert D. A novel mechanism for the regulation of amyloid precursor protein metabolism. J Cell Biol. 2002;158:79-89.
77. Chen Q, Yoshida H, Schubert D, Maher P, Mallory M, Masliah E. Presenilin binding protein is associated with neurofibrillary alterations in Alzheimer's disease and stimulates tau phosphorylation. Am J Pathol. 2001;159:1597-602.
78. Chen Q, Peto CA, Shelton GD, Mizisin A, Sawchenko PE, Schubert D. Loss of modifier of cell adhesion reveals a pathway leading to axonal degeneration. J Neurosci. 2009;29:118-30.
79. Bai N, Hayashi H, Aida T, Namekata K, Harada T, Mishina M, et al. Dock3 interaction with a glutamate-receptor NR2D subunit protects neurons from excitotoxicity. Mol Brain. 2013;6:22.
80. Ross CA. Huntington's disease: new paths to pathogenesis. Cell. 2004;118:4-7.
81. Colomer V, Engelender S, Sharp AH, Duan K, Cooper JK, Lanahan A, et al. Huntingtin-associated protein 1 (HAP1) binds to a Trio-like polypeptide, with a rac1 guanine nucleotide exchange factor domain. Hum Mol Genet. 1997;6:1519-25.
82. Mandela P, Ma XM. Kalirin, a Key Player in Synapse Formation, Is Implicated in Human Diseases. Neural Plast. 2012;2012:728161.

83. Hayashi-Takagi A, Takaki M, Graziane N, Seshadri S, Murdoch H, Dunlop AJ, et al. Disrupted-in-Schizophrenia 1 (DISC1) regulates spines of the glutamate synapse via Rac1. Nat Neurosci. 2010;13:327-32.
84. Peng YJ, He WQ, Tang J, Tao T, Chen C, Gao YQ, et al. Trio is a key guanine nucleotide exchange factor coordinating regulation of the migration and morphogenesis of granule cells in the developing cerebellum. J Biol Chem. 2010;285:24834-44.
85. Johnson R, Zuccato C, Belyaev ND, Guest DJ, Cattaneo E, Buckley NJ. A microRNA-based gene dysregulation pathway in Huntington's disease. Neurobiol Dis. 2008;29:438-45.
86. Vo N, Klein ME, Varlamova O, Keller DM, Yamamoto T, Goodman RH, et al. A cAMP-response element binding protein-induced microRNA regulates neuronal morphogenesis. Proc Natl Acad Sci. 2005;102:16426-31.
87. Holbert S, Dedeoglu A, Humbert S, Saudou F, Ferrante RJ, Néri C. Cdc42-interacting protein 4 binds to huntingtin: neuropathologic and biological evidence for a role in Huntington's disease. Proc Natl Acad Sci. 2003;100:2712-7.
88. Tian L, Nelson DL, Stewart DM. Cdc42-interacting protein 4 mediates binding of the Wiskott-Aldrich syndrome protein to microtubules. J Biol Chem. 2000;275:7854-61.
89. Pollitt SK, Pallos J, Shao J, Desai UA, Ma AA, Thompson LM, et al. A rapid cellular FRET assay of polyglutamine aggregation identifies a novel inhibitor. Neuron. 2003;40:685-94.
90. Shao J, Welch WJ, Diprospero NA, Diamond MI. Phosphorylation of profilin by ROCK1 regulates polyglutamine aggregation. Mol Cell Biol. 2008;28:5196-208.
91. Varma H, Yamamoto A, Sarantos MR, Hughes RE, Stockwell BR. Mutant huntingtin alters cell fate in response to microtubule depolymerization via the GEF-H1-RhoA-ERK pathway. J Biol Chem. 2010;285:37445-57.
92. Dawson TM, Dawson VL. Molecular pathways of neurodegeneration in Parkinson’s disease. Science. 2003;302:819-22.
93. Dickson DW, Braak H, Duda JE, Duyckaerts C, Gasser T, Halliday GM, et al. Neuropathological assessment of Parkinson's disease: refining the diagnostic criteria. Lancet Neurol. 2009;8:1150-7.
94. Tanaka M, Kim YM, Lee G, Junn E, Iwatsubo T, Mouradian MM. Aggresomes formed by alpha-synuclein and synphilin-1 are cytoprotective. J Biol Chem. 2004;279:4625-31.
95. Tsai YC, Riess O, Soehn AS, Nguyen HP. The Guanine nucleotide exchange factor kalirin-7 is a novel synphilin-1 interacting protein and modifies synphilin-1 aggregate transport and formation. PLoS One. 2012;7:e51999.
96. Chan D, Citro A, Cordy JM, Shen GC, Wolozin B. Rac1 protein rescues neurite retraction caused by G2019S leucine-rich repeat kinase 2 (LRRK2). J Biol Chem. 2011;286:16140-9.
97. Barcia C, Ros CM, Annese V, Carrillo-de Sauvage MA, Ros-Bernal F, Gómez A, et al. ROCK/Cdc42-mediated microglial motility and gliapse formation lead to phagocytosis of degenerating dopaminergic neurons in vivo. Sci Rep. 2012;2:809.
98. Fujikawa K, Iwata T, Inoue K, Akahori M, Kadotani HF, M., Watanabe M, et al. VAV2 and VAV3 as candidate disease genes for spontaneous glaucoma in mice and humans. PLoS One. 2010;5:e9050.

99. Turner M, Billadeau DD. VAV proteins as signal integrators for multi-subunit immune-recognition receptors. Nat Rev Immunol. 2002;2:476-86.
100. Fu CT, Sretavan D. Involvement of EphB/Ephrin-B signaling in axonal survival in mouse experimental glaucoma. Invest Ophthalmol Vis Sci. 2012;53:76-84.
101. Skre H. Genetic and clinical aspects of Charcot-Marie-Tooth's disease. Clin Genet. 1974;6:98-118.
102. Dyck PJ, Chance P, Lebo R, Camey AJ. Hereditary Motor and Sensory Neuropathies, in Dyck P.J., Thomas, P.K., Griffin, J.W., Low P.A. and Poduslo, J.F. (eds.), Peripheral Neuropathy(3rd edn.), Philadelphia: W.B. Saunders. 1993:1094–136.
103. Verhoeven K, De Jonghe P, Van de Putte T, Nelis E, Zwijsen A, Verpoorten N, et al. Slowed conduction and thin myelination of peripheral nerves associated with mutant rho Guanine-nucleotide exchange factor 10. Am J Hum Genet. 2003;73:926-32.
104. Chaya T, Shibata S, Tokuhara Y, Yamaguchi W, Matsumoto H, Kawahara I, et al. Identification of a negative regulatory region for the exchange activity and characterization of T332I mutant of Rho guanine nucleotide exchange factor 10 (ARHGEF10). J Biol Chem. 2011;286:29511-20.
105. Stendel C, Roos A, Deconinck T, Pereira J, Castagner F, Niemann A, et al. Peripheral nerve demyelination caused by a mutant Rho GTPase guanine nucleotide exchange factor, frabin/FGD4. Am J Hum Genet. 2007;81:158-64.
106. Horn M, Baumann R, Pereira JA, Sidiropoulos PN, Somandin C, Welzl H, et al. Myelin is dependent on the Charcot-Marie-Tooth Type 4H disease culprit protein FRABIN/FGD4 in Schwann cells. Brain. 2012;135:3567-83.
107. Maystadt I, Rezsöhazy R, Barkats M, Duque S, Vannuffel P, Remacle S, et al. The nuclear factor kappaB-activator gene PLEKHG5 is mutated in a form of autosomal recessive lower motor neuron disease with childhood onset. Am J Hum Genet. 2007;81:67-76.
108. Perona R, Montaner S, Saniger L, Sánchez-Pérez I, Bravo R, Lacal JC. Activation of the nuclear factor-kappaB by Rho, CDC42, and Rac-1 proteins. Genes Dev. 1997;11:463-75.
109. Barger SW, Moerman AM, Mao X. Molecular mechanisms of cytokine-induced neuroprotection: NFkappaB and neuroplasticity. Curr Pharm Des. 2005;11:985-98.
110. Talens-Visconti R, Peris B, Guerri C, Guasch RM. RhoE stimulates neurite-like outgrowth in PC12 cells through inhibition of the RhoA/ROCK-I signalling. J Neurochem. 2010;112:1074-87.
111. Mocholí E, Ballester-Lurbe B, Arqué G, Poch E, Peris B, Guerri C, et al. RhoE deficiency produces postnatal lethality, profound motor deficits and neurodevelopmental delay in mice. PLoS One. 2011;6:e19236.
112. Goh LL, Manser E. The RhoA GEF Syx is a target of Rnd3 and regulated via a Raf1-like ubiquitin-related domain. PLoS One. 2010;5:e12409.
113. Wennerberg K, Forget MA, Ellerbroek SM, Arthur WT, Burridge K, Settleman J, et al. Rnd proteins function as RhoA antagonists by activating p190 RhoGAP. Curr Biol. 2003;13:1106-15.
114. Riento K, Guasch RM, Garg R, Jin B, Ridley AJ. RhoE binds to ROCK I and inhibits downstream signaling. Mol Cell Biol. 2003;23:4219-29.

115. Peris B, Gonzalez-Granero S, Ballester-Lurbe B, García-Verdugo JM, Pérez-Roger I, Guerri C, et al. Neuronal polarization is impaired in mice lacking RhoE expression. J Neurochem. 2012;121:903-14.
116. Wang S, Xu B, Liou LC, Ren Q, Huang S, Luo Y, et al. α-Synuclein disrupts stress signaling by inhibiting polo-like kinase Cdc5/Plk2. Proc Natl Acad Sci. 2012;109:16119-24.